

Development of Novel Protein Kinase Inhibitors as Potential Therapeutics for Breast Cancer

Dissertation

zur Erlangung des akademischen Grades

Doctor rerum naturalium (Dr. rer. nat.)

vorgelegt der

Naturwissenschaftlichen Fakultät I
(Biowissenschaften)

der Martin-Luther-Universität Halle-Wittenberg

von

Dipl. Pharm. Kazem Ahmed Mahmoud

geb. am 06.01.1981 in Sohag, Ägypten

Gutachter:

1. PD Dr. Andreas Hilgeroth, Halle (Saale)

2. Prof. Dr. Wolfgang Sippl, Halle (Saale)

3. Prof. Dr. Christoph Ritter, Greifswald

Halle (Saale), den 03.07.2013 (Tag der Verteidigung)

Selbstständigkeitserklärung

Hiermit erkläre ich gemäß § 5 (2) b der Promotionsordnung der Naturwissenschaftlichen Fakultät I – Biowissenschaften der Martin-Luther-Universität Halle-Wittenberg, dass ich die vorliegende Arbeit selbstständig und ohne Benutzung anderer als der angegebenen Hilfsmittel und Quellen angefertigt habe. Alle Stellen, die wörtlich oder sinngemäß aus Veröffentlichungen entnommen sind, habe ich als solche kenntlich gemacht. Ich erkläre ferner, dass diese Arbeit in gleicher oder ähnlicher Form bisher keiner anderen Prüfbehörde zur Erlangung des Doktorgrades vorgelegt wurde.

Halle, April 2013

Kazem Ahmed Mahmoud

Acknowledgment

The present work was carried out at the Department of Pharmaceutical Chemistry and Clinical Pharmacy, Institute of Pharmacy, Martin Luther University Halle-Wittenberg, Halle (Saale), Germany, in the period from April 2010 to October 2012 under the supervision of PD Dr. Andreas Hilgeroth (the leader of Drug Development and Analysis research group).

First and foremost, I would like to express my deep thanks and gratitude to my supervisor PD Dr. Andreas Hilgeroth, who allowed me to perform this research in his group, as well as the hiring of the interesting topic, his guidance during this work and the scope for creativity.

Furthermore, I thank Mrs. Manuela Woigk for the production of ESI-MS spectra, Mrs. Heike Rudolph for recording the IR spectra and Dr. Dieter Ströhl, Department of Chemistry, and his staff for carrying out the NMR spectra. I also thank Dr. Frank Totzke from the *ProQinase* GmbH in Freiburg for the protein kinase assay achievement. I acknowledge all the staff of the National Cancer Institute (NCI) in the United States for the execution of the 60-cell-line screenings. My thanks also should go to Prof. Dr. Wolfgang Sippl for carrying out the docking studies in this work.

A special thanks to Dr. Marc Hemmer for his deep proofreading of the manuscript and continues help. Felix Neubauer, I appreciate his kindly help in translations. My thanks to all members of our research group for creating a nice atmosphere in the lab. I also thank all other members of the Institute of Pharmacy who have contributed in making this work.

The most special thanks belong to my father, my mother, my sister and my brothers in Egypt for their understanding about my leaving during all these years.

Great thanks are owed to my wonderful family, my wife Mardia and my children Ahmed and Rabab. Mardia has been my inspiration and motivation for continuing to improve my knowledge and move my career forward. I appreciate your sustainable support and encouragement, thank you my love.

Contents:

List of Abbreviations	IV
List of Tables	VI
List of Figures	VII
Glossary	X
1. INTRODUCTION	1
1.1. Breast Cancer.....	1
1.1.1. Female Breast Cancer.....	1
1.1.1.1. Background.....	1
1.1.1.2. Anatomy.....	2
1.1.1.3. Pathophysiology.....	3
1.1.1.4. Etiology.....	3
1.1.1.5. Signs and Symptoms.....	4
1.1.1.6. Diagnosis.....	4
1.1.1.7. Medication Summary.....	5
1.1.2. Male Breast Cancer.....	6
1.1.3. Therapeutic Targets in Breast Cancer.....	6
1.1.3.1. Protein Tyrosine Kinases.....	6
1.1.3.1.1. Breast tumor kinase/protein tyrosine kinase 6.....	7
1.1.3.1.2. Brk signaling substrates, protein interactions and biology.....	9
1.1.3.2. Epidermal Growth Factor Receptor (EGFR) family.....	12
1.1.3.2.1. Human Epidermal Growth Factor Receptor (HER)-2.....	13
1.1.3.2.2. HER2 dimerization.....	14
1.1.3.2.3. MAPK signaling.....	15
1.1.3.2.4. PI3K signaling.....	15
1.1.4. Inhibitors of Breast Cancer-Relevant Kinases.....	17
1.1.4.1. BRK/PTK6 Inhibitors.....	17
1.1.4.2. HER2 Inhibitors.....	18
2. OBJECTIVES	22
3. RESULTS & DISCUSSION	26
3.1. Chemistry.....	26
3.1.1. Synthesis of the 4-substituted α -carbolines.....	26
3.1.1.1. Reaction of the 4-chloro- α -carboline with aromatic amines.....	28
3.1.1.2. Reduction of compound 19 into the amino form 29	30
3.1.2. Substitutions on the 6-position of the α -carboline derivatives.....	32
3.1.2.1. Synthesis of the 6-sulfonamide-4-chloro- α -carbolines (Sulfonation).....	33
3.1.2.1.1. Reaction of the 6-sulfonamide 4-chloro- α -carboline with aromatic amines.....	34
3.1.2.2. <i>Friedel-Crafts</i> -Acylation Reaction (Acetylation).....	36
3.1.2.2.1. Reaction of the 6-acetyl 4-chloro- α -carboline with aromatic amines.....	36
3.1.2.2.2. Aldol Condensation of the 6-acetyl 4-chloro- α -carboline with DMF/DMA.....	37
3.1.2.3. Synthesis of the 6-bromo-4-chloro- α -carboline (Bromination).....	42

3.1.2.3.1.	Reaction of the 6-bromo-4-chloro- α -carboline with aromatic amines.....	43
3.1.2.3.2.	Reaction of the 6,8-dibromo-4-chloro- α -carboline with aromatic amines.....	44
3.1.2.3.3.	Cyanation of the 6-bromo-4-(<i>m</i> -hydroxyphenylamino)- α -carboline derivative 69	45
3.1.2.4.	Synthesis of the 6-nitro 4-chloro- α -carboline (Nitration).....	46
3.1.2.4.1.	Reaction of the 6-nitro 4-chloro- α -carboline with aromatic amines.....	48
3.1.2.4.1.1.	Reduction of some 6-nitro-4-phenylamino- α -carboline derivatives.....	49
3.1.2.4.2.	Reaction of the 6,8-dinitro 4-chloro- α -carboline with aromatic amines.....	49
3.1.2.4.2.1.	Reduction of some 6,8-dinitro-4-phenylamino- α -carboline derivatives.....	50
3.2.	Biology.....	51
3.2.1.	Protein Kinase Assay.....	51
3.2.1.1.	Results of the 4-phenylamino- α -carboline derivatives.....	53
3.2.1.2.	Results of the 6-sulfonamide-4-phenylamino- α -carboline derivatives.....	55
3.2.1.3.	Results of the 6-acetyl-4-phenylamino- α -carboline derivatives.....	56
3.2.1.4.	Results of the 6-heterocycle-4-phenylamino- α -carboline derivatives.....	56
3.2.1.5.	Results of the 6-bromo-4-phenylamino- α -carboline derivatives.....	58
3.2.1.6.	Results of the 6,8-dibromo-4-phenylamino- α -carboline derivatives.....	59
3.2.1.7.	Results of the 6-nitro- and 6-amino-4-phenylamino- α -carboline derivatives.....	60
3.2.1.8.	Results of the 6,8-dinitro-4-phenylamino- α -carboline derivatives.....	61
3.2.2.	Results of the NCI 60-cell-line-screenings.....	62
3.2.2.1.	Results of one-dose screenings.....	66
3.2.2.2.	Results of five-dose screenings.....	67
3.2.3.	Structure Activity Relationship (SAR).....	74
3.2.4.	Docking Studies.....	76
3.2.4.1.	Computational Methods.....	76
3.2.4.1.1.	Protein structure preparation.....	76
3.2.4.1.2.	Molecular Docking.....	78
3.2.4.2.	Results.....	78
3.2.4.2.1.	Examination of Brk and HER2 structural similarity.....	78
3.2.4.2.2.	Results' Discussion.....	79
3.2.4.3.	Figures.....	80
4.	SUMMARY & OUTLOOK.....	82
4.1.	Summary.....	82
4.2.	Zusammenfassung.....	91
4.3.	Outlook.....	100
5.	EXPERIMENTAL SECTION.....	101
5.1.	Synthetic part.....	101
5.1.1.	Materials and Methods.....	101
5.1.2.	Synthetic procedures.....	105

5.2. Biological part.....	185
5.2.1. Protein Kinase Assay.....	185
5.2.2. 60-cell-line-screenings.....	187
6. APPENDIX.....	189
7. CURRICULUM VITAE.....	222
8. BIBLIOGRAPHY.....	224

Abbreviations:

μM	Micromolar
AcOH	Acetic acid
aq	Aqueous
ATP	Adenosine triphosphate
br	broad (NMR)
Brk	Breast tumor kinase
Brk/PTK6	Breast tumor kinase/protein tyrosine kinase 6
conc.	Concentrated
dd	Double doublet
DMF	<i>N,N</i> -dimethyl formamide
DMF/DMA	<i>N,N</i> -dimethyl formamide dimethyl acetal
DMSO	Dimethyl sulfoxide
DTP	Developmental Therapeutics Programme
EGF	Epidermal growth factor
eq	Equivalent
ER	Estrogen receptor
ErbB2	Erythroblastic leukemia viral oncogene homolog 2
ERK5	Extracellular signal-regulated kinase 5
ESI	Electro-spray ionization
EtOAc (or) EE	Ethyl acetate
FDA	US Food and Drug Association
Fig.	Figure
GI₅₀	50% growth inhibition
h	hour (s)
H₂SO₄	Sulfuric acid
HCl	Hydrochloric acid
HER1	Human epidermal growth factor receptor 1
HER2	Human epidermal growth factor receptor 2
HER3	Human epidermal growth factor receptor 3
HER4	Human epidermal growth factor receptor 4
IC₅₀	Inhibition concentration 50%
IR	Infrared
IRS-4	Insulin receptor substrate-4
<i>J</i>	Coupling constant
KOH	Potassium hydroxide
LC₅₀	Lethal concentration 50%
m	multiplet (NMR)
M	Molar
MAPK	Mitogen-activated protein kinase
MeOH	Methanol
MG-MID	Mean graph midpoint
min	minute (s)
mmol	Millimole

MS	Mass spectroscopy
mTOR	mammalian target of rapamycin
n.a.	not active
NaOH	Sodium hydroxide
NCCN	The National Comprehensive Cancer Network
NCI	The National Cancer Institute
nM	Nanomolar
NMP	<i>N</i> -methyl-2-pyrrolidone
NMR	Nuclear magnetic resonance
NRTK	Non-receptor tyrosine kinase
PBMCs	Peripheral blood mononuclear cells
PI3K	Phosphatidylinositol 3-kinase
PPA	Poly phosphoric acid
PR	Progesterone receptor
PSF	Poly primidine tract-binding (PTB) protein associated splicing factor
PTK	Protein tyrosine kinase
q	quartet (NMR)
RT	Room temperature
RTK	Receptor tyrosine kinase
s	singlet (NMR)
Sam68	Src associated in mitosis, 68 kDa
SAR	Structure activity relationship
SH2	Src homology-2
SH3	Src homology-3
SLM-1	Sam68-like mammalian protein 1
SLM-2	Sam68-like mammalian protein 2
STAT3/5	Signal transducer and activator of transcription 3/5
t	triplet
TGFα	Transforming growth factor α
TGI	Total growth inhibition
THF	Tetrahydrofuran
TKI	Tyrosine kinase inhibitor
TLC	Thin layer chromatography
TNBC	Triple-negative breast cancer

List of Tables

Table 1:	Known Brk substrates.....	9
Table 2:	Derivatives 11-28 , which were produced from the reaction of 9 with Aromatic Amines.....	29
Table 3:	Assay parameters for the tested protein kinases.....	51
Table 4:	Substitutions of compounds 11-29	53
Table 5:	Results of 4-phenylamino- α -carboline derivatives 11-29	53
Table 6:	Substitution of sulfonamide derivatives.....	55
Table 7:	Results of 6-sulfonamide 4-phenylamino- α -carboline derivatives.....	55
Table 8:	Substitution of 48, 49 and 51	56
Table 9:	Results of 6-acetyl derivatives 48, 49 and 51	56
Table 10:	Substitutions of compounds 59, 60, 63 & 64	56
Table 11:	Results of 6-heterocyclic substituted derivatives 59, 60, 63 & 64	57
Table 12:	Substitution of derivatives 69-72	58
Table 13:	Results of 6-bromo derivatives 69-72	58
Table 14:	Substitutions of compounds 73-76	59
Table 15:	Results of 6,8-dibromo derivatives 73-76	59
Table 16:	Substitutions of derivatives 87-92	60
Table 17:	Results of compounds 87-92	60
Table 18:	Substitutions of compounds 93, 94 and 95	61
Table 19:	Results of 6,8-dinitro α -carboline derivatives 93, 94 and 95	61
Table 20:	Results of one-dose screenings.....	66
Table 21:	Results of the five-dose screenings for the 11 selected compounds.....	68
Table 22:	The most remarkable results of the test compounds on cell lines of breast cancer panel.....	69
Table 23:	Summarization of the Protein Kinase Assay results for all tested compounds.....	89

List of Figures

Figure 1:	Anatomy of Breast.....	2
Figure 2:	Breast Cancer subtypes.....	3
Figure 3:	Structure of Src and Brk Tyrosine Kinases.....	8
Figure 4:	Brk Signaling.....	11
Figure 5:	HER family of receptors.....	12
Figure 6:	ErbB2 (HER2) Structure.....	13
Figure 7:	HER2 Dimerization.....	16
Figure 8:	Dasatinib (Sprycel®).....	17
Figure 9:	Reported Brk/PTK6 Inhibitors.....	17
Figure 10:	The structure of human HER2/Herceptin complex.....	19
Figure 11:	Structure of Lapatinib (Tykerb®/Tyverb®).....	19
Figure 12:	The structure of HER2/Pertuzumab complex.....	20
Figure 13:	Structure of Neratinib.....	20
Figure 14:	Summarization of Available HER2-Inhibitors Mechanisms.....	21
Figure 15:	Preparation of 1-pyridine-2-ylbenzotriazol (3).....	26
Figure 16:	Mechanism of α -carboline base-unit preparation (7).....	27
Figure 17:	Preparation of 4-Chloro- α -carboline (9).....	27
Figure 18:	¹ H-NMR differences between 9 & 10	28
Figure 19:	Reaction of 9 with Aromatic Amines.....	29
Figure 20:	Reduction of 19 to produce 29	30
Figure 21:	Expected plan for preparation of 30 and 31 from 29	31
Figure 22:	Formation of 32 instead of the expected 30	31
Figure 23:	Synthesis of 6-Sulfomanide-4-Cl- α -carbolines 34-36	33
Figure 24:	Synthesis of 6-sulfonylmorpholino-4-anilino- α -carboline derivatives 37-40	34
Figure 25:	Synthesis of 6-sulfonylpiperazino-4-anilino- α -carboline derivatives 41-43	35
Figure 26:	Synthesis of 6-sulfonylthanolpiperazino-4-anilino- α -carboline derivatives 44-46	35
Figure 27:	<i>Friedel-Crafts</i> Acylation of 9	36
Figure 28:	Reaction of 47 with aromatic amines.....	36
Figure 29:	Reduction of 49 to prepare 51	37
Figure 30:	Aldol Condensation of 47 with DMF/DMA.....	38
Figure 31:	Condensation of 53 with hydrazine hydrate.....	38
Figure 32:	<i>N</i> -Benzylation of compound 47	39
Figure 33:	Condensation of 55 with DMF/DMA.....	39
Figure 34:	Condensation of 56 with Hydrazine hydrate.....	40
Figure 35:	<i>N</i> -Debenzylation of 57	40
Figure 36:	Reaction of 58 with aromatic amines.....	41
Figure 37:	Condensation of 56 with hydroxylamine HCl.....	41
Figure 38:	Synthesis of 6-isoxazolo-4-phenylamino- α -carbolines 63 and 64	42
Figure 39:	Possible subsequent reactions on 56	42
Figure 40:	Bromination of compound 9	43
Figure 41:	Reaction of 67 with aromatic amines.....	43
Figure 42:	Reaction of 68 with aromatic amines.....	44

Figure 43:	<i>Suzuki-Miyaura</i> coupling of compound 69	44
Figure 44:	<i>Rosenmund-von Braun</i> reaction of 69 (Cyanation).....	45
Figure 45:	Cycloaddition of 78 with sodium azide.....	46
Figure 46:	Hydrolysis of compound 78	46
Figure 47:	Possible subsequent pathways for the 6-amino substituted α -carboline derivatives.....	47
Figure 48:	Nitration reaction of compound 9	48
Figure 49:	Reaction of 81 with aromatic amines.....	48
Figure 50:	Reduction of 87 and 88	49
Figure 51:	Reaction of 86 with aromatic amines.....	49
Figure 52:	Reduction of 93 and 94	50
Figure 53:	Derivatives 11-29	53
Figure 54:	6-Sulfonamide derivatives 37-40 & 42-46	55
Figure 55:	Derivatives 48, 49 and 51	56
Figure 56:	Derivatives 59, 60, 63 and 64	56
Figure 57:	6-Bromo derivatives 69-72	58
Figure 58:	6,8-dibromo-derivatives 73-76	59
Figure 59:	Compounds 87-92	60
Figure 60:	6,8-dinitro derivatives 93-95	61
Figure 61:	Selected twenty compounds by NCI for one- dose 60-cell-line-screening...	63
Figure 62:	Results of one-dose-screenings for compound 69	64
Figure 63:	NCI five-dose screening obtained data for compound 69	72
Figure 64:	NCI five-dose screening obtained data for compound 37	73
Figure 65:	Structure-Activity Relationship Summary.....	74
Figure 66:	Suppl. Material: Sequence alignment of BRK and HER2.....	77
Figure 67:	GOLD docking solutions of compound 15 for Brk and HER2.....	80
Figure 68:	GOLD docking solutions of compound 69 for Brk and HER2.....	80
Figure 69:	GOLD docking solutions of compound 95 for Brk and HER2.....	81
Figure 70:	Desired synthetic final products.....	82
Figure 71:	Preparation of the desired starting structure 9 and subsequent reaction.....	83
Figure 72:	Substances of the 1 st series that showed a potent Brk and HER2 inhibitory activity.....	84
Figure 73:	6-Chlorosulfonation derivatives (37-46).....	84
Figure 74:	Route A and B in the preparation of enamine structure.....	85
Figure 75:	General pathway to prepare the 6-heteroaryl 4-phenylamino- α -carboline...	86
Figure 76:	Mono- and di-brominated α -carboline derivatives.....	86
Figure 77:	Compound 69 and its further derivatization.....	87
Figure 78:	Mono- and dinitration and further reduced amino-derivative.....	87
Figure 79:	Docking of the active <i>meta</i> -hydroxyaniline derivative (12) to Brk (active form). Hydrogen bonds are shown in magenta.....	189
Figure 80:	Results of One-dose screenings of compound 12	190
Figure 81:	Results of One-dose screenings of compound 13	191
Figure 82:	Results of One-dose screenings of compound 15	192
Figure 83:	Results of One-dose screenings of compound 20	193
Figure 84:	Results of One-dose screenings of compound 21	194
Figure 85:	Results of One-dose screenings of compound 24	195

Figure 86:	Results of One-dose screenings of compound 27	196
Figure 87:	Results of One-dose screenings of compound 28	197
Figure 88:	Results of One-dose screenings of compound 37	198
Figure 89:	Results of One-dose screenings of compound 38	199
Figure 90:	Results of One-dose screenings of compound 42	200
Figure 91:	Results of One-dose screenings of compound 43	201
Figure 92:	Results of One-dose screenings of compound 44	202
Figure 93:	Results of One-dose screenings of compound 45	203
Figure 94:	Results of One-dose screenings of compound 59	204
Figure 95:	Results of One-dose screenings of compound 60	205
Figure 96:	Results of One-dose screenings of compound 70	206
Figure 97:	Results of One-dose screenings of compound 71	207
Figure 98:	Results of One-dose screenings of compound 73	208
Figure 99:	Results of Five-dose screenings of compound 12 (first).....	209
Figure 100:	Results of Five-dose screenings of compound 12 (second).....	210
Figure 101:	Results of Five-dose screenings of compound 21	211
Figure 102:	Results of Five-dose screenings of compound 27	212
Figure 103:	Results of Five-dose screenings of compound 37 (second).....	213
Figure 104:	Results of Five-dose screenings of compound 69 (second).....	214
Figure 105:	Results of Five-dose screenings of compound 70	215
Figure 106:	Results of Five-dose screenings of compound 71	216
Figure 107:	Results of Five-dose screenings of compound 73	217
Figure 108:	Dose-response curves for the second Five-dose screenings of compound 37	218
Figure 109:	Superposition of all the growth curves for compound 37 (second screenings).....	219
Figure 110:	Dose-response curves for the second Five-dose screenings of compound 69	220
Figure 111:	Superposition of all the growth curves for compound 69 (second screenings).....	221

Glossary:

A

Angiogenesis

The induction of the growth of blood vessels from surrounding tissue into a tumor by a diffusible protein factor released by the tumor cells.

[Reprinted from *Dorland's Illustrated Medical Dictionary, 31st edition*. Copyright Elsevier (2007).]

Apoptosis

Also called programmed cell death, it is a signaling pathway that leads to cellular suicide in an organized manner. Several factors and receptors are specific to the apoptotic pathway. The net result is that cells shrink and develop blebs on their surface, and their DNA undergoes fragmentation.

[*J Clin Oncol.* 2005;23:7365-7374. Reprinted with permission from the American Society of Clinical Oncology.]

C

Conformation

The particular shape of an entity. In chemistry, the spatial arrangement of atoms in a molecule produced by rotations about single bonds, the property that distinguishes different conformers (conformational isomers) from each other.

[Reprinted from *Dorland's Illustrated Medical Dictionary, 31st edition*. Copyright Elsevier (2007).]

D

Differentiation

The act or process of acquiring completely individual characteristics, increasing morphologic or chemical heterogeneity.

[Adapted from *Dorland's Illustrated Medical Dictionary, 31st edition*. Copyright Elsevier (2007).]

Dimerization

The process through which 2 simpler molecular entities combine to form a unit, such as when 2 receptors join to form a receptor pair.

[Adapted from *Dorland's Illustrated Medical Dictionary, 31st edition*. Copyright Elsevier (2007).]

L

Ligand

A molecule that binds to another molecule; used especially to refer to a small molecule that binds specifically to a larger molecule, eg, an antigen binding to an antibody, a hormone or neurotransmitter binding to a receptor, or a substrate or allosteric effector binding to an enzyme.

[Reprinted from *Dorland's Illustrated Medical Dictionary, 31st edition*. Copyright Elsevier (2007).]

M

Mitogen-activated protein kinase (MAPK)

Any of a group of protein-serine/threonine kinases that when activated enter the cell nucleus and catalyze the phosphorylation of serine and threonine residues in transcription factors that regulate gene expression; it is the final member of a signal transduction cascade of 3 protein kinases that is initiated by stimulation of a wide variety of membrane receptors and is important in the regulation of cell growth and differentiation.

[Reprinted from *Dorland's Illustrated Medical Dictionary, 31st edition*. Copyright Elsevier (2007).]

Malignant

A tumor that becomes progressively worse. Characteristics include anaplasia, invasion, and metastasis.

[Adapted from *Dorland's Illustrated Medical Dictionary, 31st edition*. Copyright Elsevier (2007).]

Metastasis

The transfer of disease from one organ or part to another not directly connected with it.

[Reprinted from *Dorland's Illustrated Medical Dictionary, 31st edition*. Copyright Elsevier (2007).]

O

Oncogenic

Giving rise to tumors (either benign or malignant) or causing tumor formation.

[Reprinted from *Dorland's Illustrated Medical Dictionary, 31st edition*. Copyright Elsevier (2007).]

Overexpression

Excessive expression of a gene by producing too much of its effect or product.

[Reprinted from *Dorland's Illustrated Medical Dictionary, 31st edition*. Copyright Elsevier (2007).]

P

Phosphatidylinositol 3-kinase (PI3K)

A family of related enzymes that add a phosphate group to phosphatidylinositol 3 (PI3), which is a downstream signaling molecule involved in survival/proliferative pathways mediated by growth factors.

[*J Clin Oncol.* 2005;23:5406-5415. Reprinted with permission from the American Society of Clinical Oncology.]

Phosphorylation

The metabolic process of introducing a phosphate group into an organic molecule.

[Adapted from *J Clin Oncol.* 2005;23:5406-5415. Reprinted with permission from the American Society of Clinical Oncology.]

Proliferation

The reproduction or multiplication of similar forms, especially of cells and morbid cysts.

[Reprinted from *Dorland's Illustrated Medical Dictionary, 31st edition*. Copyright Elsevier (2007).]

T

Tumorigenesis

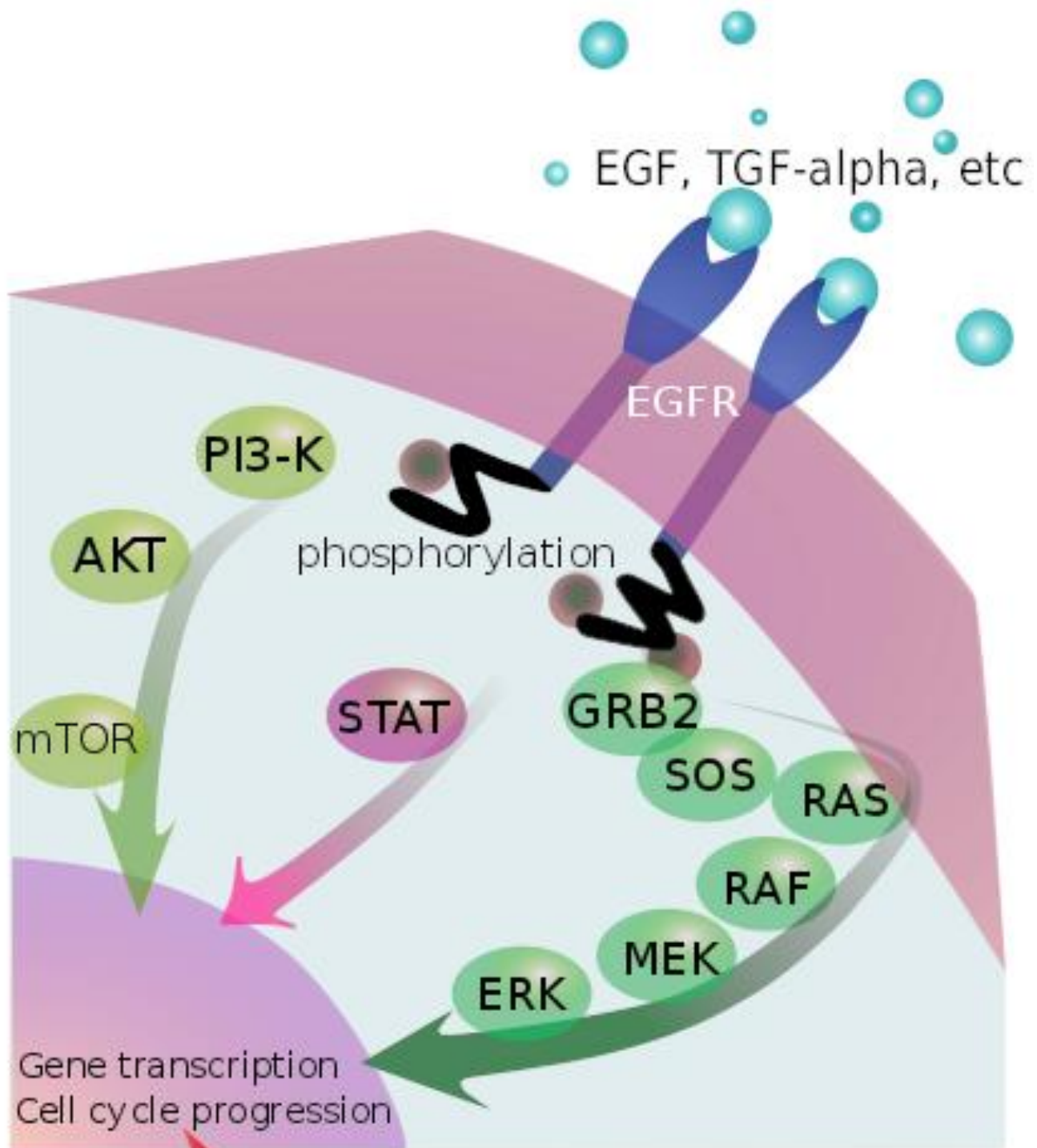
The production of tumors. Called also oncogenesis.

[Reprinted from *Dorland's Illustrated Medical Dictionary, 31st edition*. Copyright Elsevier (2007).]

Tyrosine kinase

Generic name for an enzyme that phosphorylates tyrosine molecules in proteins.

[*J Clin Oncol.* 2005;23:5406-5415. Reprinted with permission from the American Society of Clinical Oncology.]



Cell proliferation

Inhibition of apoptosis

Angiogenesis

Migration, Adhesion, Invasion

Breast Cancer:

Cancer is a disease of uncontrolled cell division. Under normal conditions, somatic cells divide, quiescent or die when appropriate but when a cell becomes cancerous, it divides uncontrollably and eventually forms a tumor. Often early cancers are in the form of benign, encapsulated lesions confined to a single tissue and lots of these rep-malignant lesions do not represent a danger to health. Some of these benign lesions go into a process called metastasis, which acquire the ability to invade the surrounding tissues and eventually spread to distant areas of the body. The maximum percentage of cancer death cases are related to these metastatic lesions. Cancer comprises a large number of diseases that can affect every tissue of the body and can afflict people at all ages. In 2008 cancer caused about 14% of all human death.¹

Breast cancer is one of the most common cancers with more than 1,300,000 cases and 450,000 deaths each year worldwide and accounts about 20% of all cancers in Western Europe and the USA. Approximately, 5-10% of breast cancer cases showed clear heritage through families where mutations in BRCA1 and BRCA2 genes represent the most frequent disease risk. Clinically, this heterogeneous disease is classified into three essential therapeutic groups. Estrogen receptor (ER) positive group which is the most various with several genomic tests to assist in predicting outcomes for ER-positive patients receiving endocrine therapy.^{1,2} The second is HER2 (also called ErbB2) amplified group which is of a great clinical success because of successful therapeutic targeting of HER2, which has assisted to characterize other DNA copy number deviations.^{3,4} Finally, the triple-negative breast cancers (TNBCs, lacking expression of ER, progesterone receptor (PR) and HER2), also known as basal-like breast cancers⁵, are a group with only chemotherapy options, and have a high prevalence in patients with germline BRCA1 mutations^{6,7} or of African origin.⁸

Female Breast Cancer:

Background:

Breast cancer is the most worldwide commonly diagnosed life-threatening cancer in women and the leading cause of cancer death of women.

Introduction

Early breast carcinomas may be asymptomatic; discomfort or pain is not usually a symptom of breast cancer. Breast cancer is frequently first distinguished as an abnormality on a mammogram before it is felt by the patient or healthcare provider. The general approach to evaluate breast cancer has become formalized as triple assessment: clinical examination, imaging (typically mammography and/or ultrasonography) and needle biopsy.

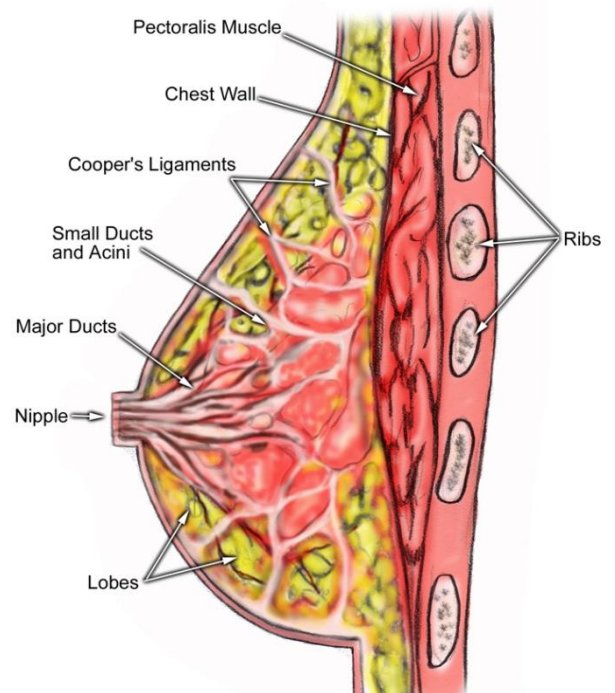
Increased public consciousness and enhanced screening have led to earlier diagnosis, at stages amenable to complete surgical resection and medicinal therapies. Consequently, survival rates for breast cancer patients have improved (particularly in younger women).

The primary treatment for breast cancer is considered to be *via* surgery. Mostly, early-stage breast cancer cases are cured with surgery alone.

Adjuvant therapy of breast cancer is considered to treat micrometastatic disease, or breast cancer cells that have escaped the breast and regional lymph nodes but which have not yet had a conventional particular metastasis. Adjuvant treatment has been estimated, depending on the model of risk reduction, to be responsible for 35-72% of the reduction in death rate. Breast cancer research has led to remarkable development in our understanding of the disease in the last two decades, resulting in more effective treatment with less toxicity.⁹

Anatomy:

The breasts of an adult woman are milk-producing glands located on the front of the chest wall. They lie on the pectoralis muscle and are supported by and attached to the front of the chest wall on each side of the sternum by ligaments. Each breast has 15-20 lobes fixed in a circular form. The fat layer that covers the lobes is the responsible for the breast size and shape. Each lobe includes many lobules which at their end are glands where milk is produced in response to hormones.⁹ (Fig. 1)



<http://emedicine.medscape.com/article/1947145-overview>

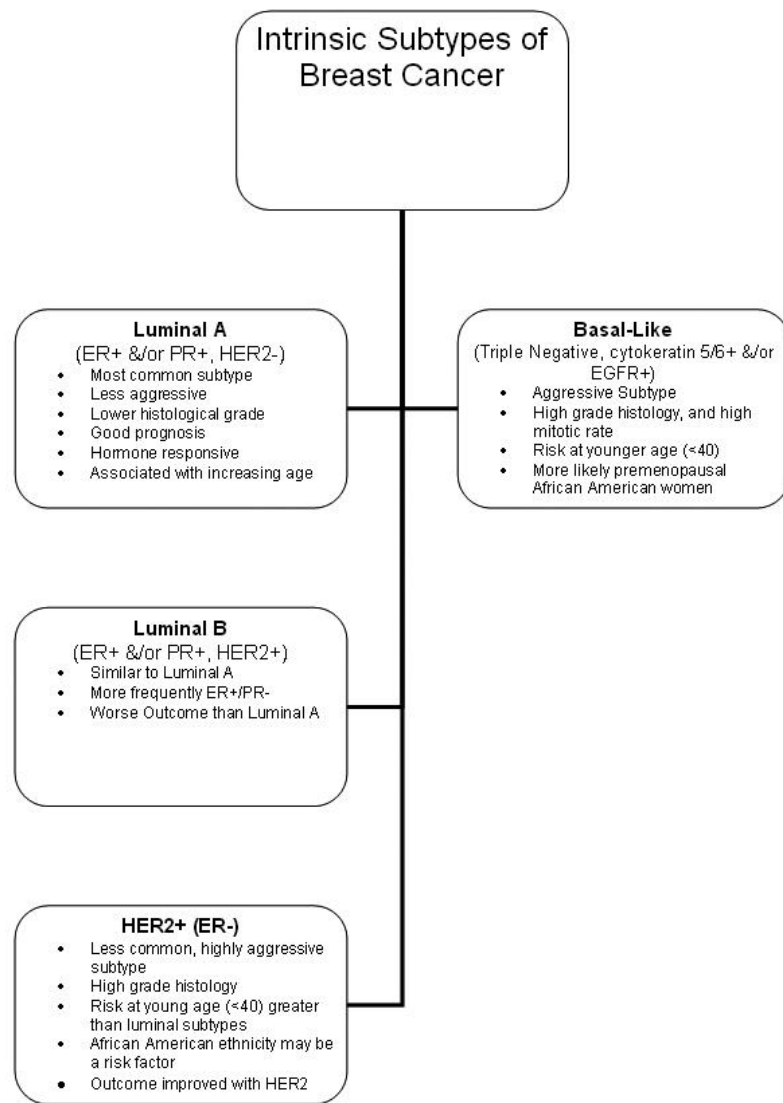
Fig.1. Anatomy of Breast

Pathophysiology:

The current understanding of breast tumorigenesis is that invasive cancers arise through a sequence of molecular alterations at the cellular level, causing the outgrowth and spread of breast epithelial cells with immortal countenance and uncontrolled growth.

Genomic profiling has confirmed the presence of distinct breast tumor subtypes with numerous clinical behaviors (e.g., 4 subclasses: luminal A, luminal B, basal and human epidermal growth factor receptor 2 [HER2]-positive). These subtypes generally align closely with the presence or absence of hormone receptor and mammary epithelial cell type (luminal or basal). Cancer Genome Atlas Network showed that the four main breast tumor subtypes are caused by different subsets of genetic and epigenetic deviations.¹⁰

Figure 2 summarizes the current general understanding of breast tumor subtypes, predominance, and the major associated molecular modifications.



<http://emedicine.medscape.com/article/1947145-overview>

Fig.2. Breast Cancer subtypes

Etiology:

Epidemiologic studies have recognized many risk factors that increase the chance of a woman to develop breast cancer. The common denominator for lots of these risk factors is their effect on the level and duration of exposure to endogenous estrogen.⁹

Risk Factors for Breast Cancer:

- Advanced age
- Family history
- Personal history
- Reproductive history
 - a) Early age at menarche (< 12 years)
 - b) Late age of menopause
 - c) Late age of first term pregnancy (>30 years)/nulliparity
- Use of combined estrogen/progesterone HRT (hormone replacement therapy)
- Current or recent use of oral contraceptives
- Lifestyle factors
 - a) Adult weight gain
 - b) Sedentary lifestyle
 - c) Alcohol consumption

Signs and symptoms

Early breast cancers may be asymptomatic, and pain and discomfort are usually not present. If a lump is detected, the following signs may indicate the possibility of breast cancer presence:

- Change in breast size or shape
- Skin dimpling or skin changes
- Recent nipple inversion or skin change, or nipple abnormalities
- Single-duct discharge, particularly if blood-stained
- Axillary lump

Diagnosis

Breast cancer is often first discovered as an abnormality on a mammogram before it is felt by the patient or health care provider.

Evaluation of breast cancer involves the following:

- Clinical examination
- Imaging
- Needle biopsy

Physical examination

The following physical conditions should elevate concern:

- Lump or contour change
- Skin tethering
- Nipple inversion
- Dilated veins
- Ulceration
- Paget disease
- Edema or peau d'orange

If a palpable lump is found and contains any of the following symptoms, breast cancer may exist:

- Hardness
- Irregularity
- Focal nodularity
- Fixation to skin or muscle

Screening

Early detection has the main role in preventing breast cancer. Screening modalities include the following:

- Breast self-examination
- Clinical breast examination
- Mammography
- Ultrasonography
- Magnetic resonance imaging

Medication Summary:

Adjuvant treatment for breast cancer includes radiation therapy and different biologic and chemotherapeutic agents. Adjuvant treatment of breast cancer is proposed to treat micrometastatic disease, or breast cancer cells that have escaped the breast and regional lymph nodes but which have not yet established a particular metastasis. Treatment is focused on decreasing the risk of recurrence in the future, thus reducing breast cancer-related morbidity and mortality.

As breast cancer adjuvant therapies, the 2011 NCCN (The National Comprehensive Cancer Network) guidelines involve recommendations for the use of two new drugs, denosumab (**Xgeva**®) and eribulin (**Halaven**®), both of which had FDA approval in 2010. These 2011 guidelines support the use of biologic denosumab for the prevention of skeletal episodes. When compared with zoledronic acid (**Zometa**®), denosumab, which is injected subcutaneously, delayed the onset of skeletal episodes by 8% and the time to multiple skeletal episodes by 23%. In addition, toxicities such as hypercalcemia and renal failure were less common. The guidelines also recommend eribulin, an antimicrotubular drug, as the "preferred single agent" in chemotherapy treatment for the advanced cases. Trials have shown considerable improvement in survival when compared with patients receiving "treatment by physician's choice."

In June 2011, FDA council recommended that bevacizumab (**Avastin**®) no longer be used to treat breast cancer, and in November they officially canceled its approval because it has been associated with several other serious and potentially life-threatening side effects including the risk of stroke, wound healing complications, organ damage or failure as well as the development of a neurological condition called reversible posterior leukoencephalopathy syndrome (RPLS), characterized by high blood pressure, headaches, confusion, seizures and vision loss from swelling of the brain.¹¹

Male Breast Cancer:

Male breast cancer is analogous to breast cancer in females in its etiology, family history, diagnosis and treatment. In nearly 30% of breast cancer cases in men, the family history is positive for the disease.⁹

Therapeutic Targets in Breast Cancer:

Protein Tyrosine Kinases

Protein tyrosine kinase (PTK) activity is raised in breast cancer¹² and is associated with poor prognosis.¹³ PTKs are responsible for mediating numerous critical biological functions, such as cellular differentiation, growth, metabolism and apoptosis.¹⁴⁻¹⁷ There are two types of PTKs: transmembrane receptor tyrosine kinases (RTKs) and soluble cytoplasmic non-receptor tyrosine kinases (NRTKs).

RTKs activate intracellular signaling events *via* extracellular ligand binding. Receptor dimerization occurs when a similar growth factor binds to this receptor's extracellular ligand binding domain. This dimerization consecutively activates the kinase activity of the receptor, followed by transphosphorylation of the intracellular domains of the dimerized receptors. The phosphotyrosine residues on the receptors are now recognized by the Src homology 2 (SH2) domains of adaptor or scaffold proteins that also contain Src homology 3 (SH3) domains. These SH3 domains bind to proline-rich regions on downstream effector proteins which propagate phosphorylation mediated signaling events in the cytoplasm. Thus, these kinases either activate or inhibit downstream effector proteins upon phosphorylation. After ligand-induced activation, signal termination can be obtained by the activity of tyrosine phosphatases directed towards the activated RTK or effectors, or by receptor endocytosis and degradation.¹⁶

Soluble NRTKs are activated by the same manner like the RTKs, however they do not bind ligand, and are located in the cellular cytoplasm, nucleus or near the cell membrane. Each non-receptor tyrosine kinase consists of one catalytic kinase domain and two non-catalytic domains, an enzymatic kinase domain (SH1), a proline-rich binding domain (SH3) and a phosphotyrosine binding domain (SH2).¹⁶

The physiological effect of PTK activation is dependent upon the interaction between protein kinases and protein phosphatases. Phosphorylation is the mechanism by which oncogenes deregulate signaling pathways and induce transformation and is essential for maintaining cellular homeostasis. Consequently, PTKs are considered as important targets for normal biology and cancer related research.

Breast Tumor Kinase/Protein Tyrosine Kinase 6

Breast tumor kinase/protein tyrosine kinase 6 (Brk/PTK6) is a cytoplasmic non-receptor PTK that is significantly overexpressed in a majority of breast tumors and whose cDNA was originally cloned in a screen for tyrosine kinases expressed in a metastatic breast tumor. Normal mammary tissues or benign lesions express low or undetectable levels of Brk.¹⁸ In addition to human breast tumors, Brk is also expressed in colon, prostate, melanoma, lymphoma and ovarian cancer cell lines.¹⁹⁻²³

Brk is a 48 kDa protein and is a member of a novel family of soluble PTK. Brk's kinase domain shares approximately 56% homology with the kinase domain

of c-Src.²⁴ Similar to c-Src, Brk contains N-terminal SH2 and SH3 domains with a soluble tyrosine kinase domain, and is capable of autophosphorylation.²⁴⁻²⁶ (Fig. 3)

Although Brk and Src kinases have a homology percentage in their domains, they are considered as distant relatives. Differing from Src-family kinases, Brk lacks the Src-characteristic N-terminal myristoylation consensus sequences necessary for fatty acid acylation and membrane association.^{26,27} (Fig. 3)

Recent studies report that Brk SH2 domain is also structurally different from most SH2 domains due to its weak affinity towards the predictable autoinhibitory phosphotyrosine of Brk (Y447). Consequently, and as a result of all these previously mentioned differences between Brk and Src, it has been suggested that Brk regulation is dissimilar to other Src-family tyrosine kinases, and/or that Brk may have some alternative signaling pathways.²⁸

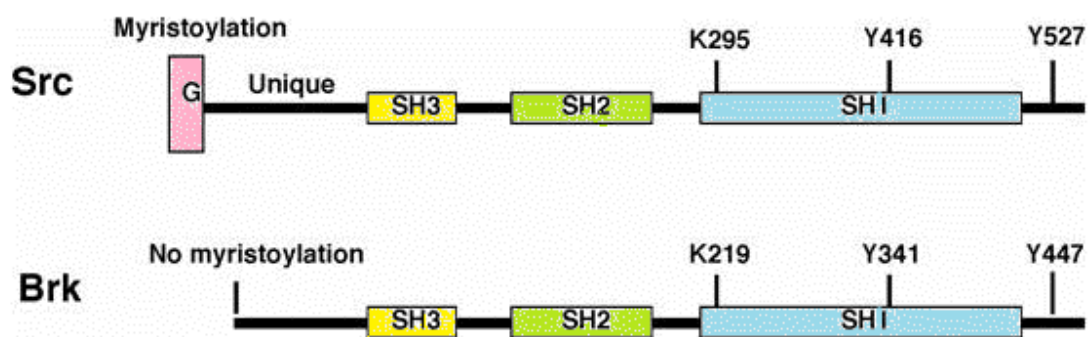


Fig.3. Structure of Src and Brk Tyrosine Kinases:²⁸

Src and Brk tyrosine kinases share 44% amino acid identity. Both Src and Brk proteins hold SH3 and SH2 domains that regulate protein-protein interactions as well as a conserved catalytic SH1 domain. The tyrosine at 527 in Src and at 447 in Brk controls kinase activity. Phosphorylation on these tyrosine residues results in the intramolecular formation of an inactive conformation connecting both SH2 and SH3 domains. The lysine at 295 in Src and at 219 in Brk correlates with the ATP-binding site and its mutation results in a dominant-negative protein. Tyrosines 416 in Src and 341 in Brk reside in the activation loop and are autophosphorylated resulting in improved kinase activity. In contrast to Src, Brk lacks an aminoterminal consensus myristoylation sequence.

The *brk* gene is located on chromosome 20q13.3-13.4 and consists of 8 exons, which display distinct precincts relative to other family members, suggesting a functional divergence. Recently, a substantial co-amplification of the region of chromosome 20, where the *brk* gene (Chr 20q13.3) is localized, and chromosome 17q21-22, the position of the *erbB2* gene, had been reported. The *brk* gene was found amplified in about 28% of tested samples.^{29,30}

Brk Signaling Substrates, Protein Interactions and Biology

One key to understand the function of Brk in normal tissue homeostasis and malignancy is to recognize its endogenous physiological substrates. So far there are three categories of potential Brk substrates and interacting proteins have been identified (Table 1).

Brk Substrate	Function	Signaling Pathway	Biology	Phosphorylation sites
Sam68	RNA-binding protein	EGF	Cell cycle	Y345, Y440, Y434
SLM-1/SLM-2	RNA-binding protein			
PSF	RNA-binding protein	EGF	Cell cycle	C-terminus
STAT3	Transcription factor		Cell cycle	Y705
STAT5a/b	Transcription factor		Cell cycle	Y694/Y699
Paxillin	Adapter protein	EGF	Migration	Y31, Y118
P190RhoGAP	GTPase activating protein		Migration	Y1109
KAP3A	Subunit of kinesin-2 complex		Migration	C-terminus
BKS/STAP-2	Adapter protein	STAT3 activation		Y250
Akt	Serine/threonine kinase	EGF	Intestinal epithelial cell cycle & differentiation	
IRS-4	Adapter protein	IGF		

Table 1: Known Brk substrates. The left hand column lists all proteins that have been identified as potential Brk substrates. The column labeled ‘Function’ refers to the intracellular function of the Brk substrate. ‘Signaling pathway’ refers to the signaling pathway where the substrate and Brk have been shown to play a role in, while ‘Biology’ refers the biological significance of Brk-induced phosphorylation of the substrate. The tyrosine residues found to be phosphorylated by Brk are indicated in the column labeled ‘Phosphorylation sites’ in the right hand column.

RNA-binding proteins: Sam68 (Src associated in mitosis, 68 kDa) which was the first identified and the most extensively studied substrate for Brk

phosphorylation *in vivo*,³¹ SLM-1 (Sam68-like mammalian protein 1) and SLM-2³², and PSF (Polyprimidine Tract-binding (PTB) protein-associated Splicing Factor).³³(Fig. 4. [a])

The transcription factors: the well-known signal transducer and activator of transcription (STAT) 3 and STAT5b are the most frequent factors which are considered as direct substrates of Brk, *in vitro*,^{34,35} and critical regulators of mammary function.^{36,37} (Fig. 4. [b])

Finally, a variety of signaling molecules: several studies have been reported investigating the effect of Brk in tyrosine phosphorylation of numerous substrates. Brk-induced phosphorylation of Paxillin at Y31 and Y118 leads to enhanced Rac activation.³⁸ Brk was shown to phosphorylate Y1109 on p190RhoGAP-A which increases its association with p120RasGAP, leading to Rho inhibition and Ras activation.^{39,40} Recently, Brk has been reported to directly phosphorylate BKS/ATAP-2,^{41,42} KAP3A,⁴³ Akt/pkB⁴⁴ and beta-catenin.⁴⁵ (Fig. 4. [c])

An immunoprecipitation study has shown some proteins that can associate with Brk including the RTKs EGFR/ErbB1, ErbB2, ErbB3,⁴⁶⁻⁴⁸ IRS-4 (Insulin receptor substrate-4 protein)⁴⁹ and ERK5 (Extracellular signal-regulated kinase-5)/MAPK.⁵⁰

Brk, similar to other protein kinases, mediates a range of cellular processes related to the progression or maintenance of malignancy. It has been reported that Brk expression sensitizes mammary epithelial cells to the mitogenic effect of EGF (Epidermal growth factor),⁴⁶ and increases PI3K (Phosphatidylinositol 3-kinase) signaling through enhanced ErbB3 phosphorylation and consequently enhancing the strength of potentially oncogenic signaling events.⁴⁷

Recently, some studies revealed that Brk-mediated Rac activation and phosphorylation of paxillin as a result of EGF effect and Brk-mediated p38 MAPK activity as a result of heregulin action play an important role in regulating cellular migration and invasion.^{51,52}

In non-transformed mammary epithelial cells, Brk enhances anchorage-independent growth when expressed⁴⁶ and prevents detachment induced-autophagic cell death in cancer cells,⁵³ accordingly suggesting a potential mechanism for Brk-positive cancer cells to survive the dissemination phase of

metastasis. Brk also supports proliferative phosphorylation of Erk5 and p38 MAPK, as well as cyclin D1 expression as a response to heregulin.⁵²

Brk in non-transformed epithelial cells *in vivo* appears to play an inhibitory role in regards to cell growth. Studies with PTK6 knock-out mice demonstrated Brk expression downregulates Akt mediated cellular proliferation in the intestinal crypts⁵⁴ *via* inhibiting beta-catenin mediated transcription.⁴⁵

Despite the fact that Brk expression has been shown to induce tyrosine phosphorylation of each of these previously mentioned proteins, not all of these proteins have been shown to be real Brk substrates *in vitro*.³⁰

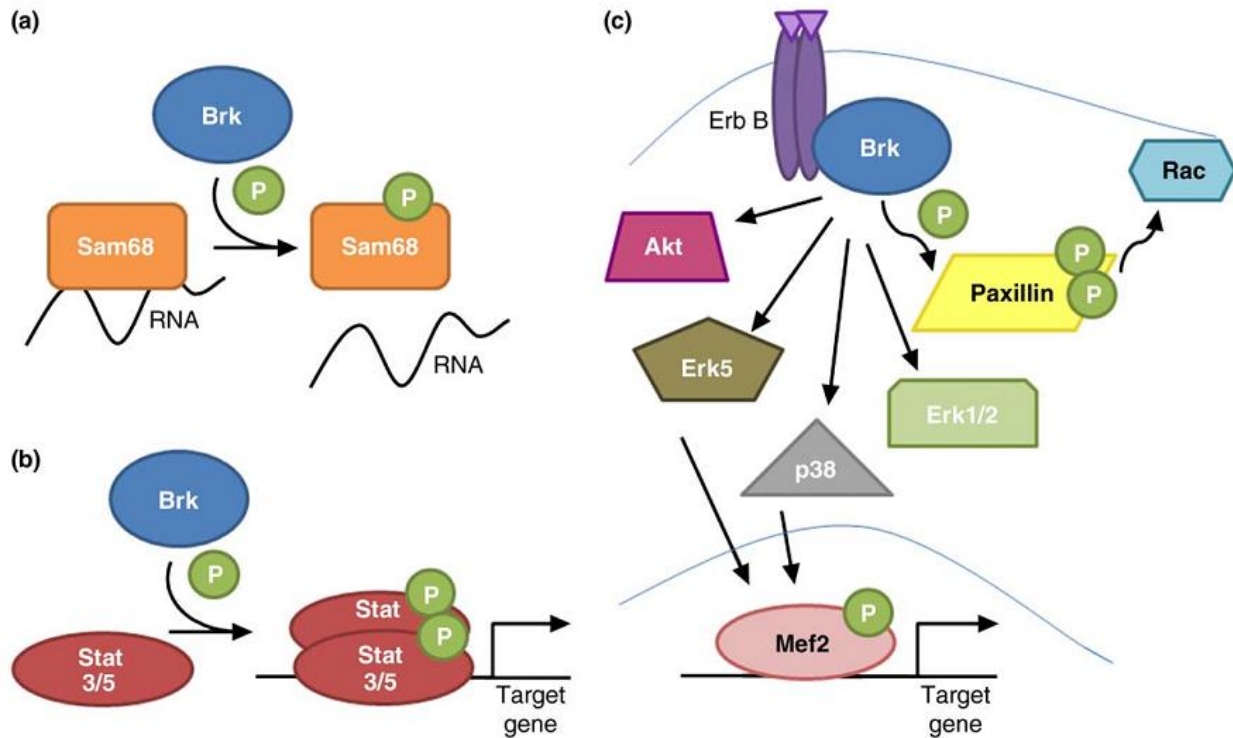
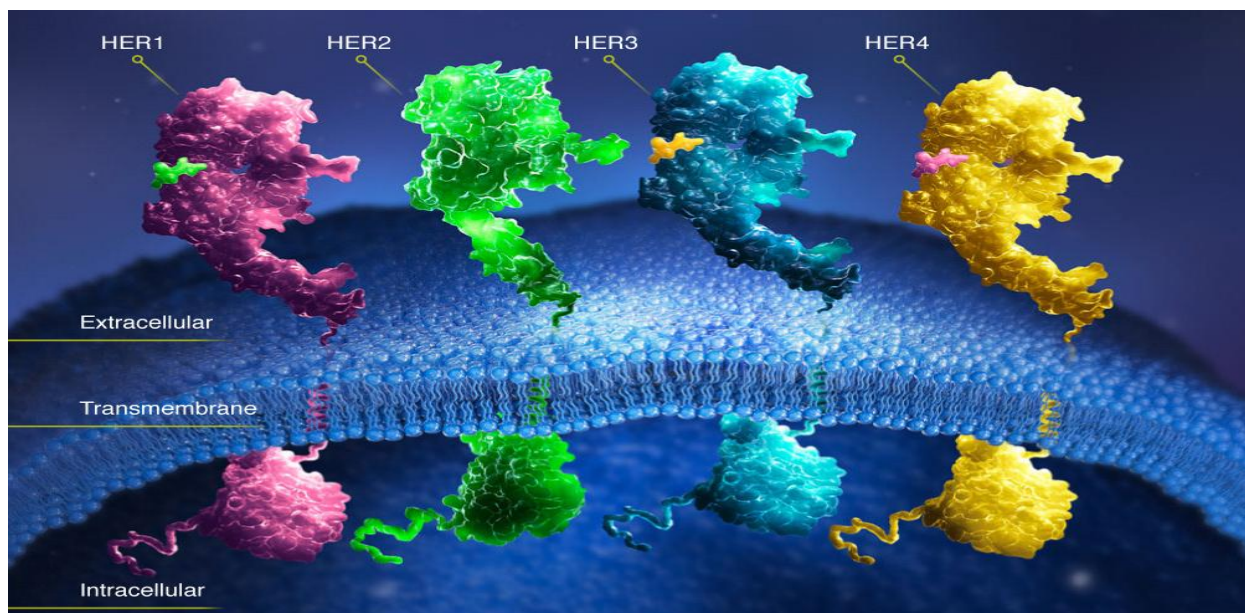


Fig.4. Brk Signaling:³⁰ Brk acts as a mediator for multiple signaling pathways. (a) Tyrosine phosphorylation by Brk decreases Sam68 (as well as SLM-1 and SLM-2, not shown) RNA-binding activity. (b) Brk phosphorylation enhances Stat3 and Stat5 transcriptional activity.(c) Brk signaling downstream of ErbB receptors activates multiple signaling pathways which can lead to changes in the gene programs expressed by cells.

Epidermal Growth Factor Receptor (EGFR) family

Epidermal growth factor receptors, also known as ErbBs, and their ligands subsist in all higher eukaryotes, involving *C. elegans*⁵⁵ and *Drosophila*⁵⁶, and have been associated in a number of cancers due to deregulation or mutation of the ErbB genes.⁵⁷ The mammalian ErbB family consists of four receptors with a homology of 40–45% to each other which arises from some gene duplications occurred early in the vertebrate progression.⁵⁸ ErbB family members include ErbB1 (EGFR, also known as HER1), ErbB2 (HER2), ErbB3 (HER3) and ErbB4 (HER4). (Fig. 5) These cell membranous receptors consist of four extracellular ligand binding domains, a transmembrane domain and C-terminal intracellular tail containing a number of tyrosine phosphorylation sites. Several ligands have been found that bind to HER1, HER3 and HER4 including, among at least 12 ligands, transforming growth factor α (TGF- α), epidermal growth factor (EGF) and heregulin. No known natural ligand exists for HER2, but there is evidence that recommends that HER2 is the preferred dimerization partner for activation of the other ErbB receptors.⁵⁹ All these receptors, except HER3, contain an intracellular tyrosine kinase domain, whereas the intracellular part of HER3 contains multiple binding sites for the phosphatidylinositol 3-kinase (PI3K) and is considered as a potent activator in combination with HER1 and HER2 of this signal pathway. Key proteins involved in the signal transduction cascade containing mitogen-activated protein kinases (MAPK), PI3K and signal transducer and activator of transcriptions (STATs). These cascades eventually lead to cellular changes in growth, differentiation, migration, apoptosis and angiogenesis.^{60,61}



<http://www.biooncology.com/research-education/hdis/her2-dimerization/index.html>

Fig. 5. HER family of receptors.

Human Epidermal Growth Factor Receptor (HER)-2

Patients diagnosed with human epidermal growth factor receptor 2-positive (HER2+) breast cancer have a more aggressive disease with an increased risk of metastases and generally a shorter survival.^{62,63} Overall, in approximately 20-30 % cases of breast cancers, there is amplification of HER2 gene and/or overexpression of the associated protein product.⁶⁴

HER2, similar to all ErbB family members, contains extra-cellular, transmembrane, and intracellular domains. The intracellular domain is responsible for phosphorylation and recruitment of proteins while the extracellular domain, which consists of 4 sub-domains (I, II, III, IV), is where signal transduction is initiated through dimerization with other HER receptors.⁶⁵ Recent researchers try to identify the individual roles of each sub-domain in receptor activation and signaling. As shown in figure 6, it has been reported that, unlike other receptors in the HER family, sub-domain I (green) of HER2 is constantly linked to sub-domain III (violet). Permanent interaction between these two sub-domains keeps HER2 in an open conformation, whereas the extracellular sub-domain II (blue) is the dimerization domain which enables HER2 to bind with other receptors in the HER family to initiate downstream signaling.⁶⁶ While the exact role of sub-domain IV (gray) in HER functioning is still unknown, it is believed to stabilize and lock the receptor in an open conformation or may play a role in the HER2 signaling, but sub-domain IV is not directly involved in the dimerization.⁶⁵

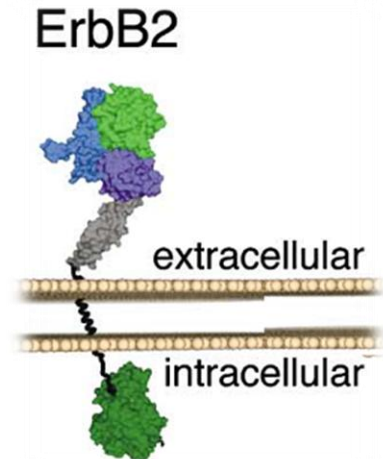


Fig. 6. ErbB2 (HER2) Structure

HER receptors, like all the erythroblastic leukemia viral oncogene homolog (ErbB) family of tyrosine kinases, are enzymatically inactive in the absence of EGF, requiring EGF binding to the extracellular domain in order to dimerize and undergo cross-phosphorylation and activation.⁶⁷ HER-mediated signaling plays an important role in the regulation of cell growth, differentiation, metabolism, and migration.⁶⁸ In humans, the abnormal activation or overexpression of these RTK signals often causes cellular developmental abnormalities or cancer.⁶⁸ The human epidermal growth factor-2 receptor (HER2) as a specific EGF family tyrosine kinase receptor, unlike other EGFR family, is unique in the fact that it does not have to undergo ligand binding, such as with EGF, in order to dimerize and undergo activation. This unique characteristic makes HER-2 positive cancers much more aggressive.

Owing to this fundamental role of epidermal growth factors (EGFs) in cell proliferation and differentiation in developing adult tissue, overexpression or inappropriate activation of EGF proteins, such as human epidermal growth factor receptor 2, HER2, is linked to the development and severity of many cancers.

HER2 dimerization: a key component of oncogenic signaling in HER2+ breast cancer

The 4 receptor tyrosine kinases of HER family must pair, or dimerize, to activate downstream signaling.⁶⁹

Preclinical studies indicate that HER dimerization, or receptor pairing, is a critical step in HER activation.⁶⁹ While the receptors of the HER family are important mediators of normal cell growth and development, HER activation has also been implicated in cancer development and progression.⁷⁰

In normal cell growth, dimerization is an important requirement of HER functionality and signaling, and it occurs between two identical receptors, known as homodimerization, or two different receptors, known as heterodimerization.⁶⁹

In HER2-positive breast cancer, HER2 overexpression is associated with excessive dimerization that plays a role in cell survival, cell proliferation and tumorigenesis.⁷¹

Each HER family receptor possesses 3 domains: the extracellular, transmembrane, and intracellular domains, all of which are essential for receptor activation and intracellular signaling. In order to activate downstream signaling, receptors must dimerize using the dimerization sub-domain, known as sub-domain II, located on the extracellular domain of the receptor.⁷⁰

As it was discussed above, EGFR (HER1), HER3, and HER4 naturally exist in a “closed” conformation. In the closed position, the dimerization sub-domain (sub-domain II) is concealed or inaccessible, and as a result, the receptor is not able to form dimers. Ligand binding to these receptors, such as EGF, leads to a conformational change, exposing sub-domain II and enabling the receptor to dimerize and initiate downstream signaling. HER2 is the only receptor in the HER family that exists in a continuously open conformation ready to dimerize without the need for ligand binding.^{66,72}

When HER family members dimerize, the intracellular domains of the two paired receptors are phosphorylated, resulting in the activation of cell proliferation and cell survival pathways.⁷³

Although HER2 has the ability to dimerize with any HER family member, recent preclinical studies suggest that HER2:HER3 is the most potent oncogenic HER dimer and may play a fundamental role in disease progression.⁷⁴

In normal cells, HER2 activates the MAPK pathway, whereas HER3 is the only receptor that can directly activate the PI3K (phosphatidylinositol 3-kinase) pathway. Consequently, the activation of this dimer results in the activation of both the cell proliferation (MAPK pathway) and cell survival (PI3K pathway), ultimately resulting in cell growth.^{75,76}

In tumor cells, an overactive dimerization of HER2 and HER3 leads to increased tumorigenesis due to abnormal MAPK signaling which results in the activation of the tumor cell proliferation pathway.⁷³ Moreover the increased HER3-mediated PI3K signaling results in the activation of cell survival mechanisms and resistance to apoptosis.⁷⁶

MAPK signaling

- HER2-mediated MAPK signaling is responsible for a number of key cellular functions, including cell proliferation, migration, differentiation and angiogenesis.^{77,78}
- Following HER2 activation, adapter molecules are recruited to the membrane to initiate a signaling cascade which causes phosphorylation and activation of MAPK and, ultimately, increased cell proliferation.⁷⁸

PI3K signaling

- Activation of PI3K is mediated by HER3 and its principal role is to recruit Akt and mTOR to regulate cell survival signaling.⁷⁹
- Continued PI3K signaling leads to continued tumor cell survival and the possibility for disease progression.⁷³

Preclinical studies show that this dimerization may be responsible for continued tumor cell survival signaling, even when HER2-mediated signaling is inhibited.⁸⁰ Additionally, the HER2:HER3 dimer may be crucial for the aggressive tumor growth seen in HER2+ breast cancer.⁸¹

In HER2+ breast cancer disease, the overexpression of HER2 is associated with overactive HER2 dimerization, abnormal signaling, and ultimately tumor growth.⁷¹

Dimerization, ligand binding and intracellular signaling mechanism associated to HER2 are summarized in figure 7.

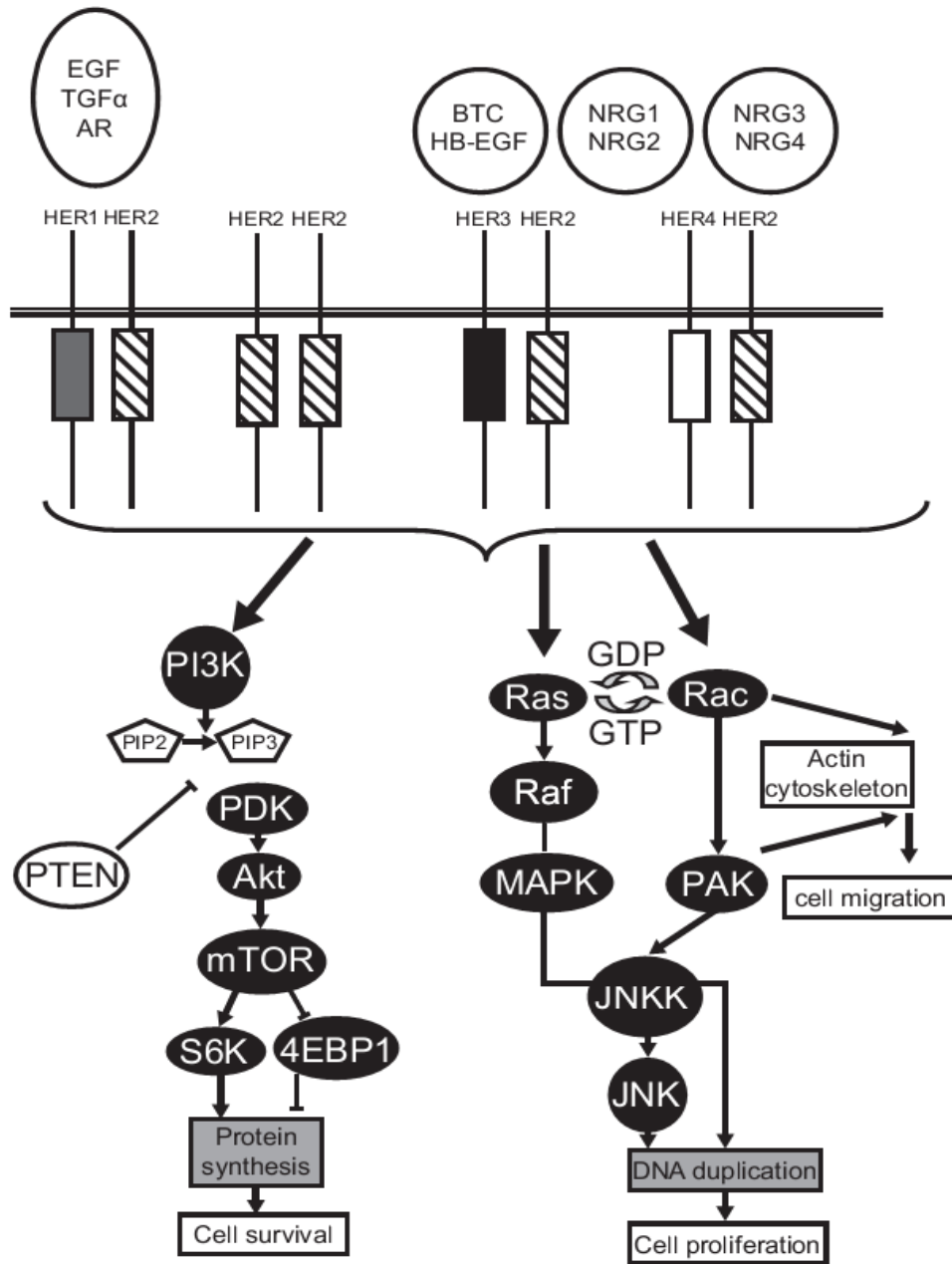


Fig. 7. HER2 Dimerization:⁸² Human epidermal growth factor receptor 2 (HER2) signal transduction pathways. Homodimerization and heterodimerization of HER2 leads to TK activation and downstream signaling via the PI3K/Akt/mTOR pathway and the Ras/Raf/MAPK pathway to stimulate processes involved in cell survival and proliferation.

Inhibitors of Breast Cancer-Relevant Kinases

BRK/PTK6 Inhibitors

Although there are no specific Brk/PTK6 inhibitors have been reported to date, specific inhibition of this kinase may provide a potentially novel approach to inhibit the progression of selected tumors, sensitize the response of the tumor cells to other chemotherapeutics and prevent/inhibit metastasis of cancer with enhanced therapeutic windows.

Dasatinib, previously known as **BMS-354825** (Fig. 8), is a cancer drug produced by Bristol-Myers Squibb and commercialized under the trade name **Sprycel**[®]. Dasatinib is an oral multi- BCR/ABL and Src family tyrosine kinase inhibitor approved for use in patients with chronic myelogenous leukemia (CML).⁸³ It has been reported as a potent Brk/PTK6 inhibitor with an IC_{50} of 9 nM.⁸⁴

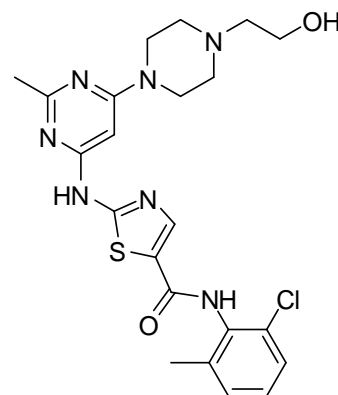
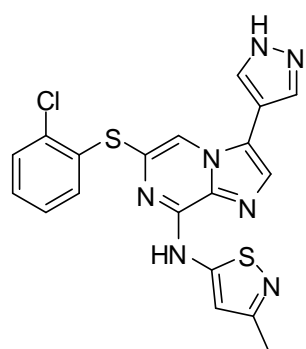
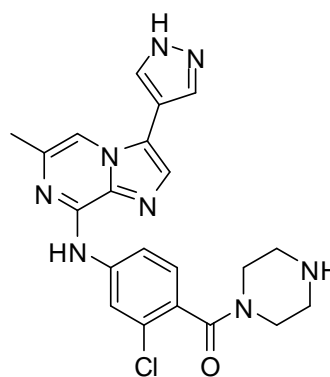


Fig. 8. Dasatinib (Sprycel[®])

Novel imidazo[1,2- α]pyrazin-8-amines have been recently reported as Brk/PTK6 inhibitors with different IC_{50} values, as shown in figure 9.⁸³



$IC_{50} = 500$ nM



$IC_{50} = 7$ nM

Fig. 9. Reported Brk/PTK6 Inhibitors

HER2 Inhibitors

Advances in translational science have led to the development of a growing range of therapies which targeting HER2. To date, only two drugs have been approved by the US Food and Drug Administration (FDA) and the European Medicines Agency: the monoclonal antibody, trastuzumab, and the small molecule tyrosine kinase inhibitor (TKI), lapatinib. Despite these advances, some tumors eventually develop resistance to these agents, leading to shortened survival for patients. Novel anti-HER2 agents, some of which are in advanced stages of clinical development, have been recently discovered and may be approved in the near future.⁶²

Trastuzumab is a fully humanized version of a murine HER2-targeted monoclonal antibody produced by Roche under the trade name **Herceptin**[®]. Trastuzumab binds to domain IV of the extracellular domain of the HER2 receptor⁸⁵ (Fig. 10) and thus, It has been suggested to induce some of its effect by downregulation of HER2 leading to disruption of receptor dimerization and signaling through the downstream PI3K cascade.⁸⁶ Cells treated with trastuzumab undergo arrest during the G1 phase of the cell cycle causing a reduced proliferation. In addition, trastuzumab suppresses angiogenesis both by induction of antiangiogenic factors and repression of proangiogenic factors. Proteolytic cleavage of HER2 that results in the release of the extracellular domain is thought to contribute to the unregulated growth observed in cancer, whereas it has been reported that trastuzumab inhibits HER2 ectodomain cleavage in breast cancer cells.^{87,88}

Although the exact mechanisms of action of trastuzumab have not been defined, it is also thought to include antibody-dependent cell-mediated cytotoxicity which induces the immune cells to destroy the tumor cells by the aid of trastuzumab.⁸⁹

In general, it has been reported that trastuzumab is well tolerated, but is associated with a small but significant increase in the risk of symptomatic cardiac failure (up to 4% at 4 years) particularly after anthracycline-based chemotherapy.⁹⁰

Despite significant progress of trastuzumab therapy, many patients will experience disease progression due to a lot of reported mechanisms which underly trastuzumab resistance. Trastuzumab resistance encourages the development of novel agents to overcome resistance and improve the outcomes.⁶²

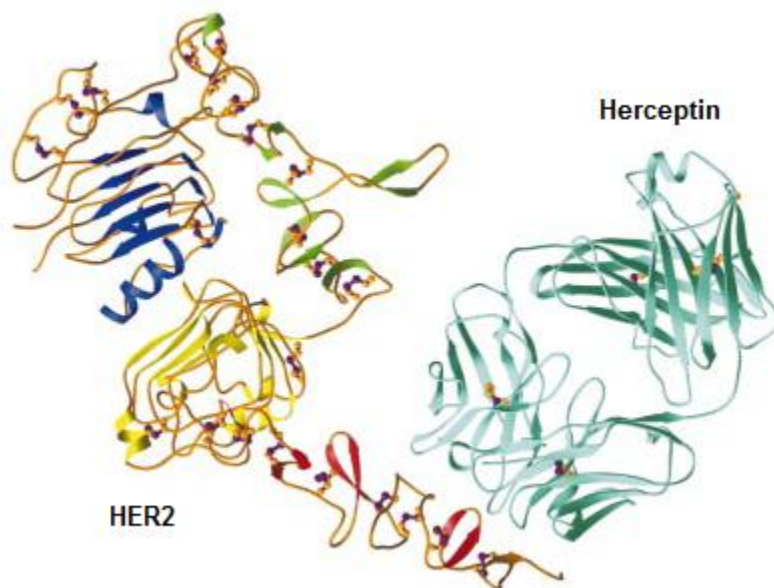


Fig. 10. The structure of human HER2/Herceptin complex:⁸⁵ Ribbon diagram of the human HER2. Domains I (blue), II (green), III (yellow) and IV (red), and the amino and carboxy termini, are indicated. Disulphide bonds are shown in purple and gold and Herceptin Fab (cyan) complex.

Lapatinib, (Tykerb[®]/Tyverb[®], produced by GlaxoSmithKline in the form of lapatinib ditosylate, Fig. 11), is an orally active small molecule drug for breast cancer and other solid tumours.⁹¹ It is a dual tyrosine kinase inhibitor which interrupts the HER2 and epidermal growth factor receptor (EGFR or HER1) pathways.⁹² It is used in combination therapy for HER2-positive breast cancer. It is used for the treatment of patients with advanced or metastatic breast cancer whose tumors overexpress HER2 (ErbB2).⁶²

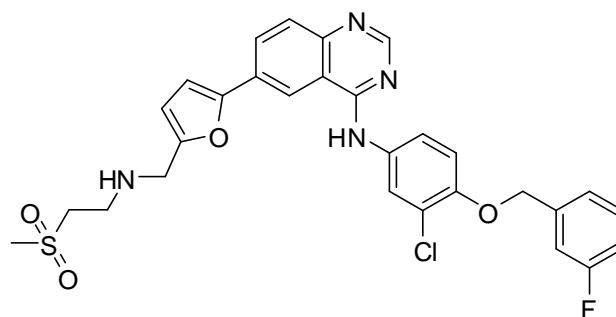


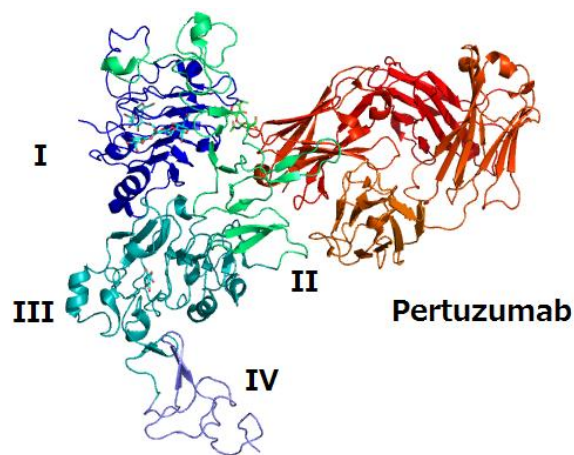
Fig. 11. Structure of Lapatinib (Tykerb[®]/Tyverb[®])

Lapatinib is a member of the 4-anilinoquinazoline class of kinase inhibitors. Members of this class of molecules have been shown to bind to the ATP binding site of protein kinases and compete with the ATP substrate. This blocks receptor phosphorylation and activation, preventing subsequent downstream signalling events.⁹³

Lapatinib was shown to inhibit phosphorylation of an exogenous peptide substrate with IC_{50} values of 9.2 nM (HER1) and 10.8 nM (HER2).⁹⁴

Preclinical studies have shown that lapatinib was active in trastuzumab-resistant HER2-positive human breast cancer cells and could increase the activity of anti-HER2 antibodies when used in combination.⁹⁵

Pertuzumab (Perjeta[®], made by Roche). On June 8, 2012, US Food and Drug Administration (FDA) approved pertuzumab injection for use in combination with trastuzumab and docetaxel for the treatment of patients with HER2-positive metastatic breast cancer who have not received prior anti-HER2 therapy or chemotherapy for metastatic disease. Pertuzumab is a recombinant humanized monoclonal antibody which targets the extracellular domain (sub-domain II) of HER2, dimerization sub-domain, and thereby blocks ligand-dependent hetero-dimerization of HER2 with other HER family members, including EGFR (HER1), HER3, and HER4.⁹⁶



HER2

Fig. 12. The structure of HER2/Pertuzumab complex. <http://en.wikipedia.org/wiki/Pertuzumab>

Perjeta[®] inhibits ligand-initiated intracellular signalling through two major signal pathways of mitogen-activated-protein kinases (MAPK) and phosphatidylinositol 3- kinases (PI3K). Inhibition of these signalling pathways can result in cell growth arrest and apoptosis, respectively. In addition, Pertuzumab mediates antibody-dependent cell mediated cytotoxicity (ADCC).^{97,98}

Recently, on December 13, 2012, the Committee for Medicinal Products for Human Use (CHMP) adopted a positive opinion, recommending the granting of a marketing authorization for the medicinal product Perjeta[®] as a first step to be approved in the European market.⁹⁹

Neratinib, (Fig. 13, HKI-272, is now part of Pfizer's expanded oncology portfolio, following the recent acquisition of Wyeth), is a potent, orally administered, small-molecule, 6,7-disubstituted-4-anilinoquinoline-3-carbonitrile pan-ErbB inhibitor

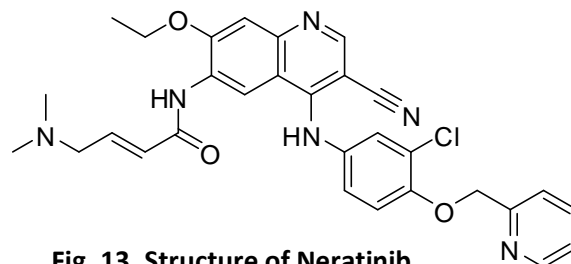


Fig. 13. Structure of Neratinib.

that irreversibly blocks signal transduction with potential antineoplastic activity *via* inhibition of ErbB1 (HER1), ErbB2 (HER2) and ErbB4 (HER4). Neratinib binds to HER receptors irreversibly, thereby reducing autophosphorylation in cells, apparently by targeting a cysteine residue in the ATP-binding pocket of these receptors. Treatment of cells with this agent results in inhibition of downstream signal transduction events and cell cycle regulatory pathways, arrest at the G1-S (Gap 1/DNA synthesis)-phase transition of the cell division cycle, and ultimately decreased cellular proliferation.^{100,101}

Neratinib has shown high selectivity towards HER2 and EGFR with IC₅₀ values of 59 nM and 92 nM, respectively.¹⁰⁰ Consequently, it has shown promising antitumor activity in a variety of solid tumors, including breast cancer, especially for the treatment of early- and late-stage HER2-positive breast cancer and non-small cell lung cancer.¹⁰²

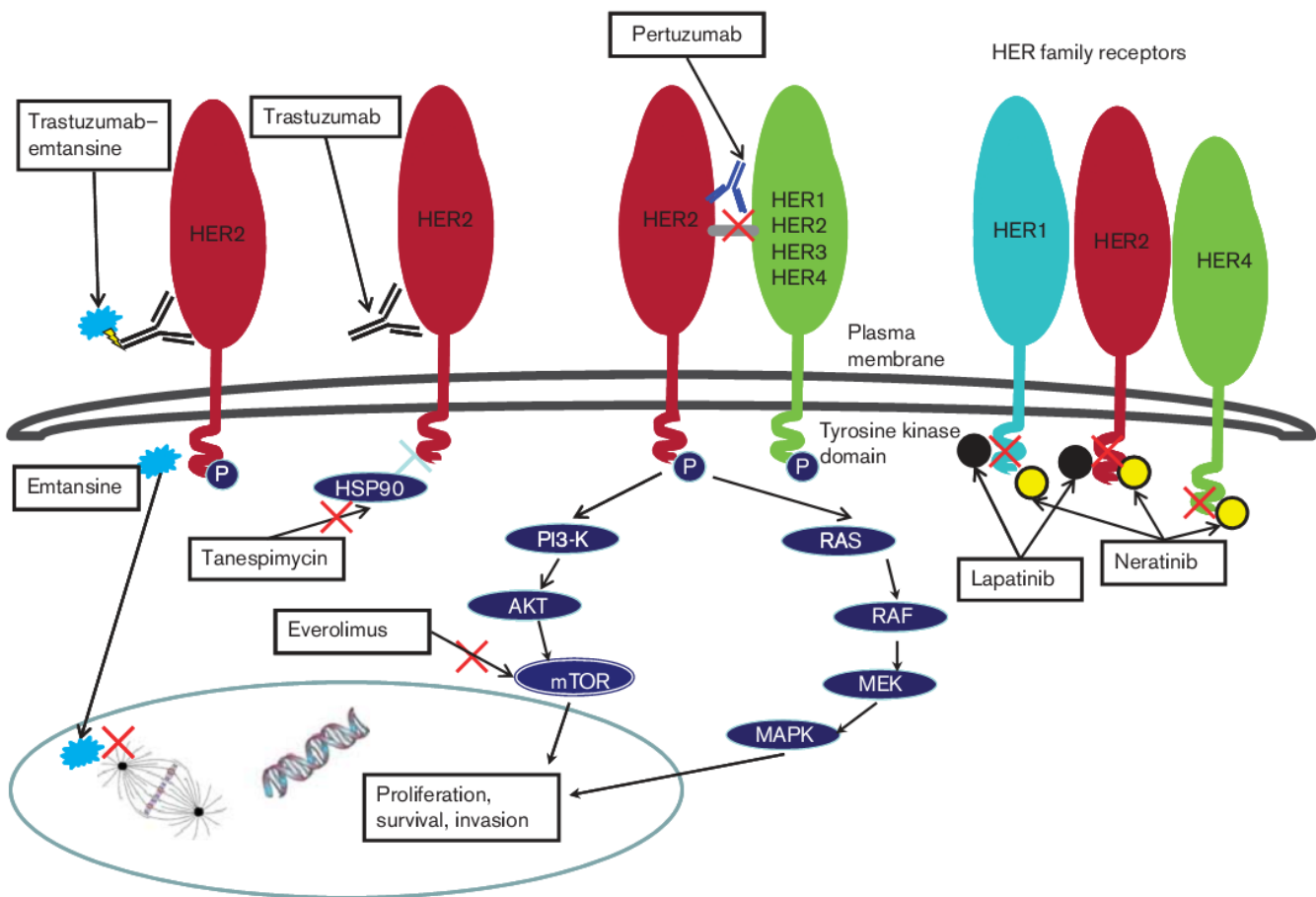


Fig. 14. Summarization of Available HER2-Inhibitors Mechanisms⁶²

Objectives

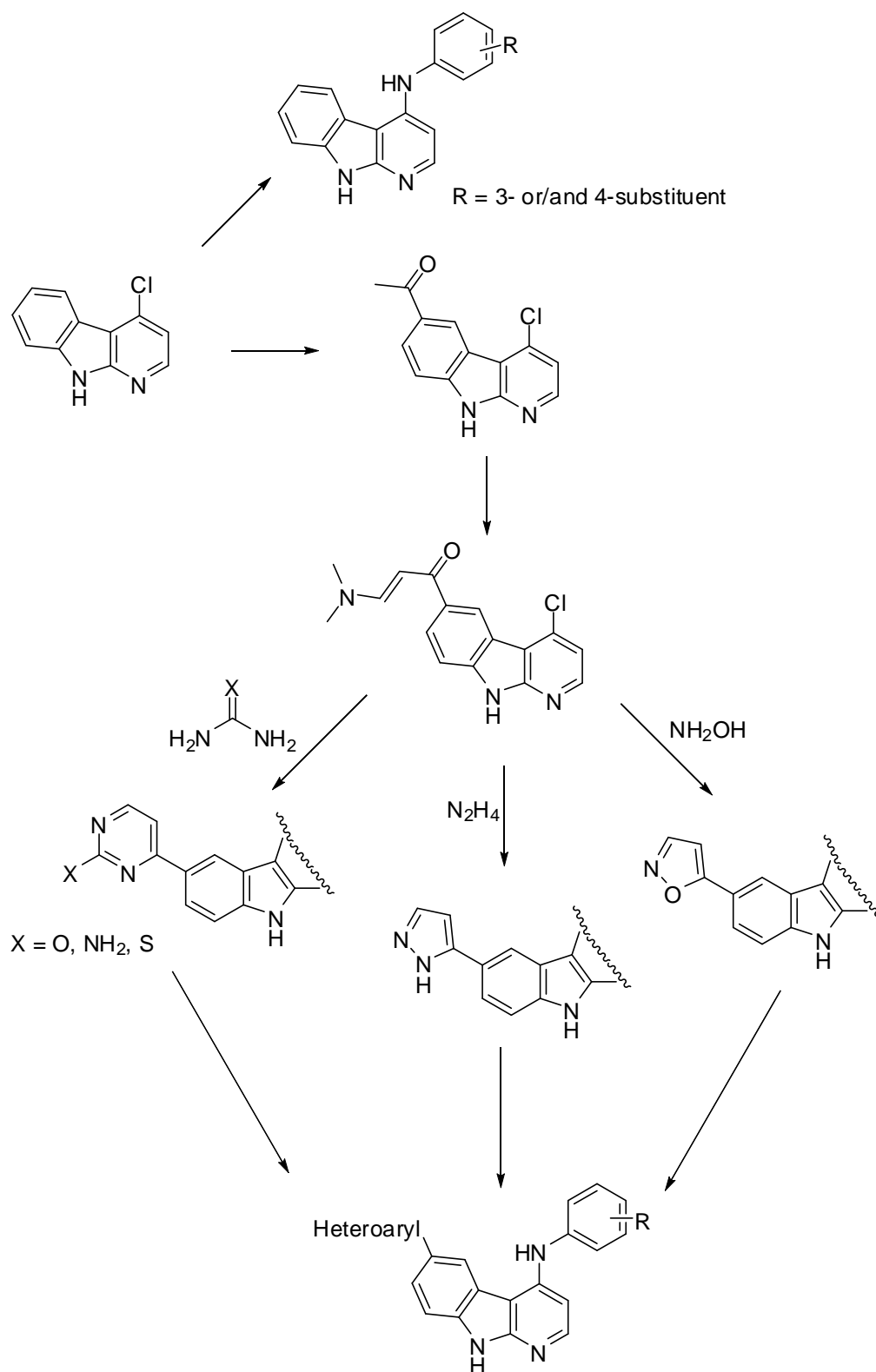
The main principle of this work was to continue the study of our research group (Drug Development and Analysis) investigating and evaluating the anti-proliferative activity of the 4-substituted α -carboline basic core.¹⁰³

Based on the results from the National Cancer Institute (NCI) 60-cell-line screenings executed in the biological exploration part of *Martin Krug* dissertation¹⁰⁴ for some derivatives, especially the 4-anilino-substituted α -carboline derivatives exhibited a promising antitumor activity, particularly against breast cancer subpanel cells. In further screening experiments, first 4-anilino-substituted α -carbolines could identify another kinase as a target structure, named Brk, breast tumor kinase. This cellular tyrosine kinase had been inhibited by the effect of *meta*- and *para*-substituted 4-anilino- α -carbolines in a nanomolar range (*m*-chloro-*p*-fluoroanilino, $IC_{50} = 69$ nM, and *m*-chloro-*p*-methylanilino, $IC_{50} = 75$ nM) and in a lowest nanomolar concentration with the *meta*-hydroxyanilino derivative ($IC_{50} = 3$ nM).

In addition, initial docking studies on the potent *meta*-hydroxyanilino α -carboline structure were conducted in cooperation with the group of Prof. Dr. *Wolfgang Sippl* (Martin Luther University Halle-Wittenberg) with the first created Brk homology model and resulted in the hypothesis that the hydroxy function forms a strong hydrogen bond with a glutamate residue in the binding pocket of the kinase. Therefore, the aim of the synthetic part was to synthesize other derivatives to support the postulated binding mode. (see Appendix part, Fig. 79)

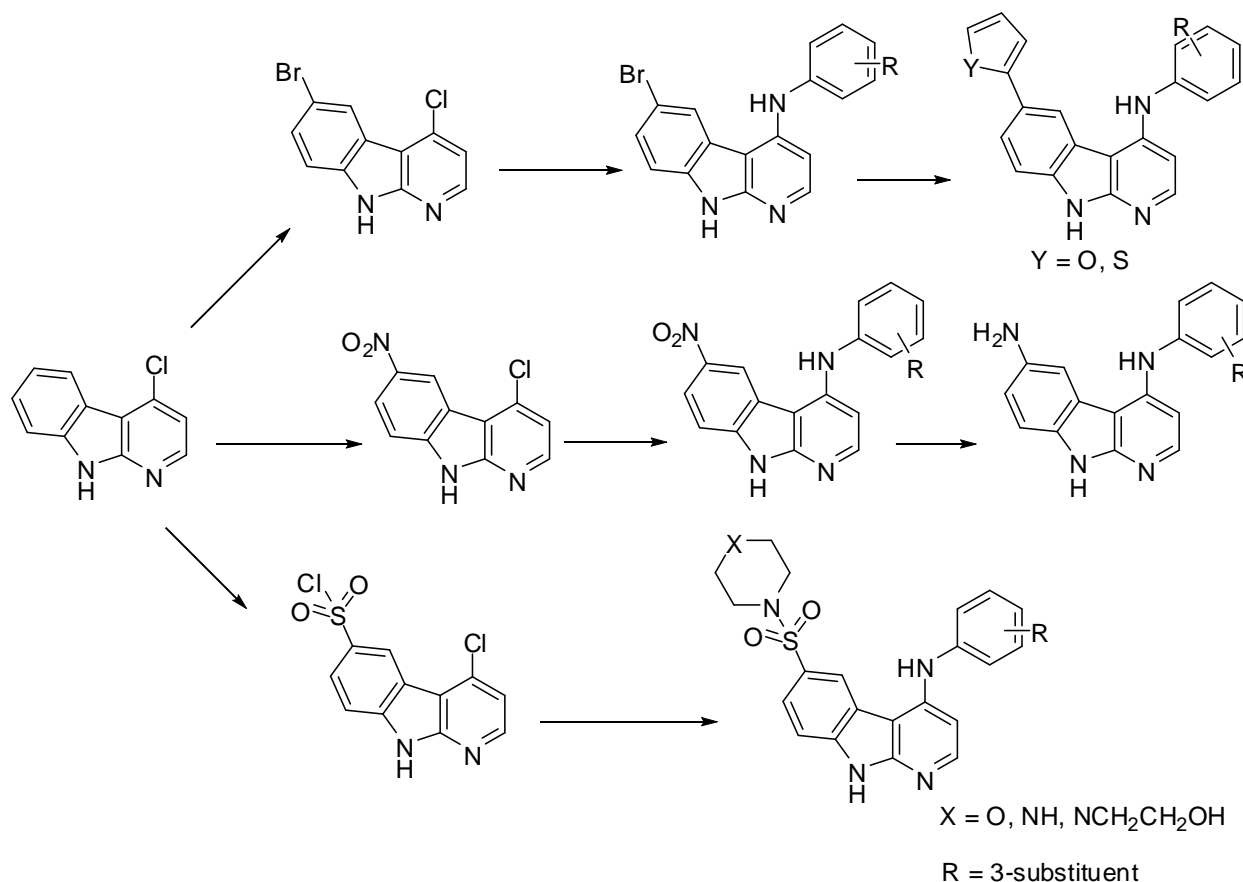
As the first tested 4-anilino-substituted α -carbolines exhibited nanomolar inhibitory activities of the tyrosine kinase Brk for first *meta*-substituted derivatives and on the way to characterize their structure-activity relationships, a series of substituted 4-anilino derivatives were synthesized with substitutions in the *meta*-position, and a *meta*- and *para*-disubstitution to be evaluated at the target structure (Scheme 1). Due to the possible significance of the amino-anilino function as hydrogen bond donor/acceptor, derivatization to the amine moiety was in our strategy. Primary acylation in the 6-position and a subsequent derivatization by the introduction of heterocycles was thought to augment the possibility for the

formation of hydrogen bonds that may influence the effectiveness of the derived products.



Scheme 1. First synthetic strategy.

Electrophilic aromatic substitutions like sulfonation, halogenation, cyanation and nitration at the 6-position followed by variable further reactions which were also assumed to improve the potential ATP-binding mode to targeted kinases. (Scheme 2)



Scheme 2. Second synthetic strategy.

The kinase Brk, against which there are currently no described inhibitors, plays an important role in numerous aggressive cancers, such as breast cancer.¹⁰⁵⁻¹⁰⁹ Reportedly, Brk reinforces the activity of the kinase HER2, which is overexpressed in many breast cancers,^{105,107} and on the other hand, it promotes the formation of metastases by the development of new tumor cell aggregates created from the detachment of the non-died tumor cells from the cell structure.^{105,110} A recent study suggests that Brk is responsible for IGF-1R regulation.¹⁰⁸ Brk kinase is also hardly expressed in normal cells and thus it is an interesting, but so far not studied as a target structure for the therapy of tumors, in particular there are no Brk inhibitors yet.¹⁰⁷⁻¹¹²

Aside from hurrying along tumor progression, Brk was also found to diminish the effectiveness of HER2-inhibiting drugs on tumor growth. This finding reinforces the need for combination therapies. Thus, we might need to hit HER2-expressing cancers with drugs against both Brk and HER2. Brk inhibitors might also be useful on their own. These inhibitors might fight tumors that never react to or become resistant to HER2-inhibitors.¹⁰⁶

Targeting Brk is also a safe strategy because it does not promote the proliferation of normal cells, and its expression in normal tissues is restricted to non-proliferating cells. Inhibiting this protein might thus produce fewer unwanted side effects than targeting other cancer-promoting proteins which may be present in larger numbers.¹⁰⁶

Initial studies in breast cancer cell lines obtained from the NCI have suggested that an association of Brk inhibition of the first α -carboline structures and anti-proliferative activity in breast cancer cells is authentic. Furthermore, the *meta*-hydroxyaniline derivative with significantly stronger Brk inhibition than the *m*-chloro-*p*-fluoroanilino derivative displayed a sub-micromolar GI₅₀ value of 0.8 μ M in MCF-7 breast cancer cells which is tenfold better growth inhibitory activity than the effective *m*-chloro-*p*-fluoroanilino derivative with a GI₅₀ of 8 μ M.

Therefore, the synthesized final derivatives (Scheme 1 & 2) are then anticipated to be investigated against the Brk as well as HER2, well documented in breast cancer therapy, *via* a protein kinase assay in collaboration with the *ProKinase GmbH* in Freiburg. Moreover, *in vitro* NCI 60-cell-line screenings using the Developmental Therapeutics Programme (DTP) in USA are also probable to estimate the anti proliferative parameters, growth inhibition, cytostatic activity and cytotoxicity of the test compounds.

Chemistry

Synthesis of 4-substituted α -carbolines

Synthesis of the desired 4-substituted α -carbolines could be done by presenting the unsubstituted base, α -carboline nucleus-structure, on which chlorination and then nucleophilic substitution of the chlorine atom with the preferred substituent can be introduced.

*Graebe-Ullmann*¹¹³ reaction basics were used for the preparation of the α -carboline basic body. The first step for this reaction was the preparation of 1-pyridinylbenzotriazole **3** which has been produced *via Katritzky* method.¹¹⁴ 2-Bromopyridine **1** is refluxed with 1*H*-benzotriazole **2** in toluene to produce 1-(pyridin-2-yl)-1*H*-benzo[*d*][1,2,3]triazole **3**, which was obtained nearly in a quantitative yield (97%). The isomeric product, 2-pyridinyl-2*H*-benzotriazole **4**, was obtained as a byproduct of this reaction as repeatedly described in the literature.¹¹⁶⁻¹¹⁹

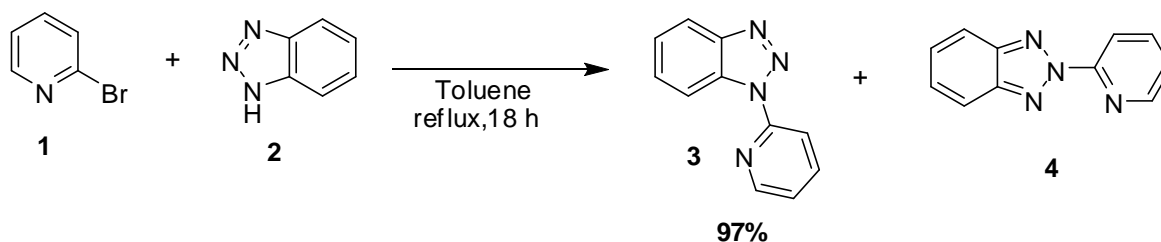


Fig. 15. Preparation of 1-pyridine-2-ylbenzotriazole (**3**).

The second step then was done according to the procedure of *WITKOP*¹¹⁵ by heating the 1-pyridin-2-ylbenzotriazole **3** in polyphosphoric acid to produce the α -carboline **7**. The product resulting from the black oily reaction mixture could be well-suspended in water by the effect of multiple ultrasonic bath treatment and the addition of 10 M sodium hydroxide solution to crystallize. Although, compound **7** has been obtained in only a moderate yield of 47%, its purity was high and accordingly a further purification of the product was not necessary.

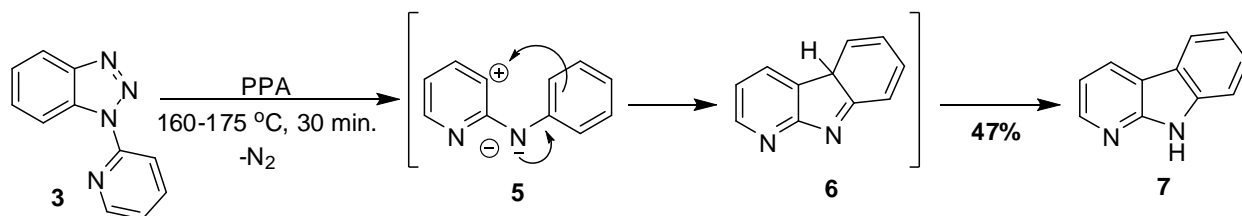


Fig. 16. Mechanism of α -carboline base-unit preparation (**7**).

By the release of molecular nitrogen from compound **3**, the zwitterionic intermediate **5** is formed, which reacts by cyclization and intramolecular recombination to produce the intermediate **6**, which in turn switches into the desired product **7** *via* tautomerism.¹²⁰ (Fig. 16)

Compound **7** was then transferred into the *N*-oxide structure **8** because of the low solubility of **7** in non-polar solvents. Using the method of *ELKS* and *STEPHENSON*,¹²¹⁻¹²³ compound **8** has been formed by heating the α -carboline **7** in a 30% aqueous solution of hydrogen peroxide in acetic acid. Subsequently, **8** was chlorinated by mixing with phosphorus oxychloride at room temperature for 24 hours in dry DMF to give the desired 4-chloro- α -carboline. The TLC of the crude product of the reaction of **8** with phosphorus oxychloride shows the presence of two distinct spots. These two substances were separated by column chromatography, characterized by NMR spectroscopy and have been identified as the two regioisomeric 2- and 4-chloro- α -carbolines **10** and **9**, respectively.

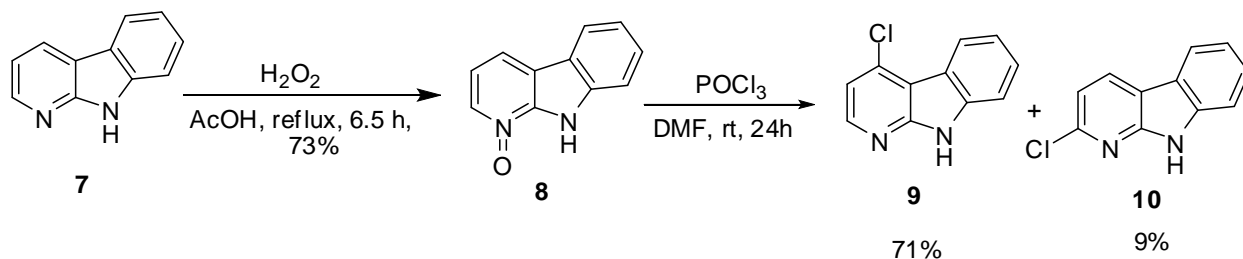


Fig. 17. Preparation of 4-Chloro- α -carboline (**9**).

The ^1H - and ^{13}C -NMR spectra of the two α -carboline compounds **9** and **10** differ only slightly from each other. The essential difference between the two compounds was the coupling constant between two protons of the pyridine ring. (Fig. 18) While the coupling constant $J_{2,3}$ between H-2 and H-3 of compound **9** was 5.3 Hz, the coupling constant $J_{3,4}$ between H-3 and H-4 of compound **10** was significantly greater (8.0 Hz). From the chemical shift of the two protons of the two regioisomers there was no reliable distinction, because the chemical shifts of the two protons H-3 $\delta_{\text{H}3}$, with 7.27 ppm in **9** and with 7.25 ppm in **10**, were nearly identical, moreover, the chemical shift of H-2 $\delta_{\text{H}2}$ was at 8.33 ppm in **9**, also only slightly different from that of the H-4 $\delta_{\text{H}4}$ of **10** which was 8.53 ppm.¹⁰⁴

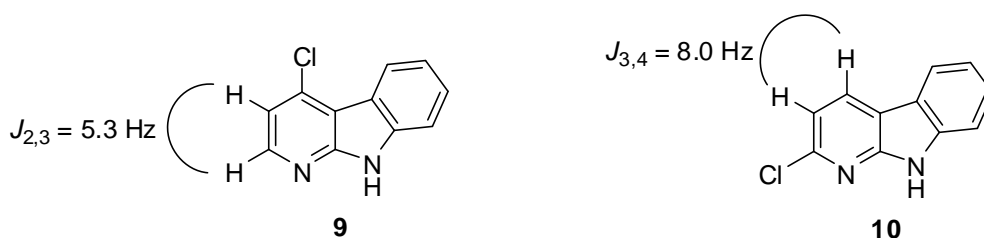


Fig. 18. ^1H -NMR differences between **9** & **10**.

Reaction of 4-chloro- α -carboline with aromatic amines

Nucleophilic substitution reactions of several mono- and disubstituted anilines with the 4-chloro- α -carboline compound **9** were simply proceeded in accordance to the available docking studies. Variable sizes of nucleophile and electrophile substitutions on the aniline phenyl ring were used to verify the pharmacological investigation and identify the impact of these variations on the activity and the selectivity towards the targeted kinases by exploring the structure-activity relationships (SARs).

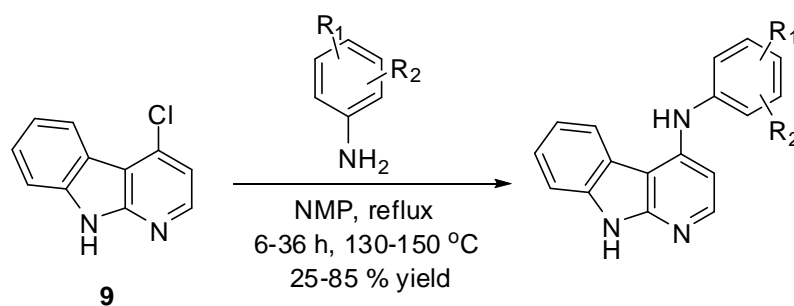


Fig. 19. Reaction of compound 9 with aromatic amines.

Nucleophile	Product
2-Toluidine	11
3-Aminophenole	12
3-Anisidine	13
3-Phenetidine	14
3-Chloroaniline	15
3-Aminobenzotrifluoride	16
3-(Methylmercapto)aniline	17
3-Benzyloxyaniline	18
3-Nitroaniline	19
4-Chloroaniline	20
4-Anisidine	21
3,5-Dichloroaniline	22
3-Chloro-4-toluidine	23
3-Chloro-4-fluoroaniline	24
3-Ethoxy-4-bromoaniline	25
3-Chloro-4-benzyloxyaniline	26
3-Methoxy-4-bromoaniline	27
1-Naphthylamine	28

Table 2. Derivatives 11-28, which were produced from the reaction of compound 9 with aromatic amines.

This reaction has been done by using an excess amount of the substituted aniline (~ 10 equivalents of compound 9) and *N*-methyl-2-pyrrolidone (NMP) as a solvent. NMP was the most suitable high-boiling solvent among other candidate solvents such as DMF, diphenyl ether and xylene in which 9 could not be sufficiently

dissolved. The other possibility was the usage of DMSO in which compound **9** is well-dissolved. However it decomposes by the fast increase of heat to reach the reflux temperature. The reaction mixture was refluxed under argon conditions and at an elevated temperature from 130 °C to 150 °C with a reaction time of 6-36 h, according to the aniline substituent used. TLC was used to detect the progression of the reaction and the ideal time for reaction termination. The crude product was then purified using column chromatography to separate the desired end products which were yielded in moderate to good percentages (25-85%).

Reduction of compound **19** to form the amino-derivative **29**

Tin (II) chloride (stannous chloride) was used as a reducing agent in the reduction reaction of the nitro group of derivative **19** to form the amino-derivative **29**. According to *Xing*¹²⁵ and *Bellamy*,¹²⁴ the reaction takes place by using excess tin (II) chloride (~ 6 equivalents of compound **19**) suspended in a 10% aqueous solution of HCl. Then, the reaction mixture was refluxed under argon conditions for about 80 minutes and observed by TLC. Termination of the reaction occurs by the alkalization with a solution of 10 M NaOH to pH 12. The amino-derivative **29** is produced in a good yield (85 %).

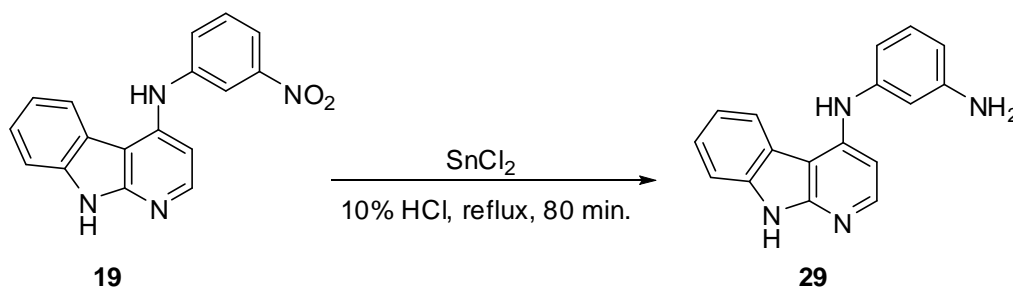


Fig. 20. Reduction of compound **19** to produce **29**.

For further investigations, we expected in this part of the work that the introduction of the amino functional group may allow further acetylation **30** or synthesis of diphenyl urea¹²⁶ derivative **31** (Fig. 21), trying to increase the possibilities of the formation of hydrogen bonds to the amino acid residues of the ATP-binding pocket of targeted kinases, and thus enable improved binding properties of these polar derivatives.

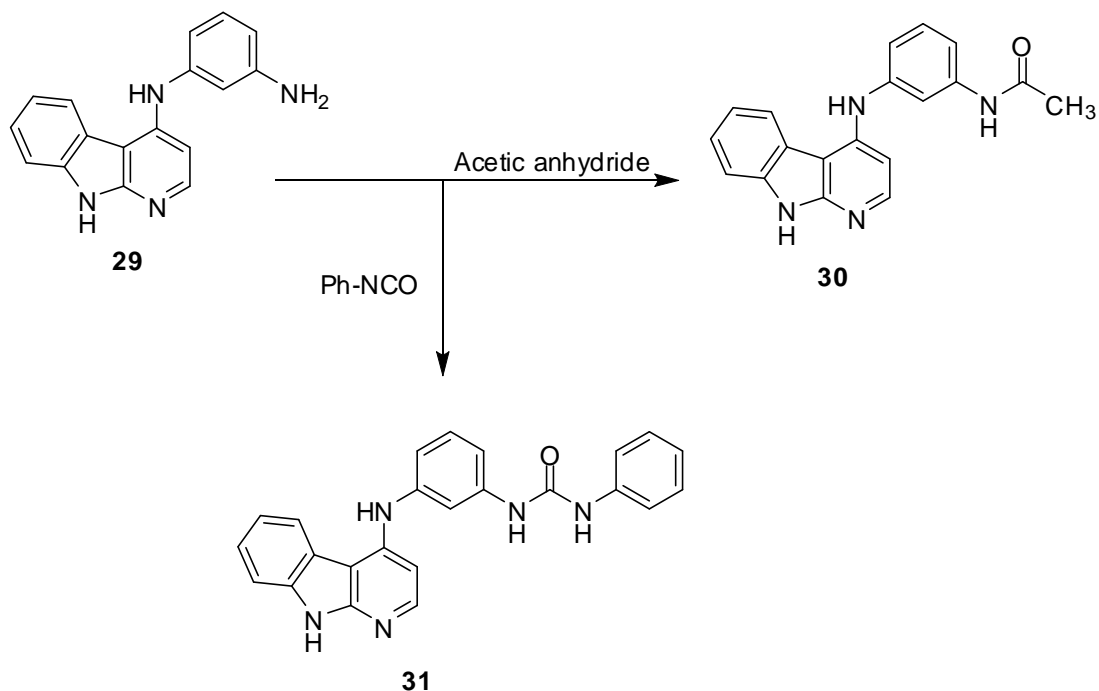


Fig. 21. Expected plan for preparation of compounds **30** and **31** from **29**.

The expected product **30** was not formed by the reaction of **29** with acetic anhydride, which reacted together immediately and at room temperature, but yielded the bis-acetylated derivative **32** and not the expected mono-acetylated candidate **30**. (Fig. 22)

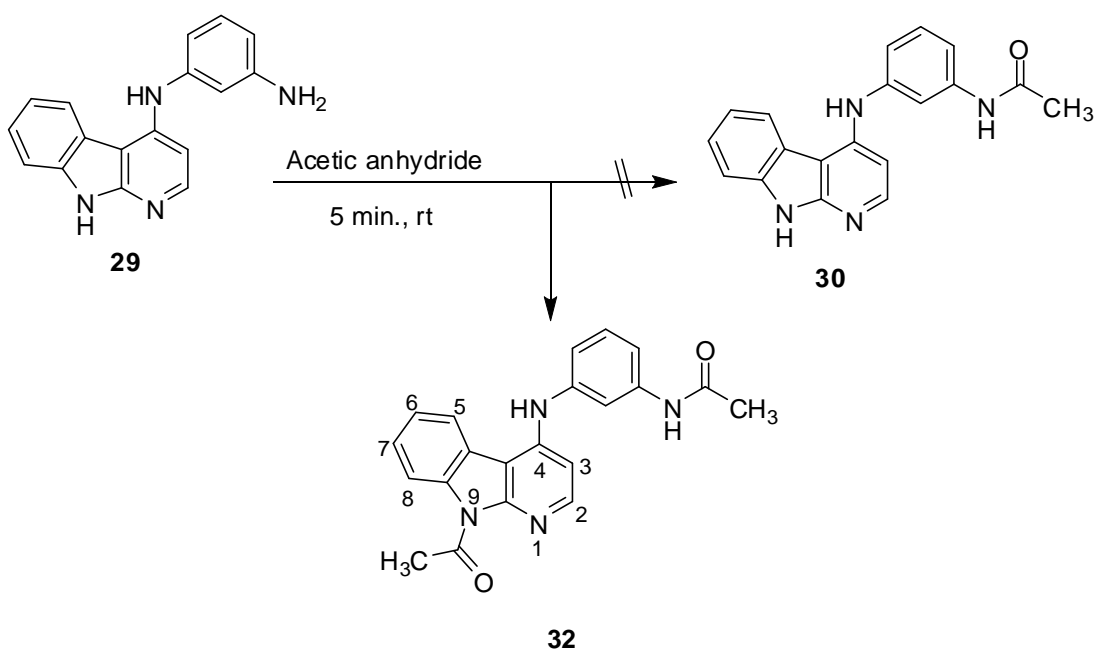


Fig. 22. Formation of compound **32** instead of the expected **30**.

The $^1\text{H-NMR}$ spectrum of compound **32** showed the disappearance of the *NH-9* proton signal in comparison with other derivative spectra, which proved that the acetyl-substitution occurs at the aniline-residue amino function and at *NH-9* of compound **29** (Fig. 22).

Since the free *NH-9* of the 4-substituted- α -carboline is essential for the pharmacological activity in targeted kinase binding, according to docking studies, it was necessary to find a way to protect this *NH-9* by a protecting group, benzyl group, and after finishing the acetylation reaction, a debenzilation reaction was performed. However, during the experienced deprotecting procedure there was a risk of structure destruction, due to the possibility of hydrolysis or cleavage of both 4-*NH* of the 4-phenyl amino moiety and the new amide linkage created by the acetylation reaction to the amino group.

Substitution on 6-position of α -carboline derivatives

From the docking binding mode studies, it was assumed that the 6-position of the α -carboline structure points to the solvent-exposed region of the ATP binding site. Thus it would be useful in this area to introduce different molecular groups to improve the physicochemical properties of these substances, such as the water solubility, moreover the expected possible hydrogen bond formation.

In this part of the work, we expected a significant contribution to the binding affinity and selectivity of these compounds according to the substituents which are introduced in this position.

For the introduction of substituents in the 6-position there are basically two possibilities: either one that leads to a substituent during the synthesis of the tricyclic α -carboline structure by the use of appropriately substituted starting materials, or one that leads to the 6-substituent by an electrophilic aromatic substitution in the final 4-substituted- α -carboline. However, the synthesis of 6-substituted α -carbolines could not follow the established route, because it required substituted derivatives of benzotriazole **2** which are not commercially available. Subsequent introduction of the substituents in the 6-position by an electrophilic aromatic substitution therefore seemed to be of interest. Some of the most used electrophilic aromatic substitutions in this part are aromatic sulfonation, aromatic nitration, aromatic halogenation and alkylating (acylation) *Friedel-Crafts* reaction.

Because of the *p*-position to the *N*-9 of the α -carboline and the structural analogy to an indole partial structure, it was assumed that a selective substitution at the 6-position of the tricyclic scaffold should be possible with the usual methods of electrophilic aromatic substitution. Therefore it should be examined whether and under what conditions the electrophilic aromatic substitution by sulfonation, halogenation, *Friedel-Crafts* acylation and nitration is possible. The aim of this study was to investigate the potential of the individual substitutions for further structural optimization of kinase inhibitors for future research to explore.

Synthesis of 6-sulfonamide-4-chloro- α -carbolins (sulfonation)

As a further possibility of variation, the introduction of a sulfonic acid group at the 6-position of the α -carboline skeleton was investigated. Furthermore, the introduction of hydrophilic sulfonamides should allow the solvent-exposed region of the ATP-binding pocket to be occupied, which was our final synthetic protocol.

There is no reported example for the regioselective sulfonation of α -carbolins in the literature other than a co-related response.¹²⁷⁻¹³¹

The reaction took place in two successive steps (Fig. 23). The first step was the addition of the chlorosulfonic acid to compound **9** at 0 °C and the reaction mixture then was left stirring at room temperature for ~ 2 hours. Then the resulting sulfonyl chloride **33**, which was isolated as a crude product, reacted further with the respective amines to achieve the targeted hydrophilic sulfonamides **34-36** in moderate yields of 35-50 % with high purities.

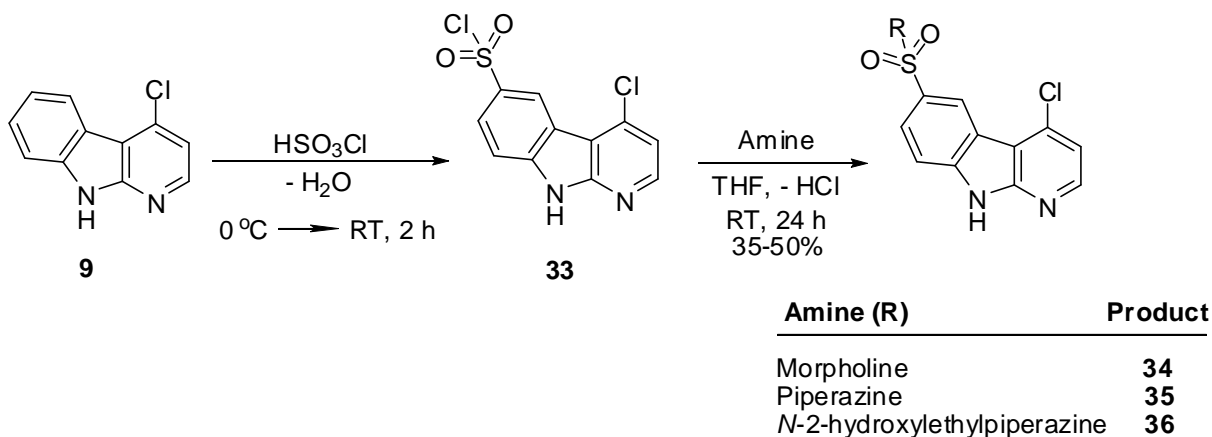


Fig. 23. Synthesis of 6-Sulfonamide-4-Cl- α -carbolins **34-36**.

Reaction of 6-sulfonamide-4-chloro- α -carbolines with aromatic amines:

Further nucleophilic substitution reaction was carried out to introduce *m*-substituted anilines in the 4-position of the 6-sulfonamide- α -carbolines **34-36**, which was expected to improve ATP-binding affinity.

The reaction took place by refluxing the recently synthesized 6-sulfonamide- α -carbolines (**34-36**) with the selected substituted anilines in NMP at relatively high temperature of about 210 °C for 8 hours and under argon conditions. (Fig. 24, 25 & 26) The detection of the products was performed by TLC and the end products were purified by column chromatography using a highly polar separating eluent mixture of EtOAc/cyclohexane/MeOH (40:40:20), due to the considerable high basicity of the end products.

Reaction of 6-morpholinosulfonyl-derivative **34** with aromatic amines

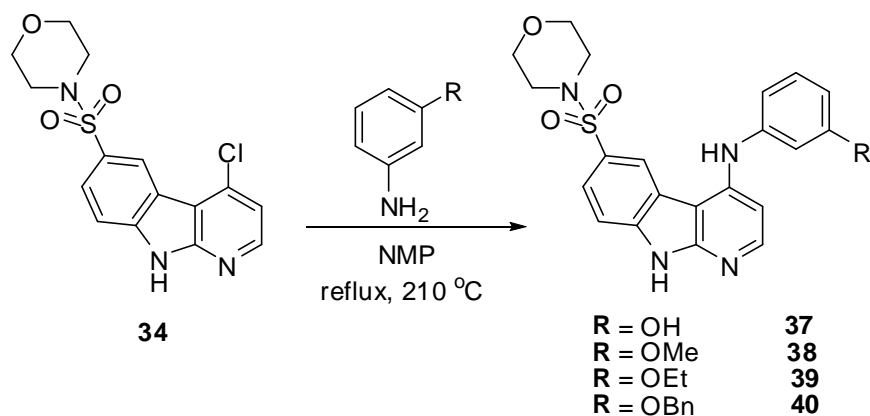


Fig. 24. Synthesis of 6-morpholinosulfonyl-4-anilino- α -carboline derivatives **37-40**.

Reaction of 6-piperazinosulfonyl-derivative 35 with aromatic amines

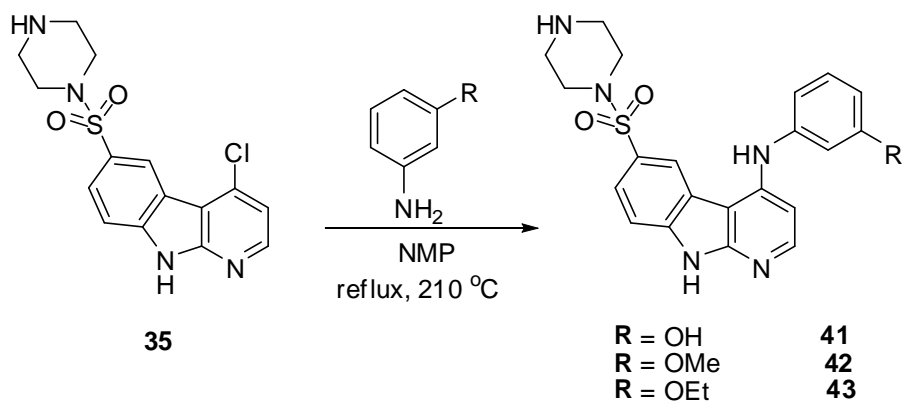


Fig. 25. Synthesis of 6-piperazinosulfonyl-4-anilino- α -carboline derivatives 41-43.

Reaction of 6-hydroxyethylpiperazinosulfonyl-derivative 36 with aromatic amines

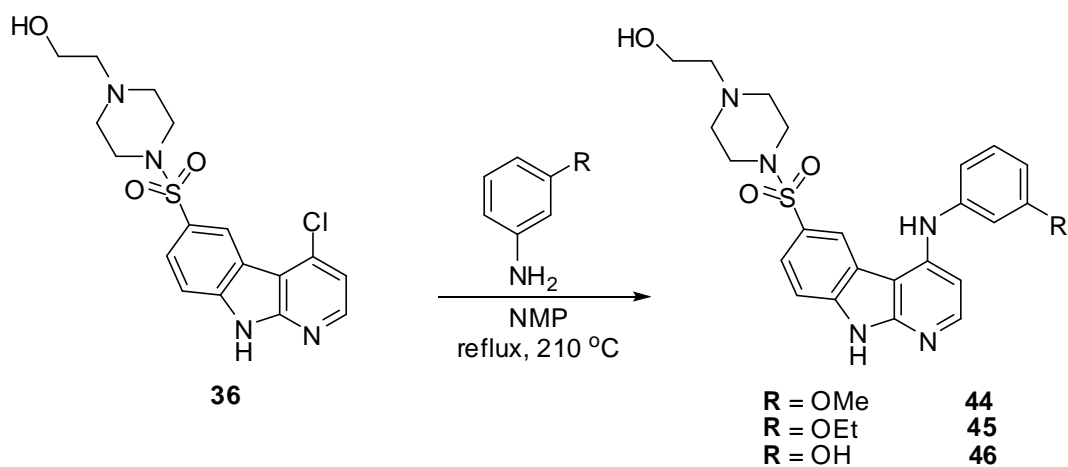


Fig. 26. Synthesis of 6-hydroxyethylpiperazinosulfonyl-4-anilino- α -carboline derivatives 44-46.

For further derivatization, a reduction reaction of the nitro function of the nitro derivative **49** was made using tin (II) chloride (SnCl_2) in 10% HCl to produce the amino-residue compound **51**. (Fig. 29)

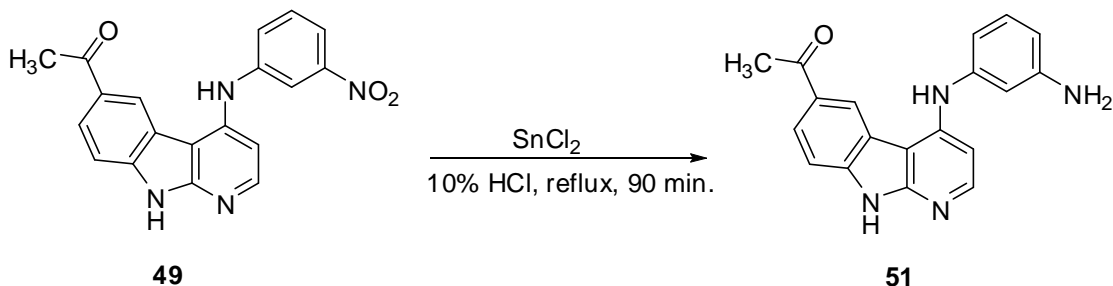


Fig. 29. Reduction of derivative **49** to prepare compound **51**.

Aldol Condensation of 6-acetyl-4-chloro- α -carboline

In this part of the work, we thought about a subsequent derivatization of the acetylated derivative **47** and the introduction of heterocycles at the 6-position estimating the possibility for the formation of hydrogen bonds and consequently influencing the activity. Product **47** underwent an aldol condensation with *N,N*-dimethylformamide dimethyl acetal (DMF/DMA) to convert into the corresponding 3-(dimethylamino) propenone **53** (Fig. 30). Subsequently, condensation of the 3-(dimethylamino) propenone fragment **53** took place with different nucleophiles to introduce various five- and six-membered hydrophilic heterocycles in the 6-position of the α -carboline skeleton. Unexpectedly, during the detection of the reaction progression by TLC we found the presence of two products. The two resulting products were then separated by column chromatography and were spectroscopically investigated. The major product **52**, which has been given in 85% yield, was the *N*-9 methylated 3-(dimethylamino) propenone derivative. While the byproduct **53**, in a 5% yield, was the desired product.

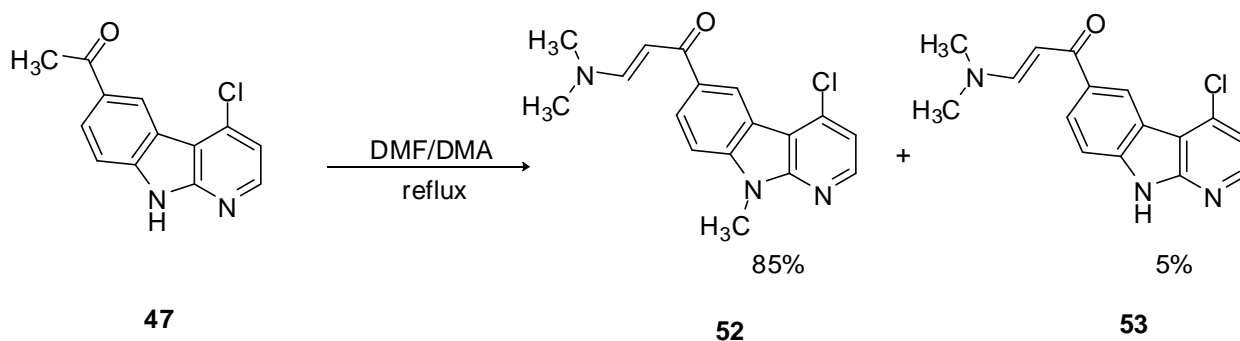


Fig. 30. Aldol Condensation of derivative **47** with DMF/DMA.

Moreover, an additional condensation reaction^{132,133} has been made with compound **52** in order to demonstrate its structure. Hydrazine hydrate was used to form the pyrazole ring structure *via* condensation reaction of **52** producing compound **54** in a very good yield (90%). Data analysis, NMR and ESI-MS, for **54** proved the methyl substitution at *N*-9 of the α -carboline derivative.

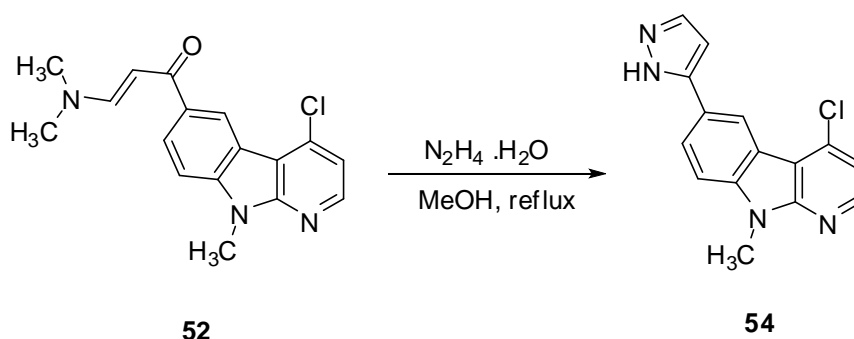


Fig. 31. Condensation of compound **52** with hydrazine hydrate.

From the above mentioned inspections, it was clear that a condensing reaction with DMF/DMA, as a source of the methyl group to react with the free *NH*-9 of our α -carboline moiety **47**, will produce the corresponding *N*-methyl derivative **52** as the major product, in addition to the formation of the targeted 3-(dimethylamino) propenone structure **53**. *NH*-9 methylation is disadvantageous for our further biological investigations because the free *NH*-9 is involved in hydrogen bonding to the hinge region of the protein backbone.

To attain the free *NH*-9 there were two possible pathways. The first was a *N*-demethylation of the produced compound **54**. The other pathway was to protect the

NH-9 of **47** by an easily removable functional group. After the condensation reactions, such a deprotection reaction should be done.

The *N*-methyl group exhibited a superior stability towards many types of reaction conditions, so that its cleavage is an obstacle in molecules with other functional groups. Although several procedures are known to realize *N*-demethylations, they are often incompatible with common reaction requirements such as chemoselectivity, high yields and mild reaction conditions.^{134,135} Hence, we decided to follow the second strategy to overcome this problem.

N-Benzylation has been our choice to protect the NH-9 of **47** during the formation of the desired enamine **53**. Benzyl chloride reacted with **47** in THF at room temperature stirring in presence of KOH to give the *N*-protected structure **55**.¹³⁶

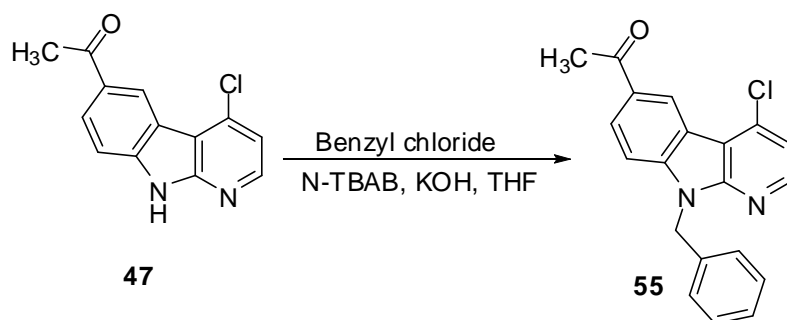


Fig. 32. *N*-Benylation of compound **47**.

Product **55** has then been reacted with DMF/DMA at 130 °C for 24 hours under argon conditions. After two hours, TLC indicated that only one product had been formed (**56**). (Fig. 33)

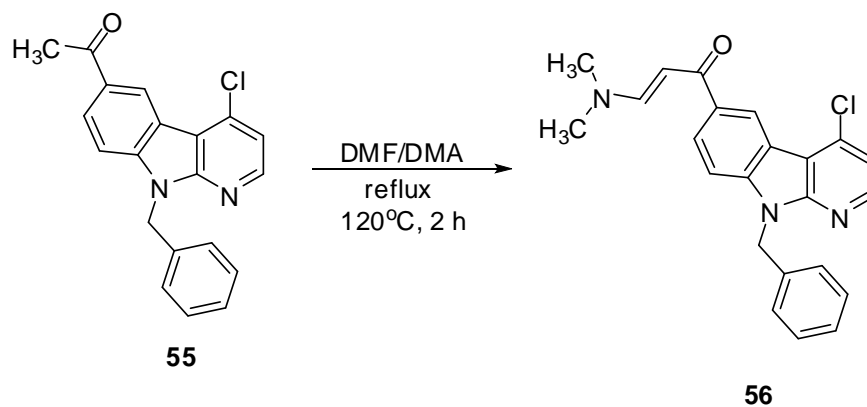


Fig. 33. Condensation of compound **55** with DMF/DMA.

Afterwards, the dimethylaminoprop-2-en-1-one **56** was refluxed with hydrazine hydrate in methanol to form the cyclic pyrazole structure **57**. The reaction took place under argon conditions for 4 hours at 120 °C and then the mixture was left stirring overnight at RT. Compound **57** was given in a good yield of 76%. (Fig. 34)

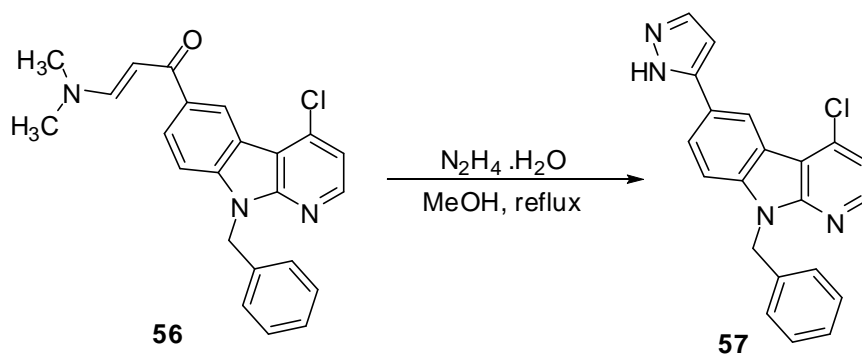


Fig. 34. Condensation of **56** with hydrazine hydrate.

Acid-catalyzed *N*-debenzylation¹³⁷ was then achieved to form compound **57** using 95% sulfuric acid to yield the desired derivative **58**.

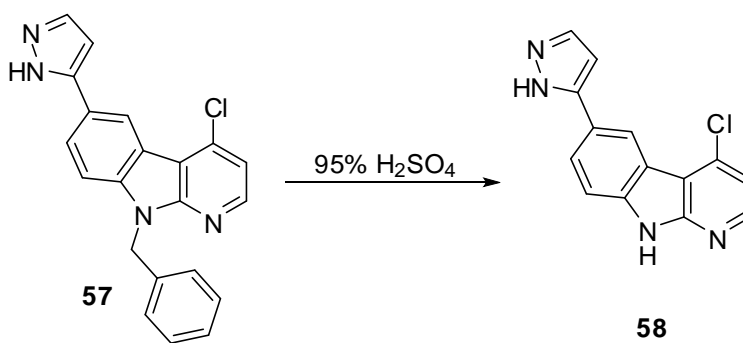


Fig. 35. *N*-Debenzylation of deivative **57**.

Final step was the nucleophilic substitution of the candidate *m*-substituted aniline in the 4-position of the formed 6-pyrazolo- α -carboline structure **58**. The reaction took place in NMP for 10 hours at 130 °C under argon conditions. (Fig. 36) The end products, **59** and **60**, were isolated and purified by column chromatography.

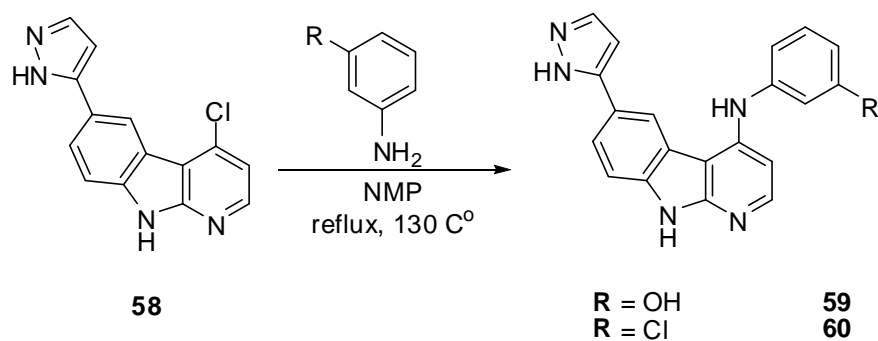


Fig. 36. Reaction of pyrazole-compound **58** with aromatic amines.

To introduce an isoxazole ring as another hydrophilic heterocycle in the 6-position of the α -carboline basic structure we decided to use the same procedures starting with the *N*-benzylated enaminone compound **56** which condensed with hydroxylamine hydrochloride.^{138,139} The reaction mixture was refluxed in absolute ethanol for 80 minutes at 100 °C under inert conditions and was then left stirring at RT for 2 hours. Structure **61** precipitated and was collected with a 65% yield.

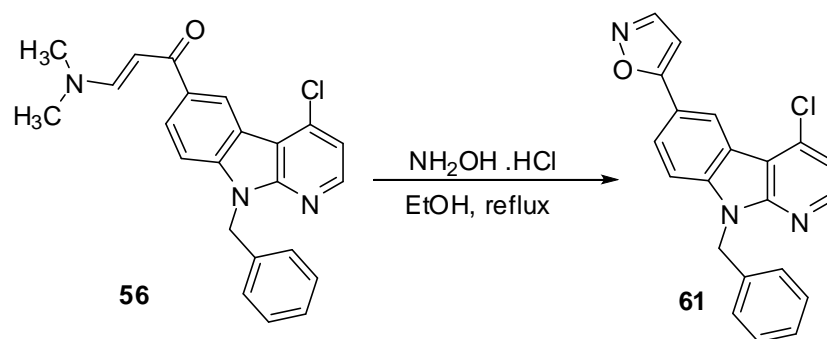


Fig. 37. Condensation of compound **56** with hydroxylamine HCl.

N-Debenzylation carried out for compound **61** by using 95% sulfuric acid to gain **62** which in turn then underwent a subsequent nucleophilic substitution at 4-position with the chosen *m*-substituted anilines in order to produce the candidate end structures **63** and **64**. By the same way as described before, the reaction mixture was refluxed in NMP at 130 °C for 10 hours (Fig. 38) and the end products were isolated and purified from the reaction mixture by column chromatography.

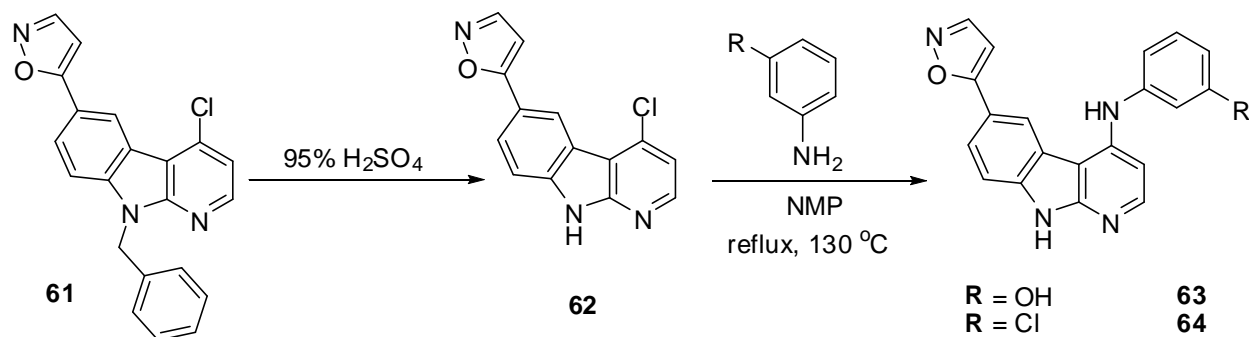


Fig. 38. Synthesis of 6-isoxazolo-4-phenylamino- α -carbolines **63** and **64**.

It was also conceivable to introduce 2-hydroxy-, 2-amino- or 2-mercapto-pyrimidines at the 6-position of the α -carboline structure by the condensation reaction of compound **56** with urea, guanidine or thiourea, respectively.¹⁴⁰⁻¹⁴³

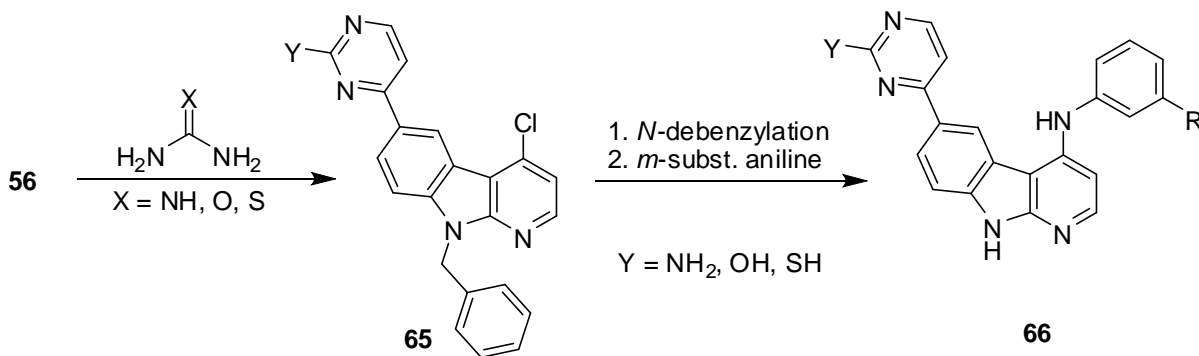


Fig. 39. Possible subsequent reactions on derivative **56**.

Synthesis of 6-bromo-4-chloro- α -carboline (bromination)

Another aim of the investigations of the electrophilic aromatic substitution was the halogenation at the 6-position of the α -carboline base body, in particular, the bromination which is of synthetic and biological interest. In addition to the pharmacological importance of the bromine itself, the introduction of a bromine substituent in the 6-position would also open up the possibility of carrying out further reactions such as contributing in the direct attachment of polar heterocycles, thiophene or furan ring, by palladium-catalyzed coupling reactions such as the *Suzuki-Miyaura* coupling.^{144,145} On the other hand, bromine could participate in the course of the *Rosenmund-von Braun* reaction¹⁴⁶⁻¹⁴⁸ with copper (I) cyanide in DMF to give the corresponding carbonitrile derivative.

Bromination was proceeded at room temperature in glacial acetic acid. Using 1.5 eq. of bromine, a complete conversion of **9** and desired product **67** was achieved after a reaction time of 24 h and was isolated in a good yield of 69%. Surprisingly, the usage of excess bromine which could under the same reaction conditions showed the presence of two distinct products by TLC. Multiple bromination was then indicated by spectral analysis, which proved the existence of a 6- and 8-bromine substitution. (Fig. 40)

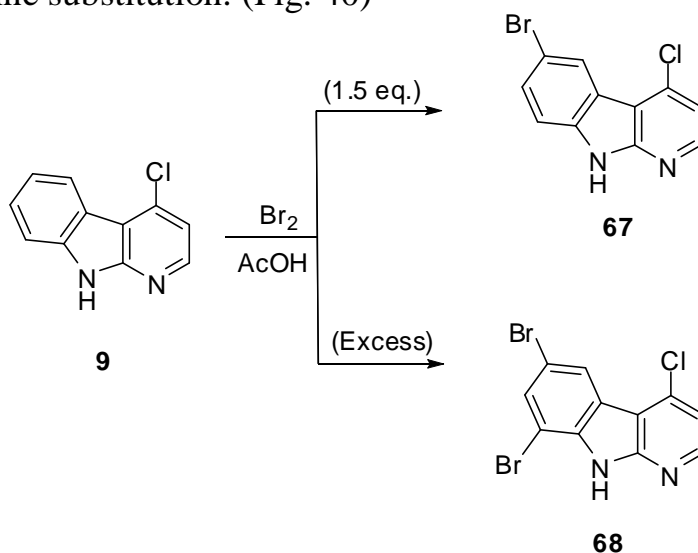


Fig. 40. Bromination of compound 9.

Reaction of 6-bromo-4-chloro- α -carboline with aromatic amines

Addition of *m*-substituted anilines into the 4-position of the 6-brominated α -carboline basic structure **67** was performed in NMP at 130 °C for 4-12 h under argon condition. End products were finally isolated and purified by column chromatography. The yields of the different products were slightly low (< 20%).

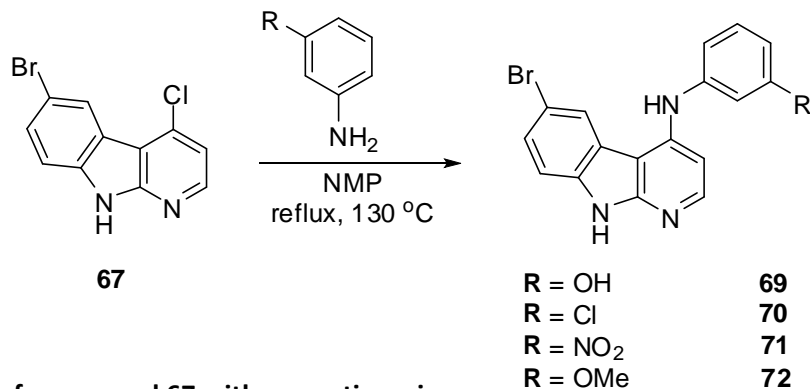


Fig. 41. Reaction of compound 67 with aromatic amines.

Reaction of 6,8-di-bromo-4-chloro- α -carboline with aromatic amines

For further investigations, the dibromo substituted α -carboline **68** underwent a nucleophilic substitution with selected anilines at 4-position. The reaction took place in NMP at high temperature (140 °C) and for a longer reaction time (36 h). (Fig. 42) The desired final products were given in considerably low yields (< 10%) after two consecutive column chromatography purifications.

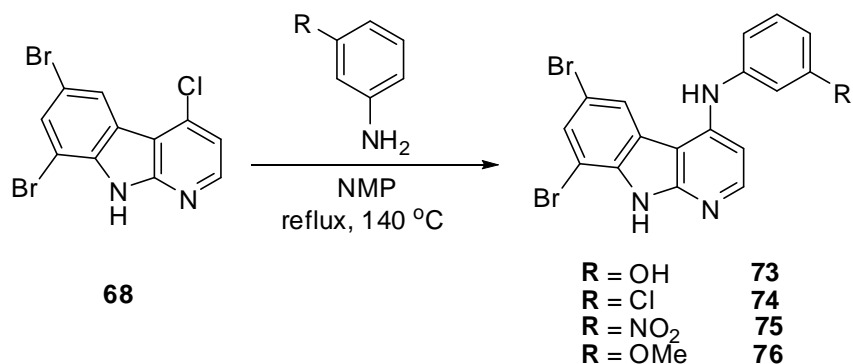


Fig. 42. Reaction of compound **68** with aromatic amines.

Suzuki-Miyaura coupling reaction was the next objective for direct replacement of the 6-bromine atom by polar heterocycles such as thiophene or furan ring *via* a palladium-catalyzed coupling reaction.

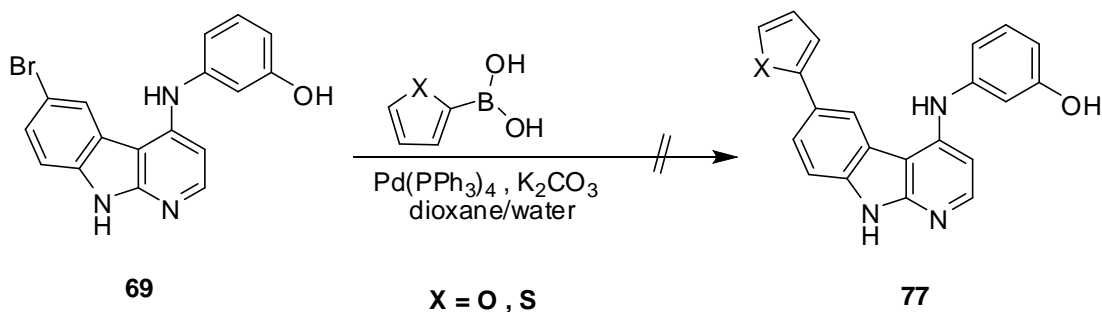


Fig. 43. Suzuki-Miyaura coupling of compound **69**.

The reaction was realized using **69** with both furan-2-yl and thiophen-2-ylboronic acid, each in a separate reaction, and tetrakis(triphenylphosphine) palladium as well as potassium carbonate in 1,4-dioxane/water.¹⁴⁹ (Fig. 43)

By increasing the temperature to 150 °C and after 20 minutes, a TLC of the reaction mixture was made and there were numerous products observed in both reactions. Therefore, it was not possible to isolate the desired products from the reaction mixture, so that the interesting class of these substances could not be developed in this work.

Cyanation of the 6-bromo-4-(*m*-hydroxyphenylamino)- α -carboline **69**

For further derivatization of compound **69**, the *Rosenmund-von Braun* reaction was carried out by heating the compound with sodium cyanide in NMP at 150 °C (Fig. 44) to produce the corresponding nitrile substituted α -carboline derivative, which was obtained in a yield of 65%.

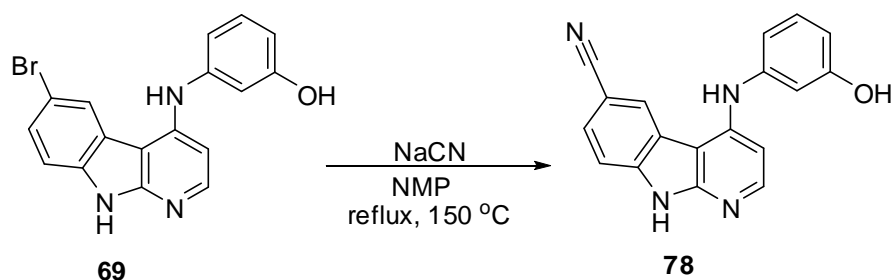


Fig. 44. Rosenmund-von Braun reaction of **69** (cyanation).

Compound **78** could also serve as a starting material for interesting secondary reactions. Thus, derivative **78** could be hydrolyzed to the corresponding carboxylic acid **80** or reacted in a 1,3-dipolar cycloaddition with sodium azide to produce the tetrazole **79** (Fig. 45& 46). Both target compounds would be considered from the standpoint of medicinal chemistry as interesting derivatives because tetrazoles have generally a similar acidity than the corresponding carboxylic acids, but simultaneously have a higher lipophilicity than the latter, which could be advantageous for the membrane permeability of the compounds.

A plethora of synthetic protocols and variations have been reported in the literature regarding the formation of tetrazoles from organic nitriles. We chose to reflux compound **78** with sodium azide in NMP/AcOH/H₂O (7:2:1) as solvent mixture.¹⁵⁰ Many TLCs were constantly made during reaction time without any

noticed changes or conversion of **78**. Increasing the reaction temperature to 210 °C and duration to 36 h did not also indicate any progress.

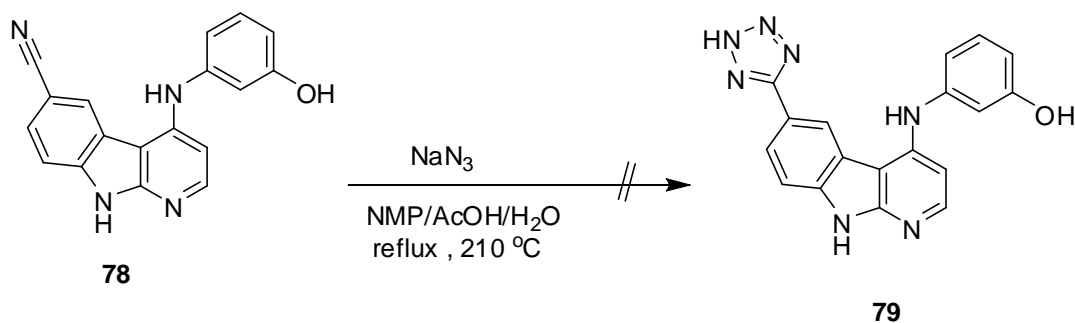


Fig. 45. Cycloaddition of **78** with sodium azide.

The other approach was to hydrolyze the nitrile function **78** to a carboxylic acid which was somewhat easy by heating the compound in concentrated hydrochloric acid¹⁵¹ under reflux for 6 hours. The resulting acid **80** was given in a 65% yield.

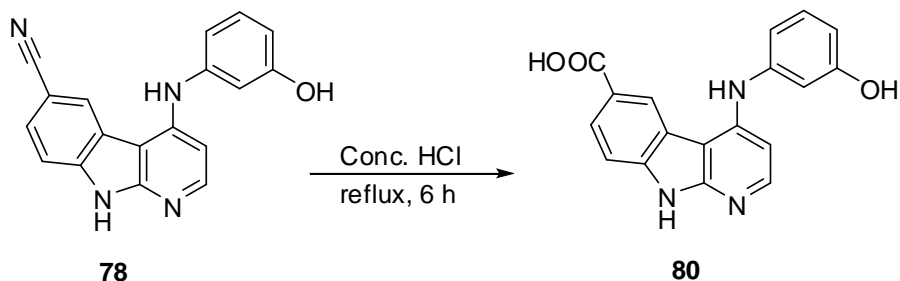


Fig. 46. Hydrolysis of compound **78**.

Synthesis of 6-nitro-4-chloro- α -carboline (nitration)

The main aim in this part of work was to synthesize the 6-nitro derivative **81** in order to obtain the 4-(*m*-anilino)-substituted products, which in turn should then be reduced to the corresponding amino derivatives.

Although the introduction of the primary amino function was aimed to improve the water solubility of the 6-unsubstituted compounds, the amino group can additionally be used for the easy attachment of other various hydrophilic residues by the reaction with isocyanates to form ureas **82**, by the reaction with carboxylic acid and sulfonic acid chlorides to amides **83** and sulfonamides **84**, or by the reaction with chloroformic esters to reach carbamates **85**. (Fig. 47)

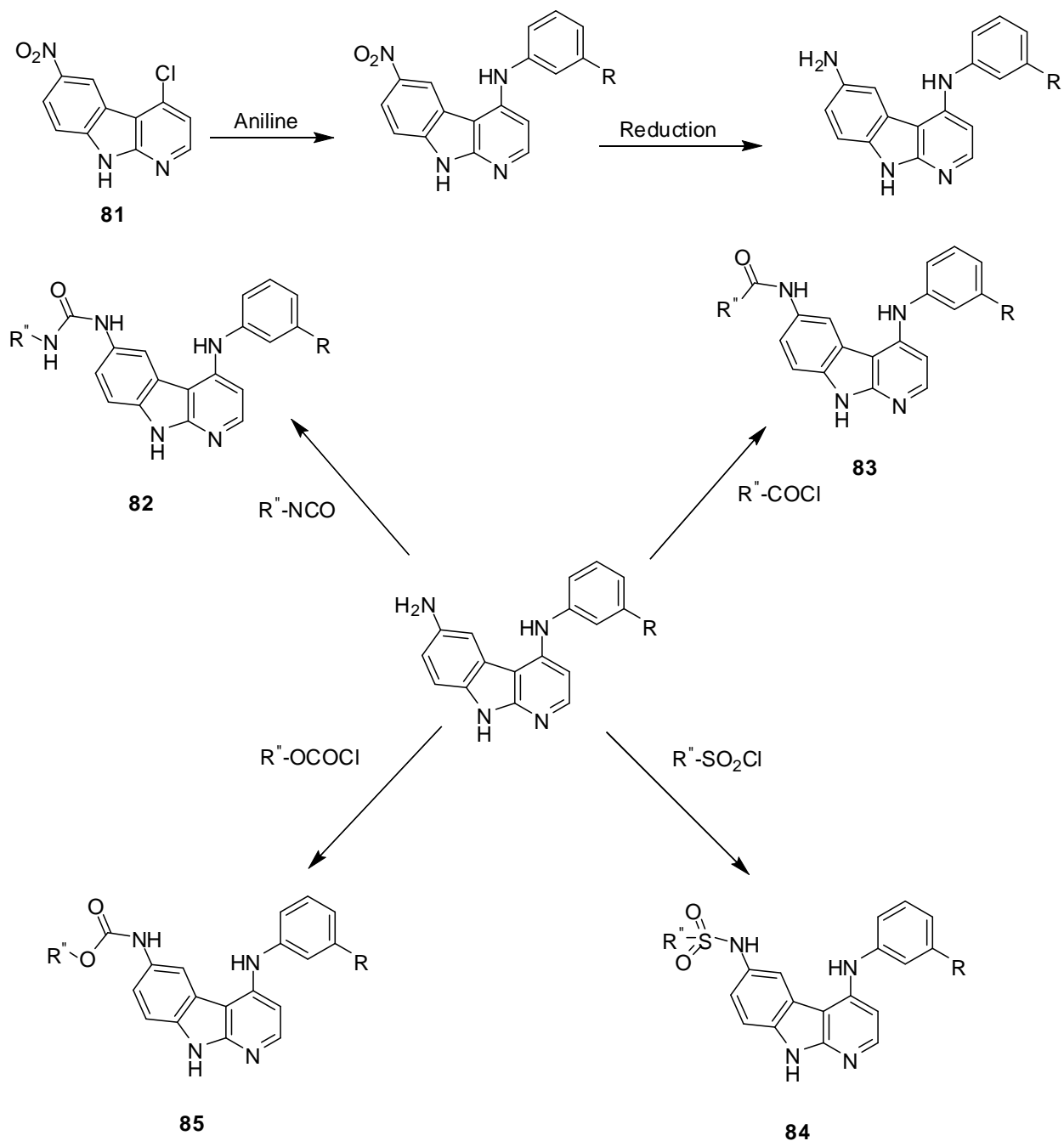


Fig. 47. Possible subsequent pathways for the 6-amino substituted α -carboline derivatives.

Nitration reaction (Fig. 48) was accomplished by slow addition of the 4-chloro- α -carboline **9** to an excess of red, fuming conc. nitric acid at 0 °C and followed by stirring at RT for 20 minutes. Termination of the reaction occurred by water addition and alkalination with sodium carbonate. Surprisingly, no selective

mononitration took place as expected. Spectral analysis proved that the 6,8-dinitro derivative **86** was produced under these reaction conditions. The yield was about 50%.

By trying to use an equivalent molar ratio from the red, fuming nitric acid, we finally have had the selective mononitro derivative **81** by the same reaction procedure. Compound **81** was produced in a moderate yield of 47%.

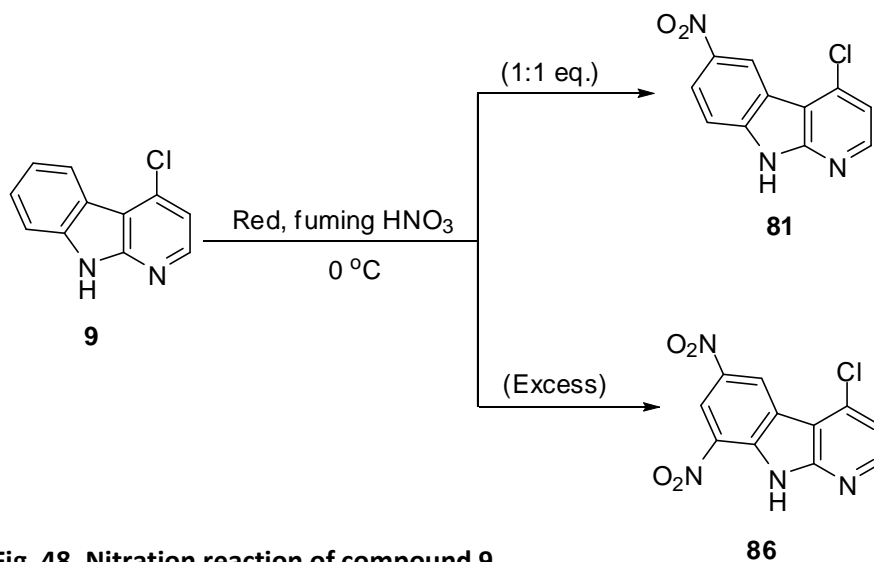


Fig. 48. Nitration reaction of compound 9.

Reaction of 6-nitro-4-chloro- α -carboline with aromatic amines

As usual, a nucleophilic substitution with different *m*-substituted anilines was carried out by heating them with compound **81** in NMP at 135 °C for 36 h under inert argon atmosphere (Fig. 49). The formed end products were then isolated and purified by column chromatography. The reaction yield differed according to the substituted aniline used (18-70%).

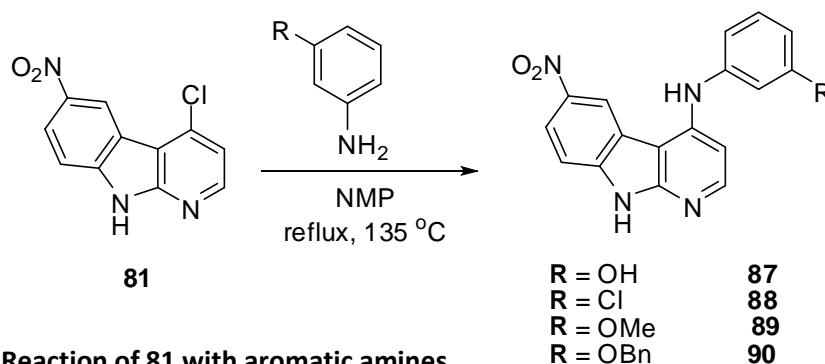


Fig. 49. Reaction of **81** with aromatic amines.

Reduction of some 6-nitro-4-chloro- α -carboline derivatives

For auxiliary biological investigations, reduction of the nitro group of some selected derivatives was proceeded so as to estimate the influence of the resulting amino function on structure-activity relationships.

In this reaction, tin (II) chloride was used as a reducing agent and it took place in 10% hydrochloric acid (Fig. 50). The amino derivatives **91** and **92** were collected in good yields.

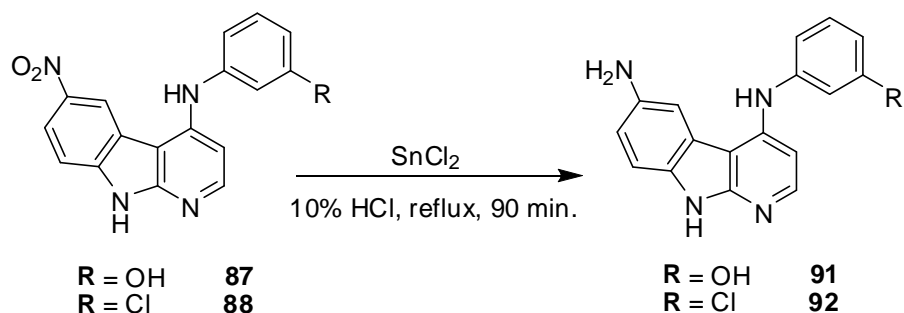


Fig. 50. Reduction of compounds **87** and **88**.

Reaction of 6,8-dinitro-4-chloro- α -carboline with aromatic amines

Replacement of the chlorine at 4-position of the 6,8-dinitro α -carboline basic structure **86** by a substituted aniline was the objective of this step. The reaction mixture was refluxed in NMP at 135 °C for 36 h. The desired product was isolated and purified by column chromatography, and was given in good yields (52-80%).

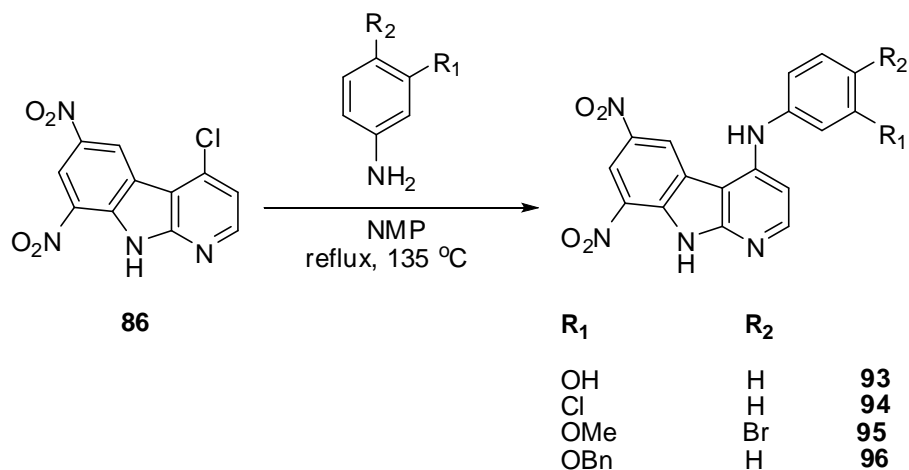


Fig. 51. Reaction of compound **86** with aromatic amines.

Reduction of some 6,8-dinitro-4-chloro- α -carboline

By using tin(II) chloride in 10% HCl as we did before, it was unexpected that the reduction did not work by the same reaction procedures. Increasing reaction time and elevating reaction temperature as well did not cause any changes to the starting nitro derivatives according to the TLC. Hence, it seems that we were in a need to use another procedure to reduce the resulting new dinitro structures.

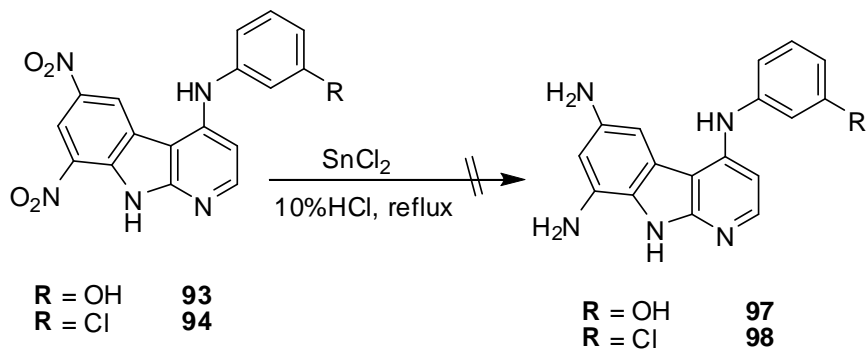


Fig. 52. Reduction of compounds 93 and 94.

Biology

Protein Kinase Assay

The main purpose of this part of work was to study the possible kinase inhibitory activity of the targeted compounds. These compounds were studied in collaboration with the *ProQinase GmbH* Company (Freiburg, www.proqinase.com). A radiometric protein kinase assay (³³PanQinase[®] Activity Assay) was used for measuring the kinase activity of the two protein kinases (Brk and HER2). All kinase assays were performed in 96-well FlashPlates[™] from PerkinElmer (Boston, AM, USA) in a 50 µl reaction volume. The reaction cocktail was pipetted in four steps in the following order:

- 20 µl of assay buffer (standard buffer)
- 5 µl of ATP solution (in H₂O)
- 5 µl of test compound (in 10% DMSO)
- 10 µl of substrate/ 10 µl of enzyme solution (premixed)

The assay for all protein kinases contained 70 mM HEPES-NaOH pH 7.5, 3 mM MgCl₂, 3 mM MnCl₂, 3 µM Na-orthovanadate, 1.2 mM DTT, 50 µg/ml PEG₂₀₀₀₀, 1 µM ATP, [γ -³³P]-ATP (approx. 5 x 10⁵ cpm per well), protein kinase (variable amounts), and substrate (variable amounts).

The following amounts of enzyme and substrate were used per well:

#	Kinase	Kinase	Kinase	Kinase Conc.	Kinase Conc.	ATP Conc.	Substrate	Substrate	Substrate
	Name	ProQinase Lot	External/Vendor Lot	ng/50µl	nM*	µM	Name	Lot	µg/50µl
1	BRK	003		25	6.1	1.0	Poly(Glu, Tyr) 4:1	SIG_20K5903	0.125
2	HER2	012		25	5.3	1.0	Poly(Glu, Tyr) 4:1	SIG_20K5903	0.125

* Maximal molar enzyme assay concentrations, implying enzyme preparations exclusively containing 100% active enzyme

Table 3. Assay parameters for the tested protein kinases.

The reaction cocktails were incubated at 30 °C for 60 minutes. The reaction was stopped with 50 µl of 2 % (v/v) H₃PO₄, plates were aspirated and washed two times with 200 µl 0.9 % (w/v) NaCl. Incorporation of ³³P_i was determined with a microplate scintillation counter (Microbeta, Wallac). All assays were performed with a BeckmanCoulter/SAGIANTM Core System.

For determining the inhibitory activity of tested compounds against protein kinases, the assay was performed in the presence of each test compound, in ten different concentrations ranging from 3 nM to 100 µM, and the control, in the absence of tested compound which was taken as the “high control” whereas in absence of the kinase as “low control”. The difference between high and low control was taken as 100 % residual activity and was calculated according to equation 1.

$$\text{Res. Activity (\%)} = 100 \times \frac{\text{cpm of compound} - \text{low control}}{\text{high control} - \text{low control}}$$

Equation 1. Calculation of the percentage residual activity

The residual activities for each concentration and the compound IC₅₀ values (50 % inhibition concentration) were calculated using *Quattro Workflow V3.1.0* (Quattro Research GmbH, Munich, Germany; www.quattro-research.com). The fitting model for the IC₅₀ determinations was “Sigmoidal response (variable slope)” with parameters “top” fixed at 100 % and “bottom” at 0 %. The fitting method used was least-squares fit.

The IC₅₀ value is the concentration of the tested substance that inhibits half-maximal activity of the particular kinase, and is a measure of the strength of the inhibitory effect of the tested substance.

As a parameter for assay quality, the Z'-factor (Zhang et al., *J. Biomol. Screen.* 2:67-73, 1999) for the low and high controls of each assay plate was used. The Z'-factors for this project did not drop below 0.44 and were above 0.6 in most cases, indicating a good to excellent assay quality.

The substances in this work were tested against the Brk and HER2 kinases. The determination of IC₅₀ values were performed *via* double measurements.

IC₅₀ values represent the arithmetic mean of the two measurement values obtained for a single substance measurement in each case.

Results of 4-phenylamino- α -carboline derivatives:

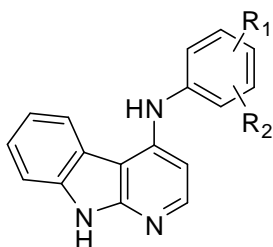


Fig. 53. Derivatives 11-29.

<i>R</i> ₁	<i>R</i> ₂	<i>Product</i>
2-CH ₃	H	11
3-OH	H	12
3-OMe	H	13
3-OEt	H	14
3-Cl	H	15
3-CF ₃	H	16
3-SCH ₃	H	17
3-OBn	H	18
3-NO ₂	H	19
4-Cl	H	20
4-OMe	H	21
3-Cl	5-Cl	22
3-Cl	4-CH ₃	23
3-Cl	4-F	24
3-OEt	4-Br	25
3-Cl	4-OBn	26
3-OMe	4-Br	27
1-Naphthylamine		28
3-NH ₂	H	29

Table 4. Substitutions of compounds 11-29.

#	<i>IC</i> ₅₀ value [nM]																		
	11	12	13	14	15	16	17	18	19	20	21	22	23	24	25	26	27	28	29
Brk	<i>n.a.</i>	3.2	<i>n.a.</i>	155	4.8	59.4	<i>n.a.</i>	40.7	5.7	<i>n.a.</i>	190	53.4	75	70	154	64.5	4.4	44	<i>n.a.</i>
HER2	978	1300	279	20100	65.5	1640	2270	2000	233	310	>10000	<i>n.a.</i>	6600	600	2420	120	628	800	148

n.a.: not active (*IC*₅₀ > 100 μ M)

Table 5. Results of 4-phenylamino- α -carboline derivatives 11-29.

Investigation of the nineteen 4-substituted phenylamino- α -carboline derivatives highlighted the potent inhibitory activity of this series against Brk and a comparative low effect against HER2. Despite the large structural homogeneity

within this series, no uniform selectivity profile towards both kinases was observed for the tested compounds. This difference is thought to be owing to the difference in the type and position of substitution on the 4-phenylamino ring of the α -carboline base structure. Resulting IC_{50} values were in nanomolar scales which emphasize the innovative character of these compounds as potent inhibitors of breast cancer-relevant kinases. Amongst the 19 tested substances we found four subcategories: potent Brk inhibitors with a relatively moderate selectivity towards HER2 such as the 3-hydroxy- (**12**), 3-chloro- (**15**), 3-nitro- (**19**) and 3-methoxy-4-bromo derivative (**27**) with IC_{50} values against Brk of 3.2, 4.8, 5.7 and 4.4 nM, respectively. Compound **15** shows also a strong inhibitory effect against HER2 with an IC_{50} value of 65.5 nM, thus it can be considered as a dual inhibitory active structure. The second class comprises the selective HER2 inhibitors which show no activity against Brk such as the 3-amino- (**29**), 3-methoxy- (**13**), 4-chloro- (**20**) and 2-methyl-derivative (**11**) which exhibit moderate IC_{50} values of 0.148, 0.279, 0.31 and 0.978 μ M, respectively. Moreover, 3,5-dichloro-derivative (**22**) was the only one which shows selective inhibitory activity against Brk ($IC_{50} = 53.4$ nM) while no activity was perceived for HER2. Finally, the rest of the tested compounds in this series present relatively moderate activities against both Brk and HER2 kinases with different nanomolar values.

SAR demonstrates that substitution on *m*-position of the 4-phenylamino residue could improve the activity and selectivity of the products especially towards Brk as shown in **12**, **15** and **19**. In case of **27** the situation was different, relative to **13** it was clear that the potency against Brk is due to the *p*-bromine substitution and not because of the *m*-methoxy group.

Evaluation of the inhibitory activity for the bis-acetylated compound **32** allowed investigating the influence of the *N*-9 acetylation on Brk/HER2 inhibition. The compound showed a comparatively low inhibitory effect against both kinases with IC_{50} values of 923 and 15400 nM for Brk and HER2 respectively and thus indicating the importance of the free NH-9 in binding properties towards both kinases. Accordingly, in our further synthesizing strategy we were more cautious not to substitute the *N*-9 position of the main α -carboline structure.

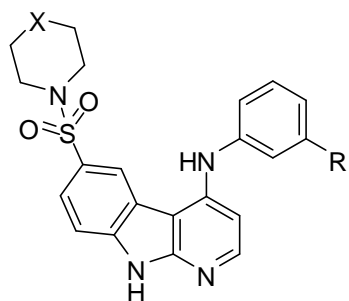
Results of 6-sulfonamide-4-phenylamino- α -carboline:

Fig. 54. 6-Sulfonamide derivatives 37-40 & 42-46.

<i>X</i>	<i>R</i>	<i>Product</i>
O	OH	37
O	OMe	38
O	OEt	39
O	OBn	40
NH	OMe	42
NH	OEt	43
NCH ₂ CH ₂ OH	OMe	44
NCH ₂ CH ₂ OH	OEt	45
NCH ₂ CH ₂ OH	OH	46

Table 6. Substitution of sulfonamide derivatives.

#	<i>IC</i> ₅₀ value [nM]								
	37	38	39	40	42	43	44	45	46
Brk	<i>n.a.</i>	5.8	410	55.2	4.8	26.2	9.2	479	<i>n.a.</i>
HER2	298	1240	54800	28300	390	576	629	6530	376

n.a.: not active (*IC*₅₀ > 100 μM)

Table 7. Results of 6-sulfonamide 4-phenylamino- α -carboline derivatives.

Investigation of the first 6-substituted α -carboline, 6-sulfonamides, shows improvement in the inhibition activity profile of this series against Brk and/or to some extent towards HER2. It was remarkable that the presence of methoxy function in *m*-position for all three sub-series, morpholino (**38**), piperazino (**42**) and ethanolpiperazino (**44**), contributes to a potent selectivity towards Brk with *IC*₅₀ values of 5.8, 4.8 and 9.2 nM, respectively. *m*-Hydroxy substitution in both **37** and **46** shows a loss of activity against BRK whereas, a relatively good sub-micromolar inhibitory action for HER2, *IC*₅₀ = 0.298 μM and 0.376 μM. Additionally, the presence of large *m*-substitutions of the 4-phenylamino moiety such as ethoxy or benzyloxy functions displays a moderate inhibitory effect comparing to the small substituted active groups (OMe or OH). Furthermore, these results clearly show that the addressing of polar substituents to the 6-position of the basic α -carboline structure plays an important role in renovating the inhibitory profile of the tested compounds.

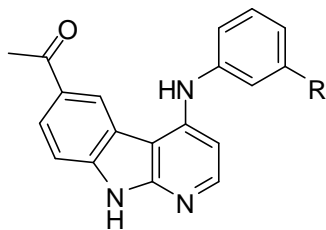
Results of 6-acetyl-4-phenylamino- α -carboline derivatives:

Fig. 55. Derivatives 48, 49 and 51.

<i>R</i>	<i>Product</i>
OH	48
NO ₂	49
NH ₂	51

Table 8. Substitution of 48, 49 and 51.

#	<i>IC</i> ₅₀ value [nM]		
	48	49	51
<i>Brk</i>	<i>n.a.</i>	21	7.6
<i>HER2</i>	12.8	801	1670

n.a.: not active (*IC*₅₀ > 100 μM)

Table 9. Results of 6-acetyl derivatives 48, 49 and 51.

Persuasive selectivity against HER2 was shown by compound **48** with *IC*₅₀ = 12.8 nM without any inhibitory effect for Brk. In contrast, compounds **49** and **51** show a potent activity towards Brk, 21 nM and 7.6 nM, with a relatively moderate activity versus HER2 with *IC*₅₀ values of 0.801 μM and 1.67 μM, respectively.

From these results, compound **48** could be a precursor for further investigations and modifications to improve the selectivity profile against HER2.

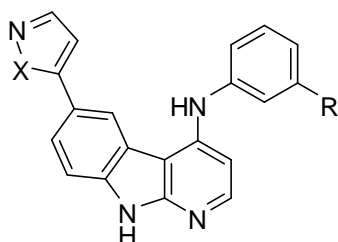
Results of 6-heterocycle-4-phenylamino- α -carbolines:

Fig. 56. Derivatives 59, 60, 63 and 64.

<i>X</i>	<i>R</i>	<i>Product</i>
NH	OH	59
NH	Cl	60
O	OH	63
O	Cl	64

Table 10. Substitutions of compounds 59, 60, 63 & 64.

#	<i>IC</i> ₅₀ value [nM]			
	59	60	63	64
<i>Brk</i>	< 3	3.85	< 3	9.15
<i>HER2</i>	429	91.6	642	851

Table 11. Results of 6-heterocyclic substituted derivatives **59**, **60**, **63** & **64**.

Inevitable, introduction of different hydrophilic heterocyclic rings into the 6-position of the α -carboline basic body was shown to influence the binding activity and selectivity of this series of derivatives towards both kinases, especially Brk.

From the obtained results, compounds **59** and **63** are considered as novel potent inhibitors against Brk with excellent *IC*₅₀ values (both < 3 nM) and with a relatively moderate HER2 activity (*IC*₅₀ = 0.429 μ M and 0.642 μ M, respectively). Moreover, compound **60** shows a potent inhibitory effect against Brk, *IC*₅₀ = 3.85 nM, as well a strong activity towards HER2 with *IC*₅₀ value of 91.6 nM. Thus, derivative **60** could be considered to have a dual inhibitory profile for both targeted breast cancer-relevant kinases. Substance **64** also shows a strong activity against Brk (*IC*₅₀ = 9.15 nM) with a reasonably moderate sub-micromolar HER2 inhibition effect (*IC*₅₀ = 0.851 μ M).

SAR investigations regarding to this series illustrate that the presence of hydrophilic residues at the 6-position presumes to augment the ATP-binding activity and hence increases the selectivity effect towards the targeted kinases. In addition, the presence of *m*-hydroxy substitution on the 4-phenylamino moiety demonstrates an excellent binding activity and well-developed selectivity of compounds **59** and **63** against Brk.

These four derivatives, **59**, **60**, **63** and **64**, open the itinerary for further investigations as excellent novel Brk inhibitors with strong pharmaceutical approaches.

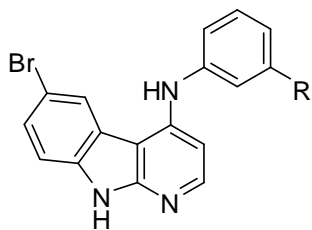
Results of 6-bromo-4-phenylamino- α -carboline derivatives:

Fig. 57. 6-Bromo derivatives 69-72.

<i>R</i>	<i>Product</i>
OH	69
Cl	70
NO ₂	71
OMe	72

Table 12. Substitution of derivatives 69-72.

#	<i>IC</i> ₅₀ value [nM]			
	69	70	71	72
Brk	<i>n.a.</i>	12.7	4.08	186
HER2	29.3	1150	8830	91200

n.a.: not active ($IC_{50} > 100 \mu M$)

Table 13. Results of 6-Bromo derivatives 69-72.

Introduction of bromine to the 6-position of the α -carboline structure affects the inhibitory activity profile with different outcomes concerning to both Brk and HER2.

Compound **69** shows a potent inhibitory as well as selectivity against HER2 with an IC_{50} value of 29.3 nM whereas no activity has been observed towards Brk. By replacing the hydroxyl group at the *m*-position with a chlorine moiety (**70**), the activity outline of the formed structure was changed. An increased inhibitory tendency towards Brk was noticed with an IC_{50} value of 12.7 nM, while the activity against HER2 was dropped off to micromolar value of 1.15 μM . High affinity towards Brk was demonstrated by the introduction of the *m*-nitro function of derivative **71** which shows potent inhibitory and selectivity effects for Brk with a low IC_{50} value of 4.08 nM. In case of compound **72**, the reactivity towards Brk was in a comparatively moderate sub-micromolar range with an IC_{50} value 0.186 μM and with a weak or nearly no activity towards HER2 ($IC_{50} = 91.2 \mu M$).

For further inspections on the α -carboline basic structure, we also examined the 6,8-disubstituted derivatives to estimate the pharmacological effects of these substitutions against both targeted kinases.

Results of 6,8-dibromo-4-phenylamino- α -carboline derivatives:

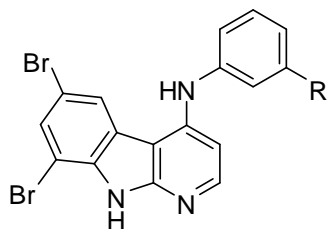


Fig. 58. 6,8-Bibromo-derivatives 73-76.

<i>R</i>	<i>Product</i>
OH	73
Cl	74
NO ₂	75
OMe	76

Table 14. Substitutions of compounds 73-76.

#	<i>IC₅₀ value [nM]</i>			
	73	74	75	76
<i>Brk</i>	550	11600	95.9	33.9
<i>HER2</i>	16300	30000	523	7450

Table 15. Results of 6,8-bibromo derivatives 73-76.

Unpredictably, the dibrominated α -carboline derivatives results did not match with our previously probable expectations.

Compounds **75** and **76** displayed a relatively moderate nanomolar inhibitory activity against Brk with IC_{50} values of 95.9 nM and 33.9 nM, respectively, while they showed an inhibition activity for HER2 in a micromolar scale with IC_{50} values equal to 0.523 μ M and 7.45 μ M, respectively. Derivative **73** reveals some inhibitory effect concerning Brk with a sub-micromolar value, 0.55 μ M, and a weak affinity towards HER2 (IC_{50} = 16.3 μ M). On the other hand, compound **75** showed the lowest affinity against both embattled kinases.

From the attained results of this series, it was clear that introduction of one more bromine atom to 8-position of the 6-monobromo α -carboline structure did not improve the inhibitory nor selectivity towards the targeted kinases, Brk and HER2, but only provide relatively moderate to low activity outcomes.

Results of 6-nitro- and 6-amino-4-phenylamino- α -carboline derivatives:

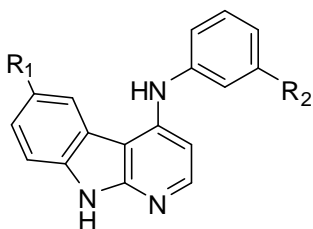


Fig. 59. Compounds 87-92.

R_1	R_2	Product
NO ₂	OH	87
NO ₂	Cl	88
NO ₂	OMe	89
NO ₂	OBn	90
NH ₂	OH	91
NH ₂	Cl	92

Table 16. Substitutions of derivatives 87-92.

#	IC_{50} value [nM]					
	87	88	89	90	91	92
Brk	< 3	13.2	6.1	132	3.3	61.4
HER2	1690	1370	13300	9810	7650	1990

Table 17. Results of compounds 87-92.

Potent inhibitory and selectivity effects were obtained from this series. Starting with both the 6-nitro derivative **87** and its reduced form, the 6-amino derivative **91**, we observed a strong inhibition activity towards Brk with low nanomolar IC_{50} values of < 3 nM and 3.3 nM, respectively, turning over the Brk inhibitory activity of compound **89** with IC_{50} of 6.1 nM. Those three compounds, **87**, **89** and **91**, exhibited a moderate activity for HER2 in a micromolar scale with IC_{50} values of 1.69 μ M, 13.3 μ M and 7.65 μ M, respectively. Derivative **88** shows a relatively moderate inhibitory effect towards Brk (IC_{50} = 13.2 nM) with a micromolar inhibitory value of 1.37 μ M for HER2. The reduced 6-amino derivative **92** similar to its 6-nitro analogue **88** shows a relatively moderate effect with an IC_{50} value of 61.4 nM and a weak activity against HER2 (IC_{50} = 1.99 μ M).

Results of 6,8-dinitro-4-phenylamino- α -carboline derivatives:

For more explorations we examined the 6,8-dinitro α -carboline derivatives in order to investigate the effect of the introduction of a 8-nitro moiety on both inhibitory and selectivity profiles.

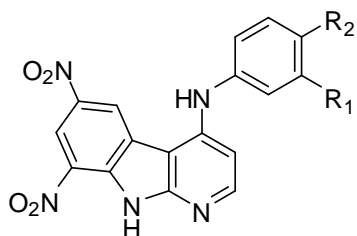


Fig. 60. 6,8-Dinitro derivatives 93-95.

R_1	R_2	Product
OH	H	93
Cl	H	94
OMe	Br	95

Table 18. Substitutions of compounds 93, 94 and 95.

#	IC_{50} value [nM]		
	93	94	95
Brk	< 3	104	13
HER2	24700	631	n.a.

n.a.: not active ($IC_{50} > 100 \mu\text{M}$)

Table 19. Results of 6,8-dinitro α -carboline derivatives 93, 94 and 95.

Surprisingly, the introduction of one more nitro group in the 8-position of the α -carboline differs from what happened in the case of the 8-bromine substitution.

The dinitro derivatives exhibited also a potent inhibitory and selectivity affinity especially against Brk. The most powerful and selective activity was recorded for the *m*-hydroxy substituted derivative **93** with a low IC_{50} value of < 3 nM concerning Brk, whereas it had a weak affinity towards HER2 ($IC_{50} = 24.7 \mu\text{M}$). A dual inhibitory effect was revealed by compound **94** which shows a sub-micromolar IC_{50} value against both Brk and HER2, 0.104 μM and 0.631 μM , respectively. On the other hand, derivative **95** displayed a relatively good inhibitory profile with a very high selectivity towards Brk with an IC_{50} value of 13 nM.

Results of the 60-cell-line-screenings

For further investigations, some of the synthesized substances in this work were examined in the context of the 60-cell-line screenings of the Developmental Therapeutics Program (DTP) of the National Cancer Institute (NCI, NIH, Bethesda, Maryland, USA) to identify the possible human cytostatic effect on tumor cell lines. The NCI-selected compounds on the basis of the kinase observed activity are shown in figure 61.

The 60-cell-line of the NCI screening comprises 60 different tumor cell lines, which are originated from nine different organs or tumor types (lung, colon, breast, ovaries, kidney, prostate, central nervous system, as well as melanoma and leukemia).¹⁵² The screening method consists of two stages: In the first stage of the screening, the one-dose screening, each cell line is incubated for 48 h with the respective tested substance in a concentration of 10 μ M. End point determinations were made with a protein binding dye, sulforhodamine B. Subsequently, a mean graph is obtained of the percent growth of the treated cells when compared to the untreated control cells. This relation is expressed as a percentage value (Growth Percent). Accordingly, once this value is less than 100 means that the substance exerts an inhibitory effect on the growth of the respective cell line, whereas when the value is more than 100 it points to a growth-stimulating effect. If the value is negative, this means that the cell number has shrunk during the incubation with the tested substance. Therefore, this substance exerts a cytotoxic effect to the cells of the particular cell line. The average cell growth rate (Mean Growth Percent) is given by calculating the impact on the individual cell lines except the growth percent value. To facilitate the evaluation and the graphic presentation of the test results, the mean growth percent value and the deviation of the growth percent values of each cell line from this value are displayed in a bar chart.

In figure 62, a bar chart example of the one-dose screening is shown for compound **69**.

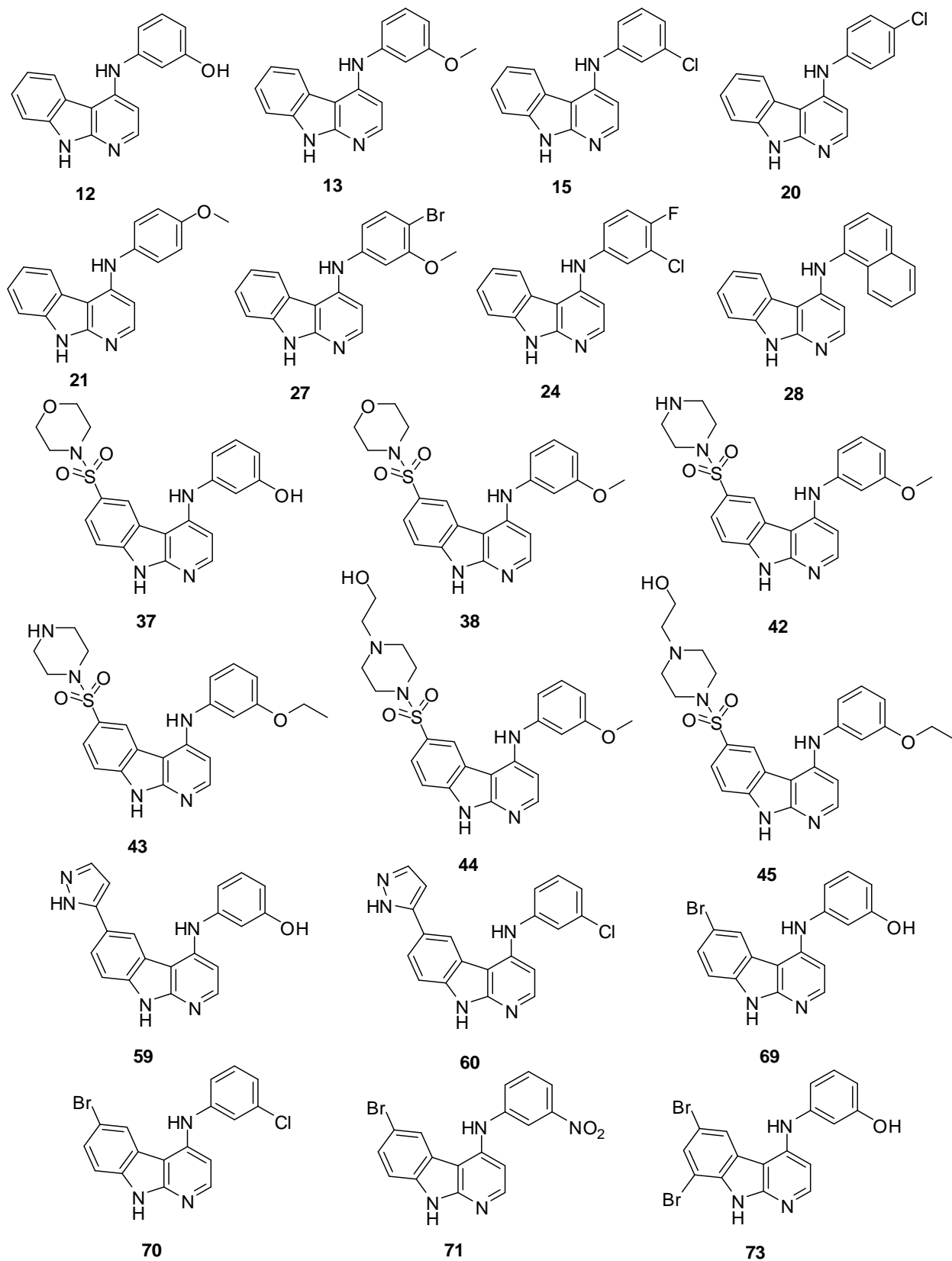


Fig. 61. Selected twenty compounds by NCI for one-dose 60-cell-line-screening

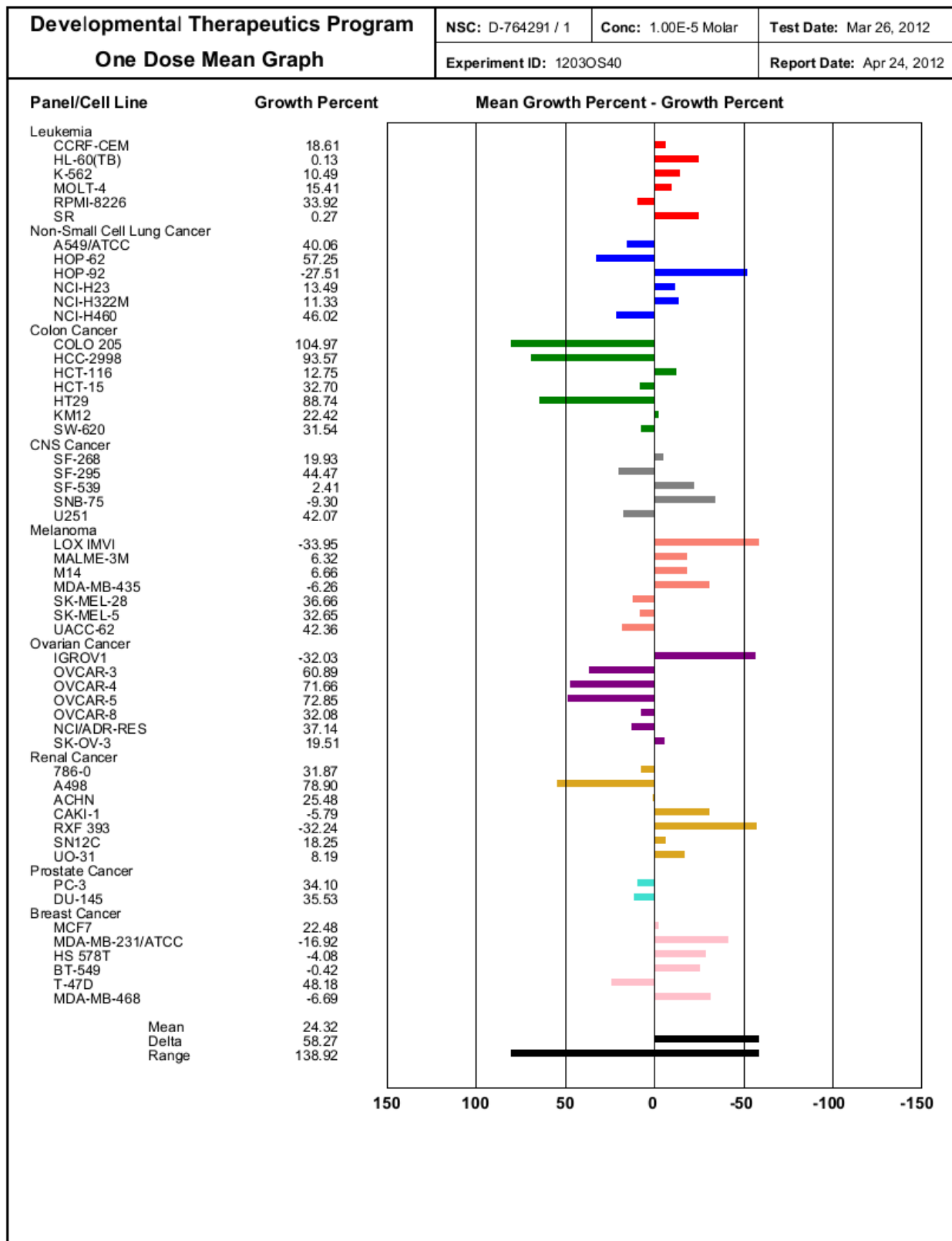


Fig. 62. Results of one-dose-screenings for compound 69

In this diagram, the mean growth percent value is the central vertical axis of the graph. Pointing to the right bars indicate that the individual cell line is more sensitive to the tested substance as the average, left-pointing bars represent accordingly for less sensitivity of the cell line. The length of the beam is the size of the deviation of the value of the mean proportional. Based on the data obtained in the first stage of the assay, analysis was performed by the Development Therapeutics Programme (DTP). Hence, the NCI decides whether the respective tested substance is investigated in the next screening stage, the five-dose screening. If the decision is positive, then the selected substance is tested again in the manner described above against the 60 cell lines, but the substance was administered in five different concentrations (10 nM to 100 μ M), and thus a dose-response curve is determined for each cell line. Subsequently, the outcomes were used to create log concentration versus % growth inhibition curves and three response parameters (GI_{50} , TGI and LC_{50}) were calculated for each cell line. the GI_{50} value (growth inhibition 50%), which describes the molar concentration of the tested substance that causes 50% inhibition of cell growth, the TGI value (total growth inhibition), which describes the concentration of tested compound which causes complete inhibition of cell growth, and the LC_{50} (lethal concentration 50%), which expresses the concentration of the tested substance that causes the death of 50% of the initially present cells. In other words, the three characteristic parameters can be used as an indication for growth inhibitory activity (GI_{50}), cytostatic activity (TGI) and cytotoxic activity (LC_{50}) of the investigated compound at the end the of incubation time of 48 h. The average of the decadic logarithmic values for each of the three parameters is calculated over all cell lines, which is called the Mean graph midpoint (MG-MID). The criterion for selectivity of a compound depends upon the ratio obtained by dividing the full panel MID (the average sensitivity of all cell lines toward the test agent) by their individual subpanel MID (the average sensitivity of all cell lines of a particular subpanel toward the test agent). Ratios between 3 and 6 refer to moderate selectivity; ratios greater than 6 indicate high selectivity toward the corresponding cell line, while compounds not meeting either of these criteria are rated non-selective.¹⁵³

In the course of interpreting the obtained results from the NCI, we focused our attention onto the data with respect to the breast cancer subpanel cell lines recorded values more than other cancer panels in order to explore the activity and selectivity of the selected compounds with regards to breast cancer cells.

Results of one-dose screenings:

Twenty derivatives had been selected to interrogate the NCI60 anticancer drug screening program.¹⁵⁴ With respect to our concern in breast cancer cell lines; we made a comparison between the obtained overall mean growth percent values for the twenty one-dose screening tested compounds with calculated mean growth percent values only for breast cancer cell lines. (Table 20)

<i>Compounds</i>	<i>Overall Mean Growth %</i>	<i>Breast cancer-Mean Growth %</i>	<i>Selected for 5-dose screening</i>
12	47.29	29.20	<i>Selected</i>
13	36.53	23.48	<i>Selected</i>
15	72.46	64.86	<i>Non selected</i>
20	64.95	56.05	<i>Non selected</i>
21	50.22	26.29	<i>Selected</i>
24	65.63	64.69	<i>Selected</i>
27	56.05	43.03	<i>Selected</i>
28	27.37	24.41	<i>Selected</i>
37	73.80	68.43	<i>Selected</i>
38	86.28	83.55	<i>Non selected</i>
42	90.86	83.85	<i>Non selected</i>
43	100.45	102.26	<i>Non selected</i>
44	89.41	83.49	<i>Non selected</i>
45	93.46	77.96	<i>Non selected</i>
59	102.05	102.28	<i>Non selected</i>
60	91.40	99.87	<i>Non selected</i>
69	24.32	7.09	<i>Selected</i>
70	24.46	35.29	<i>Selected</i>
71	62.97	60.59	<i>Selected</i>
73	54.36	49.45	<i>Selected</i>

Table 20. Results of one-dose screenings.

The average strongest cytostatic effects were scored for compounds **69**, **70** and **28** with a mean growth of 24.32%, 24.46% and 27.37% respectively. Compound **69** exhibited the highest growth inhibition activity concerning breast cancer cell lines, MCF7 (22.48%), MDA-MB-231/ATCC (-16.92%), HS 578T (-4.08%), BT-549 (-0.42%), T-47D (48.18%) and MDA-MB-468 (-6.69%), in addition to its previously reported potent HER2 inhibitory profile with IC₅₀ value of 29.3 nM. Compounds **70** and **28** also showed a good nanomolar inhibitory activity in the kinase assay. Some compounds displayed a good to moderate cytostatic activity

such as **12**, **13**, **21**, **24**, **27**, **37**, **71** and **73** with an overall mean growth percent range from 36.53 to 73.80% and had been selected for further study *via* the five-in-box screenings. As shown in table 20, all abovementioned compounds demonstrate comparatively lower mean growth percent values for the breast cancer cell lines subpanel if compared to the overall values of the 60-cell lines. This indicates their higher cytostatic activity against these particular cell lines and is compatible with their reported kinase inhibitory effects.

Moderate activities were recorded for compounds **15**, **20**, **38**, **42**, **44**, **45** and **60** with relatively high overall mean growth percent rates (64.9 to 93.46%) as well as high breast cancer growth values from 56.05 to 99.87%. Interestingly, derivatives **15**, **38**, **42**, **44** and **60** had been reported previously to be particularly potent in the kinase assay.

Both derivatives **43** and **59** were inactive in the one-dose screening cell panels with an overall mean growth percent $> 100\%$ (100.45% and 102.05% respectively), nevertheless compound **59** showed a very strong inhibition of Brk ($IC_{50} < 3$ nM) and HER2 ($IC_{50} = 0.429$ μ M).

Results of five-dose screenings

After obtaining the results of the one dose assay, an analysis was achieved by Development Therapeutics Programme (DTP) and eleven compounds which satisfied predetermined as effective inhibition criteria were selected for further NCI full panel 5-dose assays.

In the five-dose screening specific parameters, log GI_{50} , log TGI and log LC_{50} were determined for these 11 substances and are summarized in Table 21. Additionally, the corresponding values for nine well-known cytostatic drugs are also listed eligible for comparison. These drugs had been previously tested in the five-dose screening and are currently used as anti-breast cancer therapies in clinic such as dasatinib (Sprycel[®]), lapatinib (Tykerb[®]), raloxifene (Evista[®]), tamoxifen (Nolvadex[®]), capecitabine (Xeloda[®]), irinotecan (Camptosor[®]), cisplatin (Platinol[®]), paclitaxel (Taxol[®]) and vincristin (Oncovin[®]). The three parameter values of these drugs could be purchased through the website of the DTP.¹⁵⁵ For a better description of the parameters and to make them more intuitively accessible, the values are not only given in a logarithmic way but also in the respective non-logarithmic form.

<i>Products</i>	<i>Overall MG-MID</i>					
	<i>Log GI₅₀</i>	<i>GI₅₀</i>	<i>Log TGI</i>	<i>TGI</i>	<i>Log LC₅₀</i>	<i>LC₅₀</i>
12*	-5.49	3.24 μ M	-4.79	16.2 μ M	-4.24	57.5 μ M
	-5.58	2.63 μ M	-4.74	18.2 μ M	-4.18	66.1 μ M
13	-5.58	2.63 μ M	-4.29	51.3 μ M	-4.0	100 μ M
21	-5.33	4.68 μ M	-4.06	87.1 μ M	-4.0	100 μ M
27	-5.32	4.79 μ M	-4.63	23.4 μ M	-4.1	79.4 μ M
24	-5.16	6.92 μ M	-4.1	79.4 μ M	-4.01	97.7 μ M
28	-5.66	2.19 μ M	-4.74	18.2 μ M	-4.1	79.4 μ M
37*	-5.0	10.0 μ M	-4.32	47.9 μ M	-4.03	93.3 μ M
	-5.03	9.33 μ M	-4.3	50.1 μ M	-4.06	87.1 μ M
69*	-5.67	2.14 μ M	-5.0	10.0 μ M	-4.27	53.7 μ M
	-5.66	2.19 μ M	-4.92	12.0 μ M	-4.23	58.9 μ M
70	-4.85	14.1 μ M	-4.08	83.2 μ M	-4.0	100 μ M
71	-5.83	1.48 μ M	-4.29	51.3 μ M	-4.01	97.7 μ M
73	-4.9	12.6 μ M	-4.43	37.2 μ M	-4.1	79.4 μ M
<i>Dasatinib</i>	-6.48	0.33 μ M	-5.09	8.19 μ M	-4.3	53.0 μ M
<i>Lapatinib</i>	-5.53	2.98 μ M	-4.62	23.9 μ M	-4.2	65.9 μ M
<i>Raloxifene</i>	-5.08	8.29 μ M	-4.5	28.2 μ M	-4.1	71.8 μ M
<i>Tamoxifen</i>	-5.4	3.94 μ M	-4.97	10.8 μ M	-4.5	29.3 μ M
<i>Capecitabine</i>	-4.1	80.4 μ M	-4.0	100 μ M	-4.0	100 μ M
<i>Irinotecan</i>	-4.85	14.1 μ M	-4.22	60.3 μ M	-4.02	95.5 μ M
<i>Cisplatin</i>	-5.68	2.09 μ M	-5.62	2.4 μ M	-5.6	2.51 μ M
<i>Paclitaxel</i>	-7.62	24.0 nM	-6.34	457 nM	-6.05	891 nM
<i>Vincristin</i>	-8.35	4.0 nM	-6.19	646 nM	-5.19	6.46 μ M

* Compounds 12, 37 and 69 had been selected by the NCI for second five-dose screenings.

Table 21. Results of the five-dose screenings for the 11 selected compounds

Compounds under investigation, **12, 13, 21, 24, 27, 28, 37, 69, 70, 71** and **73** exhibited an overall significant anticancer activity against most of the tested cell lines representing nine different subpanels. From the summarized results in Table 21, seven compounds had average GI₅₀ responses at low micromolar concentrations (1.48 - 4.79 μ M), whereas the remaining 4 compounds showed GI₅₀ values ranging from 6.92 to 14.1 μ M. Cytostatic effect (TGI) was also presented in values ranging from relatively good to moderate micromolar averages (10 – 87.1 μ M). Finally, the average cytotoxic effects (LC₅₀) on tested cell panels displayed a wide range from 53 μ M to 100 μ M and are considered as superior results regarding to the corresponding obtained GI₅₀ concentrations.

Results & Discussion

Focusing on our main work interest, the breast cancer subpanel, we summarized the sensitivity (GI_{50}), cytostaticity (TGI) and cytotoxicity (LC_{50}) of the tested substances towards particular breast cancer cell lines. Selectivity of test compounds, in comparison with lapatinib (Tykerb[®]), has been also estimated pertaining to these individual panel cells. Depending on the ratio obtained by dividing the full panel (overall MID or MID^a) by their individual subpanel (subpanel MID or MID^b), the decisive factor for selectivity was calculated, as shown in Table 22.

Product	Cell Line	GI_{50}	TGI	LC_{50}	MID^b	MID^a/MID^b
12	<i>MCF7</i>	891 nM	19.5 μ M	58.9 μ M	1.55	1.7
	<i>MDA-MB-468</i>	1.0 μ M	8.5 μ M	44.7 μ M		
13	<i>MCF7</i>	380 nM	>100 μ M	>100 μ M	0.97	2.7
	<i>MDA-MB-468</i>	214 nM	794 nM	>100 μ M		
21	<i>MCF7</i>	2.6 μ M	>100 μ M	>100 μ M	3.44	1.4
	<i>T-47D</i>	2.8 μ M	>100 μ M	>100 μ M		
27	<i>MCF7</i>	676 nM	16.6 μ M	>100 μ M	2.73	1.8
	<i>MDA-MB-468</i>	603 nM	4.3 μ M	>100 μ M		
24	<i>T-47D</i>	3.8 μ M	>100 μ M	>100 μ M	8.32	0.8
	<i>MDA-MB-468</i>	1.8 μ M	5.6 μ M	>100 μ M		
28	<i>MCF7</i>	1.2 μ M	7.4 μ M	50.1 μ M	1.92	1.1
	<i>T-47D</i>	1.2 μ M	6.9 μ M	>100 μ M		
	<i>MDA-MB-468</i>	1.1 μ M	5.8 μ M	>100 μ M		
37	<i>MDA-MB-231/ATCC</i>	1.5 μ M	9.1 μ M	>100 μ M	6.61	1.5
	<i>MDA-MB-468</i>	4.3 μ M	26.9 μ M	>100 μ M		
69	<i>MCF7</i>	437 nM	18.6 μ M	>100 μ M	1.19	1.8
	<i>HS 578T</i>	537 nM	5.6 μ M	>100 μ M		
70	<i>MCF7</i>	3.7 μ M	>100 μ M	>100 μ M	10.55	1.3
	<i>MDA-MB-468</i>	2.4 μ M	>100 μ M	>100 μ M		
71	<i>MCF7</i>	50 nM	>100 μ M	>100 μ M	0.89	1.7
	<i>T-47D</i>	851 nM	>100 μ M	>100 μ M		
	<i>MDA-MB-468</i>	282 nM	19.5 μ M	>100 μ M		
73	<i>MCF7</i>	10.7 μ M	27.5 μ M	70.8 μ M	13.28	0.9
	<i>MDA-MB-231/ATCC</i>	9.8 μ M	30.9 μ M	97.7 μ M		
Lapatinib	<i>MCF7</i>	2.0 μ M	6.3 μ M	25.1 μ M	2.07	1.4
	<i>MDA-MB-468</i>	13 nM	158 nM	3.2 μ M		

MID^a = Average sensitivity of all cell lines in μ M.

MID^b = Average sensitivity of all cell lines of a particular subpanel in μ M.

Table 22. The most remarkable results of the test compounds on cell lines of breast cancer panel.

According to the recapitulated data in Table 22, the test compounds exhibited a potent sensitivity profile towards breast cancer cell lines, especially; MCF7, MDA-MB-231/ATCC, HS 578T, T-47D and MDA-MB-468 with growth inhibition averages in micromolar to nanomolar concentrations.

Compounds **12**, **13**, **27**, **69** and **71** showed the strongest growth inhibitory effect regarding to the cell line MCF7 with GI₅₀ values of 891, 380, 676, 437 and 50 nM, respectively. While, derivatives **21**, **28**, **70** and **73** displayed micromolar GI₅₀ values from 2.6 μM to 10.7 μM. The promising potent activity for approximately all examined compounds with respect to the MCF7 cell line opens up the possibility to investigate their effect on both ER+/HER2⁻¹⁵⁶ and ER+/HER2⁺¹⁵⁷ breast cancer subtypes. A cytostatic activity was recorded for compounds **12**, **27**, **28**, **69** and **73** with a relatively good to moderate TGI values (7.4 μM to 27.5 μM), whereas the remnants showed no cytostatic affinity (TGI > 100 μM). Only three products (**12**, **28** and **73**) demonstrated a cytotoxic property to MCF7 cell line with high LC₅₀ values (58.9, 50.1 and 70.8 μM), while no cytotoxic activity was observed for the others (LC₅₀ > 100 μM).

MDA-MB-468 cell line showed also brilliant growth inhibitory results with compounds **13**, **27** and **71** in nanomolar average values of 214, 603 and 282 nM, respectively. In addition, compounds **12**, **24**, **28**, **37** and **70** also displayed a strong sensitivity profile with GI₅₀ extent from 1.0 μM to 4.3 μM. Compound **13** showed a nanomolar cytostatic affinity for the candidate cells, TGI = 794 nM, without any cytotoxicity effects. Derivative **27** as well as **71** exhibited a total growth inhibitory activity with TGI values of 4.3 μM and 19.5 μM, respectively. Remaining products, except **70**, presented a relatively low to moderate cytostaticity with values from 5.6 to 26.9 μM. All these derivatives showed a high LC₅₀ scale more than 100 μM excluding derivative **12** which displayed cytotoxicity in a value of 44.7 μM. It is known that MDA-MB-468 cells shows a strong overexpression of EGFR.¹⁵⁸ Screening the observed growth inhibition of the MDAMB-468 cells could therefore indicate the inhibition of EGFR in these cells and its efficacy in HER2+ breast cancer subtypes.

Conspicuously, all mentioned compounds, in this section, were shown to demonstrate an inhibitory activity against HER2 in the kinase assay, which may increase the opportunity for this inhibition mechanism.

Naturally expressed estrogen receptor T-47D cell line¹⁵⁹ had also a potent growth inhibition from compound **71** with a GI₅₀ value of 851 nM without any recorded cytostatic or cytotoxic activity. Moreover, products **21**, **24** and **28** exhibited strong micromolar growth inhibitory affinity with GI₅₀ values of 2.8, 3.8

and 1.2 μM , respectively. Nevertheless, neither cytostaticity nor cytotoxicity was detected in case of derivatives **21** and **24** whereas, compound **28** showed a cytostatic activity with a TGI value of 6.9 μM .

Both **37** and **73** presented to some extent a significant sensitivity towards the breast cancer cell line MDA-MB-321/ATCC with GI_{50} values of 1.5 μM and 9.8 μM respectively, cytostatic average of 9.1 μM and 30.9 μM , and high cytotoxic concentrations of > 100 and 97.7 μM , respectively.

Finally, compound **69** caused a forceful growth inhibition in nanomolar concentration (537 nM) concerning the cell line HS 578T, with a cytostatic effect (TGI equal to 5.6 μM) and looked like non cytotoxic product ($\text{LC}_{50} > 100 \mu\text{M}$). It has been reported in literature that the growth of HS-578T cells is largely driven by an autocrine signal that is mediated by EGFR and can be suppressed specifically with an EGFR-selective kinase inhibitor.¹⁶⁰ This authenticates the achieved protein kinase assay outcome which displays a high selectivity of **69** towards HER2 (29.3 nM).

As a consequence, the kinase inhibitory effect of the tested substances could be in a causal relationship with the acquired results in the cells growth-inhibiting effect by the NCI 60-cell line screenings (single and/or five-dose).

On the basis of the 60-cell-line screening data obtained, compounds **12**, **37** and **69** were passed to the "Biological Evaluation Committee" (BEC) of the NCI, which advises of possible further studies *via* second five-dose screenings. Corresponding results are shown in figures 63 and 64. Subsequently, both **37** and **69** have been approved by NCI-DTP for *in vivo* antitumor efficacy investigations.

Results & Discussion

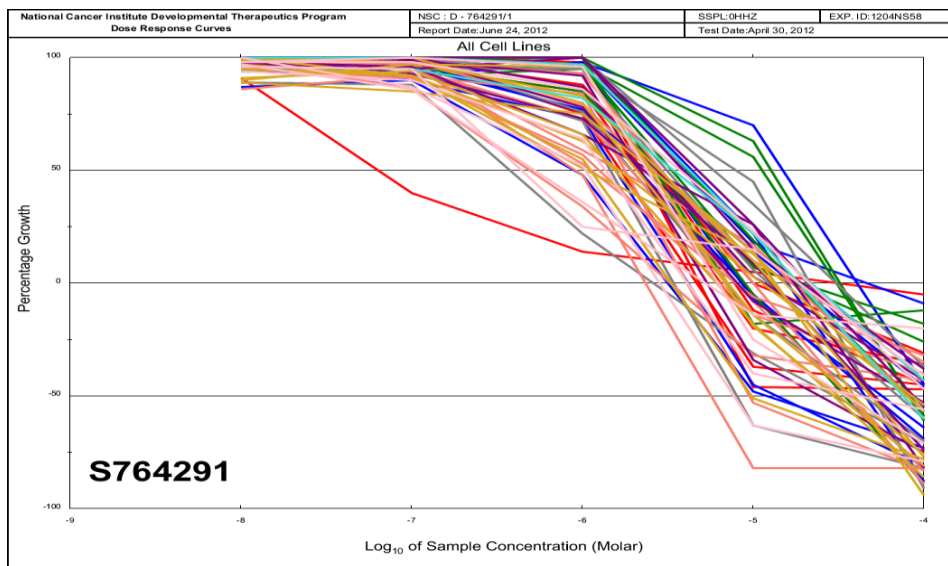
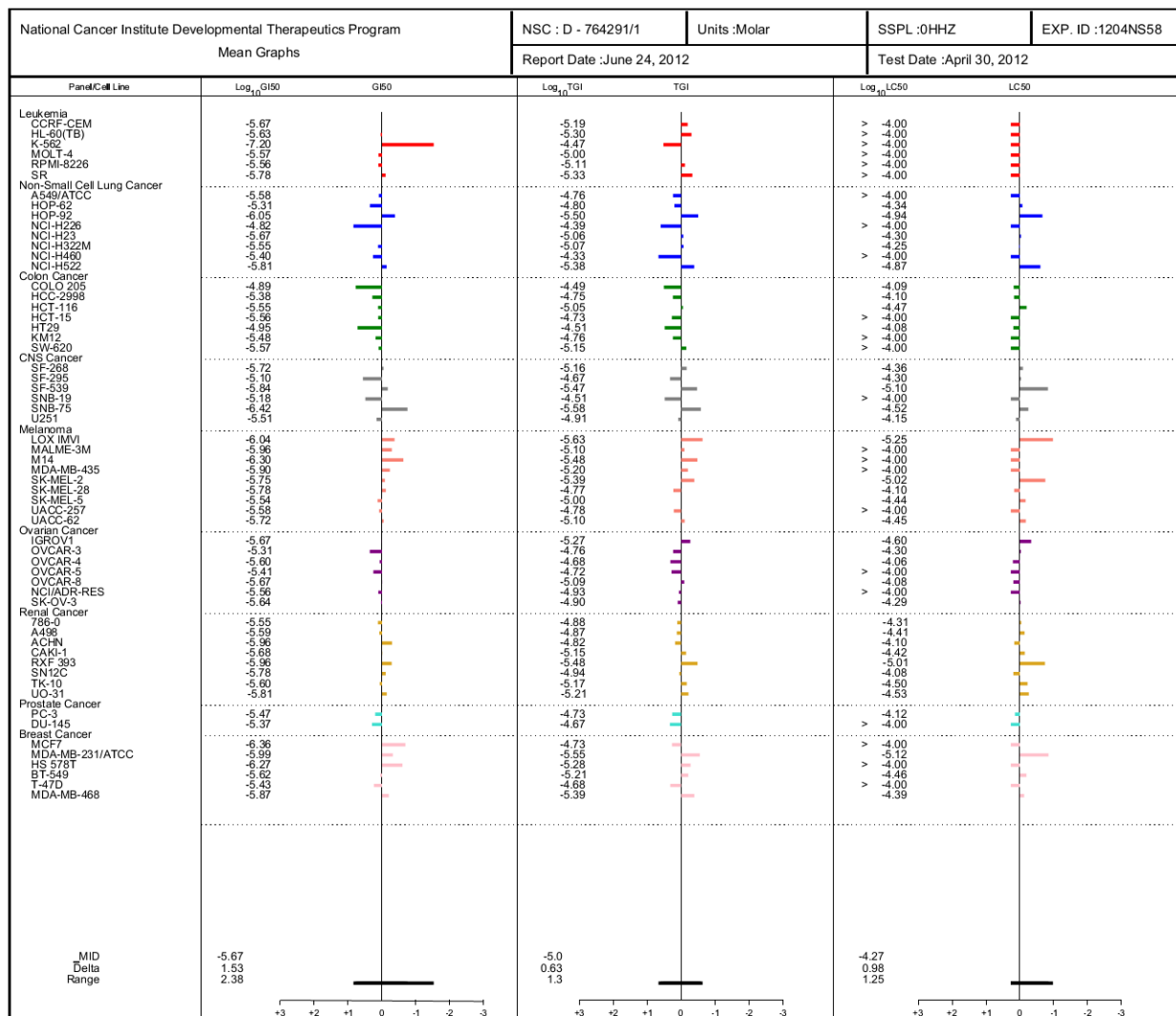


Fig. 63. NCI five-dose screening data obtained for compound 69.

Results & Discussion

National Cancer Institute Developmental Therapeutics Program		NSC : D - 764290/1		Units :Molar		SSPL:0HHZ		EXP. ID :1204NS58	
Mean Graphs		Report Date :June 24, 2012				Test Date :April 30, 2012			
Panl/Cell Line	Log ₁₀ GI50	GI50	Log ₁₀ TGI	TGI	Log ₁₀ LC50	LC50			
Leukemia									
CCRF-CEM	-4.75		-4.17		> -4.00				
HL-60(TB)	-4.72		-4.34		> -4.00				
K-562	-5.51		> -4.00		> -4.00				
MOLT-4	-4.88		-4.34		> -4.00				
RPMI-8226	-4.75		-4.35		> -4.00				
SR	-5.56		-4.78		> -4.00				
Non-Small Cell Lung Cancer									
A549/ATCC	-4.87		> -4.00		> -4.00				
HOP-62	-4.54		> -4.00		> -4.00				
HOP-92	-6.22		-5.38		> -4.00				
NCI-H226	-4.68		-4.07		> -4.00				
NCI-H23	-4.75		> -4.00		> -4.00				
NCI-H322M	-5.21		-4.32		> -4.00				
NCI-H522	-5.23		-4.45		> -4.00				
Colon Cancer									
COLO 205	-4.82		-4.53		-4.24				
HCC-2998	-4.68		-4.38		-4.07				
HCT-116	-4.98		-4.59		-4.19				
HCT-15	-4.23		> -4.00		> -4.00				
HT29	-4.67		-4.30		> -4.00				
KM12	-4.74		-4.33		> -4.00				
CNS Cancer									
SF-268	-4.95		> -4.00		> -4.00				
SF-295	-4.61		-4.05		> -4.00				
SF-539	-5.20		-4.59		-4.07				
SNB-19	-4.48		> -4.00		> -4.00				
SNB-75	-6.05		-5.28		> -4.00				
U251	-4.99		> -4.00		> -4.00				
Melanoma									
LOX IMVI	-5.58		-4.87		-4.42				
MALME-3M	-5.40		-4.40		> -4.00				
M14	-5.35		-4.63		-4.07				
MDA-MB-435	-4.97		> -4.00		> -4.00				
SK-MEL-2	-4.79		-4.39		> -4.00				
SK-MEL-28	-5.05		> -4.00		> -4.00				
SK-MEL-5	-4.82		-4.47		-4.13				
UACC-257	-5.09		-4.22		> -4.00				
UACC-62	-5.86		-5.38		-4.44				
Ovarian Cancer									
IGROV1	-5.61		-5.21		-4.22				
OVCAR-3	-4.70		-4.02		> -4.00				
OVCAR-4	-4.32		> -4.00		> -4.00				
OVCAR-5	-4.98		-4.20		> -4.00				
OVCAR-8	-4.89		> -4.00		> -4.00				
NCI/ADR-RES	> -4.00		> -4.00		> -4.00				
SK-OV-3	-4.83		> -4.00		> -4.00				
Renal Cancer									
786-0	-4.99		-4.33		> -4.00				
ACHN	-5.36		-4.07		> -4.00				
CAKI-1	-4.55		> -4.00		> -4.00				
RXF 993	-5.44		-4.75		-4.02				
SN12C	-5.09		> -4.00		> -4.00				
TK-10	-5.25		-4.61		-4.01				
UO-31	-4.90		-4.34		> -4.00				
Prostate Cancer									
PC-3	-4.87		> -4.00		> -4.00				
DU-145	-4.60		> -4.00		> -4.00				
Breast Cancer									
MCF7	-4.75		> -4.00		> -4.00				
MDA-MB-231/ATCC	-5.83		-5.04		> -4.00				
BT-549	-4.70		-4.12		> -4.00				
T-47D	-5.25		> -4.00		> -4.00				
MDA-MB-468	-5.37		-4.57		> -4.00				

MID	-5.0	-4.32	-4.03
Delta	1.22	1.06	0.41
Range	2.22	1.38	0.44

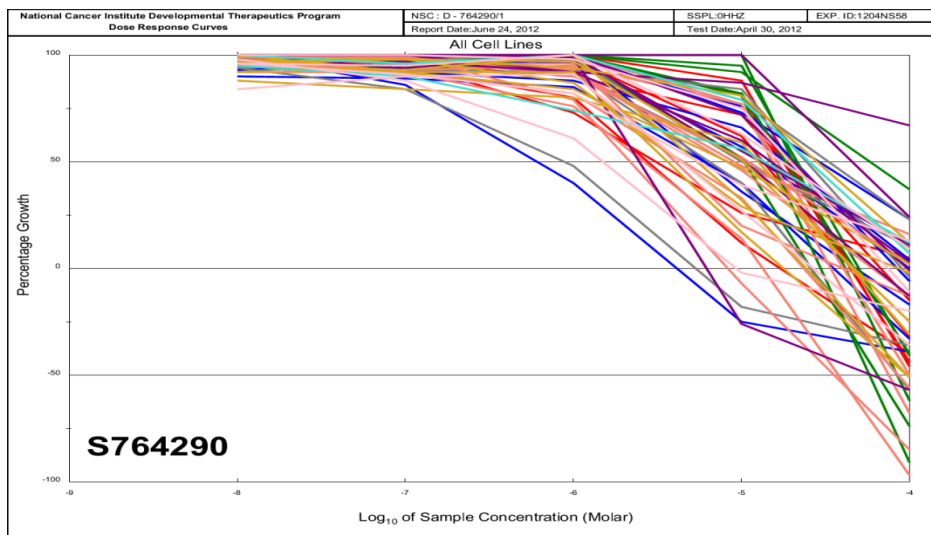


Fig. 64. NCI five-dose screening data obtained for compound 37.

Structure-Activity Relationship (SAR)

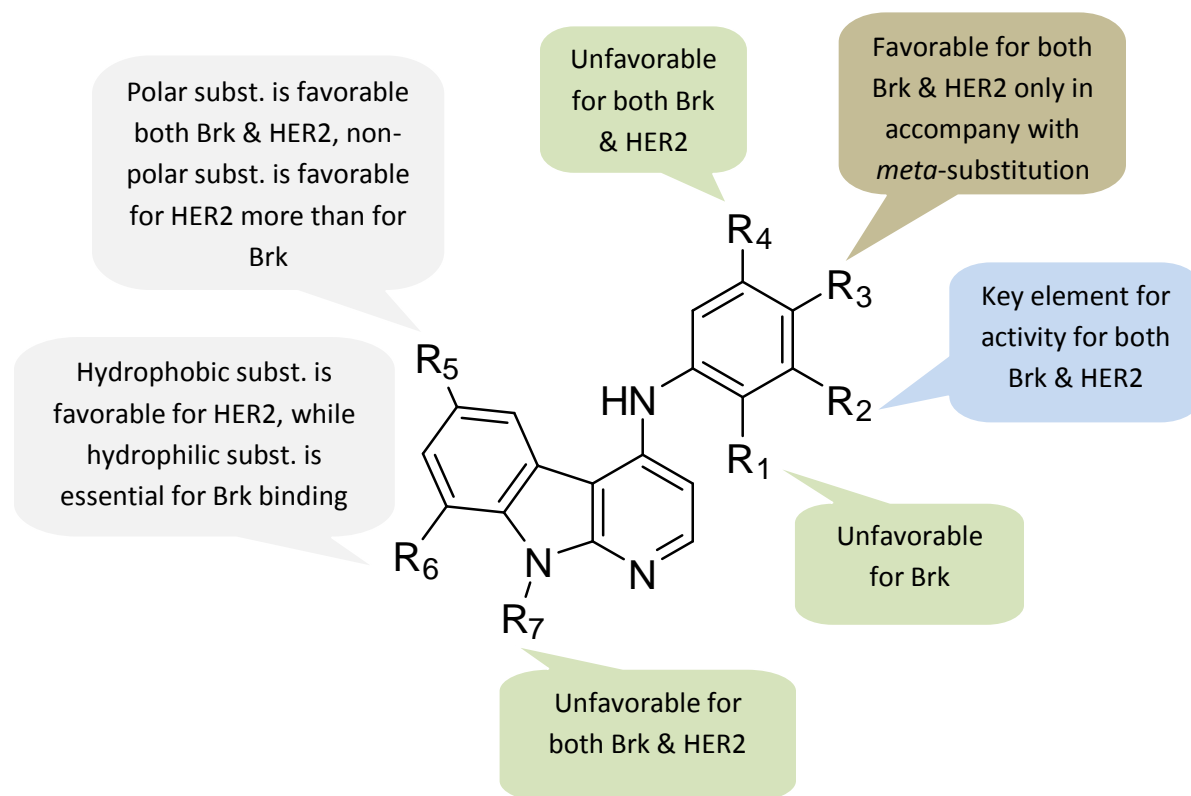


Fig. 65. Structure-Activity Relationship Summary.

Building upon the acquired *in vitro* survey data (affinity record), we can categorize the tested compounds into three classes according to the inhibitory profiles with respect to the varying substitution pattern. The first class is the series showed an improved inhibitory activity towards both Brk and HER2 target structures. Substitution at the *meta*-position as well as the *meta*- and *para*-positions of the 4-phenylamino moiety proved to be fundamental for increasing the sensitivity of the substances against both kinases. Moreover, it is clear that increasing the polarity by the introduction of a hydrophilic substituent (OH, NO₂, NH₂, etc), especially at *m*-position, boosts the potential affinity to hydrogen bond formation with the ATP-binding sites. In addition, *m*-chloro substitution ascertained to enhance the inhibitory effect, for example derivative **15** which exhibited a potent inhibition for Brk (IC₅₀= 4.8 nM) as well as for HER2 (IC₅₀= 65.5 nM). The second group displayed a high Brk selectivity as seen for compounds **89** and **95** in which the *m*-methoxy substitution on the 4-phenylamino moiety seems to improve Brk sensitivity. Furthermore, the introduction of another

nitro function at the 8-position to the mono 6-nitro derivative **87**, yielding compound **93**, indicates a selectivity development against Brk. Selective HER2 inhibitory activity recorded for both derivatives **48** and **69**, representing the third class, is estimated to be due to the essential 3'-hydroxy group as well as the 6-bromo and 6-acetyl substitution of the α -carboline core structure. Introduction of another bromo-substituent at position 8 to derivative **69** (**73**) showed increased affinity towards Brk with an abolition of HER2 selectivity.

A free 9-NH is thought to be crucial for the hydrogen bond formation with ATP-binding sites of target kinases. The acetylation of the α -carboline 9-N, as seen for compound **32**, is consequently unfavorable for both Brk and HER2.

Characteristic to sulfonamides substituted α -carboline series (**37-46**) are the *m*-substituents of the 4-phenylamino residue. In case of the 3'-hydroxy derivatives, they showed selectivity only with regard to HER2, whereas by replacing the hydroxyl group with a methoxy function a remarkable sensitivity to Brk is observed and affinity shrinkage is illustrated towards HER2. As an example, compound **37** only exhibited a submicromolar inhibitory concentration for HER2 ($IC_{50} = 0.298 \mu M$). Replacing the *m*-hydroxy group by a methoxy moiety yielded compound **38**, which displayed a potent Brk inhibitory effect with an IC_{50} value of 5.8 nM and a micromolar IC_{50} value of 1.24 μM for HER2.

Introduction of hydrophilic heteroaryl residues, pyrazoles and isoxazoles, into the 6-position of the α -carboline basic structure presented an important modification in order to amplify the sensitivity concerning both kinases, if compared to the corresponding 6-unsubstituted 4-phenylamino- α -carboline derivatives. For example, compounds **59** and **63** showed a potent activity towards Brk ($IC_{50} < 3$ nM) in comparison with the 6-unsubstituted derivative **12**, moreover the improved inhibitory effect against HER2.

In general, polar *m*-substitution of the 4-phenylamino moiety proved to be crucial for activity of the structure. Furthermore, introduction of a hydrophilic substituent to the 6-position as well as 8-position demonstrated to increase the inhibitory profile of the formed derivatives. Free 9-NH is of a fundamental necessity on the topic of the inhibitory activity.

Docking Studies

Following the synthesis of the target compounds and their evaluation in the kinase assay against both Brk and HER2, the interaction of substances with the active sites of the respective kinases was further explored by docking studies. The aim of this work was to obtain detailed knowledge about the possible binding mode of the derivatives in order to explain the difference in inhibitory activity of the tested compounds and to specify the developmental recommendations for further structural optimization of the substances. The docking studies were carried out in the group of Prof. Dr. *Wolfgang Sippl* in the Institute of Pharmacy, Martin Luther University Halle-Wittenberg.

Computational Methods

Protein structure preparation:

Brk:

Since there is no crystal structure available for Brk, the homology modeling methodology was used to predict it. The sequence of human protein kinase BRK (residues 13-450) was retrieved from the UniProtKB repository (entry number Q13882¹⁶¹). Following the NCBI *Basic Local Alignment Search Tool (BLAST)* query for the search of template structure in Protein Data Bank (PDB), it was identified that members of the Src kinase family share the highest sequence similarity (> 50%) with BRK. Crystal structure of c-Src in active conformation (PDB code: 1Y57_A, resolution 1.91 Å) was chosen as a template as it shows one of the highest sequence identity with Brk (around 53%).

The homology model was generated using MODELLER-9v11. The sequence alignment between Brk and c-Src was made using *align2d* in MODELLER (Figure 66). Based on the template structure and the alignment file, five models of Brk were generated using the “automodel” module of the program. The model with the lowest value of the Discrete Optimized Protein Energy (DOPE) assessment score was selected for further refinement. Hydrogen atoms and partial charges were assigned and the protein structure was subjected for energy minimization in implicit solvent with RMSD deviation of maximum 0.3 Å using the OPLS-AA 2005 forcefield (Maestro 9.3, Schrödinger Inc). The stereochemical analysis of Ramachandran plot with the PROCHECK program¹⁶² confirmed that this model is

Molecular Docking

Ligand selection and preparation:

Among all compounds tested on Brk and HER2 we selected three types of compounds for the docking studies. The first group includes BRK-selective inhibitors (**89**, **93** and **95**), the second group contains HER2-selective inhibitors (**48** and **69**) and the third one includes three compounds active on both enzymes (**15**, **19** and **60**).

All ligands were prepared using the LigPrep¹⁶³ utility of the Schrödinger suite. MMFF force field was used for energy minimization. Possible ionization states of each ligand were generated at pH 7.4 by using the Ionizer module. Options to generate tautomers, stereoisomers and up to 10 low energy ring conformations were set on.

Docking studies:

Ligands were docked into the ATP-binding pocket of Brk and of HER2 using GOLD version 5.1 programme.^{164,165} The center of the binding site was set at Leu319 for Brk or Leu852 for HER2 with a radius of 14 Å. Protein hydrogen bond constraint with hinge region residue (Met267 of Brk and Met801 of HER2) was additionally applied for docking. 30 poses per one compound were saved. Goldscore was chosen as fitness functions and rescoring with Chemscore was applied, since this protocol was validated on the available Src X-ray structures. Finally, the results were visually analyzed within the MOE software¹⁶⁶ and the best poses were selected according to the highest Chemscore.

Results

Examination of Brk and HER2 structural similarity:

The analysis of Brk and HER2 sequences showed that they share rather low sequence identity (36% for kinase domain). However, the overall 3D structures and especially the structure of the binding pocket is quite similar ($\text{RMSD}_{\text{all, C}\alpha} = 2.29$ Å, $\text{RMSD}_{\text{binding pocket, C}\alpha} = 1.17$ Å). It is worth to note, that most of the key residues playing an important role for binding of ATP-competitive inhibitors are identical for Brk and HER2 (e.g. Met at hinge region or Thr gatekeeper residue).

Noticeable structural differences between these two kinases can be found at conformationally flexible loops and P-loop, which conformation can have an impact on the kinase selectivity.¹⁶⁷

Results' Discussion:

Eight selected compounds mentioned above were docked into the ATP-binding pocket of refined HER2 crystal structure (3PP0) and the homology model of Brk. Docking results suggest a common binding mode for this type of inhibitors, where the NH and N atoms of the α -carboline core body are participating in two H-bond interactions with hinge region residues, namely with backbone atoms of Met267 or Met801 (for Brk and HER2, respectively). Additionally, the tricyclic α -carboline structure and phenyl rings are making a number of hydrophobic interactions with residues in the ATP binding site and adjacent gatekeeper pocket. The typical binding mode for this compound series is shown on example of **15**, which shows inhibitory activity on both Brk and HER2 (Figure 67). Furthermore, compounds **69** (Figure 68), **93** and **48** have a hydroxy group, which is making additional H-bonds with Glu235 of Brk and with Ala751, Lys753 or Asp863 of HER2.

The docking into the Brk binding site suggested the above described binding mode for all eight selected compounds, even though two of them (**48** and **69**) did not show activity on Brk in the biological assay. In case of HER2, only the inhibitors highly active on HER2 showed the expected binding mode. The weakly-active inhibitor on HER2 (compounds such as **89**, **93** and **95**) were not able to adopt a similar conformation, presumably, because of the presence of 8-nitro-substitution of the 9H-pyrido[2,3-*b*]indole ring (**93** and **95**) or the 3-methoxy-substitution of the phenyl ring (**89**). These substitutions could result in ligand geometry that causes steric clashes with the flexible loop flanking the ATP binding pocket in HER2 (Figure 69). This loop is missing in the Brk structure, hereby increasing the solvent accessibility of this region. This can explain why hydrophobic substitutes like -Br or -Acetyl (compounds **69** and **48**) have unfavorable effects on Brk binding. At the same time, the distance between -Br or -Acetyl to Val205 of Brk is slightly higher than the one to the same residue of HER2 (Val734, Figure 69). We suggest that these groups are able to participate in additional hydrophobic interactions with Val734 of HER2, thus, making binding of compounds **69** and **48** preferable to HER2 but not to Brk.

Figures:

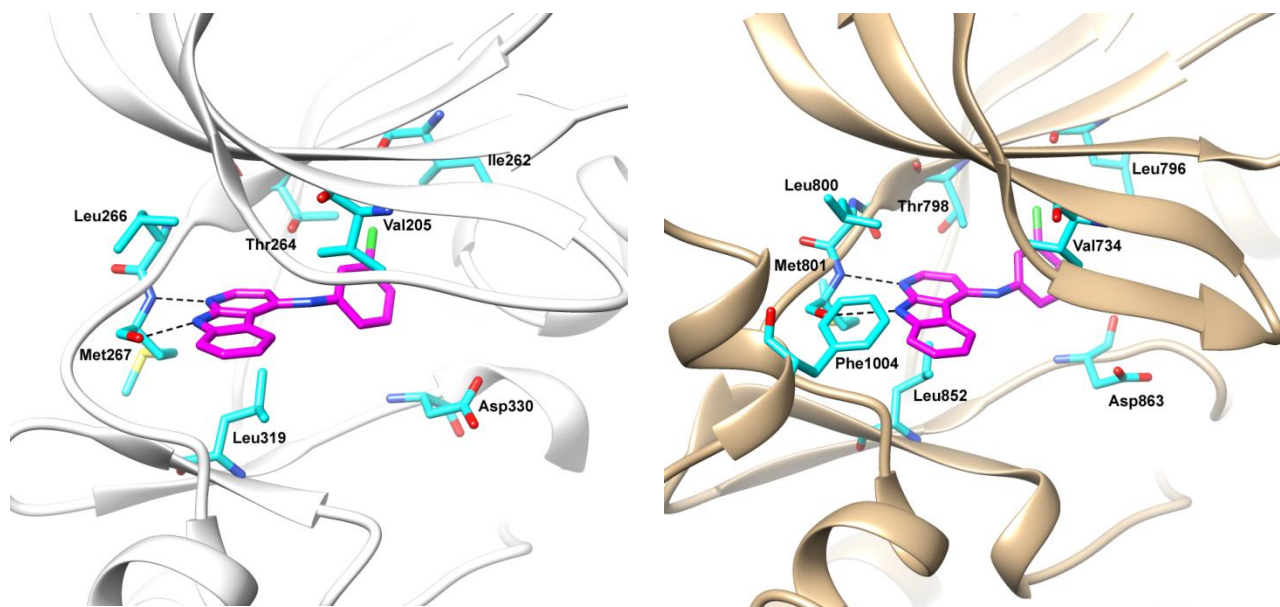


Fig. 67. GOLD docking solutions of compound **15** (magenta stick) for Brk (left site) and HER2 (right site) are shown. Brk and HER2 are represented as white and tan ribbon, respectively and important residues of the binding site are colored cyan. Hydrogen bonds between inhibitor and the kinase are displayed as dashed lines.

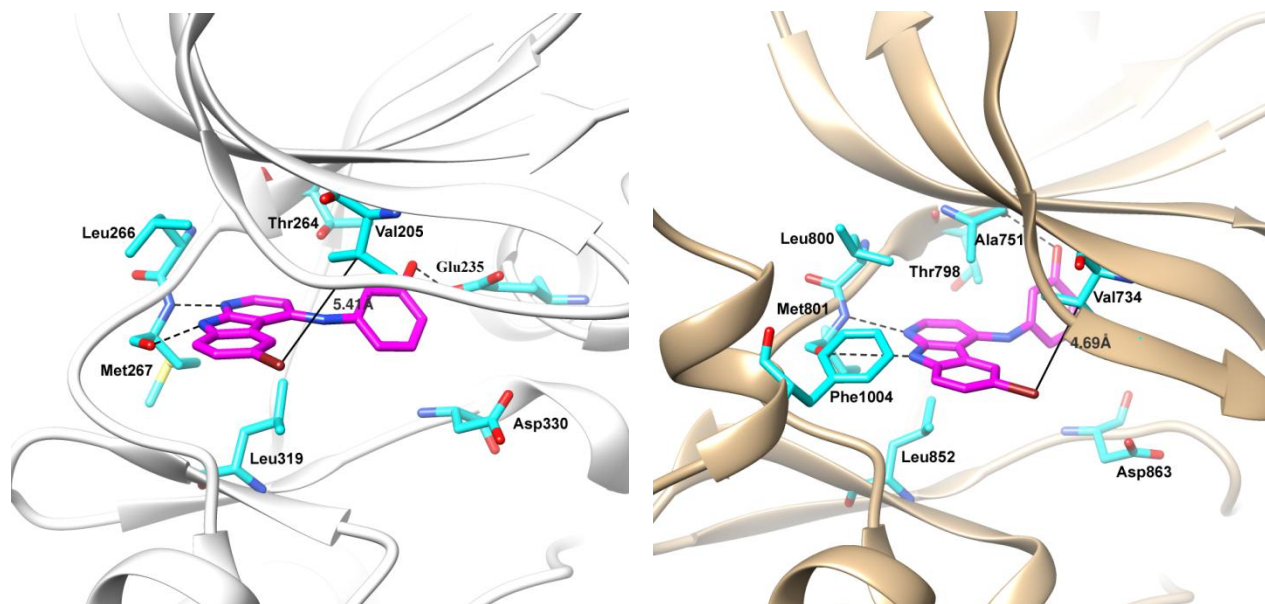


Fig. 68. Binding mode of **69** at the binding site of Brk (left site) and HER2 (right site). The distances from bromine atom of inhibitor to Val residue of kinase are shown in Å. In case of HER2 the bromo group is more buried within the hydrophobic binding pocket.

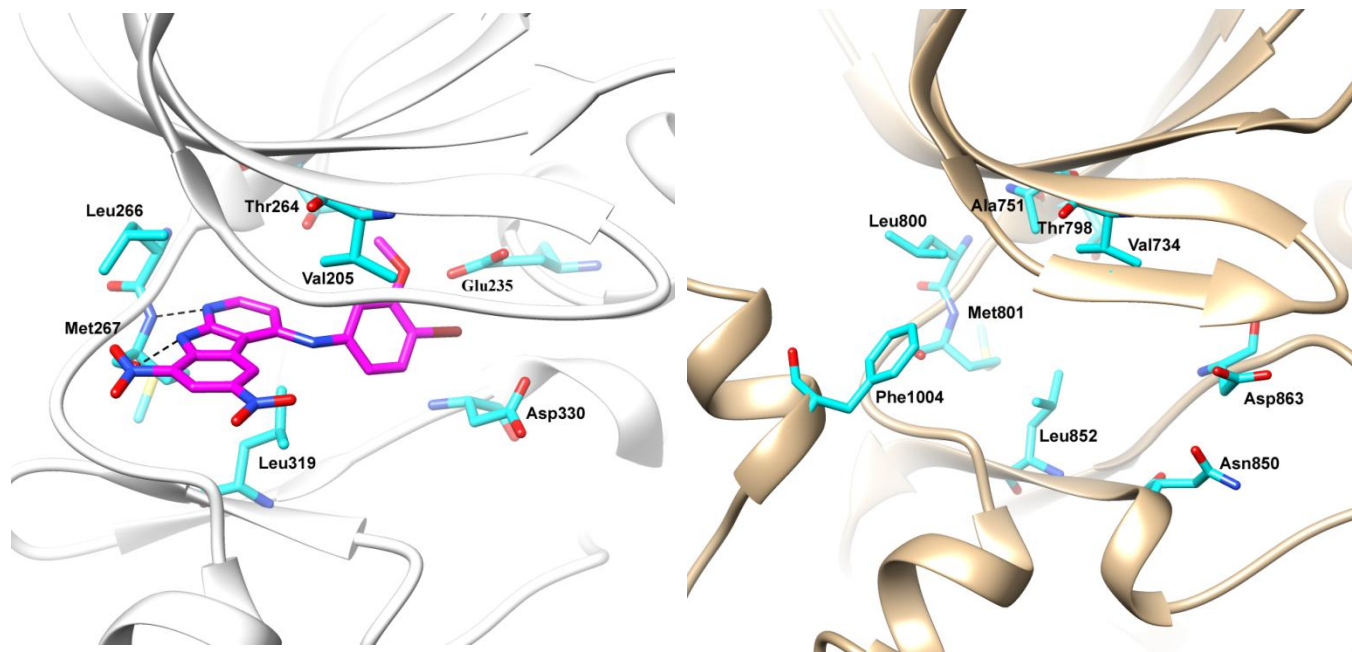


Fig. 69. Binding mode of **95** (magenta stick) at the Brk binding site (left site) in comparison with the structure of HER2 ATP-binding pocket (right site). It is shown that residues of the HER2 flexible loop (i.e. Phe1004) flanking the ATP binding pocket can cause steric hindrance for the inhibitor binding.

Summary

Breast cancer is the second most common cancer worldwide after lung cancer, the fifth most common cause of cancer death, and the leading cause of cancer death in women. The global burden of breast cancer exceeds all other cancers and the incidence rates of breast cancer are increasing. In light of these grim statistics, a special focus has been issued on breast cancer in the last decade.

Based on the results from the National Cancer Institute (NCI) 60-cell-line screenings executed in the biological exploration part in *Martin Krug* dissertation¹⁰⁴ for some derivatives, especially the 4-anilino-substituted α -carboline derivatives exhibited a promising antitumor activity, particularly against breast cancer subpanel cells. In further screening experiments, breast cancer kinase (Brk/PTK6) has been identified as target structure for first 4-anilino-substituted α -carbolines. This cellular tyrosine kinase had been inhibited by *meta*- and *para*-substituted 4-anilino- α -carbolines in nanomolar ranges.

Therefore, the objective of this work was to synthesize alternatively substituted 4-phenylamino α -carboline derivatives (figure 70, **I**), moreover, execute different electrophilic aromatic substitutions on the 6-position (figure 65, **II**, **III**, **IV**, **V**) followed by further successive reactions to support the postulated binding mode, and therefore, to evaluate their inhibitory properties against Brk as well as the well documented HER2.

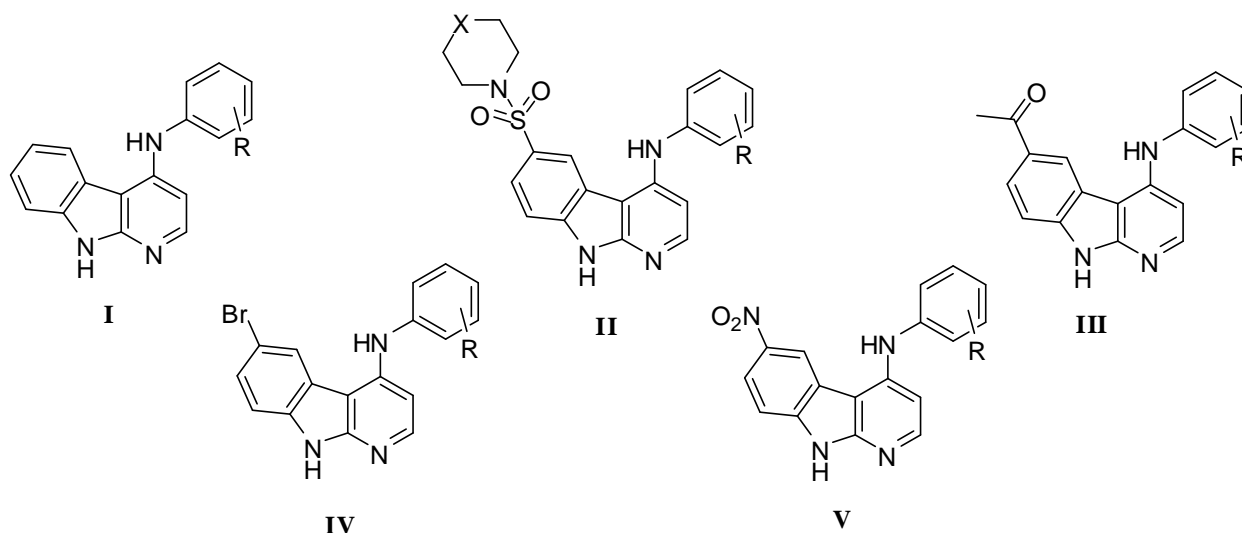


Fig. 70. Desired synthetic final products.

The 4-chloro- α -carboline **9** was prepared to serve as key intermediate for the synthesis of the desired α -carboline derivatives. Synthesis of the target structure **9** was accomplished starting from the reaction of 2-bromopyridine **1** with 1*H*-benzotriazole **2** to produce 1-pyridine-2-ylbenzotriazole **3** which in turn refluxed in polyphosphoric acid to produce the α -carboline **7**. *N*-oxide structure **8** was formed by the heating of **7** in 30% aqueous solution of hydrogen peroxide to improve the solubility in non-polar solvents. Finally, compound **8** was chlorinated by mixing with phosphorus oxychloride in DMF for 24 h at RT to produce **9**. (Fig. 71)

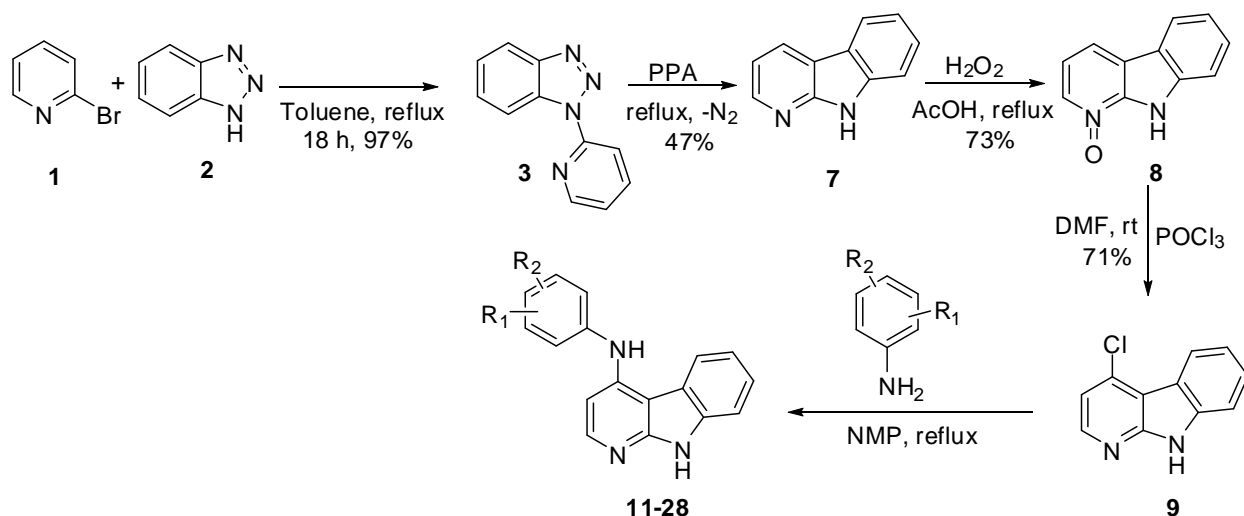


Fig. 71. Preparation of the desired starting structure **9** and subsequent reaction.

Subsequently, nucleophilic substitution reactions of several mono- and di-substituted aromatic amines, mainly anilines, with variable sizes of nucleophile and electrophile, were achieved in accordance with the available biological results and docking studies. The reaction took place in *N*-methyl-2-pyrrolidinone (NMP) as a solvent and under inert argon conditions, resulting in eighteen derivatives, **11-28**. (Fig. 71)

In cooperation with *ProQinase GmbH*, the newly synthesized compounds were evaluated for a potential inhibitory activity against the targeted kinases, Brk and HER2. Approximately all tested compounds displayed strong inhibitory activity against both of the aforementioned protein kinases, with IC_{50} values in a low nanomolar and submicromolar range. Some of the tested compounds in this series displayed both potent inhibitory affinity towards Brk (single-digit nanomolar IC_{50}), in addition to a strong activity against HER2 (submicromolar IC_{50}) such as, **12**, **15**, **19** and **27**. (Fig. 72)

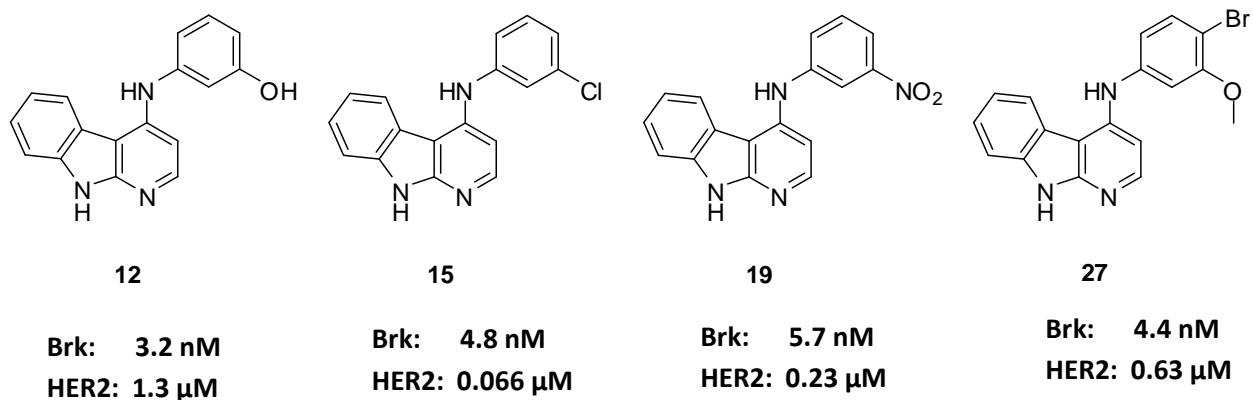


Fig. 72. Substances of the 1st series that showed a potent Brk and HER2 inhibitory activity.

The second synthetic strategy in this work was to carry out a number of classical electrophilic aromatic substitution reactions in the 6-position of the tricyclic α -carboline structure in order to introduce different functional groups that might strengthen the sensitivity as well as the selectivity towards targeted kinases. These substitution reactions should provide the possibility to attach a variable element to this position through which physico-chemical and pharmacokinetic parameters of the target compounds could be modified. As a result of these studies, chlorosulfonation, *Friedel-Crafts* acylation, halogenation, and nitration proved to be valuable synthetic tools for the introduction of the desired substituents.

Chlorosulfonation of **9** and consecutive reaction with secondary amines yielded a series of sulfonamides which by a subsequent nucleophilic substitution reaction at the 4-position with substituted anilines afforded the desired 6-sulfonamides 4-phenylamino- α -cabolines derivatives. (Fig. 73)

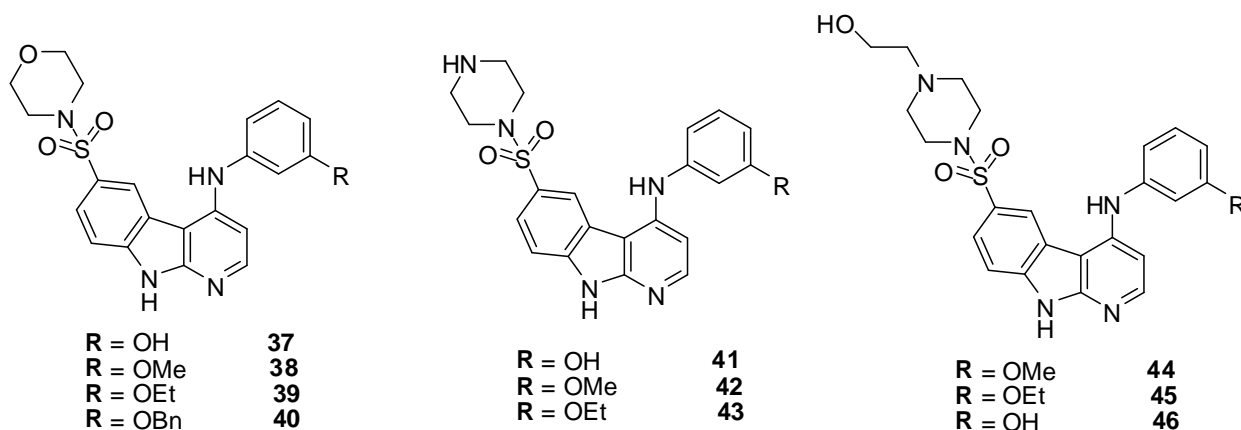


Fig. 73. 6-Chlorosulfonation derivatives (37-46).

Interestingly, the 3'-methoxy-substituted derivatives, **38**, **42** and **44**, exhibited the lowest IC₅₀ values (5.8 nM, 4.8 nM and 9.2 nM, respectively) against Brk kinase in this series.

Another main part of the synthetic strategy was a *Friedel-Crafts* acylation at the 6-position of the precursor structure **9** followed by a nucleophilic substitution with substituted anilines at the 4-position. For further inspections, the 6-acetylated 4-chloro- α -carboline derivative **47** was used as a precursor for *Aldol* condensation reaction with DMF/DMA in order to produce the corresponding enaminone. The enamine derivative in turn was supposed to act as a starting structure for an auxiliary condensation reaction with different nucleophiles to produce various five-membered hydrophilic heterocycles in the 6-position of the 4-chloro- α -carboline basic structure. Unexpectedly, the formed enaminone **52**, as a major product; 85%, was methylated at the *N*-9 which is considered to be disadvantageous according to the docking studies (Route A). As demethylation is tricky to be achieved, and to conquer this problem, a primary *N*-benzylation was executed with compound **47** followed by condensation with DMF/DMA (Route B). Afterward, a subsequent *N*-debenzylation was done using conc. H₂SO₄ yielding the desired structures. (Fig. 74 & 75)

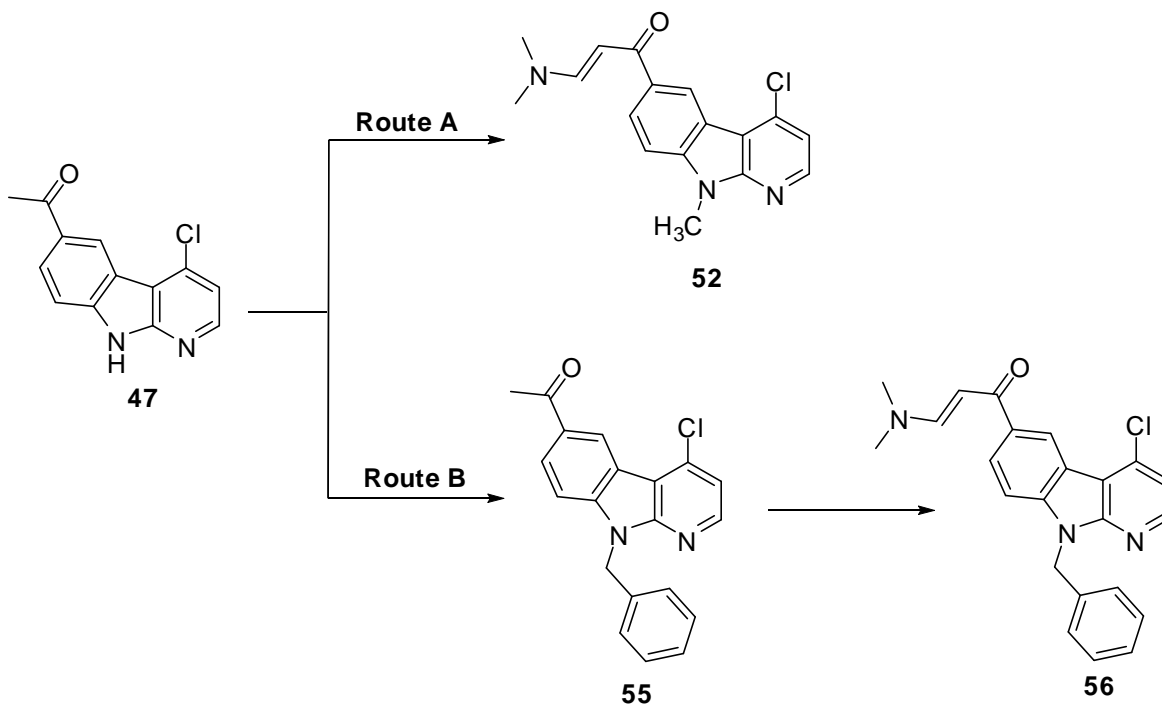


Fig. 74. Route A and B in the preparation of enamine structure.

Compound **69**, which is a 3'-hydroxy-substituted mono-brominated derivative, showed a potent inhibitory profile as well as selectivity against HER2 with an IC_{50} value of 29.3 nM, whereas no activity has been observed against BRK. Furthermore, in the NCI 60-cell line screenings, one- and five-dose, it exhibited remarkable interesting results comparable with other different derivatives (overall $GI_{50} = 2.14 \mu\text{M}$ and a moderate cytotoxicity) with a nanomolar GI_{50} value concerning particular breast cancer cell lines such as MCF7 and HS 578T. In general, the mono-brominated derivatives showed a relatively excessive activity in comparison to the dibrominated structures.

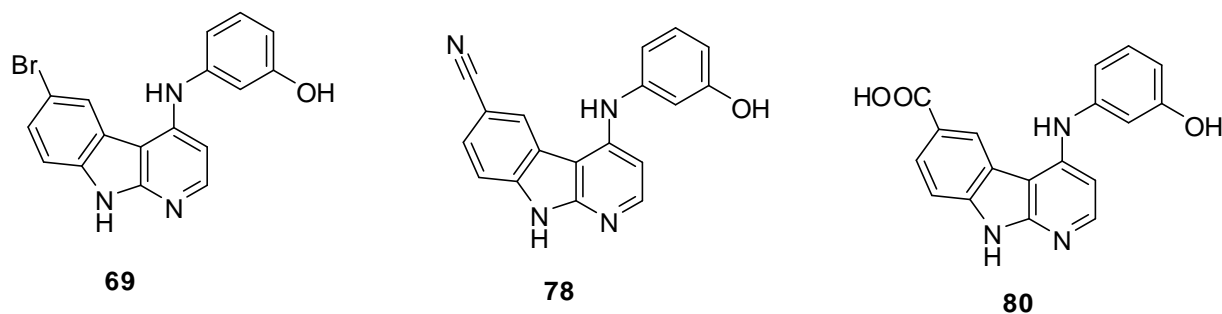


Fig. 77. Compound **69** and its further derivatizations.

Substance **69** was converted into the 6-cyano substituted derivative **78**, which in turn was hydrolyzed to the corresponding carboxylic acid **80**. (Fig. 77)

Similarly, nitration of compound **9** produced both the 6-mono and 6,8-dinitro-substituted derivatives. Subsequent reaction with different anilines led to the mono-/dinitro-substituted compounds. Further reduction was then processed to achieve the amino derivatives which succeeded with the 6-nitro-substituted compounds, but without any success in the case of the 6,8-dinitro derivatives.

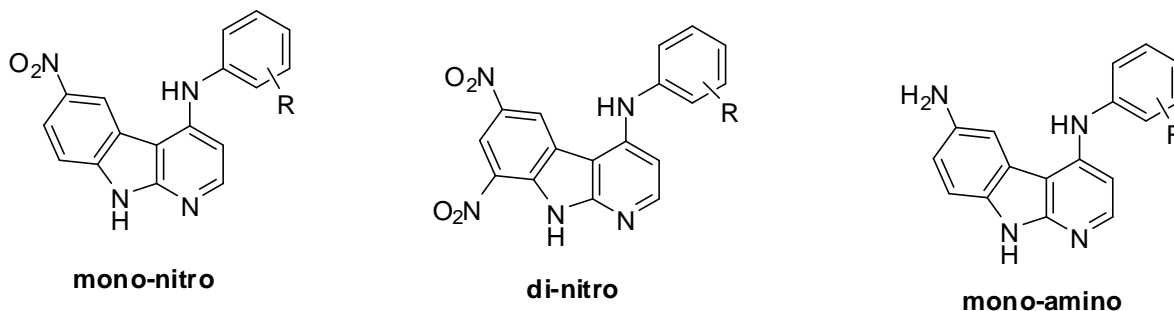


Fig. 78. Mono- and dinitration and further reduced amino-derivative.

Both mono- and dinitro-substituted derivatives as well as the 6-amino compounds demonstrated a strong activity towards Brk. In particular, the 3'-hydroxy-substituted derivatives (**87**, **91** and **93**) exhibited the highest sensitivity and selectivity with IC₅₀ concentrations ranging from < 3 nM to 3.3 nM. On the other hand, they showed a relatively decreased affinity against HER2 (7650 nM to 24700 nM).

Summary of Protein Kinase Assay results:

#	<i>IC₅₀ value [nM]</i>	
	<i>Brk</i>	<i>HER2</i>
11	n.a	978
12	3.2	1300
13	n.a.	279
14	155	20100
15	4.8	65.5
16	59.4	1640
17	n.a.	2270
18	40.7	2000
19	5.7	233
20	n.a.	310
21	190	>10000
22	53.4	n.a.
23	75	6600
24	70	600
25	154	2420
26	64.5	120
27	4.4	628
28	44	800
29	n.a.	148
37	n.a.	298
38	5.8	1240
39	410	54800
40	55.2	28300
42	4.8	390

#	<i>IC₅₀ value [nM]</i>	
	<i>Brk</i>	<i>HER2</i>
43	26.2	576
44	9.2	629
45	479	6530
46	n.a.	376
48	n.a.	12.8
49	21	801
51	7.6	1670
59	< 3	429
60	3.85	91.6
63	< 3	642
64	9.15	851
69	n.a.	29.3
70	12.7	1150
71	4.08	8830
72	186	91200
73	550	16300
74	11600	30000
75	95.9	523
76	33.9	7450
87	< 3	1690
88	13.2	1370
89	6.1	13300
90	132	9810
91	3.3	7650

#	<i>IC₅₀ value [nM]</i>	
	<i>Brk</i>	<i>HER2</i>
92	61.4	1990
93	< 3	24700

n.a.: not active (IC₅₀ > 100 μM)

#	<i>IC₅₀ value [nM]</i>	
	<i>Brk</i>	<i>HER2</i>
94	104	631
95	13	n.a.

Table 23. Summarization of the Protein Kinase Assay results for all tested compounds.

Summary of the NCI 60-Cell-Line Screenings:

Among the 20 derivatives (Fig. 61) that have been submitted to the National Cancer Institute (NCI) in the USA to be investigated for the one-dose screening, eleven compounds have been selected by the Development Therapeutics Programme (DTP) according to their overall mean growth % values for further NCI full panel 5-dose assays. (See table 20)

Compounds under five-dose screenings, **12**, **13**, **21**, **24**, **27**, **28**, **37**, **69**, **70**, **71** and **73** displayed an overall substantial anticancer activity against most of the tested cell lines representing nine different subpanels. In addition to the promising results of these compounds, GI₅₀, TGI and LC₅₀, concerning breast cancer cell lines. All tested compounds showed quite high LC₅₀ values in comparison to the obtained GI₅₀ values which indicate their non critical cytotoxicity. (See table 21)

As a consequence, the kinase inhibitory effect of the tested substances could be related to the cell growth inhibition observed in the NCI 60-cell-line screenings (single and/or five-dose).

On the basis of the 60-cell-line screening data obtained, compounds **12**, **37** and **69** were chosen for possible further studies *via* second five-dose screenings. Subsequently, both **37** and **69** have been approved by NCI-DTP for *in vivo* antitumor efficacy assessment.

Summary & Outlook

Docking studies were carried out for tested compounds to define the possible binding mode with targeted kinases and to specify the following structural optimization in the further future investigations. Docking results suggest a common binding mode, where the NH and N atoms of the tricyclic α -carboline structure participate in the formation of two hydrogen bonds with the hinge region residues. Moreover, the 4-phenylamino ring also contributes in hydrophobic interactions with residues in the ATP-binding site in both Brk and HER2. This docking survey was accomplished in the group of Prof. Dr. *Wolfgang Sippl*.

In conclusion, the results of these investigations clearly demonstrate that by using electrophilic substitution reactions, a number of 6-substituted α -carboline intermediates can be prepared. These intermediates could offer a possibility to synthesize further, structurally optimized derivatives in future studies.

Zusammenfassung

Brustkrebs ist die zweithäufigste Krebsart weltweit nach Lungenkrebs, der fünfte häufigste Ursache für Krebstod und die führende Ursache für Krebstod bei Frauen. Die globale Belastung von Brustkrebs übertrifft alle anderen Krebsarten und die Inzidenz von Brustkrebs steigt. Angesichts dieser düsteren Statistiken wurde ein besonderes Augenmerk auf Brustkrebs in den letzten zehn Jahren ausgestellt.

Basierend auf den Ergebnissen aus dem National Cancer Institute (NCI) 60-Zell-Linie Screenings in der biologischen Erforschung an *Martin Krug Dissertation*¹⁰⁴ für einige Derivate, insbesondere die 4-anilino-substituted α -Carbolinderivate ausgeführt zeigten eine vielversprechende Antitumor-Aktivität, insbesondere gegen Brustkrebs Unterpanel Zellen. In weiteren Screening-Experimenten, erste 4-Anilino-substituierte α -Carboline könnte eine andere Kinase als Zielstruktur zu identifizieren, benannt Brk, Brusttumor Kinase. Diese zelluläre Tyrosinkinase inhibiert worden war von meta- und 4-Anilino- α -Carboline in nanomolaren Bereich para-substituiert ist.

Daher war das Ziel dieser Arbeit zu synthetisieren alternativ substituierten 4-phenylamino α -Carbolinderivate (Abb. 70, I), darüber hinaus führen unterschiedliche elektrophile aromatische Substitutionen an der 6-Position (Abb. 65, II, III, IV, V) gefolgt von weiteren aufeinanderfolgenden Reaktionen auf die postulierte Bindungsmodus unterstützt, und daher wird auf ihre inhibitorische Wirkung gegen Brk sowie der gut dokumentierten HER2 auszuwerten.

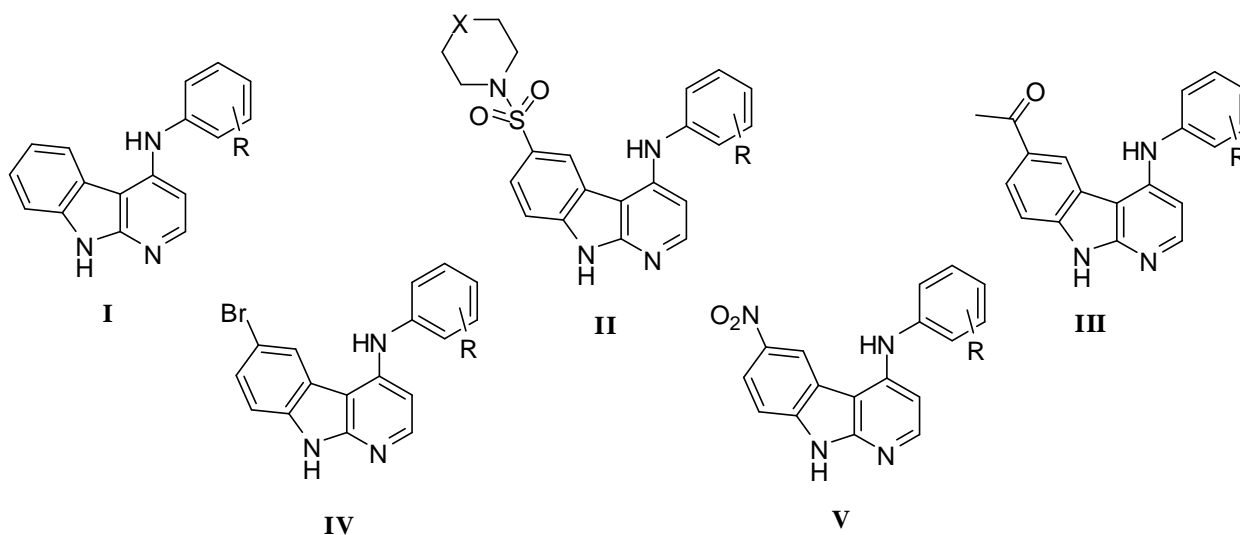


Abb. 70. Wunschpartner synthetischen Endprodukte.

Das 4-Chlor- α -carbolin **9** wurde hergestellt, um als wichtiges Zwischenprodukt für die Synthese der gewünschten α -carbolin-Derivate dienen. Synthese des Zielstruktur **9** erfolgte ausgehend von der Reaktion von 2-Brompyridin **1** mit 1H-Benzotriazol 2-1-pyridin-2-3 ylbenzotriazole die wiederum in Polyphosphorsäure refluxiert, um die α -carbolin **7** produzieren. N-Oxid-Struktur **8** wurde durch Erhitzen von **7** in 30% ige wässrige Lösung von Wasserstoffperoxid, um die Löslichkeit in unpolaren Lösungsmitteln zu verbessern **7** gebildet. Schließlich wurde **8** durch Mischen mit Phosphoroxchlorid in DMF für 24 h bei RT bis **9** zu erzeugen chloriert. (Abb. 71)

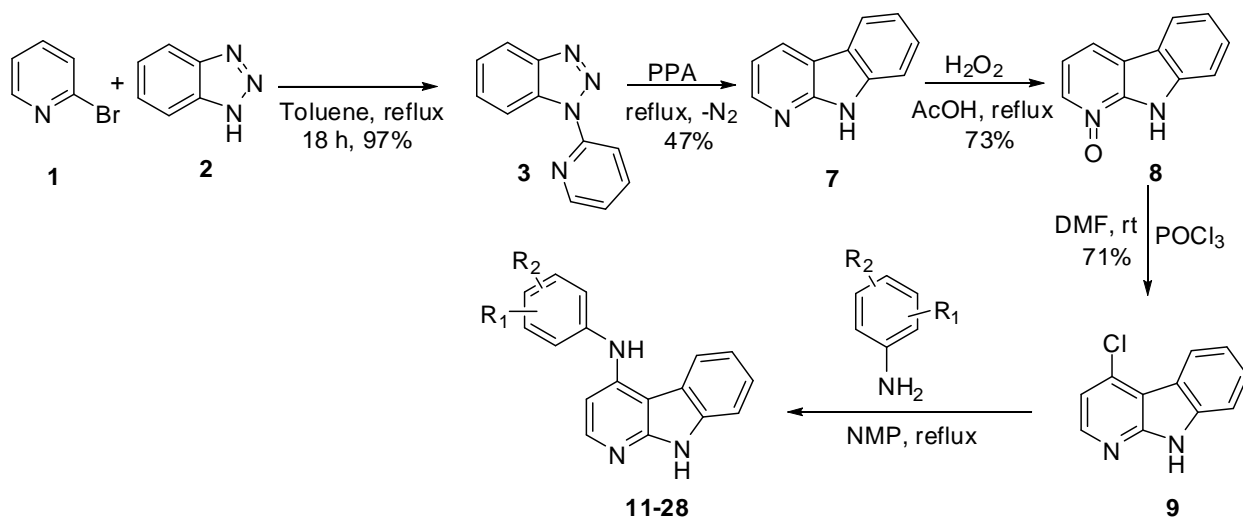


Abb. 71. Herstellung des gewünschten Ausgangsstruktur **9** und nachfolgende Reaktion.

Anschließend nukleophile Substitutionsreaktionen von mehreren mono- und disubstituierten aromatischen Aminen, insbesondere Anilinen, mit variablen Größen von Nucleophil und Elektrophil, wurden in Übereinstimmung mit den vorliegenden biologischen Ergebnisse und Dockingstudien erreicht. Die Reaktion fand in N-Methyl-2-pyrrolidinon (NMP) als Lösungsmittel und unter inerten Bedingungen unter Verwendung von Argon, was zu achtzehn Derivate, **11** bis **28** (Abb. 71).

In Zusammenarbeit mit *ProQinase GmbH*, wurden die neu synthetisierten Verbindungen für eine mögliche hemmende Aktivität gegen die gezielte Kinasen, BRK und HER2 ausgewertet. Etwa alle getesteten Verbindungen zeigten starke inhibitorische Aktivität gegen die beiden oben genannten Proteinkinasen, mit IC_{50} -Werten in einem niedrigen nanomolaren und submikromolaren Bereich. Einige der getesteten Verbindungen dieser Reihe erscheint sowohl stark hemmende Affinität gegenüber Brk (einstelligen nanomolaren IC_{50}), die neben einer starken Aktivität gegen HER2 (submikromolaren IC_{50}) wie **12**, **15**, **19** und **27** (Abb. 72).

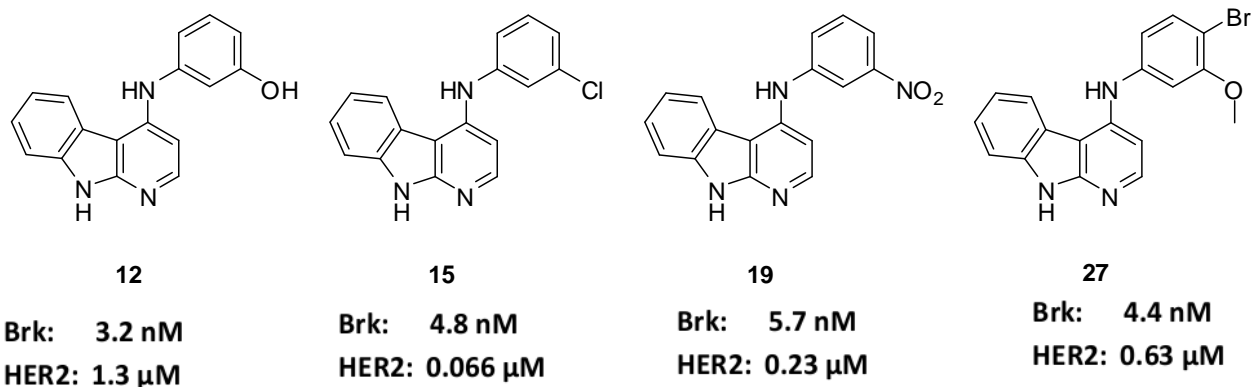


Abb. 72. Substanzen der ersten Serie, die eine starke Brk und HER2 inhibitorische Aktivität zeigte.

Die zweite Synthesestrategie in dieser Arbeit war es, eine Reihe von klassischen elektrophile aromatische Substitutionsreaktionen in der 6-Position des tricyclischen α -carboline Struktur, um verschiedene funktionelle Gruppen, die die Empfindlichkeit zu renovieren könnte sowie die Selektivität gegenüber gezielte Einführung Kinasen. Diese Substitutionsreaktionen sollten die Möglichkeit bieten, einen variablen Teil in diese Position durch die physikalisch-chemischen und die pharmakokinetischen Parameter der Zielverbindungen modifiziert werden könnte befestigen. Als ein Ergebnis dieser Studien bewiesen Chlorsulfonierung, *Friedel-Crafts*-Acylierung, Halogenierung, und Nitrierung, wertvolle synthetische Werkzeuge zur Einführung der gewünschten Substituenten sein.

Chlorsulfonierung von **9** und aufeinanderfolgende Reaktion mit sekundären Aminen ergab eine Reihe von Sulfonamiden, die durch eine nachfolgende nukleophile Substitutionsreaktion in der 4-Position mit substituierten Anilinen ergab das gewünschte 6-Sulfonamide 4-phenylamino- α -cabolines Derivate (Abb. 73).

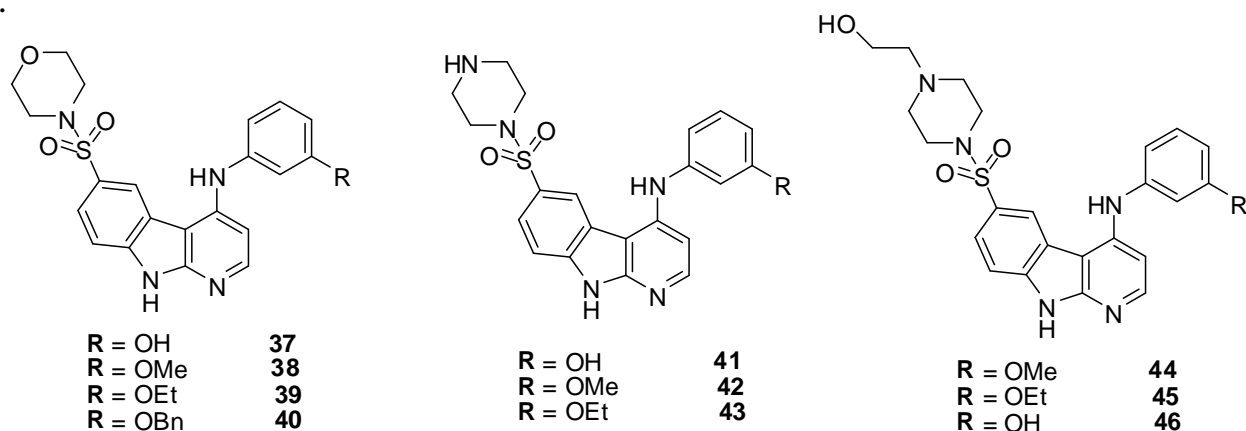


Abb. 73. 6-Chlorsulfonierung Derivate (37-46).

Interessanterweise wiesen die 3'-Methoxy-substituierten Derivaten, **38**, **42** und **44**, die niedrigsten IC₅₀-Werte in dieser Reihe von Verbindung gegen Brk Kinase, 5,8 nM, 4,8 nM und 9,2 nM.

Ein weiterer Teil der Synthesestrategie war eine *Friedel-Crafts*-Acylierungsreaktion an der 6-Position der Vorläuferstruktur **9** durch eine nucleophile Substitution mit substituierten Anilinen an der 4-Position folgt. Für weitere Untersuchungen wurde die 6-acetylierte 4-Chlor- α -carbolin-Derivat **47** als Vorläufer für Aldolkondensation Umsetzung mit DMF / DMA verwendet, um die entsprechenden Enaminon erzeugen. Die Enaminderivat wiederum sollte als Ausgangsmaterial für ein Zusatzelement Kondensationsreaktion mit verschiedenen Nukleophilen, um verschiedene fünfgliedrigen hydrophilen Heterocyclen in der 6-Stellung des 4-Chlor- α -carbolin Grundstruktur herzustellen handeln. Unerwarteterweise das gebildete Enaminon **52**, als Hauptprodukt, 85%, wurde am *N*-9, die als nachteilig angesehen gemäß der Docking-Studien (Route A) methyliert ist. Als Demethylierung ist schwierig zu erreichen ist, und um dieses Problem zu überwinden, wurde ein primärer *N*-Benzylierung zur Verbindung **47** durch Kondensation mit DMF / DMA (Route B) gefolgt ausgeführt. Danach wurde ein nachfolgender *N*-Debenzylierung erfolgt mit konz. H₂SO₄ was die gewünschten Strukturen. (Abb. 74 und 75)

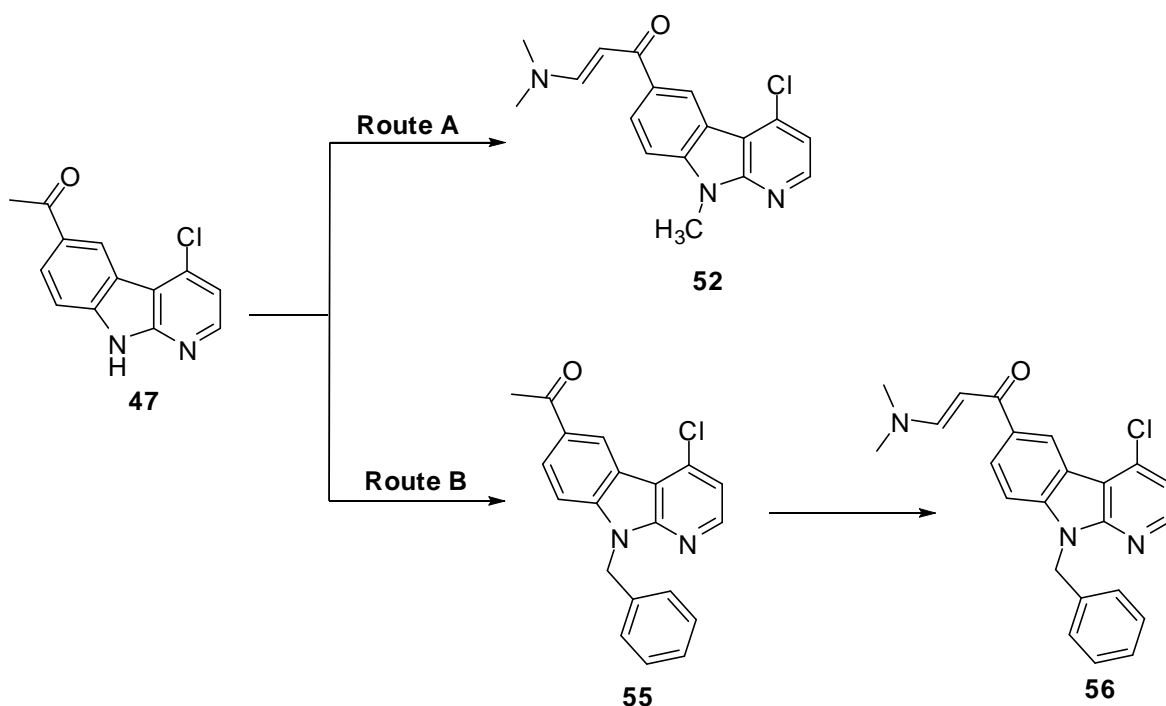


Abb. 74. Weg A und B bei der Herstellung der Enamin-Struktur.

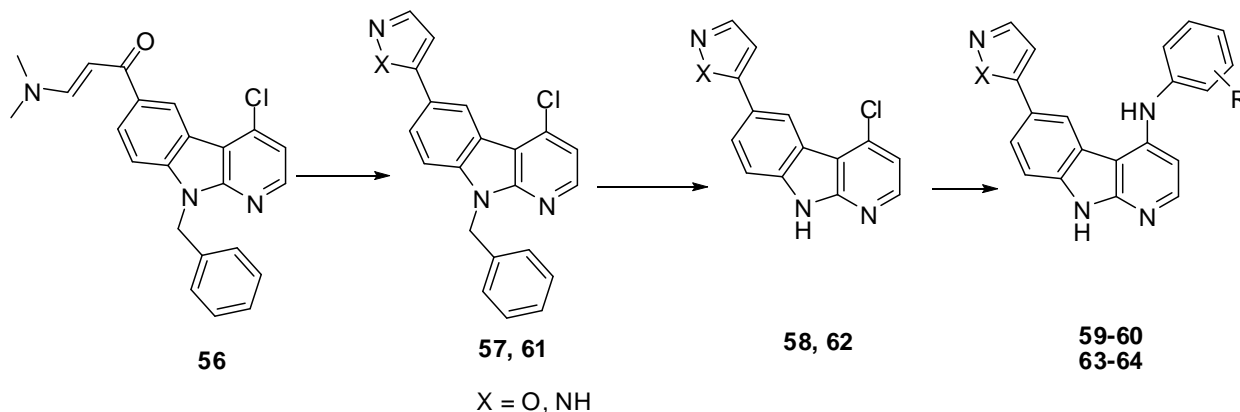


Abb. 75. Allgemeinen Weg, um den 6-Heteroaryl Herstellung von 4-phenylamino- α -Carbolinen.

Interessanterweise substituierte die 3'-Hydroxy-Derivate dieser Reihe zeigten eine sehr starke Selektivität und Empfindlichkeit gegen Brk in einem außerhalb des Bereiches nanomolaren IC_{50} -Konzentration (**59** bzw. **63** \rightarrow $\text{IC}_{50} = <3$ nM), während die 3'-Chlor substituierten Derivate, **60** und **64** zeigten eine stark hemmende Wirkung mit IC_{50} -Werten von 3,85 nM und 9,15 nM. Darüber hinaus wurde eine starke Affinität zu HER2 in submikromolaren Werte dieser Serie reichte von 0,092 μM bis 0,851 μM angezeigt.

Bromierung des 4-Chlor- α -carbolin **9** gefolgt von einer Reaktion mit verschiedenen m-substituierten Anilinen führte zu den 6-Brom-substituierte Derivate. Unvorhersehbar, durch Verwendung von überschüssigem Brom bei dieser Reaktion, zusätzlich zu dem 6-Substitution, erwiesen sich die so erhaltenen Verbindungen auf an der 8-Position substituiert sein. Für weitere Anfrage für den neuen 6,8-Dibrom 4-Chlor- α -Carboline wurde eine anschließende nukleophile Substitution mit verschiedenen Anilinen durchgeführt, um 6,8-Dibrom Serie herzustellen.

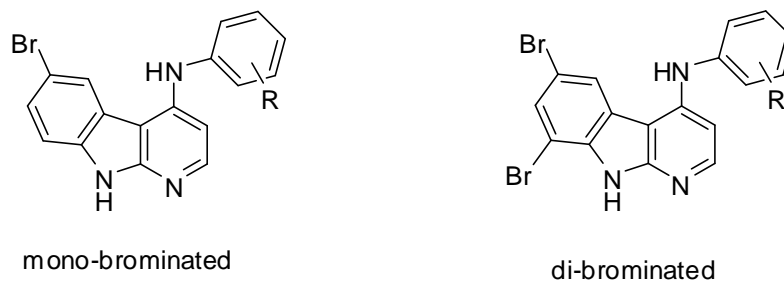


Abb. 76. Mono-und Di-bromiertes α -carbolin-Derivate.

Einführung von Brom an die 6-Position des α -carbolin Struktur beeinflusst die inhibitorische Profil mit unterschiedlichen Ergebnissen hinsichtlich sowohl BRK und HER2. Verbindung **69**, die ein 3'-Hydroxy-substituierten Mono-bromierten Derivat ist, zeigte eine stark hemmende Profil sowie Selektivität gegen HER2 mit einem IC_{50} -Wert von 29,3 nM, wohingegen keine Aktivität gegen BRK beobachtet. Ferner ist bei den NCI 60-Zelllinie Screenings, ein-und Fünf-Dosis zeigten es bemerkenswert interessanten Ergebnissen vergleichbar mit anderen verschiedener Derivate (allgemeine $GI_{50} = 2.14 \mu M$ und eine moderate Zytotoxizität) mit einem Wert über nanomolar GI_{50} besondere Brustkrebszelllinie Linien wie MCF7 und HS 578T im Allgemeinen zeigten die Mono-bromierte Derivate eine relativ übermäßige Aktivität im Vergleich zu den dibromiert Strukturen.

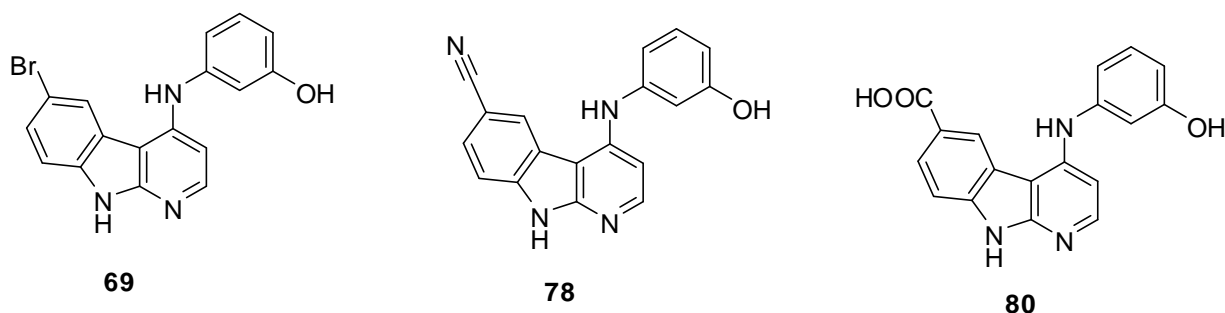


Abb. 77. Verbindung **69** und deren weitere Derivatisierungen.

Substanz **69** wurde in die 6-Cyano umgewandelt substituiertes Derivat **78**, die ihrerseits verseift zur entsprechenden Carbonsäure **80**. (Abb. 77)

Ähnlich hergestellt Nitrierung der Verbindung **9** sowohl die 6-Mono- und 6,8-Dinitro-substituierte Derivate. Die anschließende Umsetzung mit verschiedenen Anilinen führte zu den mono-/dinitro-substituted Verbindungen. Weitere Reduktion Reaktion wurde dann verarbeitet, um die Amino-Derivate, die mit den 6-nitro-substituierten Verbindungen ohne Erfolg im Fall der 6,8-Dinitro-Derivate gelang erreichen.

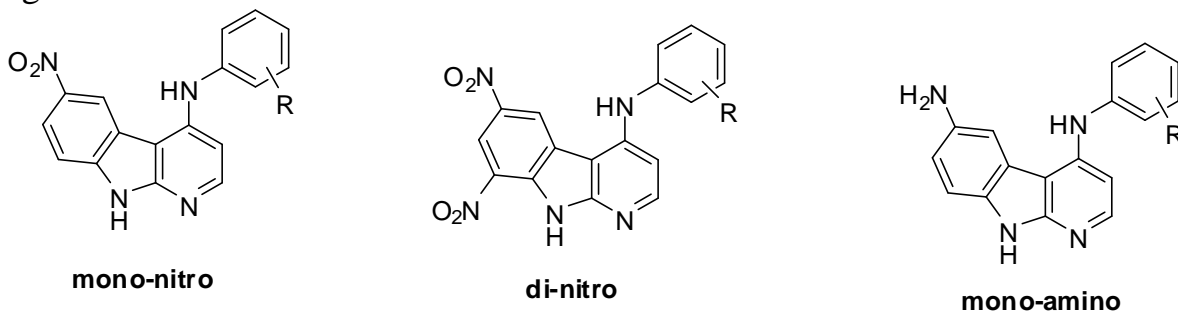


Abb. 78. Mono- und Di-Nitrierung und weiter reduziert Amino-Derivat.

Sowohl Mono- und Dinitro-substituierte Derivate sowie die 6-Amino-Verbindungen zeigte eine starke Aktivität gegenüber Brk. Insbesondere zeigten die 3'-Hydroxy-substituierten Derivaten der höchsten Empfindlichkeit und Selektivität mit IC_{50} -Konzentrationen lagen zwischen < 3 nM bis 3,3 nM. Auf der anderen Seite zeigten sie eine relativ verminderte Affinität gegen HER2 (7650 nM bis 24.700 nM).

Zusammenfassung der Protein Kinase Assay Ergebnisse:

#	<i>IC₅₀ value [nM]</i>	
	<i>Brk</i>	<i>HER2</i>
11	n.a	978
12	3.2	1300
13	n.a.	279
14	155	20100
15	4.8	65.5
16	59.4	1640
17	n.a.	2270
18	40.7	2000
19	5.7	233
20	n.a.	310
21	190	>10000
22	53.4	n.a.
23	75	6600
24	70	600
25	154	2420
26	64.5	120
27	4.4	628
28	44	800
29	n.a.	148
37	n.a.	298
38	5.8	1240
39	410	54800
40	55.2	28300
42	4.8	390

#	<i>IC₅₀ value [nM]</i>	
	<i>Brk</i>	<i>HER2</i>
43	26.2	576
44	9.2	629
45	479	6530
46	n.a.	376
48	n.a.	12.8
49	21	801
51	7.6	1670
59	< 3	429
60	3.85	91.6
63	< 3	642
64	9.15	851
69	n.a.	29.3
70	12.7	1150
71	4.08	8830
72	186	91200
73	550	16300
74	11600	30000
75	95.9	523
76	33.9	7450
87	< 3	1690
88	13.2	1370
89	6.1	13300
90	132	9810
91	3.3	7650

#	<i>IC₅₀ value [nM]</i>	
	<i>Brk</i>	<i>HER2</i>
92	61.4	1990
93	< 3	24700

#	<i>IC₅₀ value [nM]</i>	
	<i>Brk</i>	<i>HER2</i>
94	104	631
95	13	n.a.

n.a.: nicht aktiv (IC₅₀ > 100 µM)

Tabelle 23. Verdichtung des Protein Kinase Assay Ergebnisse für alle getesteten Verbindungen.

Zusammenfassung der NCI 60-Cell-Line-Screenings:

Unter den 20 Derivate (Abb. 61), die mit dem National Cancer Institute (NCI) in den USA für die ein-dose-Screening untersucht werden eingereicht wurden, haben elf Verbindungen, die durch die Development Therapeutics Programme (DTP) wurde nach ihrem ausgewählt Gesamtmittelwert Wachstum% für die weitere NCI volle Panel 5-dase-Assays. (Siehe Tabelle 20)

Verbindungen unter fünf-dose-Screenings, **12, 13, 21, 24, 27, 28, 37, 69, 70, 71** und **73** zeigten eine insgesamt erhebliche Antitumoraktivität gegen die meisten der getesteten Zelllinien, die neun verschiedene Teilfelder. Neben den vielversprechenden Ergebnisse dieser Verbindungen, GI₅₀, TGI und LC₅₀, betreffend Brustkrebs-Zelllinien. Alle getesteten Verbindungen zeigten recht hoch LC₅₀-Werte im Vergleich zu den Werten, die erhalten GI₅₀ ihre nicht kritisch Zytotoxizität anzuzeigen. (Siehe Tabelle 21)

Als Folge könnte die Kinase hemmende Wirkung der getesteten Substanzen in einem kausalen Zusammenhang mit der gewonnenen Ergebnisse aus den Zellen wachstumshemmende Wirkung vom NCI 60-Zelllinie Screenings (Einzel-und / oder Fünf-Dosis) sein.

Auf der Grundlage der 60-Zell-Linie Screening erhaltenen Daten wurden die Verbindungen **12, 37** und **69** zu dem "Biological Evaluation Committee" (BEC) des NCI, die auf eine mögliche weitere Studien über zweite Fünf-Dosis Rechengut rät geleitet. Anschließend wurden jeweils **37** und **69** NCI-DTP wurde *in vivo* antitumorale Wirksamkeit Untersuchungen zugelassen.

Nach der Synthese der Zielverbindungen und deren Bewertung in der Kinase-Assay sowohl gegen Brk und HER2, die Wechselwirkung von Substanzen mit den aktiven Zentren der jeweiligen Kinasen wurde durch weitere Studien Andocken

Summary & Outlook

definiert. Das Ziel dieser Arbeit war es, detaillierte Kenntnisse über die mögliche Bindungsmodus der Derivate zu erhalten, um den Unterschied in der Hemmwirkung der getesteten Verbindungen zu erklären und die Entwicklung von Empfehlungen für weitere strukturelle Optimierung der Stoffe angeben. Die Docking-Studien wurden in der Arbeitsgruppe von Prof. Dr. *Wolfgang Sippl* im Institut für Pharmazie, Martin-Luther-Universität Halle-Wittenberg durchgeführt.

Abschließend werden die Ergebnisse dieser Untersuchungen zeigen deutlich, dass durch die Verwendung elektrophile Substitutionsreaktionen, eine Reihe von 6-substituierten α -carbolin Zwischenprodukte hergestellt werden können. Diese Zwischenprodukte könnten eine Möglichkeit, weitere, strukturell optimiert Derivate in zukünftigen Studien zu synthetisieren.

Outlook

As a part of a project, further explorations are expected to complete the contemporary work. Consequent *in vitro* characterization of the toxicity of the first synthesized Brk-inhibitors will be measured in cooperation with Prof. Dr. *Christoph Ritter* (Department of Clinical Pharmacy, Institute of Pharmacy, Greifswald University). Preliminary investigation of toxic concentrations for normal cells will be determined in PBMCs (peripheral blood mononuclear cells) in the MTT assay.

Furthermore, *in vitro* characterization of the anti-proliferative effect is expected to be done for the first Brk inhibitors, depending on the expression and the activity of Brk (by AG Prof. Dr. *Ritter*), which will depend on the data from the toxicity studies in the normal cells exhibit in different breast cancer cell lines (MCF-7, T-47D, MDA-MB-231, MDA-MB-468, BT-474, etc.), including trastuzumab-resistant cells (BT-HR).

In addition, the ongoing *in vivo* survey for compounds **69** and **37** is expected to be accomplished soon by the National Cancer Institute (NCI) which may verify and support our selected inhibitors for further preclinical investigation progress.

In view of further structural optimizations of compounds synthesized in this work, it is also of interest to investigate the possibilities of further substitution of the phenylamino rests of the 6-/6,8-substituted 4-phenylamino- α -carboline. This is owing to the acquired results of previously synthesized α -carboline which have already shown significant differences in the activity and selectivity of the compounds with some representatives of these classes of compounds have excellent kinase inhibitory properties. Moreover, in the synthetic work, the main focus would be put on the introduction of polar functional groups in the phenyl ring to allow more interaction with the three amino acid residues of the DFG motif and to increase the tendency for hydrogen bond formation with the ATP-binding pocket.

Experimental Section

Synthetic Part

Materials and Method

All moisture and/or air-sensitive reactions were carried out under argon atmosphere in dried apparatus under vacuum.

Chemicals and Solvents

All solvents are received from the Institute of Pharmacy, Martin-Luther-University Halle-Wittenberg, dried and distilled by standard procedures.¹⁶⁸ Chemicals were purchased from commercial suppliers and were used as received without further purification.

Acetone (<i>Roth</i>)	Chlorosulfonic acid (<i>Fluka</i>)
Acetyl chloride (<i>Lancaster</i>)	Copper(I)-cyanide (<i>Sigma-Aldrich</i>)
Acetic acid (<i>Roth</i>)	Copper(I)-iodide (<i>Sigma-Aldrich</i>)
Acetic anhydride (<i>Roth</i>)	3,5-Dichloroaniline (<i>Sigma-Aldrich</i>)
Aluminium chloride (<i>Roth</i>)	Dichlormethane (<i>Roth</i>)
3-Aminobenzotrifluoride (<i>Merck</i>)	Diethylether (<i>Kraemer und Martin</i>)
3-Aminophenol (<i>Merck</i>)	<i>N,N</i> -Dimethylformamide (<i>Laborchemie Apolda</i>)
Ammonium chloride (<i>Roth</i>)	<i>N,N</i> -Dimethylformamide dimethyl acetal (<i>Sigma-Aldrich</i>)
3-Anisidin (<i>Chemapol Chechoslovakia</i>)	Dimethyl sulfoxide (<i>Roth</i>)
4-Anisidin (<i>Laborchemie Apolda</i>)	1,4-Dioxan (<i>BASF</i>)
1 <i>H</i> -Benzotriazol (<i>Acros Organics</i>)	Diphenyl ether (<i>Acros Organics</i>)
Benzyl bromide (<i>Sigma-Aldrich</i>)	Ethanol (<i>Roth</i>)
Benzyl chloride (<i>Merck</i>)	3-Ethoxy-4-bromoaniline (<i>Sigma-Aldrich</i>)
3-Benzyloxyaniline (<i>Acros Organics</i>)	Ethyl acetate (<i>Roth</i>)
Brom (<i>Merck</i>)	2-Furanylboronic acid (<i>Sigma-Aldrich</i>)
2-Brompyridine (<i>Acros Organics</i>)	Hydrazine Hydrate (<i>Sigma-Aldrich</i>)
3-Chloroaniline (<i>Riedel-deHaen</i>)	Hydrochloric acid (<i>Roth</i>)
3-Chloro-4-toluidine (<i>Sigma-Aldrich</i>)	Hydrogen peroxide (<i>AcrosOrganics</i>)
4-Chloroaniline (<i>Ferak</i>)	Hydroxylamine HCl (<i>Acros Organics</i>)
3-Chloro-4-fluoroaniline (<i>Riedel-deHaen</i>)	Lithium chloride (<i>Roth</i>)
Chloroform (<i>Roth</i>)	Methanol (<i>Roth</i>)
Cyclohexane (<i>Roth</i>)	3-(Methylmercapto)aniline (<i>Ferak</i>)
3-Chloro-4-benzyloxyaniline (<i>Acros Organics</i>)	

3-Methoxy-4-bromoaniline (<i>Sigma-Aldrich</i>)	Sodium azide (<i>Acros Organics</i>)
<i>N</i> -Methylpyrrolidin-2-on (<i>Sigma-Aldrich</i>)	Sodium carbonate (<i>Germed</i>)
Morpholine (<i>Merck</i>)	Sodium chloride (<i>Grussing</i>)
1-Naphthylamine (<i>Merck</i>)	Sodium cyanide (<i>Sigma-Aldrich</i>)
Nitric acid (<i>DMK Chemikalien GmbH</i>)	Sodium hydrogen carbonate (<i>Isocommerz</i>)
3-Nitroaniline (<i>Sigma-Aldrich</i>)	Sodium hydroxide (<i>Roth</i>)
3-Phenitidine (<i>Sigma-Aldrich</i>)	Sodium sulfate (<i>Grussing</i>)
Phosphorus oxychloride (<i>Sigma-Aldrich</i>)	Sulfuric acid (<i>DMK Chemikalien GmbH</i>)
Piperazine (<i>Fluka</i>)	Tetra-butyl ammonium bromide (<i>Acros Organics</i>)
2-(Piperazin-1-yl)ethanol (<i>Riedel-deHaen</i>)	Tetrahydrofuran (<i>Roth</i>)
Polyphosphoric acid (<i>Acros Organics</i>)	Tetrakis(triphenylphosphine)palladium (<i>Sigma-Aldrich</i>)
Potassium carbonate (<i>Merck</i>)	Tin(II)-chloride (<i>Sigma-Aldrich</i>)
Potassium hydroxide (<i>Roth</i>)	2-Thienylboronic acid (<i>Sigma-Aldrich</i>)
Potassium iodide (<i>Grussing</i>)	Toluene (<i>Roth</i>)
Red, fuming nitric acid (<i>Sigma-Aldrich</i>)	2-Toluidin (<i>Laborchemie Apolda</i>)
See sand (<i>Laborchemie Apolda</i>)	

Thin Layer Chromatography (TLC)

For the thin layer chromatographic analysis, TLC-aluminum foils with fluorescent indicator from the company *Merck KGaA* were used (silica gel 60 F254, layer thickness 0.2 mm). Detection was performed with UV light at 254 nm or 366 nm, *R_f* values were indicated (run level relative to the solvent front). Eluent mixtures used were specified in the experimental procedures.

Column Chromatography

The column chromatographic separations were carried out at atmospheric pressure on silica gel 60 (particle size from 0.063 to 0.200 mm) conducted by the company *Merck KGaA*. Eluent mixtures used were specified in the experimental procedures.

NMR spectra:

The NMR spectra were obtained on a "Gemini-2000" (400/100 MHz) or on "INOVA 500" measured (500 MHz) of the company "Varian". The residual resonance signal of the respective deuterated solvent was used as an internal standard. The interpretation of the NMR spectra was carried out using the spectral simulation tools under the "ACD / Labs 7.00" (Advanced Chemistry Development Inc.) and "ChemDraw Ultra 10.0" (CambridgeSoft).

¹H-NMR:

In which the transmitter frequency and the used deuterated solvents were specified. The chemical shifts δ are reported as parts per million (ppm). In parentheses is followed by the multiplicity of the signal. Where: s = singlet, d = doublet, t = triplet, q = quartet, qu = quintet, sep = septet, m = multiplet and b = broad signal. Combinations of multiplicities, e.g. dd = doublet doublet, are optionally included. Furthermore, the integrated number of protons, the coupling constant J and chemical interpretation of the signal are indicated.

¹³C-NMR:

The ¹³C-NMR spectra were recorded broadband decoupled. It is the transmitter frequency, the used deuterated solvent, and the chemical shifts δ in parts per million (ppm). In parentheses is following the chemical interpretation of the signals. The abbreviations mean: p = primary carbon atom, s = secondary carbon atom, t = tertiary carbon atom and q = quaternary carbon atom.

IR Spectra:

The ATR spectra were recorded on a FT-IR spectrometer, "IFS 28" Company "Bruker", the KBr spectra on a FT-IR spectrometer "Spectrum BX" Company "Perkin-Elmer". For each signal, the wave number ν in cm^{-1} , the intensity and the chemical interpretation were given. The abbreviations mean the following: s = strong, m = medium, w = weak and br = broad.

Mass Spectra (MS):

The ESI-mass spectra were measured on a "Finnigan LCQ Classic" from the company "Thermo Electron". The sample was injected directly. The EI-mass spectra were measured on a "AMD 402" of the company "AMD Intectra GmbH". The ionization energy was 70 eV. Interpretation of the EI-mass spectra was obtained using the spectral simulation tools "ACD / MS fragmenter" (Advanced Chemistry Development Inc.).

Melting Points:

The melting points were measured on a Boetius-Mikroheiztisch from the company "VEB Wägetechnik Rapido Radebeul/VEB Kombinat NAGEMA" and are not corrected.

Elemental Analysis (EA):

The carbon, hydrogen and nitrogen content of the substances were determined on a "CHNS-932" automatic analyzer of the company "LECO Corporation" in automatic micro process. The halogen content was determined by titration in the semi-micro method.

Synthetic Procedure

Synthesis of 4-chloro- α -carboline:

1-(pyridin-2-yl)-1H-benzo[d][1,2,3]triazole (3)

Molecular formula: C₁₁H₈N₄

Molecular weight: 196.21 g/mol

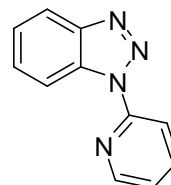
Melting point: 109-110 °C [Lit.: 110-111 °C]

R_f-value: [Cyc : EE 75 : 25 v/v] 0,76

Yield: 30 g (152.88 mmol, 97 %) white solid

Method of preparation:

A suspension of 25 g (158.23 mmol, 1 eq.) 1H-benzo [1,2,3] triazole **2** and 38 g (316.46 mmol, 2 eq.) 2-bromopyridine **1** in 110 ml of toluene was heated to reflux for 18 h. It initially formed a clear, yellowish solution, later; a white solid began to precipitate. After cooling, the reaction mixture was poured into 500 ml of ethyl acetate (EE) and by the addition of 50 ml of aq. 10% potassium hydroxide solution the white solid was obtained. The phases were separated; the organic phase was washed twice with 150 ml of aq. 10%. Potassium hydroxide and then dried over sodium sulfate. The solvent was removed under reduced pressure and the crude product is recrystallized from MeOH.¹¹⁴



¹H-NMR: [400 MHz, CDCl₃] δ (ppm) = 7.30 (ddd, $J = 7.4$ Hz, $J = 4.9$ Hz, $J = 0.7$ Hz, 1H, H- 5'); 7.43 (ddd, $J = 8.1$ Hz, $J = 7.2$ Hz, $J = 0.9$ Hz, 1H, H-5); 7.58 (ddd, $J = 8.0$ Hz, $J = 5.7$ Hz, $J = 0.8$ Hz, 1H, H-6); 7.92 (ddd, $J = 7.6$ Hz, $J = 5.7$ Hz, $J = 1.8$ Hz, 1H, H-4'); 8.10 (d, $J = 8.3$ Hz, 1H, H-4); 8.28 (d, $J = 8.3$ Hz, 1H, H-3'); 8.60 (d, $J = 4.7$ Hz, 1H, H-6'); 8.63 (d, $J = 8.4$ Hz, 1H, H-7).

¹³C-NMR: [100 MHz, CDCl₃] δ (ppm) = 114.4 (t, C-7); 114.8 (t, C-3'); 119.8 (t, C-5'); 122.2 (t, C-4); 124.8 (t, C-5); 128.7 (t, C-6); 131.6 (q, C-7a); 138.7 (t, C-4'); 146.8 (q, C-3a); 148.3 (t, C-6'); 151.7 (q, C-2').

IR: (KBr) ν (cm⁻¹) = 3113 (w, Aryl-CH-stretch); 3067 (w, Aryl-CH-stretch); 1477 (s, C=C stretch); 1443 (s, C=C-stretch); 785 (s, CH-bending); 768 (s, CH-bending); 752 (s, CH-bending).

EI-MS: m/z = 196 (24, M⁺); 168 (100, M⁺-N₂); 142 (12, C₈H₄N₃⁺); 117 (9, M⁺-C₅H₅N); 102 (2, C₆H₂N₂⁺); 90 (2, C₅H₂N₂⁺); 78 (77, M⁺-C₆H₄N₃).

9-H-pyrido[2,3-b]indole (7)

Molecular formula: C₁₁H₈N₂

Molecular weight: 168.19 g/mol

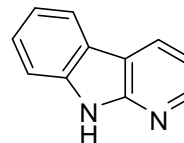
Melting point: 210-212 °C [Lit.: 211 °C]

R_f-value: [Cyc : EE 60 : 40 v/v] 0.38

Yield: 4.03 g (23.96 mmol, 47 %) beige solid

Method of preparation:

25 g of polyphosphoric acid were added to a 250 ml three-necked flask with KPG stirrer and bubbler and was then heated to 175 °C. Under vigorous stirring, 10 g (50.97 mmol) of **3** were added in portions, wherein the temperature of the mixture was maintained at 150-160 °C. After finishing the addition, the temperature was continued at 160 °C until the evolution of gas had ceased. During cooling, the dark brown viscous mixture was carefully diluted with 50 ml water and was then alkalinized by slow addition of 10 M NaOH (pH > 10). The mixture was then treated as long at 50 °C in an ultrasonic bath until the dark brown mass was completely suspended. The resulting suspension was poured into 250 ml of water and cooled in the ice bath. It was stirred for 20 min, then the precipitated solid was filtered through a Buchner funnel, washed thoroughly with water, air dried and used without further purification in the next step.¹¹⁵



¹H-NMR: [400 MHz, DMSO-d₆] δ (ppm) = 7.15 (dd, *J* = 7.8 Hz, *J* = 4.8 Hz, 1H, H-3); 7.16-7.20 (m, 1H, H-6); 7.38-7.44 (m, 1H, H-7); 7.47 (dd, *J* = 8.1 Hz, *J* = 0.8 Hz, 1H, H-8); 8.11 (d, *J* = 7.8 Hz, 1H, H-5); 8.37 (dd, *J* = 4.8 Hz, *J* = 1.6 Hz, 1H, H-2); 8.44 (dd, *J* = 7.8 Hz, *J* = 1.6 Hz, 1H, H-4); 11.72 (br, 1H, NH).

¹³C-NMR: [100 MHz, DMSO-d₆] δ (ppm) = 111.2 (t, C-8); 114.8 (t, C-3); 115.1 (q, C-4a); 119.3 (t, C-6); 120.3 (q, C-5); 121.0 (t, C-4b); 126.4 (t, C-7); 128.2 (t, C-4); 138.7 (q, C-8a); 145.9 (t, C-2); 151.8 (q, C-9a).

IR: (KBr) ν (cm⁻¹) = 3434 (br, NH-stretch); 3139 (m, Aryl-CH- stretch); 3078 (m, Aryl-CH-stretch); 1603 (m, C=C-stretch); 1457 (m, C=C-stretch).

EI-MS: m/z = 168 (100, M⁺); 140 (32, M⁺-CH₂N); 114 (19, M⁺-C₃H₄N).

9H-Pyrido[2,3-b]indol-1-oxide (8)

Molecular formula: C₁₁H₈N₂O

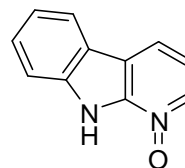
Molecular weight: 184.19 g/mol

Melting point: 234-238 °C [Lit.: 236-238 °C]

Yield: 8.75 g (43.18 mmol, 73 %) orange solid

Method of preparation:

To a solution of 10 g (59.46 mmol, 1 eq.) of **7** in 80 ml of glacial acetic acid and under stirring, 8 ml hydrogen peroxide solution (35%, 7.95 g, 94.55 mmol, 1.6 eq.) was dropped. Then the reaction mixture was heated to gentle boiling for 4 h. After cooling, further 2 ml aq. hydrogen peroxide solution (35%, 2.27 g, 27.01 mmol, 0.5 eq.) was added dropwise and the mixture was again heated to gentle boiling for 2.5 h. After cooling, the solvent was distilled off under reduced pressure. The oily residue was added dropwise with swirling to saturated potassium carbonate solution until the mixture had a pH value of 8. Then the mixture was stirred overnight at RT. Then the precipitated, orange solid was filtered through a Buchner funnel, washed with water, dried overnight in the air and used without further purification in the next step.¹²²



¹H-NMR: [400 MHz, DMSO-d₆] δ (ppm) = 7.22 (dd, *J* = 7.8 Hz, *J* = 6.3 Hz, 1H, H-3); 7.28 (dd, *J* = 7.1 Hz, *J* = 1.1 Hz, 1H, H-6); 7.52 (dd, *J* = 7.1 Hz, *J* = 1.2 Hz, 1H, H-8); 7.58 (d, *J* = 8.2 Hz, 1H, H-7); 8.16-8.20 (m, 2H, H-2 & H-5); 8.34 (dd, *J* = 6.3 Hz, *J* = 0.8 Hz, 1H, H-4); 10.25 (br, 1H, NH).

¹³C-NMR: [100 MHz, DMSO-d₆] δ (ppm) = 112.4 (t, C-8); 115.8 (t, C-6); 119.6 (q, C-4b); 119.7 (t, C-3); 120.7 (t, C-5); 120.9 (q, C-4a); 121.8 (t, C-4); 127.7 (t, C-7); 134.5 (t, C-2); 138.3 (q, C-8a); 141.9 (q, C-9a).

IR: (KBr) ν (cm⁻¹) = 3420 (br, NH-stretch); 3095 (m, Aryl-CH-stretch); 1604 (m, C=C-stretch); 1509 (m, C=C-stretch).

EI-MS: *m/z* = 184 (100, M⁺); 168 (47, M⁺-O); 140 (43, M⁺-CH₂N); 113 (13, M⁺-C₃H₃N); 102 (9, M⁺-C₄H₄NO); 92 (5, M⁺-C₆H₄O); 63 (9, 7, C₅H₃⁺).

4-Chloro-9H-pyrido[2,3-b]indole

Molecular formula: C₁₁H₇ClN₂

Molecular weight: 202.64 g/mol

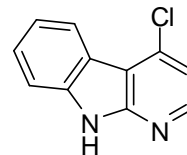
Melting point: 231-234 °C [Lit.: 232-235 °C]

R_f-value: [Cyc : EE 50 : 50 v/v] 0,50

Yield: 19.53 g (96.37 mmol, 71 %) beige crystals

Method of preparation:

25 g (135.73 mmol, 1 eq.) of **8** were placed in a 500 ml three-necked flask under argon atmosphere and were suspended in 100 ml of abs. DMF. The suspension was cooled on an ice bath and then, while stirring at 0 °C, 30 ml (49.35 g, 321.85 mmol, 2.4 eq.) of POCl₃ was slowly added dropwise with a syringe. After the addition, the mixture was stirred for 24 h at RT, and then the mixture was carefully poured into 250 ml of water. This mixture was cooled on an ice bath, and was then alkalinized by slow dropwise addition of 10% potassium hydroxide (pH 8-10). The mixture was stirred for 15 min at 0 °C, and then the resulting solid was isolated by suction filtration on a Buchner funnel, washed with water and air dried. The solid was again taken up in acetone, adsorbed onto silica gel and purified by column chromatography on silica gel with Cyc: EE 80:20 (v/v) as an eluent. Besides the main product **9**, about 2.48 g (12.22 mmol, 9%) of 2-chloro- α -carboline **10** were isolated.¹⁰⁴



¹H-NMR: [400 MHz, DMSO-d₆] δ (ppm) = 7.24-7.29 (m, 1H, H-6); 7.27 (d, J = 5.3 Hz, 1H, H-3); 7.48-7.55 (m, 2H, H-7 & H-8); 8.30 (d, J = 7.3 Hz, 1H, H-5); 8.33 (d, J = 5.3 Hz, 1H, H-2); 12.14 (br, 1H, H-9).

¹³C-NMR: [100 MHz, DMSO-d₆] δ (ppm) = 112.0 (t, C-8); 113.1 (q, C-4a); 116.0 (t, C-3); 119.5 (q, C-4b); 120.5 (t, C-6); 122.9 (t, C-5); 127.7 (t, C-7); 136.9 (q, C-4); 139.3 (q, C-8a); 146.9 (t, C-2); 153.1 (q, C-9a).

IR: (KBr) ν (cm⁻¹) = 3436 (br, NH-stretch); 3262 (s, Aryl-CH-stretch); 3090 (m, Aryl-CH-stretch); 1624 (m, NH-stretch); 1597 (s, C=C-stretch); 1573 (s, C=C-stretch); 1456 (s, C=C-stretch); 788 (m, CH-bending); 736 (s, CH-bending).

EI-MS: m/z = 202 (100, M⁺); 167 (22, M⁺-Cl); 140 (22, M⁺-C₂H₃Cl); 113 (11, C₉H₅⁺); 101 (8, C₈H₅⁺).

2-Chloro-9H-pyrido[2,3-b]indole (byproduct) (10)

Molecular formula: C₁₁H₇ClN₂

Molecular weight: 202.64 g/mol

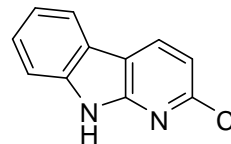
Melting point: 225-230 °C

R_f-value: [Cyc : EE 85 : 15 v/v] 0.54

Yield: 2.48 g (12.22 mmol, 9%) beige solid

Method of preparation:

It has the same procedure similar to the abovementioned method for preparation of the 4-chloro derivative (9) in which it is yielded as a side product.



¹H-NMR: [400 MHz, DMSO-d⁶] δ (ppm) = 7.22-7.27 (m, 1H, H-6); 7.25 (d, *J* = 8.0 Hz, 1H, H-3); 7.44-7.49 (m, 1H, H-7); 7.51 (d, *J* = 7.9 Hz, 1H, H-8); 8.16 (d, *J* = 7.8 Hz, 1H, H-5); 8.53 (d, *J* = 8.0 Hz, 1H, H-4); 12.01 (s, 1H, H-9).

¹³C-NMR: [100 MHz, DMSO-d⁶] δ (ppm) = 111.4 (t, C-8); 114.1 (q, C-4a); 114.3 (t, C-3); 114.3 (q, C-4b); 119.8 (q, C-4b); 119.9 (t, C-6); 121.1 (t, C-5); 126.7 (t, C-7); 131.2 (t, C-4); 138.7 (q, C-8a); 146.1 (q, C-9a); 150.9 (q, C-2).

IR: (KBr) ν (cm⁻¹) = 3436 (br, NH-stretch); 3245 (s, Aryl-CH-stretch); 1622 (m, NH-stretch); 1594 (s, C=C-stretch); 1569 (m, C=C-stretch); 1457 (s, C=C-stretch); 803 (m, CH-bending); 777 (m, CH-bending); 738 (m, CH-bending).

EI-MS: *m/z* = 202 (100, M⁺); 166 (100, M⁺-HCl); 140 (21, M⁺-C₂H₃Cl); 114 (19, M⁺-C₄H₅Cl).

Synthesis of the substituted 4-phenylamino- α -carboline:

General procedure (GP-1):

1 eq. of the 4-chloro- α -carboline **9** and 10 eq. of the respective amine were dissolved in 5 ml of anhydrous NMP, the solution was degassed under vacuum and then for 6-36 h under argon atmosphere was heated to reflux. After cooling the mixture was poured into 50 ml of ethyl acetate, and mixed with 25 ml H₂O. The phases were separated and the aq. phase was extracted three times with 25 ml ethyl acetate. The combined organic phases were dried over sodium sulfate. Then the solvent was removed under reduced pressure and the oily residue is purified by column chromatography on silica gel. The eluent used is indicated for each derivative separately.

N-o-Tolyl-9*H*-pyrido[2,3-*b*]indol-4-amine (11)

Molecular formula: C₁₈H₁₅N₃

Molecular weight: 273.33 g/mol

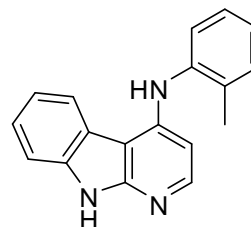
Melting point: 215-218 °C

R_f-value: [EE] 0.47

Yield: 206 mg (0.76 mmol, 61 %) light beige solid

Method of preparation:

250 mg (1.23 mmol, 1 eq.) of **9**, according to **GP1**, is implemented with 1.322 g (12.34 mmol, 10 eq.) 2-toluidine.



¹H-NMR: [400 MHz, DMSO-d₆] δ (ppm) = 2.20 (s, 3H, CH₃); 6.06 (d, *J* = 5.6 Hz, 1H, H-3); 7.09 (ddd, *J* = 7.9 Hz, *J* = 7.1 Hz, *J* = 0.7 Hz, 1H, H-6); 7.13-7.25 (m, 3H, H-4', H-5' & H-6'); 7.31 (ddd, *J* = 8.1 Hz, *J* = 7.3 Hz, *J* = 0.8 Hz, 1H, H-7), 7.33 (d, *J* = 6.3 Hz, 1H, H-3'); 7.40 (d, *J* = 8.0, 1H, H-8); 7.94 (d, *J* = 5.6 Hz, 1H, H-2); 8.00 (s, 1H, Anilin-H); 8.15 (d, *J* = 7.9 Hz, 1H, H-5), 11.52 (s, 1H, H-9).

¹³C-NMR: [100 MHz, DMSO-d₆] δ (ppm) = 18,4 (p, CH₃); 100,9 (t, C-3); 102,1 (q, C-4a); 110,8 (t, C-8); 119,3 (t, C-5); 120,8 (q, C-4b); 122,6 (t, C-6); 124,9 (t, C-7); 126,1 (t, C-6'); 126,8 (t, C-4'); 127,3 (t, C-5'); 131,4 (t, C-3'); 134,5 (q, C-2'); 137,8 (q, C-8a); 139,4 (q, C-1'); 147,2 (t, C-2); 148,2 (q, C-4); 154,0 (q, C-9a).

IR: (KBr) ν (cm⁻¹) = 3422 (br, NH-stretch); 3252 (m, Aryl-CH-stretch); 3144 (w, Aryl-CH-stretch); 3073 (w, Aryl-CH-stretch); 2984 (w, Alkyl-CH-stretch); 2842 (w, Alkyl-CH-stretch); 2764 (w, Alkyl-CH-stretch); 1692 (m, NH-bending); 1593

Experimental Section

(s, C=C-stretch); 1507 (s, C=C-stretch); 1458 (s, C=C-stretch); 1263 (s, C=C-bending); 998 (m, CH-bending); 808 (m, CH-bending); 736 (m, CH-bending).

EI-MS: $m/z = 273$ (100, M^+); 258 (43, $M^+ - CH_3$); 181 (1, $M^+ - C_7H_8$); 155 (2, $C_9H_5N_3^+$); 140 (3, $C_9H_4N_2^+$); 129 (3, $C_7H_3N_3^+$); 91 (1, $C_7H_7^+$).

EA: Calcd: C: 79.10; H: 5.53; N: 15.37
Found: C: 77.66; H: 6.56; N: 14.48

3-(9H-Pyrido[2,3-b]indol-4-ylamino)phenol (12)

Molecular formula: C₁₇H₁₃N₃O

Molecular weight: 275.30 g/mol

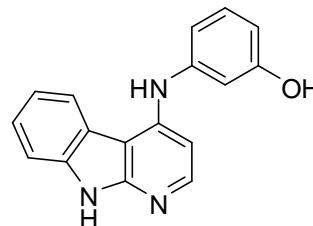
Melting point: 225-227 °C

R_f-value: [EE] 0.30

Yield: 140 mg (0.51 mmol, 41 %) yellow solid

Method of preparation:

250 mg (1.23 mmol, 1 eq.) of **9**, according to **GP1**, is implemented with 1.347 g (12.34 mmol, 10 eq.) 3-aminophenol.



¹H-NMR: [400 MHz, DMSO-d⁶] δ (ppm) = 6.44 (d, *J* = 7.1 Hz, 1H, H-4'); 6.64-6.72 (m, 2H, H-2' & H-6'), 6.78 (d, *J* = 5.5 Hz, 1H, H-2); 7.06-7.13 (m, 2H, H-3' & H-6); 7.32 (dd, *J* = 7.9 Hz, *J* = 7.2 Hz, 1H, H-7); 7.40 (d, *J* = 8.0 Hz, 1H, H-8); 8.04 (d, *J* = 8.1 Hz, 1H, H-5); 8.06 (d, *J* = 5.6 Hz, 1H, H-2); 8.35 (s, 1H, Anilin-NH o. OH); 9.33 (s, 1H, Anilin-NH o. OH); 11.58 (s, 1H, H-9).

¹³C-NMR: [100 MHz, DMSO-d⁶] δ (ppm) = 102.8 (t, C-3); 104.0 (q, C-4a); 108.5 (t, C-2'); 110.4 (t, C-6'); 110.9 (t, C-8); 112.4 (t, C-4'); 119.2 (t, C-5); 120.6 (q, C-4b); 123.2 (t, C-6); 125.2 (t, C-7); 130.2 (t, C-5'); 138.1 (q, C-8a); 143.0 (q, C-1'); 146.7 (q, C-4); 147.1 (t, C-2); 154.1 (q, C-9a); 158.5 (q, C-3').

IR: (KBr) ν (cm⁻¹) = 3420 (br, NH- & OH-stretch); 3056 (w, Aryl-CH-stretch); 1694 (m, NH-bending); 1595 (s, C=C-stretch); 1505 (s, C=C-stretch); 1458 (s, C=C-stretch); 1264 (m, C=C-bending); 808 (w, CH-bending); 739 (m, CH-bending); 733 (m, CH-bending).

EI-MS: *m/z* = 275 (100, M⁺); 257 (7, M⁺-H₂O); 167 (1, C₉H₄N₂⁺); 155 (2, C₉H₅N₃⁺); 140 (4, C₉H₄N₂⁺); 128 (3, C₉H₆N⁺); 113 (2, C₇HN₂⁺).

EA: Calcd: C: 69.61; H: 5.15; N: 14.33

Found: C: 69.91; H: 5.15; N: 14.43

N-(3-Methoxyphenyl)-9H-pyrido[2,3-b]indol-4-amine (13)

Molecular formula: C₁₈H₁₅N₃O

Molecular weight: 289.33 g/mol

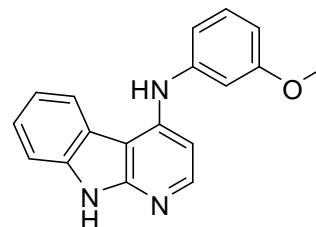
Melting point: 224-225 °C

R_f-value: [EE] 0.51

Yield: 191 mg (0.66 mmol, 54 %) beige solid

Method of preparation:

250 mg (1.23 mmol, 1 eq.) of **9**, according to **GP1**, is implemented with 1.519 g (12.34 mmol, 10 eq.) 3-anisidine.



¹H-NMR: [400 MHz, DMSO-d⁶] δ (ppm) = 3.70 (s, 3H, CH₃); 6.60 (d, *J* = 7.4 Hz, 1H, H-2'); 6.79-6.89 (m, 3H, H-4', H-6' & H-3); 7.11 (dd, *J* = 7.1 Hz, *J* = 7.1 Hz, 1H, H-6); 7.21 (dd, *J* = 8.0 Hz, *J* = 7.2 Hz, 1H, H-5'); 7.33 (dd, *J* = 7.4 Hz, *J* = 7.2 Hz, 1H, H-7); 7.41 (d, *J* = 7.4 Hz, 1H, H-8); 8.01-8.11 (m, 2H, H-5 & H-2); 8.45 (s, 1H, Anilin-H); 11.59 (s, 1H, H-9).

¹³C-NMR: [100 MHz, DMSO-d⁶] δ (ppm) = 55.6 (p, CH₃); 102.8 (t, C-3); 104.2 (q, C-4a); 107.1 (t, C-2'); 108.6 (t, C-4'); 110.9 (t, C-8); 113.5 (t, C-6'); 119.2 (t, C-5); 120.5 (q, C-4b); 123.2 (t, C-6); 125.3 (t, C-7); 130.3 (t, C-5'); 138.1 (q, C-8a); 143.2 (q, C-1'); 146.4 (q, C-4); 147.2 (t, C-2); 154.2 (q, C-9a); 160.5 (q, C-3').

IR: (KBr) ν (cm⁻¹) = 3441 (br, NH-stretch); 3145 (w, Aryl-CH-stretch); 3076 (w, Aryl-CH-stretch); 2971 (w, Alkyl-CH-stretch); 2925 (w, Alkyl-CH-stretch); 2838 (w, Alkyl-CH-stretch); 2763 (w, Alkyl-CH-stretch); 1598 (s, C=C-stretch); 1511 (m, C=C-stretch); 1493 (s, C=C-stretch); 1458 (s, C=C-stretch); 1264 (s, C=C-stretch); 1160 (s, C-O-stretch); 856 (m, CH-bending); 801 (m, CH-bending); 732 (m, CH-bending).

EI-MS: *m/z* = 289 (100, M⁺); 274 (9, M⁺-CH₃); 258 (6, M⁺-CH₃O); 140 (3, C₉H₄N₂⁺); 129 (2, C₇H₃N₃⁺); 122 (4, C₇H₈NO⁺); 113 (2, C₇HN₂⁺).

N-(3-Ethoxyphenyl)-9H-pyrido[2,3-b]indol-4-amine (14)

Molecular formula: C₁₉H₁₇N₃O

Molecular weight: 303.36 g/mol

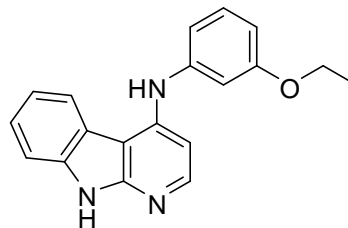
Melting point: 193-195 °C

R_f-value: [EE] 0.48

Yield: 260 mg (0.86 mmol, 70 %) light beige solid

Method of preparation:

250 mg (1.23 mmol, 1 eq.) of **9**, according to **GP1**, is implemented with 1.692 g (12.34 mmol, 10 eq.) 3-phenetidine.



¹H-NMR: [400 MHz, CDCl₃] δ (ppm) = 1.41-1.44 (t, *J* = 7.1 Hz, 3H, OCH₂CH₃); 4.03-4.08 (q, *J* = 13.9 Hz, 2H, OCH₂CH₃); 6.69-6.74 (m, 2H, H-2', H-6'); 6.90-6.95 (m, 3H, H-3, H-4', H-5'); 7.24-7.32 (m, 3H, H-6, H-7, H-8); 7.42-7.55 (m, 2H, H-2, H-5); 7.88 (d, *J* = 7.7 Hz, 1H, aniline-H); 8.20 (d, *J* = 5.8 Hz, 1H, H-9).

¹³C-NMR: [100 MHz, CDCl₃] δ (ppm) = 14.9 (p, CH₃); 63.7 (s, CH₂); 101.1 (t, C-3); 103.2 (q, C-4a); 108.6 (t, C-2'); 110.6 (t, C-4'); 111.2 (t, C-8); 114.4 (t, C-6'); 120.1 (t, C-5); 120.6 (q, C-4b); 120.9 (t, C-6); 125.3 (t, C-7); 130.3 (t, C-5'); 137.5 (q, C-8a); 140.1 (q, C-1'); 145.9 (q, C-4); 147.3 (t, C-2); 153.1 (q, C-9a); 160.1 (q, C-3').

IR: (ATR) ν (cm⁻¹) = 3445 (w, NH-stretch); 3145 (w, Aryl-CH-stretch); 3051 (w, Aryl-CH-stretch); 2956 (w, Alkyl-CH-stretch); 2916 (s, Alkyl-CH-stretch); 2848 (s, Alkyl-CH-stretch); 2785 (w, Alkyl-CH-stretch); 1596 (m, C=C-stretch); 1512 (m, C=C-stretch); 1493 (m, C=C-stretch); 1457 (m, C=C-stretch); 1263 (w, C=C-stretch); 1165 (s, C-O-stretch); 858 (m, CH-bending); 810 (m, CH-bending); 730 (m, CH-bending).

ESI-MS: *m/z* = 304.3 (M⁺+H⁺)

N-(3-Chlorophenyl)-9H-pyrido[2,3-b]indol-4-amine (15)

Molecular formula: C₁₇H₁₂ClN₃

Molecular weight: 293.75 g/mol

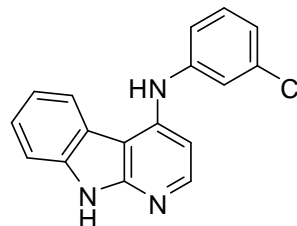
Melting point: 241-244 °C

R_f-value: [EE] 0.56

Yield: 337 mg (1.15 mmol, 78 %) light brown solid

Method of preparation:

300 mg (1.48 mmol, 1 eq.) of **9**, according to **GP1**, is implemented with 1.889 g (14.80 mmol, 10 eq.) 3-Chloroaniline.



¹H-NMR: [400 MHz, DMSO-d₆] δ (ppm) = 6.85 (d, *J* = 5.6 Hz, 1H, H-3); 7.02 (dd, *J* = 7.9 Hz, *J* = 1.0 Hz, 1H, H-6'); 7.11 (ddd, *J* = 7.9 Hz, *J* = 7.1 Hz, *J* = 0.8 Hz, 1H, H-6); 7.19 (dd, *J* = 7.9 Hz, *J* = 1.2 Hz, 1H, H-4'); 7.25 (dd, *J* = 1.8 Hz, *J* = 1.9 Hz, 1H, H-1'); 7.31 (dd, *J* = 8.0 Hz, *J* = 7.8 Hz, 1H, H-3'); 7.34 (ddd, *J* = 8.0 Hz, *J* = 7.2 Hz, *J* = 0.8 Hz, 1H, H-7); 7.43 (d, *J* = 8.1 Hz, 1H, H-8); 7.98 (d, *J* = 8.0 Hz, 1H, H-5); 8.13 (d, *J* = 5.6 Hz, 1H, H-2); 8.68 (s, 1H, Anilin-H); 11.66 (s, 1H, H-9).

¹³C-NMR: [100 MHz, DMSO-d₆] δ (ppm) = 103.5 (t, C-3); 104.9 (q, C-4a); 111.1 (t, C-8); 118.6 (t, C-2'); 119.3 (t, C-5); 119.9 (t, C-6'); 120.3 (q, C-4b); 122.0 (t, C-4'); 123.3 (t, C-6); 125.6 (t, C-7); 131.1 (t, C-5'); 134.0 (q, C-1'); 138.2 (q, C-8a); 143.9 (q, C-3'); 145.4 (q, C-4); 147.3 (t, C-2); 154.2 (q, C-9a).

IR: (KBr) ν (cm⁻¹) = 3412 (br, NH-stretch); 3238 (w, Aryl-CH-stretch); 3141 (w, Aryl-CH-stretch); 3072 (w, Aryl-CH-stretch); 1698 (w, NH-bending); 1584 (s, C=C-stretch); 1506 (s, C=C-stretch); 1457 (s, C=C-stretch); 1258 (s, C=C-bending); 878 (w, CH-bending); 807 (w, CH-bending); 750 (m, CH-bending).

EI-MS: *m/z* = 293 (100, M⁺); 257 (24, M⁺-HCl); 155 (4, C₉H₅N₃⁺); 140 (6, C₉H₄N₂⁺); 129 (11, C₇H₃N₃⁺); 113 (3, C₇HN₂⁺); 75 (1, C₆H₃⁺).

EA: Calcd: C: 69.51; H: 4.12; Cl: 12.07; N: 14.30

Found: C: 69.71; H: 4.14; Cl: 12.00; N: 14.06

N-(3-(Trifluoromethyl)phenyl)-9H-pyrido[2,3-b]indol-4-amine (16)

Molecular formula: C₁₈H₁₂F₃N₃

Molecular weight: 327.30 g/mol

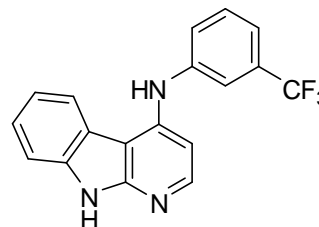
Melting point: 229-231 °C

R_f-value: [EE] 0.65

Yield: 215 mg (0.66 mmol, 53 %) light orange solid

Method of preparation:

250 mg (1.23 mmol, 1 eq.) of **9**, according to **GP1**, is implemented with 1.347 g (12.34 mmol, 10 eq.) 3-aminobenzotrifluoride.



¹H-NMR: [400 MHz, DMSO-d₆] δ (ppm) = 6.86 (d, *J* = 5.6 Hz, 1H, H-3); 7.11 (ddd, *J* = 7.9 Hz, *J* = 7.1 Hz, *J* = 0.8 Hz, 1H, H-6); 7.27-7.32 (m, 1H, H-6'); 7.35 (ddd, *J* = 8.1 Hz, *J* = 7.2 Hz, *J* = 0.8 Hz, 1H, H-7); 7.43 (d, *J* = 8.0 Hz, 1H, H-8); 7.49-7.57 (m, 3H, H-2', H-4' & H-5'); 7.99 (d, *J* = 7.8 Hz, 1H, H-5); 8.14 (d, *J* = 5.6 Hz, 1H, H-2); 8.83 (s, 1H, Anilin-NH); 11.70 (s, 1H, H-9).

¹³C-NMR: [100 MHz, DMSO-d₆] δ (ppm) = 103.3 (t, C-3); 104.9 (q, C-4); 111.1 (t, C-8); 116.4 (q, C-2'); 118.5 (t, C-4'); 119.3 (t, C-5); 120.2 (q, C-4b); 123.3 (t, C-6); 123.5 (t, C-6'); 125.6 (t, C-7); 128.2 (q, *J* = 440.3 Hz; CF₃); 130.7 (t, C-3' & C-5'); 138.3 (q, C-8a); 143.1 (q, C-1'); 145.3 (q, C-4); 147.3 (t, C-2); 154.2 (q, C-9a).

IR: (KBr) ν (cm⁻¹) = 3381 (m, NH-stretch); 3213 (w, Aryl-CH-stretch); 3144 (w, Aryl-CH-stretch); 3078 (w, Aryl-CH-stretch); 1699 (s, NH-bending); 1586 (s, C=C-stretch); 1511 (m, C=C-stretch); 1458 (m, C=C-stretch); 1334 (s, C-F-stretch); 799 (m, CH-bending); 743 (m, CH-bending); 699 (m, CH-bending).

EI-MS: *m/z* = 327 (100, M⁺); 257 (9, M⁺-HCF₃); 140 (4, C₉H₄N₂⁺); 129 (4, C₇H₃N₃⁺); 69 (1, CF₃⁺).

EA: Calcd: C: 66.05; H: 3.70; N: 12.84

Found: C: 65.49; H: 3.75; N: 12.47

N-(3-(Methylthio)phenyl)-9H-pyrido[2,3-b]indol-4-amine (17)

Molecular formula: C₁₈H₁₅N₃S

Molecular weight: 305.40 g/mol

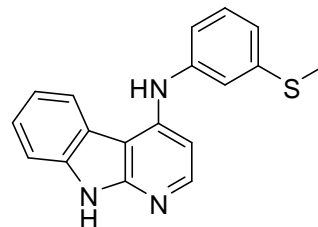
Melting point: 257-260 °C

R_f-value: [EE] 0.38

Yield: 298 mg (0.98 mmol, 79 %) beige solid

Method of preparation:

250 mg (1.23 mmol, 1 eq.) of **9**, according to **GP1**, is implemented with 1.718 g (12.34 mmol, 10 eq.) 3-(methylmercapto) aniline.



¹H-NMR: [400 MHz, DMSO-d₆] δ (ppm) = 2.43 (s, 3H, CH₃); 6.82 (d, *J* = 5.6 Hz, 1H, H-3); 6.93 (d, *J* = 7.8 Hz, 1H, H-4'); 7.07 (d, *J* = 7.6 Hz, 1H, H-6'); 7.14 (dd, *J* = 7.6 Hz, *J* = 7.5 Hz, 1H, H-6); 7.18 (s, 1H, H-2'); 7.27 (dd, *J* = 7.8 Hz, *J* = 7.6 Hz, 1H, H-5'); 7.36 (dd, *J* = 7.9 Hz, *J* = 7.4 Hz, 1H, H-7); 7.45 (d, *J* = 7.9 Hz, 1H, H-8); 8.08 (d, *J* = 7.9 Hz, 1H, H-5); 8.11 (d, *J* = 5.6 Hz, 1H, H-2); 8.54 (s, 1H, Anilin-NH); 11.65 (s, 1H, H-9).

¹³C-NMR: [100 MHz, DMSO-d₆] δ (ppm) = 15.3 (p, CH₃); 102.8 (t, C-3); 104.2 (q, C-4a); 111.0 (t, C-8); 117.5 (t, C-2'); 118.3 (t, C-6'); 119.3 (t, C-5); 120.3 (q, C-4b); 120.4 (t, C-4'); 123.2 (t, C-6); 125.3 (t, C-7); 129.9 (t, C-5'); 138.1 (q, C-8a); 139.5 (q, C-3'); 142.5 (q, C-1'); 146.2 (q, C-4); 147.2 (t, C-2); 154.1 (q, C-9a).

IR: (KBr) ν (cm⁻¹) = 3437 (br, NH-stretch); 3073 (w, Aryl-CH-stretch); 2983 (w, Alkyl-CH-stretch); 2922 (w, Alkyl-CH-stretch); 2841 (w, Alkyl-CH-stretch); 2761 (w, Alkyl-CH-stretch); 1581 (s, C=C-stretch); 1511 (s, C=C-stretch); 1481 (m, C=C-stretch); 1458 (m, C=C-stretch); 1263 (m, C=C-stretch); 730 (m, CH-bending).

EI-MS: *m/z* = 305 (100, M⁺); 290 (5, M⁺-NH); 272 (9, M⁺-SH); 257 (54, M⁺-CH₄S); 155 (2, C₉H₅N₃⁺); 140 (5, C₉H₄N₂⁺); 129 (8, C₇H₃N₃⁺); 122 (3, C₆H₄NS⁺); 113 (4, C₉H₅⁺); 77 (1, C₆H₅⁺).

EA: Calcd: C: 70.79; H: 4.95; N: 13.76; S: 10.50

Found: C: 69.89; H: 4.89; N: 13.18; S: 10.36

N-(3-Benzyloxyphenyl)-9H-pyrido[2,3-b]indol-4-amine (18)

Molecular formula: C₂₄H₁₉N₃O

Molecular weight: 365.43 g/mol

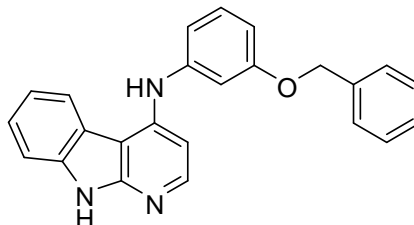
Melting point: 164-170 °C

R_f-value: [EE] 0.45

Yield: 300 mg (0.82 mmol, 67 %) light beige solid

Method of preparation:

250 mg (1.23 mmol, 1 eq.) of **9**, according to **GP1**, is implemented with 2.458 g (12.34 mmol, 10 eq.) 3-benzyloxyaniline.



¹H-NMR: [400 MHz, CDCl₃] δ (ppm) = 5.09 (s, 2H, -OCH₂-); 6.80-6.84 (m, 3H, H-2', H-6' & H-4'); 6.89 (d, *J* = 8.1 Hz, 1H, H-3); 6.96 (d, *J* = 2.3 Hz, 1H, H-5'); 7.24-7.46 (m, 9H, -OCH₂C₆H₅, H-5, H-6, H-7, H-8); 7.62 (d, *J* = 8.1 Hz, 1H, H-2); 7.87 (d, *J* = 7.9 Hz, 1H, Aniline-NH); 8.11 (d, *J* = 6.0 Hz, 1H, H-9).

¹³C-NMR: [100 MHz, CDCl₃] δ (ppm) = 70.24 (p, O-CH₂); 101.2 (t, C-3); 103.2 (q, C-4a); 108.9 (t, C-2'); 111.1 (t, C-4'); 111.3 (t, C-8); 114.9 (t, C-6'); 120.3 (t, C-5); 120.6 (q, C-4b); 120.9 (t, C-6); 125.5 (t, C-7); 127.4-128.6 (5C, OCH₂C₆H₅); 130.4 (t, C-5'); 136.7 (q, C-1''); 137.2 (q, C-8a); 140.1 (q, C-1'); 145.6 (q, C-4); 147.3 (t, C-2); 153.1 (q, C-9a); 159.8 (q, C-3').

IR: (ATR) ν (cm⁻¹) = 3423 (w, NH-stretch); 3059 (w, Aryl-CH-stretch); 2983 (w, Alkyl-CH-stretch); 2917 (w, Alkyl-CH-stretch); 2830 (w, Alkyl-CH-stretch); 2756 (w, Alkyl-CH-stretch); 1582 (s, C=C-stretch); 1511 (s, C=C-stretch); 1481 (m, C=C-stretch); 1458 (m, C=C-stretch); 1263 (m, C=C-stretch); 735 (m, CH-bending).

ESI-MS: *m/z* = 366.15 (M⁺+H⁺).

N-(3-Nitrophenyl)-9H-pyrido[2,3-b]indol-4-amine (19)

Molecular formula: C₁₇H₁₂N₄O₂

Molecular weight: 304.30 g/mol

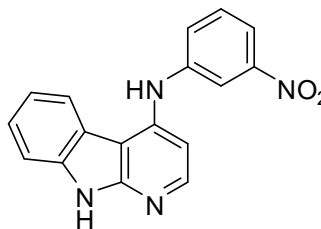
Melting point: 290-293 °C

R_f-value: [EE] 0.50

Yield: 260 mg (0.85 mmol, 70 %) orange solid

Method of preparation:

250 mg (1.23 mmol, 1 eq.) of **9**, according to **GP1**, is implemented with 1.704 g (12.34 mmol, 10 eq.) 3-nitroaniline.



¹H-NMR: [400 MHz, DMSO-d₆] δ (ppm) = 6.93 (d, *J* = 4.4 Hz, 1H, H-3); 7.36 (d, *J* = 6.8 Hz, 1H, H-2'); 7.43 (d, *J* = 7.9 Hz, 2H, H-4' & H-6'); 7.55 (d, *J* = 7.9 Hz, 2H, H-6 & H-8); 7.63-7.8.19 (m, 4H, H-5', H-5, H-7 & H-2); 9.04 (s, 1H, Aniline-NH); 11.74 (s, 1H, H-9).

¹³C-NMR: [100 MHz, Acetone-d₆] δ (ppm) = 104.8 (t, C-3); 105.0 (q, C-4a); 111.5 (t, C-8); 114.7 (t, C-2'); 117.1 (t, C-6'); 119.3 (t, C-5); 120.1 (q, C-4b); 120.4 (t, C-4'); 123.3 (t, C-6); 126.1 (t, C-7); 129.9 (t, C-5'); 131.0 (q, C-8a); 139.5 (q, C-3'); 142.6 (q, C-1'); 146.5 (q, C-4); 147.9 (t, C-2); 154.0 (q, C-9a).

IR: (ATR) ν (cm⁻¹) = 3407 (br, NH-stretch); 3075 (w, Aryl-CH-stretch); 2977 (m, Alkyl-CH-stretch); 2918 (w, Alkyl-CH-stretch); 2830 (w, Alkyl-CH-stretch); 2758 (w, Alkyl-CH-stretch); 1595 (s, C=C-stretch); 1519 (s, C=C-stretch); 1505 (m, C=C-stretch); 1457 (m, C=C-stretch); 1276 (m, C=C-stretch); 729 (m, CH-bending).

ESI-MS: *m/z* = 305.20 (M⁺+H⁺).

N-(4-Chlorophenyl)-9H-pyrido[2,3-b]indol-4-amine (20)

Molecular formula: C₁₇H₁₂ClN₃

Molecular weight: 293.75 g/mol

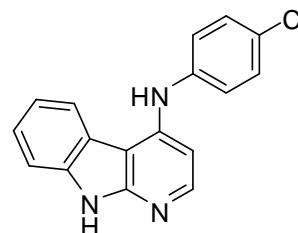
Melting point: 274-277 °C

R_f-value: [EE] 0.45

Yield: 276 mg (0.94 mmol, 64 %) beige solid

Method of preparation:

300 mg (1.48 mmol, 1 eq.) of **9**, according to **GP1**, is implemented with 1.889 g (14.80 mmol, 10 eq.) 4-Chloroaniline.



¹H-NMR: [400 MHz, DMSO-d⁶] δ (ppm) = 6.77 (d, *J* = 5.6 Hz, 1H, H-3); 7.11 (ddd, *J* = 1.0 Hz, *J* = 7.0 Hz, *J* = 8.1 Hz, 1H, H-6); 7.25 (d, *J* = 8.1 Hz, 2H, H-2' & H-6'); 7.31-7.37 (m, 3H, H-7, H-3' & H-5'); 7.42 (d, *J* = 8.0 Hz, 1H, H-8); 8.01 (d, *J* = 7.9 Hz, 1H, H-5); 8.09 (d, *J* = 5.6 Hz, 1H, H-2); 8.55 (s, 1H, Anilin-NH); 11.63 (s, 1H, H-9).

¹³C-NMR: [100 MHz, DMSO-d⁶] δ (ppm) = 102.2 (t, C-3); 103.8 (q, C-4a); 110.4 (t, C-8); 118.7 (t, C-5); 119.8 (q, C-4b); 122.0 (t, C-2' & C-6'); 122.6 (t, C-6); 124.8 (t, C-7); 125.7 (q, C-4'); 128.9 (t, C-3' & C-5'); 137.6 (q, C-8a); 140.5 (q, C-1'); 145.5 (q, C-4); 146.7 (t, C-2); 153.6 (q, C-9a).

IR: (KBr) ν (cm⁻¹) = 3424 (br, NH-stretch); 3142 (w, Aryl-CH- stretch); 3073 (m, Aryl-CH-stretch); 1588 (s, C=C-stretch); 1493 (s, C=C-stretch); 1457 (s, C=C-stretch); 1261 (s, C=C-bending); 877 (w, CH-bending); 796 (m, CH-bending); 731 (m, CH-bending).

EI-MS: *m/z* = 293 (100, M⁺); 257 (18, M⁺-HCl); 155 (1, C₉H₅N₃⁺); 140 (2, C₉H₄N₂⁺); 129 (2, C₇H₃N₃⁺); 113 (1, C₇HN₂⁺).

EA: Calcd: C: 69.51; H: 4.12; N: 14.30; Cl: 12.07

Found: C: 69.55; H: 4.09; N: 14.36; Cl: 12.17

N-(4-Methoxyphenyl)-9H-pyrido[2,3-b]indol-4-amine (21)

Molecular formula: C₁₈H₁₅N₃O

Molecular weight: 289.33 g/mol

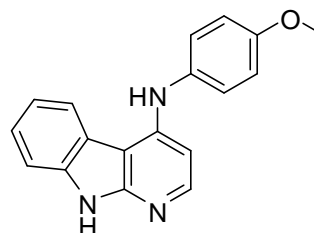
Melting point: 236-240 °C

R_f-value: [EE] 0.53

Yield: 215 mg (0.74 mmol, 61 %) brown solid

Method of preparation:

250 mg (1.23 mmol, 1 eq.) of **9**, according to **GP1**, is implemented with 1.823 g (14.80 mmol, 12 eq.) 4-anisidine.



¹H-NMR: [400 MHz, DMSO-d₆] δ (ppm) = 3.77 (s, 3H, CH₃); 6.48 (d, *J* = 5.7 Hz, 1H, H-3); 6.99 (d, *J* = 8.9 Hz, 2H, H-3' & H-5'); 7.14 (dd, *J* = 7.9 Hz, *J* = 7.1 Hz, 1H, H-6); 7.26 (d, *J* = 8.8 Hz, 2H, H-2' & H-6'); 7.34 (dd, *J* = 7.8 Hz, *J* = 7.2 Hz, 1H, H-7); 7.42 (d, *J* = 8.0 Hz, 1H, H-8); 7.99 (d, *J* = 5.7 Hz, 1H, H-2); 8.19 (s, 1H, Aniline-NH); 8.25 (d, *J* = 7.9 Hz, 1H, H-5); 11.53 (s, H-9).

¹³C-NMR: [100 MHz, DMSO-d₆] δ (ppm) = 55.9 (p, CH₃); 100.6 (t, C-3); 102.4 (q, C-4a); 110.8 (t, C-8); 115.0 (t, C-3' & C-5'); 119.2 (t, C-5); 120.8 (q, C-4b); 122.7 (t, C-6); 124.9 (t, C-7); 125.6 (t, C-2' & C-6'); 134.1 (q, C-1'); 137.8 (q, C-8a); 147.2 (t, C-2); 148.3 (q, C-4); 154.0 (q, C-9a); 156.4 (q, C-4').

IR: (KBr) ν (cm⁻¹) = 3425 (br, NH-stretch); 3208 (w, Aryl-CH-stretch); 3143 (m, Aryl-CH-stretch); 3075 (m, Aryl-CH-stretch); 3000 (m, Alkyl-CH-stretch); 2910 (m, Alkyl-CH-stretch); 2835 (m, Alkyl-CH-stretch); 2762 (m, Alkyl-CH-stretch); 1593 (s, C=C-stretch); 1508 (s, C=C-stretch); 1456 (s, C=C-stretch); 1263 (s, C=C-bending); 1241 (s, C-O-stretch); 816 (m, CH-bending); 799 (m, CH-bending).

EI-MS: *m/z* = 289 (100, M⁺); 274 (64, M⁺-CH₃); 257 (4, M⁺-CH₄O); 167 (2, C₁₁H₇N₂⁺); 140 (4, C₉H₄N₂⁺); 122 (3, C₇H₈NO⁺); 113 (1, C₇HN₂⁺).

EA: Calcd: C: 74.72; H: 5.23; N: 14.52

Found: C: 74.17; H: 5.34; N: 14.20

N-(3,5-Dichlorophenyl)-9 H-pyrido[2,3-b]indol-4-amine (22)

Molecular formula: C₁₇H₁₁Cl₂N₃

Molecular weight: 328.20 g/mol

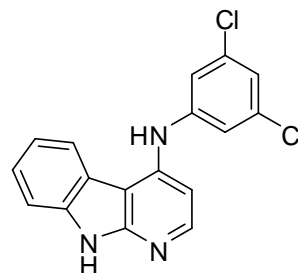
Melting point: 276-278 °C

R_f-value: [EE] 0.56

Yield: 306 mg (0.93 mmol, 68 %) light brown

Method of preparation:

300 mg (1.48 mmol, 1 eq.) of **9**, according to **GP1**, is implemented with 2.383 g (14.80 mmol, 10 eq.) 3,5-Dichloroaniline.



¹H-NMR: [400 MHz, DMSO-d₆] δ (ppm) = 6.94 (d, *J* = 5.5 Hz, 1H, H-3); 7.09 (t, *J* = 1.8 Hz, 1H, H-4'); 7.13 (ddd, *J* = 8.0 Hz, *J* = 7.1 Hz, *J* = 0.9 Hz, 1H, H-6); 7.17 (d, *J* = 1.8 Hz, 2H, H-3' & H-5'); 7.37 (ddd, *J* = 8.0 Hz, *J* = 7.2 Hz, *J* = 0.8 Hz, 1H, H-7); 7.45 (d, *J* = 8.0 Hz, 1H, H-8); 7.92 (d, *J* = 7.9 Hz, 1H, H-5); 8.20 (d, *J* = 5.5 Hz, 1H, H-2); 8.93 (s, 1H, Aniline-NH); 11.76 (s, 1H, H-9).

¹³C-NMR: [100 MHz, DMSO-d₆] δ (ppm) = 104.2 (t, C-3); 105.2 (q, C-4a); 110.6 (t, C-8); 116.6 (t, C-2' & C-6'); 118.9 (t, C-4'); 119.4 (q, C-4b); 120.1 (t, C-5); 122.8 (t, C-6); 125.3 (t, C-7); 134.3 (q, C-3' & C-5'); 137.8 (q, C-8a); 143.6 (q, C-1'); 144.7 (q, C-4); 146.8 (t, C-2); 153.6 (q, C-9a).

IR: (KBr) ν (cm⁻¹) = 3383 (s, NH-stretch); 3212 (m, Aryl-CH-stretch); 3146 (m, Aryl-CH-stretch); 3086 (m, Aryl-CH-stretch); 1697 (s, NH-bending); 1596 (s, C=C-stretch); 1503 (s, C=C-stretch); 1459 (s, C=C-stretch); 1111 (m, C-Cl-stretch); 812 (m, CH-bending); 803 (m, CH-bending); 735 (m, CH-bending); 661 (m, CH-bending).

EI-MS: *m/z* = 328 (100, M⁺); 291 (18, M⁺-HCl); 257 (21, M⁺-Cl₂); 167 (4, M⁺-C₆H₄Cl₂N); 155 (8, C₉H₅N₃⁺); 140 (13, C₉H₄N₂⁺); 128 (12, C₉H₆N⁺); 113 (8, C₇HN₂⁺).

EA: Calcd: C: 62.21; H: 3.38; N: 12.80; Cl: 21.60

Found: C: 61.44; H: 3.90; N: 12.53; Cl: 21.71

N-(3-Chloro-4-methylphenyl)-9H-pyrido[2,3-b]indol-4-amine (23)

Molecular formula: C₁₈H₁₄ClN₃

Molecular weight: 307.78 g/mol

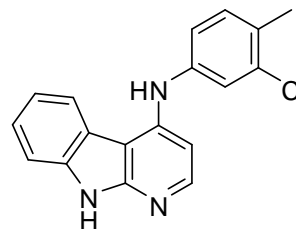
Melting point: 226-227 °C

R_f-value: [EE] 0.60

Yield: 306 mg (0.99 mmol, 81 %) light gray solid

Method of preparation:

250 mg (1.23 mmol, 1 eq.) of **9**, according to **GP1**, is implemented with 1.747 g (14.80 mmol, 12 eq.) 3-Chloro-4-methylaniline.



¹H-NMR: [400 MHz, DMSO-d₆] δ (ppm) = 2.27 (s, 3H, CH₃); 6.75 (d, *J* = 5.6 Hz, 1H, H-3); 7.09-7.18 (m, 2H, H-6 & H-6'); 7.27 (d, *J* = 8.2 Hz, 1H, H-5'); 7.30 (d, *J* = 2.3 Hz, 1H, H-2'); 7.33 (dd, *J* = 7.9 Hz, *J* = 7.3 Hz, 1H, H-7); 7.41 (d, *J* = 8.0 Hz, 1H, H-8); 8.07 (d, *J* = 7.6 Hz, 1H, H-5); 8.08 (d, *J* = 5.6 Hz, 1H, H-2); 8.50 (s, 1H, Aniline-NH); 11.63 (s, 1H, H-9).

¹³C-NMR: [100 MHz, DMSO-d₆] δ (ppm) = 19.5 (p, CH₃); 102.5 (t, C-3); 104.2 (q, C-4a); 111.0 (t, C-8); 119.3 (t, C-5); 120.0 (t, C-6'); 120.4 (q, C-4b); 121.4 (t, C-2'); 123.1 (t, C-6); 125.4 (t, C-7); 129.4 (q, C-4'); 131.9 (t, C-5'); 133.9 (q, C-3'); 138.1 (q, C-8a); 141.2 (q, C-1'); 146.1 (q, C-4); 147.2 (t, C-2); 154.1 (q, C-9a).

IR: (KBr) ν (cm⁻¹) = 3433 (br, NH-stretch); 3078 (w, Aryl-CH-stretch); 2985 (w, Alkyl-CH-stretch); 2921 (w, Alkyl-CH-stretch); 2842 (w, Alkyl-CH-stretch); 2764 (m, Alkyl-CH-stretch); 1695 (w, NH-bending); 1590 (s, C=C-stretch); 1505 (s, C=C-stretch); 1458 (m, C=C-stretch); 802 (m, CH-bending); 734 (m, CH-bending).

EI-MS: *m/z* = 307 (100, M⁺); 292 (2, M⁺-CH₃); 272 (16, M⁺-Cl); 155 (4, C₉H₅N₃⁺); 140 (7, C₇H₇ClN⁺); 113 (4, C₅H₄ClN⁺).

N-(3-Chloro-4-fluorophenyl)-9 H-pyrido[2,3-b]indol-4-amine (24)

Molecular formula: C₁₇H₁₁ClFN₃

Molecular weight: 311.74 g/mol

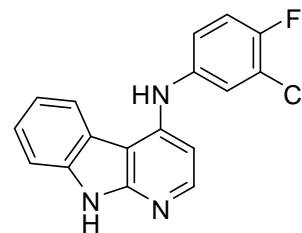
Melting point: 252-254 °C

R_f-value: [EE] 0.51

Yield: 329 mg (1.05 mmol, 85 %) sand-color solid

Method of preparation:

250 mg (1.23 mmol, 1 eq.) of **9**, according to **GP1**, is implemented with 1.796 g (14.80 mmol, 12 eq.) 3-Chloro-4-fluoroaniline.



¹H-NMR: [400 MHz, DMSO-d⁶] δ (ppm) = 6.76 (d, *J* = 5.6 Hz, 1H, H-3); 7.15 (dd, *J* = 7.8 Hz, *J* = 7.3 Hz, 1H, H-6); 7.26-7.30 (m, 1H, H-5'); 7.34-7.42 (m, 2H, H-2' & H-7); 7.42-7.48 (m, 2H, H-6' & H-8); 8.08 (d, *J* = 7.9 Hz, 1H, H-8); 8.12 (d, *J* = 5.6 Hz, 1H, H-2); 8.60 (s, 1H, Aniline-NH); 11.69 (s, 1H, H-9).

¹³C-NMR: [100 MHz, DMSO-d⁶] δ (ppm) = 102.4 (q, C-4a); 104.1 (t, C-3); 111.0 (t, C-8); 117.7 (t, *J* = 21.7 Hz, C-6'); 119.3 (t, C-5); 120.1 (q, *J* = 18.5 Hz, C-3'); 120.3 (q, C-4b); 121.6 (t, *J* = 6.9 Hz, C-5'); 122.9 (t, C-6); 123.0 (t, *J* = 18.0 Hz, C-2'); 125.4 (t, C-7); 138.1 (q, C-8a); 139.3 (q, *J* = 2.7 Hz, C-1'); 146.1 (q, C-4); 147.3 (t, C-2); 153.4 (q, *J* = 241.1 Hz, C-4'); 154.1 (q, C-9a).

IR: (KBr) ν (cm⁻¹) = 3435 (br, NH-stretch); 3077 (w, Aryl-CH-stretch); 2986 (w, Alkyl-CH-stretch); 2924 (w, Alkyl-CH-stretch); 2838 (w, Alkyl-CH-stretch); 2764 (w, Alkyl-CH-stretch); 1695 (s, NH-bending); 1586 (s, C=C-stretch); 1499 (s, C=C-stretch); 1458 (m, C=C-stretch); 1257 (m, C=C-bending); 801 (m, CH-bending); 737 (m, CH-bending).

EI-MS: *m/z* = 311 (100, M⁺); 275 (25, M⁺-HCl); 256 (2, M⁺-HClF); 155 (5, C₉H₅N₃⁺); 113 (4, C₉H₅⁺).

EA: Calcd: C: 65.50; H: 3.56; N: 13.48

Found: C: 64.06; H: 3.78; N: 12.94

N-(4-bromo-3-ethoxyphenyl)-9H-pyrido[2,3-b]indol-4-amine (25)

Molecular formula: C₁₉H₁₆BrN₃O

Molecular weight: 382.25 g/mol

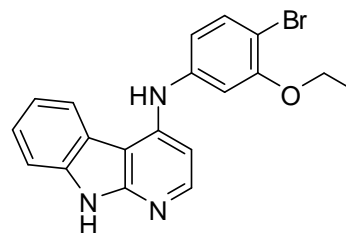
Melting point: 185-190 °C

R_f-value: [EE] 0.43

Yield: 140 mg (0.37 mmol, 28 %); light green solid

Method of preparation:

250 mg (1.23 mmol, 1 eq.) of **9**, according to **GP1**, is implemented with 2.666 g (12.34 mmol, 10 eq.) 3-ethoxy-4-bromoaniline.



¹H-NMR: [400 MHz, Acetone-d₆] δ (ppm) = 1.28-1.41 (m, 3H, OCH₂CH₃); 4.01-4.10 (m, 2H, OCH₂CH₃); 6.66 (d, *J* = 8.3 Hz, 1H, H-2'); 6.89-7.08 (m, 1H, H-3); 7.15 (t, *J* = 7.3 Hz, 1H, H-6); 7.26 (t, *J* = 8.4 Hz, 1H, H-7); 7.35-7.39 (m, 1H, H-5'); 7.48-7.55 (m, 1H, H-8); 7.89 (s, 1H, Aniline-NH); 8.04 (d, *J* = 8.3 Hz, 1H, H-5); 8.10 (d, *J* = 7.8 Hz, 1H, H-2); 10.73 (s, 1H, H-9).

¹³C-NMR: [100 MHz, DMSO-d₆] δ (ppm) = 14.9 (p, CH₃); 63.4 (s, CH₂); 103.5 (t, C-3); 106.7 (q, C-4a); 110.9 (t, C-8); 119.2 (t, C-5); 120.4 (t, C-6'); 123.3 (q, C-4b); 125.3 (t, C-2'); 125.5 (t, C-6); 127.0 (t, C-7); 129.2 (q, C-4'); 130.9 (t, C-5'); 133.4 (q, C-3'); 138.2 (q, C-8a); 142.9 (q, C-1'); 143.1 (q, C-4); 147.3 (t, C-2); 155.6 (q, C-9a).

IR: (ATR) ν (cm⁻¹) = 3428 (br, NH-stretch); 3072 (m, Aryl-CH-stretch); 2968 (m, Alkyl-CH-stretch); 2923 (m, Alkyl-CH-stretch); 2851 (m, Alkyl-CH-stretch); 2762 (w, Alkyl-CH-stretch); 1672 (w, NH-bending); 1577 (s, C=C-stretch); 1490 (m, C=C-stretch); 1454 (m, C=C-stretch); 1259 (m, C=C-bending); 875 (m, CH-bending); 732 (m, CH-bending).

ESI-MS: *m/z* = 383.30 (M⁺+H⁺).

N-(3-Chloro-4-benzyloxyphenyl)-9 H-pyrido[2,3-b]indol-4-amine (26)

Molecular formula: C₂₄H₁₈ClN₃O

Molecular weight: 399.87 g/mol

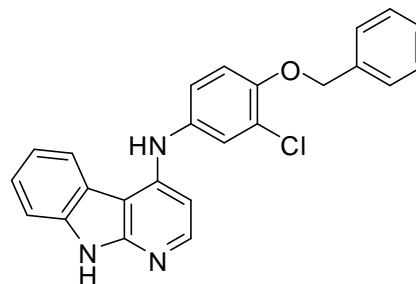
Melting point: 118-124 °C

R_f-value: [EE] 0.39

Yield: 329 mg (0.83 mmol, 67 %) black solid

Method of preparation:

250 mg (1.23 mmol, 1 eq.) of **9**, according to **GP1**, is implemented with 3.459 g (14.80 mmol, 12 eq.) 3-chloro-4-benzyloxyaniline.



¹H-NMR: [400 MHz, CDCl₃] δ (ppm) = 5.19 (s, 2H, OCH₂); 6.63 (d, *J* = 5.8 Hz, 1H, H-6'); 6.69 (s, 1H, H-2'); 7.01 (d, *J* = 8.7 Hz, 1H, H-5'); 7.17 (d, *J* = 7.3 Hz, 1H, H-3); 7.27-7.53 (m, 10 H, OCH₂C₆H₅, H-2, H-5, H-6, H-7 & H-8); 7.85 (d, *J* = 7.5 Hz, 1H, Aniline-NH); 8.05 (d, *J* = 6.0 Hz, 1H, H-9).

¹³C-NMR: [100 MHz, CDCl₃] δ (ppm) = 70.8 (p, OCH₂); 101.4 (q, C-4a); 103.5 (t, C-3); 111.1 (t, C-8); 119.3 (t, C-6'); 119.8 (t, C-5); 120.1 (q, C-3'); 120.5 (q, C-4b); 121.9 (t, C-5'); 122.7 (t, C-6); 123.2 (t, C-2'); 127.9-128.9 (5 C, OCH₂C₆H₅); 130.2 (t, C-7); 137.2 (q, C-1''); 138.7 (q, C-8a); 139.4 (q, C-1'); 143.1 (q, C-4); 147.0 (t, C-2); 152.8 (q, C-4'); 155.3 (q, C-9a).

IR: (ATR) ν (cm⁻¹) = 3443 (br, NH-stretch); 3061 (s, Aryl-CH-stretch); 3033 (m, Alkyl-CH-stretch); 2922 (m, Alkyl-CH-stretch); 2851 (m, Alkyl-CH-stretch); 2759 (w, Alkyl-CH-stretch); 1695 (s, NH-bending); 1584 (s, C=C-stretch); 1495 (s, C=C-stretch); 1456 (m, C=C-stretch); 1251 (m, C=C-bending); 843 (m, CH-bending); 750 (m, CH-bending).

ESI-MS: *m/z* = 400.24 (M⁺)

N-(3-Methoxy-4-bromophenyl)-9 H-pyrido[2,3-b]indol-4-amine (27)

Molecular formula: C₁₈H₁₄BrN₃O

Molecular weight: 368.23 g/mol

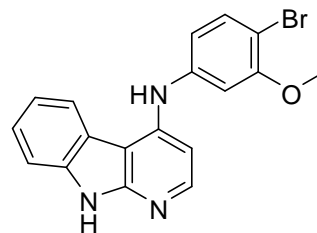
Melting point: 148-154 °C

R_f-value: [EE] 0.38

Yield: 150 mg (0.41 mmol, 33 %) brown solid

Method of preparation:

250 mg (1.23 mmol, 1 eq.) of **9**, according to **GP1**, is implemented with 2.493 g (12.34 mmol, 10 eq.) 3-methoxy-4-bromoaniline.



¹H-NMR: [400 MHz, DMSO-d₆] δ (ppm) = 3.69 (s, 3H, OCH₃); 6.59 (d, *J* = 7.7 Hz, 1H, H-2'); 6.83 (t, *J* = 9.6 Hz, 1H, H-6); 7.01-7.21 (m, 4H, H-5', H-6', H-3 & H-7); 7.33 (d, *J* = 7.5 Hz, 1H, H-8), 7.40 (d, *J* = 8.9 Hz, 1H, H-5); 8.03 (d, *J* = 7.9 Hz, 1H, H-2); 8.45 (s, 1H, Aniline-NH); 11.58 (s, 1H, H-9).

¹³C-NMR: [100 MHz, DMSO-d₆] δ (ppm) = 19.5 (p, OCH₃); 102.1 (t, C-3); 105.2 (q, C-4a); 111.1 (t, C-8); 119.3 (t, C-5); 120.4 (t, C-6'); 120.9 (q, C-4b); 122.4 (t, C-2'); 123.8 (t, C-6); 125.3 (t, C-7); 129.1 (q, C-4'); 130.9 (t, C-5'); 132.9 (q, C-3'); 137.2 (q, C-8a); 142.9 (q, C-1'); 145.1 (q, C-4); 147.0 (t, C-2); 153.9 (q, C-9a).

IR: (ATR) ν (cm⁻¹) = 3418 (br, NH-stretch); 3074 (w, Aryl-CH-stretch); 2954 (m, Alkyl-CH-stretch); 2921 (m, Alkyl-CH-stretch); 2851 (m, Alkyl-CH-stretch); 2759 (w, Alkyl-CH-stretch); 1683 (w, NH-bending); 1579 (s, C=C-stretch); 1491 (s, C=C-stretch); 1455 (m, C=C-stretch); 1258 (m, C=C-bending); 871 (m, CH-bending); 721 (m, CH-bending).

ESI-MS: m/z = 368.39 (M⁺)

N-(Naphthalene-1-yl)-9H-pyrido[2,3-b]indol-4-amine (28)

Molecular formula: C₂₁H₁₅N₃

Molecular weight: 309.36 g/mol

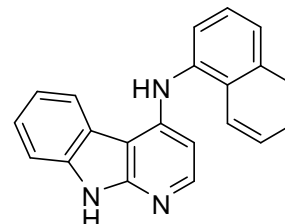
Melting point: 246-249 °C

R_f-value: [EE] 0.47

Yield: 187 mg (0.60 mmol, 49 %) light orange solid

Method of preparation:

250 mg (1.23 mmol, 1 eq.) of **9**, according to **GP1**, is implemented with 1.766 g (14.80 mmol, 12 eq.) 1-Naphthylamine.



¹H-NMR: [400 MHz, DMSO-d₆] δ (ppm) = 6.11 (d, *J* = 5.6 Hz, 1H, H-3); 7.06 (dd, *J* = 7.8 Hz, *J* = 7.4 Hz, 1H, H-6); 7.29-7.36 (m, 2H, 1 x H in naphthyl ring & H-7); 7.41-7.56 (m, 4H, 3 x H in naphthyl ring & H-8); 7.81 (d, *J* = 8.2 Hz, 1H, 1 x H in naphthyl ring); 7.93 (d, *J* = 5.6 Hz, 1H, H-2); 7.95-8.02 (m, 1H, 2 x H in naphthyl ring); 8.06 (d, *J* = 7.9 Hz, 1H, H-5); 8.60 (s, 1H, Aniline-H); 11.59 (s, 1H, H-9).

¹³C-NMR: [100 MHz, DMSO-d₆] δ (ppm) = 102.5 (t, C-3); 102.8 (q, C-4a); 110.9 (t, C-8); 119.3 (t, C-5); 120.8 (q, C-4b); 122.4 (t, Naphthyl-C); 123.0 (t, C-6); 123.8 (t, Naphthyl-C); 125.1 (t, C-7); 125.8 (t, Naphthyl-C); 126.4 (t, Naphthyl-C); 126.6 (t, Naphthyl-C); 126.7 (t, Naphthyl-C); 128.7 (t, Naphthyl-C); 129.7 (q, Naphthyl-C); 134.8 (q, Naphthyl-C); 137.4 (q, Naphthyl-C); 138.0 (q, C-8a); 147.1 (q, C-2); 148.7 (q, C-4); 154.0 (q, C-9a).

IR: (KBr) ν (cm⁻¹) = 3425 (br, NH-stretch); 3058 (w, Aryl-CH-stretch); 3008 (m, Aryl-CH-stretch); 1592 (s, C=C-stretch); 1576 (s, C=C-stretch); 1508 (s, C=C-stretch); 1456 (m, C=C-stretch); 1265 (s, C=C-stretch); 999 (w, CH-bending); 789 (m, CH-bending); 737 (m, CH-bending).

EI-MS: *m/z* = 309 (100, M⁺); 294 (4, M⁺-NH); 154 (7, C₁₀H₆N₂⁺); 140 (4, C₉H₄N₂⁺); 127 (2, C₁₀H₇⁺); 115 (3, C₈H₅N⁺).

EA: Calcd: C: 81.53; H: 4.89; N: 13.58

Found: C: 79.56; H: 4.99; N: 12.75

N-(3-Amino)-9 H-pyrido[2,3-b]indol-4-amine (29)

Molecular formula: C₁₇H₁₄N₄

Molecular weight: 274.32 g/mol

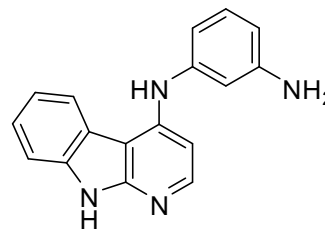
Melting point: 234-241 °C

R_f-value: [EE] 0.24

Yield: 70 mg (0.26 mmol, 37 %) dark brown solid

Method of preparation:

213 mg (0.7 mmol) of compound **19** was suspended in 15 ml of 10% hydrochloric acid. Then, 800 mg (4.21 mmol) of tin-II-chloride was added and the reaction mixture was heated for 80 min under reflux. TLC was made to detect the reaction progression. After cooling, the mixture was poured into 25 ml water and the pH was adjusted to 12 using 10 M potassium hydroxide. The water phase was then extracted by ethyl acetate for 5 times (each with 25 ml) and the unified organic layers are dried over sodium sulfate. After filtration, the eluent is removed in vacuum and the amino derivative is obtained.



¹H-NMR: [400 MHz, DMSO-d⁶] δ (ppm) = 5.07 (br, 2H, NH₂); 6.30 (d, J = 7.9 Hz, 1H, H-6'); 6.46 (d, J = 7.9 Hz, 1H, H-4'); 6.54 (s, 1H, H-2'); 6.74 (d, J = 5.6 Hz, 1H, H-3); 6.99 (t, J = 7.9 Hz, 1H, H-5'); 7.12 (t, J = 7.4 Hz, 1H, H-6); 7.33 (t, J = 7.5 Hz, 1H, H-7); 7.41 (d, J = 7.9 Hz, 1H, H-8); 8.04 (d, J = 5.6 Hz, 1H, H-5); 8.11 (d, J = 7.7 Hz, 1H, H-2); 8.18 (s, 1H, Aniline-NH); 11.54 (s, 1H, H-9).

¹³C-NMR: [100 MHz, Acetone-d⁶] δ (ppm) = 101.4 (t, C-3); 108.2 (q, C-4a); 109.3 (t, C-8); 110.7 (t, C-2'); 116.3 (t, C-6'); 119.3 (t, C-5); 120.6 (q, C-4b); 120.9 (t, C-4'); 124.8 (t, C-6); 129.1 (t, C-7); 129.7 (t, C-5'); 130.1 (q, C-8a); 137.9 (q, C-3'); 141.8 (q, C-1'); 146.3 (q, C-4); 149.4 (t, C-2); 153.9 (q, C-9a).

IR: (ATR) ν (cm⁻¹) = 3434 (br, NH-stretch); 3409 (m, NH-stretch); 3069 (m, Aryl-CH-stretch); 2961 (m, Alkyl-CH-stretch); 2920 (m, Alkyl-CH-stretch); 2849 (m, Alkyl-CH-stretch); 2758 (w, Alkyl-CH-stretch); 1599 (m, C=C-stretch); 1577 (s, C=C-stretch); 1495 (m, C=C-stretch); 1454 (m, C=C-stretch); 1258 (m, C=C-stretch); 745 (m, CH-bending).

ESI-MS: m/z = 275.35 (M⁺+H⁺).

N-(3-(9-acetyl-9H-pyrido[2,3-b]indol-4-ylamino)phenyl)acetamide (32)

Molecular formula: C₂₁H₁₈N₄O₂

Molecular weight: 358.39 g/mol

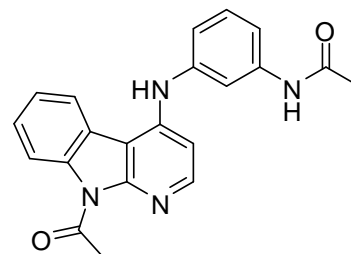
Melting point: 210-220 °C

R_f-value: [EE] 0.70

Yield: 130 mg (0.36 mmol, 100 %) light brown solid

Method of preparation:

To 100 mg (0.36 mmol) of derivative **29**, 15 ml acetic anhydride was added and the reaction mixture was stirred at RT for 5 min. A quick acetylation occurred and the product was precipitated. Filtration was then performed and the produced derivative was washed by water and left to dry over night in an open air.



¹H-NMR: [400 MHz, DMSO-d₆] δ (ppm) = 2.03 (s, 3H, NHCOCH₃); 3.04 (s, 3H, NCOCH₃); 6.95-6.99 (m, 2H, H-6', H-4'); 7.26 (d, *J* = 7.1 Hz, 2H, H-3, H-8); 7.38 (d, *J* = 7.5 Hz, 1H, H-2); 7.46 (d, *J* = 8.1 Hz, 1H, H-5'); 7.67 (s, 1H, H-2'); 8.19 (t, *J* = 6.4 Hz, 2H, H-6, H-7); 8.58 (d, *J* = 8.3 Hz, 1H, H-5); 8.68 (s, 1H, Aniline-NH); 9.94 (s, 1H, NHCOCH₃).

¹³C-NMR: [100 MHz, DMSO-d₆] δ (ppm) = 23.5 (p, CH₃); 24.6 (p, CH₃); 100.2 (t, C-3); 104.3 (q, C-4a); 110.5 (t, C-8); 119.1 (t, C-5); 120.0 (t, C-6'); 120.9 (q, C-4b); 123.4 (t, C-2'); 124.8 (t, C-6); 125.8 (t, C-7); 129.2 (q, C-4'); 130.8 (t, C-5'); 133.6 (q, C-3'); 137.7 (q, C-8a); 140.8 (q, C-1'); 142.4 (q, C-4); 147.5 (t, C-2); 151.9 (q, C-9a); 168.2 (s, C=O); 170.0 (s, C=O).

IR: (ATR) ν (cm⁻¹) = 3564 (br, NH-stretch); 3410 (m, NH-stretch); 3090 (w, Aryl-CH-stretch); 2975 (m, Alkyl-CH-stretch); 2926 (m, Alkyl-CH-stretch); 2853 (w, Alkyl-CH-stretch); 1585 (s, C=C-stretch); 1555 (m, C=C-stretch); 1494 (m, C=C-stretch); 1448 (m, C=C-stretch); 1278 (m, C=C-stretch); 731 (m, CH-bending).

ESI-MS: m/z = 381.06 (M⁺+Na⁺); 359.19 (M⁺+H⁺); 357.10 (M⁺-H⁺).

Synthesis of the 6-/6,8-substituted 4-phenylamino- α -carbolines:

Sulfonation:

General procedure (GP-2):

1 eq. of the 4-chloro- α -carboline **9** in a 100 ml two-necked flask with a reflux condenser was placed and the gas was outlet, and cooled on the ice bath. Then, while stirring, 1.5 ml (2.625 g, 59.14 mmol) of chlorosulfonic acid was added dropwise with a glass syringe. After the addition, the ice bath was removed and the mixture was stirred for 2 h at RT. Then the mixture was cooled again in the ice bath and the excess of chlorosulfonic acid is hydrolyzed by the addition of crushed ice. The precipitated solid was quickly filtered using a Buchner funnel, washed by cold water and sucked to dry on the Buchner funnel for 5 min. The solid was resuspended in 25 ml of THF and stirring with 10 eq. offset of the respective amine. The mixture was stirred overnight at RT, and then the solvent was removed under reduced pressure and the oily residue was mixed with 50 ml of water. The mixture was stirred for 24 h at RT, and then the precipitated solid was filtered through a Buchner funnel, washed with water and dried by air.

4-(4-chloro-9H-pyrido[2,3-b]indol-6-ylsulfonyl)morpholine (34)

Molecular formula: C₁₅H₁₄ClN₃O₃S

Molecular weight: 351.81 g/mol

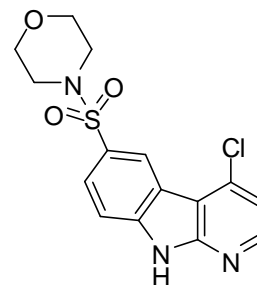
Melting point: 285-292 °C

R_f-value: [EE] 0.51

Yield: 602 mg (1.71 mmol, 35 %) beige solid

Method of preparation:

1 g (4.94 mmol, 1 eq.) **9**, according to **GP-2**, is implemented with 1.5 ml (2.625 g, 59.14 mmol, 12 eq.) of chlorosulfonic acid and 4.3 ml (4.304 g, 49.40 mmol, 10 eq.) of morpholine.



¹H-NMR: [400 MHz, DMSO-d₆] δ (ppm) = 2.87 (t, J = 4.4 Hz, 4H, 2 x CH₂-N); 3.60 (t, J = 4.4 Hz, 4H, 2 x CH₂-O); 7.42 (d, J = 5.3 Hz, 1H, H-3); 7.76 (d, J = 8.6 Hz, 1H, H-8); 7.86 (dd, J = 8.6 Hz, J = 1.5 Hz, 1H, H-7); 8.46 (d, J = 5.3 Hz, 1H, H-2), 8.62 (d, J = 1.5 Hz, 1H, H-5); 12.21 (s, 1H, H-9).

¹³C-NMR: [100 MHz, DMSO-d₆] δ (ppm) = 45.9 (s, 2 x CH₂-N); 65.2 (s, 2 x CH₂-O); 112.1 (t, C-8); 112.2 (q, C-4a); 116.5 (t, C-3); 118.7 (q, C-4b); 122.4 (t, C-5);

Experimental Section

125.7 (q, C-6); 126.2 (t, C-7); 137.1 (q, C-4); 141.2 (q, C-8a); 148.0 (t, C-2); 153.1 (q, C-9a).

IR: (KBr) ν (cm^{-1}) = 3428 (br, NH-stretch); 3208 (m, Aryl-CH-stretch); 3128 (m, Aryl-CH-stretch); 2963 (m, Alkyl-CH-stretch); 2897 (m, Alkyl-CH-stretch); 2860 (m, Alkyl-CH-stretch); 1624 (m, NH-bending); 1598 (s, C=C-stretch); 1570 (s, C=C-stretch); 1455 (s, C=C-stretch); 1306 (s, Sulfonamide); 1160 (s, Sulfonamide); 1114 (s, CH-stretch); 943 (s, CH-bending); 742 (s, CH-bending); 560 (s, CH-bending).

EI-MS: m/z = 351 (24, M^+); 265 (21, $\text{M}^+ - \text{C}_5\text{H}_{11}\text{N}_2\text{O}_2\text{S}$); 216 (19, $\text{C}_9\text{H}_{14}\text{NO}_3\text{S}^+$); 201 (51, $\text{M}^+ - \text{C}_7\text{H}_3\text{ClN}_2$); 174 (14, $\text{C}_{10}\text{H}_5\text{ClN}^+$); 166 (26, $\text{C}_{11}\text{H}_6\text{N}_2^+$); 86 (100, $\text{C}_4\text{H}_8\text{NO}^+$); 56 (30, $\text{C}_3\text{H}_4\text{O}^+$).

EA: Calcd: C: 51.21; H: 4.01; Cl: 10.08; N: 11.94; S: 9.11
Found: C: 51.06; H: 4.10; Cl: 10.18; N: 11.77; S: 8.51

4-chloro-6-(piperazin-1-ylsulfonyl)-9H-pyrido[2,3-b]indole (35)

Molecular formula: C₁₅H₁₅ClN₄O₂S

Molecular weight: 350.82 g/mol

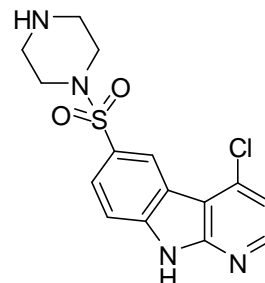
Melting point: > 320 °C

R_f-value: [EE : MeOH 50 : 50 v/v] 0.29

Yield: 789 mg (2.25 mmol, 50 %) light beige solid

Method of preparation:

1 g (4.94 mmol, 1 eq.) **9**, according to **GP-2**, is implemented with 1.5 ml (2.625 g, 59.14 mmol, 12 eq.) of chlorosulfonic acid and 4.254 g (49.40 mmol, 10 eq.) of piperazine.



¹H-NMR: [400 MHz, DMSO-d⁶] δ (ppm) = 2.68-2.75 (m, 4H, 2 x CH₂-NH); 2.78-2.84 (m, 4H, 2 x CH₂-N-SO₂); 3.06 (br, 1H, NH); 7.45 (d, *J* = 5.2 Hz, 1H, H-3); 7.78 (d, *J* = 8.4 Hz, 1H, H-8); 8.34 (d, *J* = 8.4 Hz, 1H, H-8); 8.49 (d, *J* = 5.2 Hz, 1H, H-2); 8.62 (s, 1H, H-5), H-9 not detected.

¹³C-NMR: [100 MHz, DMSO-d⁶] δ (ppm) = 44.6 (s, 2 x CH₂-NH); 46.7 (s, 2 x CH₂-N-SO₂); 112.0 (t, C-8); 112.2 (q, C-4a); 116.5 (t, C-3); 118.6 (q, C-4b); 122.2 (t, C-5); 126.2 (q, C-6); 126.3 (t, C-7); 137.1 (q, C-4); 141.0 (q, C-8a); 147.9 (t, C-2); 153.0 (q, C-9a).

IR: (KBr) ν (cm⁻¹) = 3323 (br, NH-stretch); 3121 (m, Aryl-CH-stretch); 2949 (m, Alkyl-CH-stretch); 2856 (m, Alkyl-CH-stretch); 2743 (m, Alkyl-CH-stretch); 1624 (m, NH-bending); 1596 (s, C=C-stretch); 1570 (s, C=C-stretch); 1456 (m, C=C-stretch); 1306 (s, Sulfonamide); 1159 (s, Sulfonamide); 945 (m, C-Cl-stretch); 740 (s, CH-bending).

EI-MS: *m/z* = 350 (4, M⁺); 265 (1, M⁺-C₄H₉N₂); 201 (8, M⁺-C₄H₉N₂O₂S); 174 (3, M⁺-C₄H₅ClN₂); 166 (6, C₁₁H₆N₂⁺); 85 (100, C₄H₉N₂⁺); 56 (26, C₃H₆N⁺).

EA: Calcd: C: 51.35; H: 4.31; Cl: 10.11; N: 15.97; S: 9.14

Found: C: 50.80; H: 3.97; Cl: 10.30; N: 15.05; S: 9.15

2-(4-(4-chloro-9H-pyrido[2,3-b]indol-6-ylsulfonyl)piperazin-1-yl)ethanol (36)

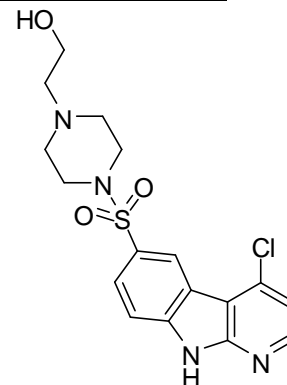
Molecular formula: C₁₇H₁₉ClN₄O₃S

Molecular weight: 394.88 g/mol

Melting point: 213-215 °C

Rf- value: [EE : MeOH 50 : 50 v/v] 0.66

Yield: 941 mg (2.38 mmol, 48 %) light beige solid



Method of preparation:

1 g (4.94 mmol, 1 eq.) **9**, according to **GP-2**, is implemented with 1.5 ml (2.625 g, 59.14 mmol, 12 eq.) of chlorosulfonic acid and 6.50 g (49.40 mmol, 10 eq.) of 2-hydroxyethyl piperazine.

¹H-NMR: [400 MHz, DMSO-d⁶] δ (ppm) = 2.31 (t, *J* = 6.1 Hz, 2H, N-CH₂-CH₂-OH); 2.44-2.50 (m, 4H, 2 x CH₂-N-CH₂-CH₂-OH); 2.84-2.95 (m, 4H, 2 x CH₂-N-SO₂); 3.28-3.40 (m, 2H, CH₂-OH); 4.29 (br, 1H, OH); 7.44 (d, *J* = 5.4 Hz, 1H, H-3); 7.78 (d, *J* = 8.6 Hz, 1H, H-8); 7.87 (dd, *J* = 8.6 Hz, *J* = 1.7 Hz, 1H, H-7); 8.48 (d, *J* = 5.4 Hz, 1H, H-2); 8.63 (d, *J* = 1.7 Hz, 1H, H-5); 12.59 (br, 1H, H-9).

¹³C-NMR: [100 MHz, DMSO-d⁶] δ (ppm) = 45.9 (s, 2 x CH₂-N-SO₂); 51.9 (s, 2 x CH₂-N-CH₂-CH₂-OH); 58.3 (s, N-CH₂-CH₂-OH); 59.4 (s, N-CH₂-CH₂-OH); 112.1 (t, C-8); 112.2 (q, C-4a); 116.5 (t, C-3); 118.6 (q, C-4b); 122.3 (t, C-5); 125.9 (q, C-6); 126.2 (t, C-7); 137.1 (q, C-4); 141.1 (q, C-8a); 147.9 (t, C-2); 153.1 (q, C-9a).

IR: (KBr) ν (cm⁻¹) = 3430 (br, NH-stretch); 2947 (m, Alkyl-CH-stretch); 2822 (m, Alkyl-CH-stretch); 1624 (m, NH-bending); 1596 (m, C=C-stretch); 1569 (m, C=C-stretch); 1456 (m, C=C-stretch); 1306 (s, Sulfonamide); 1161 (s, Sulfonamide); 743 (s, CH-bending).

EI-MS: *m/z* = 394 (6, M⁺); 363 (82, M⁺-CH₄O); 265 (6, M⁺-C₆H₁₃N₂O); 201 (36, M⁺-C₆H₁₃N₂O₃S); 166 (18, C₁₁H₆N₂⁺); 129 (100, C₆H₁₃N₂O⁺); 111 (2, C₆H₁₁N₂⁺); 70 (11, C₄H₈N⁺).

EA: Calcd: C: 51.71; H: 4.85; Cl: 8.98; N: 14.19; S: 8.12

Found: C: 50.44; H: 5.00; Cl: 8.55; N: 13.59; S: 8.50

3-(6-(morpholinosulfonyl)-9H-pyrido[2,3-b]indol-4-ylamino)phenol (37)

Molecular formula: C₂₁H₂₀N₄O₄S

Molecular weight: 424.47 g/mol

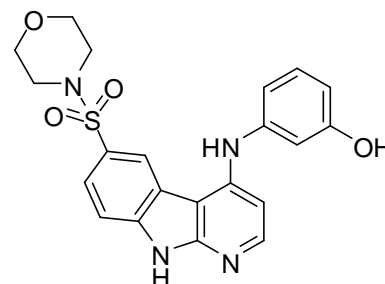
Melting point: > 300 °C

R_f-value: [EE] 0.22

Yield: 110 mg (0.26 mmol, 37%) dark brown solid

Method of preparation:

250 mg (0.71 mmol, 1 eq.) of **34**, according to **GP-1**, is implemented with 775 mg (7.1 mmol, 10 eq.) 3-aminophenol.



¹H-NMR: [400 MHz, Acetone-d₆] δ (ppm) = 2.86 (t, *J* = 4.6 Hz, 4H, 2x CH₂-N); 3.63 (t, *J* = 4.6 Hz, 4H, 2x CH₂-O); 6.59 (dd, *J* = 1.8 Hz, *J* = 8.0 Hz, 1H, H-2'); 6.72-6.77 (m, 2H, H-6', H-4'); 6.93 (d, *J* = 5.6 Hz, 1H, H-3); 7.18 (t, *J* = 8.0 Hz, 1H, H-5'); 7.71-7.79 (m, 2H, H-7, H-8); 8.22 (d, *J* = 5.4 Hz, 2H, H-5, H-2); 8.32 (s, 1H, Aniline-NH); H-9 not detected.

¹³C-NMR: [100 MHz, DMSO-d₆] δ (ppm) = 46.5 (s, 2 x CH₂-N); 65.7 (s, 2 x CH₂-O); 104.5(q, C-4a); 105.4 (t, C-3); 107.7 (t, C-2'); 110.3 (t, C-6'); 111.1 (t, C-4'); 112.0 (t, C-8); 120.3 (q, C-4b); 124.0 (t, C-5); 124.6 (q, C-6); 124.8 (t, C-7); 130.5 (t, C-5'); 140.8 (q, C-8a); 143.1 (q, C-1'); 147.0 (q, C-4); 148.5 (t, C-2); 154.9 (q, C-9a); 158.6 (q, C-3').

IR: (ATR) ν (cm⁻¹) = 3330 (br, NH-stretch); 3070 (m, Aryl-CH-stretch); 2956 (m, Alkyl-CH-stretch); 2921 (s, Alkyl-CH-stretch); 2852 (m, Alkyl-CH-stretch); 1630 (m, NH-bending); 1598 (s, C=C-stretch); 1502 (s, C=C-stretch); 1455 (m, C=C-stretch); 1295 (m, Sulfonamide); 1155 (m, Sulfonamide); 1110 (m, CH-stretch); 967 (m, CH-bending); 731 (w, CH-bending); 550 (w, CH-bending).

ESI-MS: *m/z* = 425.22 (M⁺+H⁺).

N-(3-methoxyphenyl)-6-(morpholinylsulfonyl)-9H-pyrido[2,3-b]indol-4-amine

(38)

Molecular formula: C₂₂H₂₂N₄O₄S

Molecular weight: 438.50 g/mol

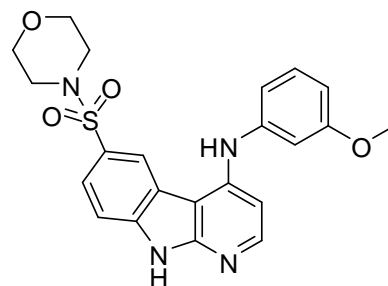
Melting point: 230-240 °C

R_f-value: [EE] 0.26

Yield: 134 mg (0.31 mmol, 44%) brown solid

Method of preparation:

250 mg (0.71 mmol, 1 eq.) of **34**, according to **GP-1**, is implemented with 875 mg (7.1 mmol, 10 eq.) 3-anisidine.



¹H-NMR: [400 MHz, Acetone-d₆] δ (ppm) = 2.85-2.87 (m, 4H, 2x CH₂-O); 3.63-3.65 (m, 4H, 2x CH₂-N); 3.75 (s, 3H, OCH₃); 6.69-6.11 (m, 1H, H-2'); 6.82-6.86 (m, 2H, H-6', H-4'); 6.93 (d, *J* = 5.6 Hz, 1H, H-3); 7.27 (t, *J* = 8.1 Hz, 1H, H-5'); 7.74-7.76 (m, 2H, H-7, H-8); 8.22-8.25 (m, 2H, H-2, Aniline-NH); 8.32 (d, *J* = 1.5 Hz, 1H, H-5); 11.21 (br, 1H, H-9).

¹³C-NMR: [100 MHz, Acetone-d₆] δ (ppm) = 44.3 (s, 2 x CH₂-N); 50.9 (p, OCH₃); 64.2 (s, 2 x CH₂-O); 103.1(q, C-4a); 104.1 (t, C-3); 109.0 (t, C-2'); 110.4 (t, C-6'); 111.5 (t, C-4'); 119.2 (t, C-8); 120.7 (q, C-4b); 124.1 (t, C-5); 125.2 (q, C-6); 127.5 (t, C-7); 130.0 (t, C-5'); 141.2 (q, C-8a); 142.1 (q, C-1'); 146.7 (q, C-4); 149.0 (t, C-2); 153.4 (q, C-9a); 156.4 (q, C-3').

IR: (ATR) ν (cm⁻¹) = 3410 (br, NH-stretch); 3040 (m, Aryl-CH-stretch); 2960 (s, Alkyl-CH-stretch); 2922 (s, Alkyl-CH-stretch); 2850 (m, Alkyl-CH-stretch); 1602 (m, NH-bending); 1579 (s, C=C-stretch); 1508 (m, C=C-stretch); 1456 (m, C=C-stretch); 1298 (s, Sulfonamide); 1151 (m, Sulfonamide); 1113 (m, CH-stretch); 973 (m, CH-bending); 724 (m, CH-bending); 546 (m, CH-bending).

ESI-MS: m/z = 439.25 (M⁺+H⁺); 437.29 (M⁺-H⁺).

N-(3-ethoxyphenyl)-6-(morpholinosulfonyl)-9H-pyrido[2,3-b]indol-4-amine
(39)

Molecular formula: C₂₃H₂₄N₄O₄S

Molecular weight: 452.53 g/mol

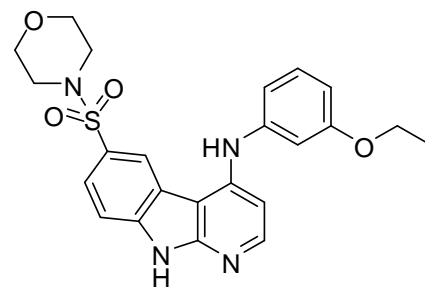
Melting point: 237-241 °C

R_f-value: [EE] 0.30

Yield: 160 mg (0.35 mmol, 50%) beige solid

Method of preparation:

250 mg (0.71 mmol, 1 eq.) of **34**, according to **GP-1**, is implemented with 975 mg (7.1 mmol, 10 eq.) 3-phenitidine.



¹H-NMR: [400 MHz, CDCl₃] δ (ppm) = 1.41 (t, *J* = 7.1 Hz, 3H, OCH₂CH₃); 3.0 (t, *J* = 4.6 Hz, 4H, 2x CH₂-N); 3.72 (t, *J* = 4.6 Hz, 4H, 2x CH₂-O); 4.02 (q, *J* = 6.8 Hz, 2H, OCH₂CH₃); 6.68 (s, 1H, H-2'); 6.74 (dd, *J* = 1.8 Hz, *J* = 8.4 Hz, 1H, H-6'); 6.86-6.95 (m, 3H, H-4', H-3 & H-8); 7.32 (t, *J* = 8.1 Hz, 1H, H-5'); 7.61 (d, *J* = 8.5 Hz, 1H, H-7); 7.79 (d, *J* = 1.5 Hz, 1H, H-2); 8.22 (s, 1H, H-5); 8.28 (d, *J* = 5.8 Hz, 1H, Aniline-NH); 11.49 (br, 1H, H-9).

¹³C-NMR: [100 MHz, Acetone-d₆] δ (ppm) = 14.8 (p, OCH₂CH₃); 44.8 (s, 2 x CH₂-N); 56.4 (s, OCH₂CH₃); 65.0 (s, 2 x CH₂-O); 101.3(q, C-4a); 103.2 (t, C-3); 106.9 (t, C-2'); 110.1 (t, C-6'); 111.9 (t, C-4'); 115.7 (t, C-8); 120.0 (q, C-4b); 122.3 (t, C-5); 123.7 (q, C-6); 128.1 (t, C-7); 130.2 (t, C-5'); 140.9 (q, C-8a); 144.6 (q, C-1'); 146.5 (q, C-4); 148.1 (t, C-2); 151.6 (q, C-9a); 156.1 (q, C-3').

IR: (ATR) ν (cm⁻¹) = 3414 (br, NH-stretch); 3060 (m, Aryl-CH-stretch); 2960 (m, Alkyl-CH-stretch); 2921 (m, Alkyl-CH-stretch); 2852 (s, Alkyl-CH-stretch); 1604 (m, NH-bending); 1580 (s, C=C-stretch); 1507 (m, C=C-stretch); 1451 (m, C=C-stretch); 1298 (m, Sulfonamide); 1152 (s, Sulfonamide); 1112 (s, CH-stretch); 972 (m, CH-bending); 725 (w, CH-bending); 556 (m, CH-bending).

ESI-MS: m/z = 453.28 (M⁺+H⁺); 451.29 (M⁺-H⁺).

N-(3-(benzyloxy)phenyl)-6-(morpholinosulfonyl)-9H-pyrido[2,3-b]indol-4-amine (40)

Molecular formula: C₂₈H₂₆N₄O₄S

Molecular weight: 514.60 g/mol

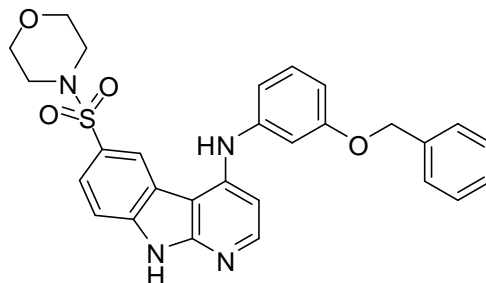
Melting point: 100-110 °C

R_f-value: [EE] 0.31

Yield: 110 mg (0.21 mmol, 30%) brown solid

Method of preparation:

250 mg (0.71 mmol, 1 eq.) of **34**, according to **GP-1**, is implemented with 1.416 g (7.1 mmol, 10 eq.) 3-benzyloxyaniline.



¹H-NMR: [400 MHz, Acetone-d₆] δ (ppm) = 2.86 (t, *J* = 4.7 Hz, 4H, 2x CH₂-N); 3.63-3.68 (m, 4H, 2x CH₂-O); 5.08 (s, 2H, OCH₂); 6.78 (dd, *J* = 2.2 Hz, *J* = 8.4 Hz, 1H, H-2'); 6.86-6.92 (m, 2H, H-4', H-6'); 7.26-7.42 (m, 8H, OCH₂C₆H₅, H-3, H-8 & H-5'); 7.75-7.77 (m, 2H, H-7, H-5); 8.21 (d, *J* = 5.6 Hz, 1H, H-5); 8.30 (d, *J* = 9.7 Hz, 1H, Aniline-NH); H-9 not detected.

¹³C-NMR: [100 MHz, Acetone-d₆] δ (ppm) = 46.1 (s, 2 x CH₂-N); 66.1 (s, 2 x CH₂-O); 70.2 (s, OCH₂); 102.2 (q, C-4a); 109.6 (t, C-3); 111.5 (t, C-2'); 111.8 (t, C-6'); 113.9 (t, C-4'); 115.4 (t, C-8); 120.4 (q, C-4b); 121.6 (t, C-5); 124.8 (q, C-6); 126.2-128.1 (p, 5C-Bnz.); 128.7 (t, C-7); 130.5 (t, C-5'); 136.6 (q, C-1''); 140.1 (q, C-8a); 140.3 (q, C-1'); 146.4 (q, C-4); 148.2 (t, C-2); 153.6 (q, C-9a); 159.9 (q, C-3').

IR: (ATR) ν (cm⁻¹) = 3214 (br, NH-stretch); 3062 (m, Aryl-CH-stretch); 2955 (m, Alkyl-CH-stretch); 2922 (s, Alkyl-CH-stretch); 2853 (m, Alkyl-CH-stretch); 1665 (w, NH-bending); 1579 (s, C=C-stretch); 1508 (m, C=C-stretch); 1453 (m, C=C-stretch); 1325 (m, Sulfonamide); 1154 (s, Sulfonamide); 1111 (m, CH-stretch); 993 (m, CH-bending); 730 (w, CH-bending); 565 (m, CH-bending).

ESI-MS: *m/z* = 515.20 (M⁺+H⁺).

N-(3-methoxyphenyl)-6-(piperazin-1-ylsulfonyl)-9H-pyrido[2,3-b]indol-4-amine (42)

Molecular formula: C₂₂H₂₃N₅O₃S

Molecular weight: 437.51 g/mol

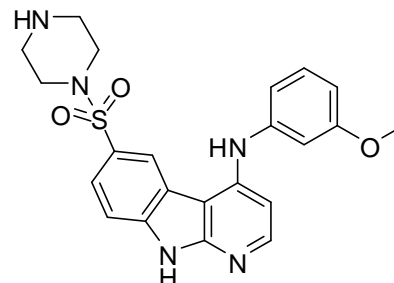
Melting point: 137-140 °C

R_f-value: [EE] 0.11

Yield: 98 mg (0.21 mmol, 30%) dark brown solid

Method of preparation:

250 mg (0.71 mmol, 1 eq.) of **35**, according to **GP-1**, is implemented with 875 mg (7.1 mmol, 10 eq.) 3-anisidine.



¹H-NMR: [400 MHz, DMSO-d₆] δ (ppm) = 1.76 (s, 4H, 2x CH₂-NH); 2.04 (s, 1H, Piperazine-NH); 2.65 (s, 4H, 2x CH₂-N-SO₂); 3.67 (s, 3H, OCH₃); 6.61 (d, *J* = 8.1 Hz, 1H, H-2'); 6.71 (d, *J* = 8.8 Hz, 1H, H-3); 6.81 (d, *J* = 5.4 Hz, 2H, H-4', H-6'); 7.05-7.41 (m, 1H, H-5'); 7.59-7.7.79 (m, 2H, H-7, H-8); 8.16 (d, *J* = 7.7 Hz, 2H, H-2, H-5); 8.87 (s, 1H, Aniline-NH); 12.27 (br, 1H, H-9).

¹³C-NMR: [100 MHz, DMSO-d₆] δ (ppm) = 44.3 (s, 2 x CH₂-NH); 48.2 (s, 2 x CH₂-N-SO₂); 54.4 (p, OCH₃); 102.4(q, C-4a); 103.9 (t, C-3); 110.0 (t, C-2'); 110.7 (t, C-6'); 112.4 (t, C-4'); 119.3 (t, C-8); 120.2 (q, C-4b); 123.5 (t, C-5); 124.7 (q, C-6); 128.1 (t, C-7); 130.3 (t, C-5'); 140.5 (q, C-8a); 143.4 (q, C-1'); 147.8 (q, C-4); 148.2 (t, C-2); 154.6 (q, C-9a); 157.1 (q, C-3').

IR: (ATR) ν (cm⁻¹) = 3212 (br, NH-stretch); 2920 (s, Alkyl-CH-stretch); 2851 (s, Alkyl-CH-stretch); 1663 (m, NH-bending); 1579 (s, C=C-stretch); 1491 (m, C=C-stretch); 1453 (m, C=C-stretch); 1318 (m, Sulfonamide); 1156 (s, Sulfonamide); 1131 (s, CH-stretch); 937 (m, CH-bending); 735 (w, CH-bending); 561 (m, CH-bending).

ESI-MS: m/z = 438.31 (M⁺+H⁺); 436.36 (M⁺-H⁺).

N-(3-ethoxyphenyl)-6-(piperazin-1-ylsulfonyl)-9H-pyrido[2,3-b]indol-4-amine
(43)

Molecular formula: C₂₃H₂₅N₅O₃S

Molecular weight: 451.54 g/mol

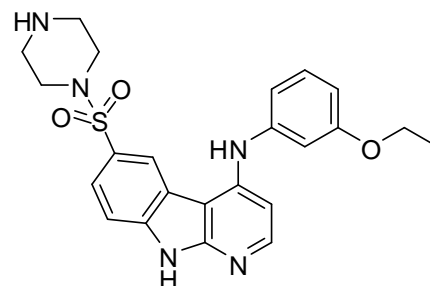
Melting point: 280-286 °C

R_f-value: [EE] 0.14

Yield: 100 mg (0.22 mmol, 31%) light beige solid

Method of preparation:

250 mg (0.71 mmol, 1 eq.) of **35**, according to **GP-1**, is implemented with 975 mg (7.1 mmol, 10 eq.) 3-phenitidine.



¹H-NMR: [400 MHz, DMSO-d₆] δ (ppm) = 1.27 (t, *J* = 6.8 Hz, 3H, OCH₂CH₃); 2.07 (s, 1H, Piperazine-NH); 2.68 (d, *J* = 2.5 Hz, 8H, 4x Piperazine-CH₂); 3.91 (q, *J* = 6.9 Hz, 2H, OCH₂CH₃); 6.61 (d, *J* = 8.3 Hz, 1H, H-3); 6.69 (s, 1H, H-2'); 6.73 (d, *J* = 8.1 Hz, 1H, H-8); 6.84 (d, *J* = 5.6 Hz, 2H, H-4', H-6'); 7.21 (t, *J* = 8.0 Hz, 1H, H-5'); 7.65 (d, *J* = 2.9 Hz, 1H, H-7); 8.16 (s, 1H, H-5); 8.19 (d, *J* = 5.6 Hz, 1H, H-2); 8.92 (s, 1H, Aniline-NH); H-9 not detected.

¹³C-NMR: [100 MHz, DMSO-d₆] δ (ppm) = 14.7 (p, CH₃); 46.2 (s, 2 x CH₂-NH); 48.8 (s, 2 x CH₂-N-SO₂); 64.1 (s, CH₂); 100.8(q, C-4a); 101.8 (t, C-3); 109.1 (t, C-2'); 110.6 (t, C-6'); 111.9 (t, C-4'); 117.6 (t, C-8); 119.9 (q, C-4b); 122.3 (t, C-5); 125.2 (q, C-6); 127.6 (t, C-7); 130.0 (t, C-5'); 142.2 (q, C-8a); 145.7 (q, C-1'); 147.9 (q, C-4); 149.2 (t, C-2); 155.3 (q, C-9a); 158.4 (q, C-3').

IR: (ATR) ν (cm⁻¹) = 3335 (br, NH-stretch); 2956 (m, Alkyl-CH-stretch); 2853 (m, Alkyl-CH-stretch); 1661 (m, NH-bending); 1576 (s, C=C-stretch); 1505 (m, C=C-stretch); 1453 (m, C=C-stretch); 1318 (m, Sulfonamide); 1155 (m, Sulfonamide); 1113 (m, CH-stretch); 934 (w, CH-bending); 758 (w, CH-bending); 536 (w, CH-bending).

ESI-MS: *m/z* = 452.36 (M⁺+H⁺); 450.33 (M⁺-H⁺).

2-(4-(4-(3-methoxyphenylamino)-9H-pyrido[2,3-b]indol-6-ylsulfonyl)piperazin-1-yl)ethanol (44)

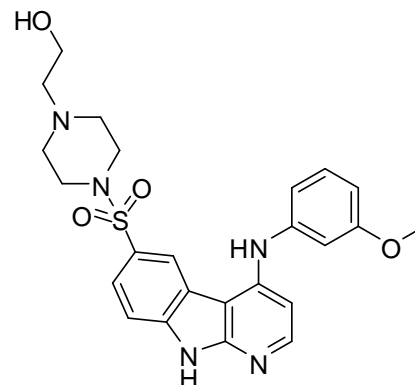
Molecular formula: C₂₄H₂₇N₅O₄S

Molecular weight: 481.57 g/mol

Melting point: 138-143 °C

R_f-value: [EE] 0.07

Yield: 170 mg (0.35 mmol, 56%) brown solid



Method of preparation:

250 mg (0.63 mmol, 1 eq.) of **36**, according to **GP-1**, is implemented with 779 mg (6.3 mmol, 10 eq.) 3-anisidine.

¹H-NMR: [400 MHz, CDCl₃] δ (ppm) = 2.51 (t, *J* = 5.0 Hz, 2H, N-CH₂-CH₂-OH); 2.58 (s, 4H, 2x OH-CH₂-CH₂-N-CH₂); 3.03 (s, 4H, 2x SO₂-N-CH₂); 3.54 (t, *J* = 5.2 Hz, 2H, N-CH₂-CH₂-OH); 3.81 (s, 3H, OCH₃); 6.74-6.77 (m, 2H, H-2', H-3); 6.87-6.92 (m, 3H, H-4', H-6' & H-5); 7.32 (t, *J* = 8.2 Hz, 1H, H-5'); 7.54 (d, *J* = 8.5 Hz, 1H, H-8); 7.74 (d, *J* = 8.7 Hz, 1H, H-7); 8.21-8.24 (m, 2H, H-2, Aniline-NH); H-9 not detected.

¹³C-NMR: [100 MHz, CDCl₃] δ (ppm) = 45.4 (s, 2 x CH₂-N-SO₂); 52.1 (s, 2 x CH₂-N-CH₂-CH₂-OH); 55.4 (p, OCH₃); 58.5 (s, N-CH₂-CH₂-OH); 59.8 (s, N-CH₂-CH₂-OH); 103.1(q, C-4a); 105.7 (t, C-3); 107.9 (t, C-2'); 109.8 (t, C-6'); 111.1 (t, C-4'); 115.2 (t, C-8); 120.3 (q, C-4b); 123.5 (t, C-5); 127.2 (q, C-6); 129.0 (t, C-7); 130.3 (t, C-5'); 140.6 (q, C-8a); 143.2 (q, C-1'); 144.9 (q, C-4); 147.4 (t, C-2); 153.4 (q, C-9a); 156.8 (q, C-3').

IR: (KBr) ν (cm⁻¹) = 3340 (br, NH-stretch); 2958 (m, Alkyl-CH-stretch); 2852 (m, Alkyl-CH-stretch); 1580 (s, C=C-stretch); 1455 (m, C=C-stretch); 1322 (m, Sulfonamide); 1157 (s, Sulfonamide); 747 (m, CH-bending).

ESI-MS: m/z = 482.10 (M⁺+H⁺).

2-(4-(4-(3-ethoxyphenylamino)-9H-pyrido[2,3-b]indol-6-ylsulfonyl)piperazin-1-yl)ethanol (45)

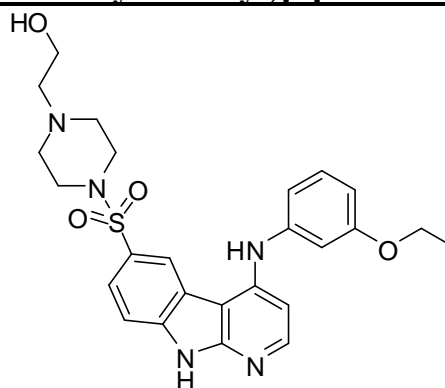
Molecular formula: C₂₅H₂₉N₅O₄S

Molecular weight: 495.59 g/mol

Melting point: 148-155 °C

R_f-value: [EE] 0.08

Yield: 110 mg (0.22 mmol, 35%) beige solid



Method of preparation:

250 mg (0.63 mmol, 1 eq.) of **36**, according to **GP-1**, is implemented with 779 mg (6.3 mmol, 10 eq.) 3-phenitidine.

¹H-NMR: [400 MHz, CDCl₃] δ (ppm) = 1.41 (t, *J* = 6.9 Hz, 3H, OCH₂CH₃); 2.53-2.65 (m, 6H, OH-CH₂-CH₂-N, 2x OH-CH₂-CH₂-N-CH₂); 3.05-3.9 (m, 4H, 2x SO₂-N-CH₂); 3.57 (t, *J* = 5.0 Hz, 2H, OH-CH₂-CH₂-N); 4.01 (q, *J* = 6.9 Hz, 2H, OCH₂CH₃); 6.74 (d, *J* = 8.9 Hz, 1H, H-2'); 6.86-6.93 (m, 2H, H-4', H-6'); 7.23-7.31 (m, 1H, H-5'); 7.58 (d, *J* = 8.5 Hz, 2H, H-3, H-8); 7.75 (d, *J* = 8.9 Hz, 1H, H-7); 8.21-8.24 (m, 1H, H-2); 8.42 (d, *J* = 5.2 Hz, 1H, H-5); 8.78 (s, 1H, Aniline-NH); 10.98 (br, 1H, H-9).

¹³C-NMR: [100 MHz, CDCl₃] δ (ppm) = 14.8 (p, CH₃); 44.3 (s, 2 x CH₂-N-SO₂); 53.2 (s, 2 x CH₂-N-CH₂-CH₂-OH); 56.8 (s, N-CH₂-CH₂-OH); 59.1 (s, N-CH₂-CH₂-OH); 65.2 (s, OCH₂); 101.5(q, C-4a); 104.0 (t, C-3); 105.8 (t, C-2'); 110.2 (t, C-6'); 112.5 (t, C-4'); 117.3 (t, C-8); 120.4 (q, C-4b); 124.6 (t, C-5); 127.1 (q, C-6); 130.1 (t, C-7); 130.8 (t, C-5'); 138.9 (q, C-8a); 142.6 (q, C-1'); 145.2 (q, C-4); 146.1 (t, C-2); 151.9 (q, C-9a); 155.0 (q, C-3').

IR: (KBr) ν (cm⁻¹) = 3208 (br, NH-stretch); 3123 (m, Aryl-CH-stretch); 2923 (s, Alkyl-CH-stretch); 2851 (s, Alkyl-CH-stretch); 1661 (s, NH-bending); 1579 (s, C=C-stretch); 1454 (s, C=C-stretch); 1324 (s, Sulfonamide); 1155 (s, Sulfonamide); 784 (m, CH-bending).

ESI-MS: m/z = 496.10 (M⁺+H⁺).

3-(6-(4-(2-hydroxyethyl)piperazin-1-ylsulfonyl)-9H-pyrido[2,3-b]indol-4-ylamino)phenol (46)

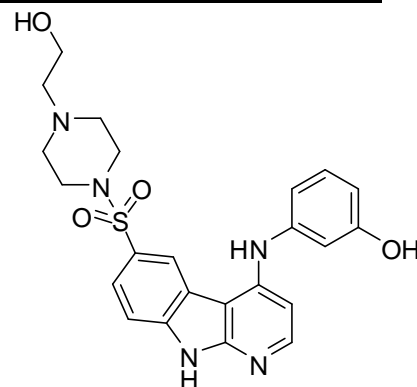
Molecular formula: C₂₃H₂₅N₅O₄S

Molecular weight: 467.54 g/mol

Melting point: 173-179 °C

R_f-value: [EE] 0.06

Yield: 110 mg (0.22 mmol, 35%) brown solid



Method of preparation:

250 mg (0.63 mmol, 1 eq.) of **36**, according to **GP-1**, is implemented with 688 mg (6.3 mmol, 10 eq.) 3-Aminophenol.

¹H-NMR: [400 MHz, Acetone-d₆] δ (ppm) = 1.28 (s, 4H, 2x OH-CH₂-CH₂-N-CH₂); 2.44 (t, *J* = 5.6 Hz, 2H, OH-CH₂-CH₂-N); 2.53 (t, *J* = 4.8 Hz, 4H, 2x SO₂-N-CH₂); 3.52 (t, *J* = 5.6 Hz, 2H, OH-CH₂-CH₂-N); 6.59 (d, *J* = 7.9 Hz, 1H, H-2'); 6.74 (d, *J* = 8.1 Hz, 2H, H-4', H-6'); 6.93 (d, *J* = 5.6 Hz, 1H, H-3); 7.18 (t, *J* = 8.0 Hz, 1H, H-5'); 7.70-7.78 (m, 2H, H-7, H-8); 8.19 (s, 1H, H-5); 8.22 (d, *J* = 5.6 Hz, 1H, H-2); 8.30 (s, 1H, Aniline-NH); 11.21 (br, 1H, H-9).

¹³C-NMR: [100 MHz, Acetone-d₆] δ (ppm) = 44.3 (s, 2 x CH₂-N-SO₂); 53.2 (s, 2 x CH₂-N-CH₂-CH₂-OH); 56.8 (s, N-CH₂-CH₂-OH); 59.1 (s, N-CH₂-CH₂-OH); 102.3(q, C-4a); 105.1 (t, C-3); 109.4 (t, C-2'); 110.8 (t, C-6'); 115.0 (t, C-4'); 118.5 (t, C-8); 121.6 (q, C-4b); 123.9 (t, C-5); 128.2 (q, C-6); 129.5 (t, C-7); 130.9 (t, C-5'); 135.2 (q, C-8a); 140.8 (q, C-1'); 142.4 (q, C-4); 147.2 (t, C-2); 154.1 (q, C-9a); 157.7 (q, C-3').

IR: (KBr) ν (cm⁻¹) = 3214 (br, NH-stretch); 3145 (br, Aryl-CH-stretch); 2922 (s, Alkyl-CH-stretch); 2852 (m, Alkyl-CH-stretch); 1582 (s, C=C-stretch); 1455 (s, C=C-stretch); 1323 (m, Sulfonamide); 1155 (s, Sulfonamide); 757 (m, CH-bending).

ESI-MS: *m/z* = 468.15 (M⁺+H⁺).

Friedel-Crafts Acylation:

1-(4-chloro-9H-pyrido[2,3-b]indol-6-yl)ethanone (47)

Molecular formula: C₁₃H₉ClN₂O

Molecular weight: 244.68 g/mol

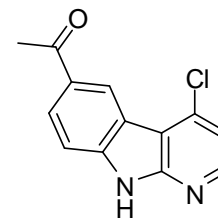
Melting point: 297-302 °C

R_f value: [EE] 0.40

Yield: 3.122 g (12.76 mmol, 86 %) light yellow solid

Method of preparation:

A suspension of 3 g (14.80 mmol, 1 eq.) **9** and 8.88 g (66.62 mmol, 4.5 eq.) of aluminum chloride in 75 ml dry CH₂Cl₂ was cooled in an ice bath. Then, with stirring, 2.1 ml (2.32 g, 29.61 mmol, 2 eq.) of acetyl chloride was slowly added dropwise with a syringe. After the addition, the mixture was heated 4 h under argon atmosphere to reflux. After cooling to RT, the mixture was cooled in the ice bath and 120 ml of water was dropped slowly with stirring. After the addition, the mixture was stirred for 15 min at RT. The precipitated solid was filtered through a Buchner funnel, washed with water and dried overnight in an open air.



¹H-NMR: [400 MHz, DMSO-d₆] δ (ppm) = 2.65 (s, 3H, CH₃); 7.38 (d, *J* = 5.3 Hz, 1H, H-3); 7.60 (d, *J* = 8.6 Hz, 1H, H-8); 8.13 (dd, *J* = 8.6 Hz, *J* = 1.4 Hz, 1H, H-7); 8.42 (d, *J* = 5.3 Hz, 1H, H-2); 8.88 (d, *J* = 1.4 Hz, 1H, H-5); 12.58 (s, 1H, H-9).

¹³C-NMR: [100 MHz, DMSO-d₆] δ (ppm) = 27.2 (p, CH₃); 111.8 (t, C-8); 113.4 (q, C-4a); 116.9 (t, C-3); 119.3 (q, C-4b); 123.7 (t, C-5); 128.1 (t, C-7); 129.9 (q, C-6); 137.3 (q, C-4); 142.2 (q, C-8a); 147.8 (t, C-2); 153.8 (q, C-9a); 197.0 (q, C=O).

IR: (KBr) ν(cm⁻¹) = 3435 (br, NH-stretch); 3209 (m, Aryl-CH-stretch); 3124 (m, Aryl-CH-stretch); 3004 (m, Aryl-CH-stretch); 2959 (m, Alkyl-CH-stretch); 2836 (m, Alkyl-CH-stretch); 2769 (m, Alkyl-CH-stretch); 1671 (s, C=O-stretch); 1574 (s, C=C-stretch); 1299 (s, C=C-bending); 1218 (s, C=C-bending); 967 (m, CH-bending); 890 (m, CH-bending); 734 (m, CH-bending); 584 (m, CH-bending).

EI-MS: *m/z* = 244 (40, M⁺); 229 (100, M⁺-CH₃); 201 (39, M⁺-C₂H₃O); 174 (11, C₁₀H₅ClN⁺); 166 (21, C₁₁H₆N₂⁺); 114 (4, C₇H₂N₂⁺); 87 (3, C₃H₂ClN⁺).

1-(4-(3-hydroxyphenylamino)-9H-pyrido[2,3-b]indol-6-yl)ethanone (48)

Molecular formula: C₁₉H₁₅N₃O₂

Molecular weight: 317.34 g/mol

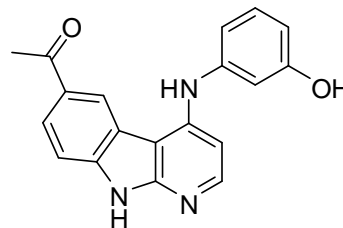
Melting point: 250-260 °C

R_f-value: [EE] 0.24

Yield: 135 mg (0.43 mmol, 42 %) dark orange solid

Method of preparation:

250 mg (1.02 mmol, 1 eq.) of **47**, according to **GP-1**, is implemented with 1.115 g (10.2 mmol, 10 eq.) 3-Aminophenol.



¹H-NMR: [400 MHz, Acetone-d₆] δ (ppm) = 2.41 (s, 3H, COCH₃); 6.50 (dd, *J* = 7.4 Hz, *J* = 1.7 Hz, 1H, H-2'); 6.69-6.71 (m, 3H, H-4', H-6' & H-3); 6.80 (d, *J* = 5.6 Hz, 1H, H-8); 7.07-7.11 (m, 1H, H-5'); 7.46 (d, *J* = 8.4 Hz, 1H, H-7); 7.92 (dd, *J* = 8.5 Hz, *J* = 1.7 Hz, 1H, H-2); 7.99 (s, 1H, -OH); 8.06 (d, *J* = 5.7 Hz, 1H, H-5); 8.49 (d, *J* = 1.1 Hz, 1H, Aniline-NH); 11.15 (br, 1H, H-9).

¹³C-NMR: [100 MHz, Acetone-d₆] δ (ppm) = 26.6 (p, CH₃); 103.9 (t, C-3); 109.8 (t, C-2'); 111.1 (t, C-6'); 111.6 (t, C-4'); 113.5 (q, C-4a); 117.9 (t, C-8); 121.2 (q, C-4b); 124.8 (t, C-5); 126.2 (q, C-6); 130.4 (t, C-7); 130.9 (t, C-5'); 141.8 (q, C-8a); 143.2 (q, C-1'); 148.1 (q, C-4); 148.3 (t, C-2); 155.6 (q, C-9a); 159.4 (q, C-3'); 197.3 (q, C=O).

IR: (ATR) ν(cm⁻¹) = 3217 (br, NH-stretch); 3144 (br, Aryl-CH-stretch); 2923 (m, Alkyl-CH-stretch); 2851 (m, Alkyl-CH-stretch); 2764 (br, Alkyl-CH-stretch); 1652 (m, C=O-stretch); 1583 (s, C=C-stretch); 1300 (m, C=C-bending); 1217 (m, C=C-bending); 957 (w, CH-bending); 889 (w, CH-bending); 739 (m, CH-bending); 562 (m, CH-bending).

ESI-MS: *m/z* = 318.26 (M⁺+H⁺).

1-(4-(3-nitrophenylamino)-9H-pyrido[2,3-b]indol-6-yl)ethanone (49)

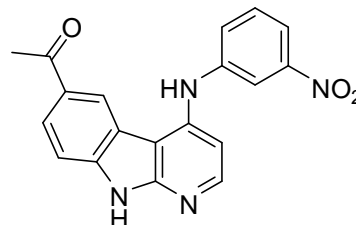
Molecular formula: C₁₉H₁₄N₄O₃

Molecular weight: 346.34 g/mol

Melting point: 290-300 °C

R_f-value: [EE] 0.31

Yield: 140 mg (0.40 mmol, 39 %) yellowish brown solid



Method of preparation:

250 mg (1.02 mmol, 1 eq.) of **47**, according to **GP-1**, is implemented with 1.410 g (10.2 mmol, 10 eq.) 3-nitroaniline.

¹H-NMR: [400 MHz, Acetone-d₆] δ (ppm) = 2.67 (s, 3H, COCH₃); 6.99 (d, *J* = 5.5 Hz, 1H, H-3); 7.52 (d, *J* = 8.4 Hz, 1H, H-6'); 7.58 (d, *J* = 8.0 Hz, 1H, H-5'); 7.67 (dd, *J* = 8.1 Hz, *J* = 1.1 Hz, 1H, H-2'); 7.84 (dd, *J* = 8.0 Hz, *J* = 1.4 Hz, 1H, H-8); 8.01-8.06 (m, 2H, H-7, H-2'); 8.24 (d, *J* = 5.6 Hz, 1H, H-2); 8.53 (d, *J* = 0.8 Hz, 1H, H-5); 9.33 (s, 1H, Aniline-NH); 12.19 (s, 1H, H-9).

¹³C-NMR: [100 MHz, DMSO-d₆] δ (ppm) = 26.9 (p, CH₃); 105.3 (t, C-3); 109.2 (t, C-2'); 110.7 (t, C-6'); 111.8 (t, C-4'); 114.2 (q, C-4a); 117.4 (t, C-8); 120.1 (q, C-4b); 123.9 (t, C-5); 127.0 (q, C-6); 129.2 (t, C-7); 130.5 (t, C-5'); 140.7 (q, C-8a); 144.3 (q, C-1'); 146.7 (q, C-4); 149.4 (t, C-2); 156.2 (q, C-9a); 158.6 (q, C-3'); 197.5 (q, C=O).

IR: (ATR) ν(cm⁻¹) = 3393 (br, NH-stretch); 3293 (s, Aryl-CH-stretch); 3095 (s, Aryl-CH-stretch); 3038 (s, Aryl-CH-stretch); 2956 (m, Alkyl-CH-stretch); 2851 (m, Alkyl-CH-stretch); 2783 (m, Alkyl-CH-stretch); 1657 (s, C=O-stretch); 1565 (s, C=C-stretch); 1299 (m, C=C-bending); 1238 (m, C=C-bending); 952 (m, CH-bending); 884 (w, CH-bending); 765 (m, CH-bending); 590 (w, CH-bending).

ESI-MS: m/z = 347.17 (M⁺+H⁺); 345.28 (M⁺-H⁺).

1-(4-(3-chlorophenylamino)-9H-pyrido[2,3-b]indol-6-yl)ethanone (50)

Molecular formula: C₁₉H₁₄ClN₃O

Molecular weight: 335.79 g/mol

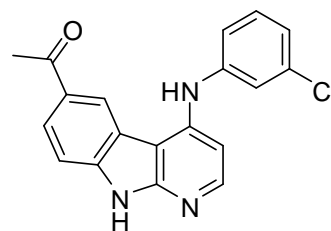
Melting point: 233-236 °C

R_f-value: [EE] 0.33

Yield: 85 mg (0.25 mmol, 25 %) dark yellow solid

Method of preparation:

250 mg (1.02 mmol, 1 eq.) of **47**, according to **GP-1**, is implemented with 1.301 g (10.2 mmol, 10 eq.) 3-chloroaniline.



¹H-NMR: [400 MHz, DMSO-d₆] δ (ppm) = 2.48 (s, 3H, COCH₃); 6.94 (d, *J* = 5.7 Hz, 1H, H-3); 7.07 (d, *J* = 7.9 Hz, 1H, H-2'); 7.25-7.37 (m, 4H, H-4', H-5', H-6' & H-8); 8.09 (d, *J* = 7.8 Hz, 1H, H-7); 8.23 (d, *J* = 5.6 Hz, 1H, H-2); 8.33 (d, *J* = 7.6 Hz, 1H, H-5); 8.85 (s, 1H, Aniline-NH); 11.39 (s, 1H, H-9).

¹³C-NMR: [100 MHz, DMSO-d₆] δ (ppm) = 27.5 (p, CH₃); 102.7 (t, C-3); 104.2 (t, C-2'); 109.9 (t, C-6'); 111.5 (q, C-4a); 113.4 (t, C-4'); 118.6 (t, C-8); 120.4 (q, C-4b); 122.5 (t, C-5); 128.3 (q, C-6); 128.27 (t, C-7); 131.2 (t, C-5'); 134.1 (q, C-8a); 143.5 (q, C-1'); 145.9 (q, C-4); 148.2 (t, C-2); 152.3 (q, C-9a); 154.6 (q, C-3'); 199.8 (q, C=O).

IR: (ATR) ν(cm⁻¹) = 3223 (br, NH-stretch); 3152 (m, Aryl-CH-stretch); 2922 (m, Alkyl-CH-stretch); 2855 (m, Alkyl-CH-stretch); 2770 (m, Alkyl-CH-stretch); 1654 (s, C=O-stretch); 1585 (s, C=C-stretch); 1299 (w, C=C-bending); 1219 (m, C=C-bending); 959 (w, CH-bending); 885 (w, CH-bending); 745 (m, CH-bending).

ESI-MS: m/z = 336.23 (M⁺+H⁺).

1-(4-(3-aminophenylamino)-9H-pyrido[2,3-b]indol-6-yl)ethanone (51)

Molecular formula: C₁₉H₁₆N₄O

Molecular weight: 316.36 g/mol

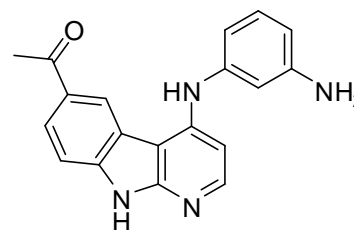
Melting point: > 300 °C

R_f-value: [EE] 0.14

Yield: 210 mg (0.66 mmol, 95 %) dark brown solid

Method of preparation:

243 mg (0.7 mmol) of compound **49** was suspended in 15 ml of 10% hydrochloric acid. Then, 800 mg (4.21 mmol) of tin-II-chloride was added and the reaction mixture was heated for 80 min under reflux. TLC was made to detect the reaction progression. After cooling, the mixture was poured into 25 ml water and the pH was adjusted to 12 using 10 M potassium hydroxide. The water phase was then extracted by ethyl acetate for 5 times (each with 25 ml) and the unified organic layers are dried over sodium sulfate. After filtration, the eluent is removed in vacuum and the amino derivative is obtained.



¹H-NMR: [400 MHz, DMSO-d₆] δ (ppm) = 5.11 (br, 2H, NH₂); 6.34 (d, *J* = 7.8 Hz, 1H, H-6'); 6.43 (d, *J* = 7.9 Hz, 1H, H-4'); 6.51 (s, 1H, H-2'); 6.75 (d, *J* = 5.7 Hz, 1H, H-3); 7.02 (t, *J* = 7.8 Hz, 1H, H-5'); 7.46 (d, *J* = 8.6 Hz, 1H, H-8); 7.96 (d, *J* = 8.6 Hz, 1H, H-7); 8.09 (d, *J* = 5.6 Hz, 1H, H-2); 8.55 (s, 1H, H-5); 8.60 (s, 1H, Aniline-NH); 11.99 (s, 1H, H-9).

¹³C-NMR: [100 MHz, DMSO-d₆] δ (ppm) = 27.1 (p, CH₃); 103.4 (t, C-3); 103.6 (t, C-2'); 108.1 (t, C-6'); 109.4 (q, C-4a); 110.1 (t, C-4'); 110.4 (t, C-8); 110.6 (q, C-4b); 120.3 (t, C-5); 125.1 (q, C-6); 125.2 (t, C-7); 129.0 (t, C-5'); 130.0 (q, C-8a); 141.1 (q, C-1'); 146.6 (q, C-4); 147.7 (t, C-2); 150.1 (q, C-9a); 154.9 (q, C-3'); 197.6 (q, C=O).

IR: (ATR) ν(cm⁻¹) = 3476 (br, NH-stretch); 3310 (m, Aryl-CH-stretch); 3084 (m, Aryl-CH-stretch); 2959 (m, Aryl-CH-stretch); 2923 (m, Alkyl-CH-stretch); 2852 (m, Alkyl-CH-stretch); 2688 (m, Alkyl-CH-stretch); 1643 (m, C=O-stretch); 1578 (s, C=C-stretch); 1306 (m, C=C-bending); 1248 (s, C=C-bending); 954 (m, CH-bending); 893 (m, CH-bending); 735 (m, CH-bending); 576 (m, CH-bending).

ESI-MS: *m/z* = 317.24 (M⁺+H⁺); 315.42 (M⁺-H⁺).

Aldol Condensation:

(E)-1-(4-chloro-9-methyl-9H-pyrido[2,3-b]indol-6-yl)-3-(dimethylamino)prop-2-en-1-one (52)

Molecular formula: C₁₇H₁₆ClN₃O

Molecular weight: 313.78 g/mol

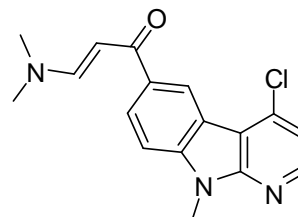
Melting point: > 300 °C

R_f-value: [EE] 0.15

Yield: 544 mg (1.73 mmol, 85 %) light yellow solid

Method of preparation:

7 ml (6.23 g, 52.28 mmol, 25.5 eq.) DMF-DMA was placed in a 25 ml round bottom flask. Under stirring, 500 mg (2.04 mmol, 1 eq.) of **47** was added. Then the mixture was heated under argon atmosphere to reflux for 3 h. After cooling, a dark brownish solid began to fall. By the addition of 40 ml of diethyl ether the precipitation was completed, and after 30 minutes the crude product was collected by filtration through a Buchner funnel and dried in an open air. Purification by column chromatography was then carried out to separate the two products, **52** and **53**.



¹H-NMR: [400 MHz, DMSO-d₆] δ (ppm) = 2.95-3.17 (br 2 s, 6H, N-(CH₃)₂); 3.95 (s, 3H, CH₃); 5.93 (d, *J* = 12.2 Hz, 1H, CO-CH=CH-N); 7.39 (d, *J* = 5.3 Hz, 1H, H-3); 7.72-7.76 (m, 2H, H-7, H-8); 8.20 (dd, *J* = 8.7 Hz, *J* = 1.7 Hz, 1H, H-2); 8.45 (d, *J* = 5.3 Hz, 1H, H-5); 8.90 (d, *J* = 1.4 Hz, 1H, CO-CH=CH-N).

¹³C-NMR: [100 MHz, DMSO-d₆] δ (ppm) = 28.5 (p, N-CH₃, N-(CH₃)₂); 91.3 (t, CO-CH=CH-N); 109.7 (t, C-8); 113.3 (q, C-4a); 116.6 (t, C-3); 118.5 (q, C-4b); 127.6 (t, C-5); 133.4 (t, C-7); 137.2 (q, C-6); 141.2 (q, C-4); 141.8 (q, C-8a); 147.1 (t, C-2); 152.9 (t, CO-CH=CH-N); 154.3 (q, C-9a); 185.6 (q, C=O).

IR: (ATR) ν(cm⁻¹) = 3081 (br, Aryl-CH-stretch); 3023 (w, Aryl-CH-stretch); 2882 (w, Alkyl-CH-stretch); 2798 (w, Alkyl-CH-stretch); 1643 (m, C=O-stretch); 1551 (s, C=C-stretch); 1297 (m, C=C-bending); 1265 (m, C=C-bending); 960 (m, CH-bending); 872 (m, CH-bending); 730 (s, CH-bending); 580 (m, CH-bending).

ESI-MS: m/z = 314.11 (M⁺+H⁺).

(E)-1-(4-chloro-9H-pyrido[2,3-b]indol-6-yl)-3-(dimethylamino)prop-2-en-1-one (53)

Molecular formula: C₁₆H₁₄ClN₃O

Molecular weight: 299.75 g/mol

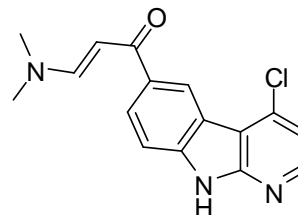
Melting point: > 300 °C

R_f-value: [EE] 0.19

Yield: 31 mg (0.10 mmol, 5 %) white solid

Method of preparation:

The same procedure was used for the preparation of derivative 52. It was yielded as a by-product and isolated during the purification by column chromatography.



¹H-NMR: [400 MHz, DMSO-d₆] δ (ppm) = 2.94-3.28 (br 2 s, 6H, N-(CH₃)₂); 5.90 (d, *J* = 12.1 Hz, 1H, CO-CH=CH-N); 7.36 (d, *J* = 5.4 Hz, 1H, H-3); 7.54 (d, *J* = 9.0 Hz, 1H, H-8); 7.73 (d, *J* = 12.1 Hz, 1H, H-7); 8.12 (dd, *J* = 8.6 Hz, *J* = 1.6 Hz, 1H, H-5); 8.39 (d, *J* = 5.5 Hz, 1H, H-2); 8.87 (d, *J* = 1.2 Hz, 1H, CO-CH=CH-N); 12.38 (br, 1H, H-9).

¹³C-NMR: [100 MHz, DMSO-d₆] δ (ppm) = 30.6 (p, N-(CH₃)₂); 90.7 (t, CO-CH=CH-N); 109.5 (t, C-8); 110.8 (q, C-4a); 113.0 (t, C-3); 118.7 (q, C-4b); 121.9 (t, C-5); 127.1 (t, C-7); 132.6 (q, C-6); 136.7 (q, C-4); 140.6 (q, C-8a); 146.9 (t, C-2); 153.2 (t, CO-CH=CH-N); 153.8 (q, C-9a); 185.3 (q, C=O).

IR: (ATR) ν(cm⁻¹) = 3447 (br, NH-stretch); 3205 (m, Aryl-CH-stretch); 3109 (m, Aryl-CH-stretch); 3033 (m, Aryl-CH-stretch); 2943 (m, Alkyl-CH-stretch); 2859 (m, Alkyl-CH-stretch); 2769 (m, Alkyl-CH-stretch); 1638 (s, C=O-stretch); 1568 (s, C=C-stretch); 1294 (s, C=C-bending); 1218 (m, C=C-bending); 988 (m, CH-bending); 867 (m, CH-bending); 742 (m, CH-bending); 566 (m, CH-bending).

ESI-MS: *m/z* = 300.22 (M⁺+H⁺); 298.23 (M⁺-H⁺).

4-chloro-9-methyl-6-(1H-pyrazol-5-yl)-9H-pyrido[2,3-b]indole (54)

Molecular formula: C₁₅H₁₁ClN₄

Molecular weight: 282.73 g/mol

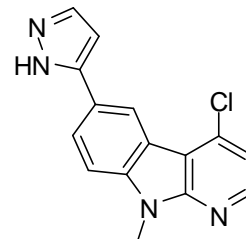
Melting point: > 300 °C

R_f-value: [EE] 0.20

Yield: 82 mg (0.29 mmol, 90 %) light yellow solid

Method of preparation:

In a 25 ml rounded flask, 100 mg (0.32 mmol, 1 eq.) of **52** was heated to reflux for 10 min. with 0.02 ml (0.38 mmol, 1.2 eq.) hydrazine hydrate in MeOH. Then, the reaction mixture was left stirring at RT overnight. The desired heterocyclic structure **54** precipitated and was collected by filtration and dried in an open air.



¹H-NMR: [400 MHz, DMSO-d₆] δ (ppm) = 3.87 (s, 3H, N-CH₃); 6.73 (d, J = 1.9 Hz, 1H, H-5''); 7.26 (d, J = 7.8 Hz, 1H, H-8); 7.64-7.77 (m, 2H, H-7, H-5); 8.01 (d, J = 7.9 Hz, 1H, H-3); 8.37 (d, J = 8.0 Hz, 1H, H-4''); 8.75 (d, J = 2.4 Hz, 1H, H-2); 12.97 (br, 1H, H-2'').

¹³C-NMR: [100 MHz, DMSO-d₆] δ (ppm) = 27.8 (p, N-CH₃); 101.3 (t, C-5''); 109.9 (t, C-8); 112.5 (q, C-4a); 115.7 (t, C-3); 118.5 (q, C-4b); 125.2 (t, C-5); 127.1 (t, C-7); 132.6 (q, C-6); 136.7 (q, C-4); 139.2 (t, C-4''); 140.8 (q, C-8a); 142.0 (q, C-1''); 146.2 (t, C-2); 152.2 (q, C-9a).

ESI-MS: m/z = 283.21 (M⁺+H⁺).

1-(9-benzyl-4-chloro-9H-pyrido[2,3-b]indol-6-yl)ethanone (55)

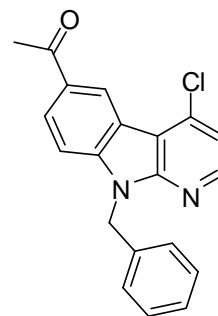
Molecular formula: C₂₀H₁₅ClN₂O

Molecular weight: 334.80 g/mol

Melting point: 149-157 °C

R_f-value: [EE] 0.97

Yield: 1.25 g (3.73 mmol, 91 %) beige solid



Method of preparation:

1 g (4.09 mmol, 1 eq.) of **47** was added to 3.4 ml (0.78 g, 6.14 mmol, 1.5 eq.) of benzyl chloride in presence of 50 mg KOH and 10 mg N-TBAB in THF. The mixture was stirred overnight at RT. After the detection of the formed product using TLC, 50 ml of water was added and the mixture was extracted by ethyl acetate 3 times. The organic fragments were collected and dried over sodium sulfate. After filtration, the solvent was evaporated under vacuum and the desired *N*-benzylated product was isolated.

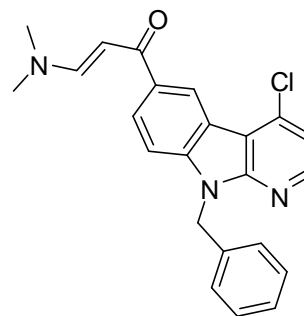
¹H-NMR: [400 MHz, DMSO-d₆] δ (ppm) = 2.72 (s, 3H, CH₃); 5.83 (s, 2H, N-CH₂-C₆H₅); 7.25-7.35 (m, 5H, N-CH₂-C₆H₅); 7.52 (d, *J* = 5.3 Hz, 1H, H-3); 7.84 (d, *J* = 8.8 Hz, 1H, H-7); 8.23 (dd, *J* = 8.6 Hz, *J* = 1.6 Hz, 1H, H-8); 8.56 (d, *J* = 5.3 Hz, 1H, H-5); 8.98 (d, *J* = 1.3 Hz, 1H, H-2).

¹³C-NMR: [100 MHz, DMSO-d₆] δ (ppm) = 27.1 (p, CH₃); 45.1 (s, CH₂-Bnz.); 110.8 (t, C-8); 113.3 (q, C-4a); 117.6 (t, C-3); 118.9 (q, C-4b); 123.6 (t, C-5); 127.5- 128.5 (t, 5x C-Bnz.); 129.1 (t, C-7); 130.4 (q, C-6); 137.3 (q, C-4); 137.8 (q, C-Bnz.); 142.3 (q, C-8a); 147.9 (t, C-2); 152.9 (q, C-9a); 199.2 (q, C=O).

IR: (ATR) ν(cm⁻¹) = 3089 (m, Aryl-CH-stretch); 3007 (m, Aryl-CH-stretch); 2959 (m, Alkyl-CH-stretch); 2854 (m, Alkyl-CH-stretch); 2640 (w, Alkyl-CH-stretch); 1677 (s, C=O-stretch); 1558 (s, C=C-stretch); 1301 (s, C=C-bending); 1214 (m, C=C-bending); 935 (m, CH-bending); 871 (s, CH-bending).

ESI-MS: *m/z* = 335.10 (M⁺).

(E)-1-(9-benzyl-4-chloro-9H-pyrido[2,3-b]indol-6-yl)-3-(dimethylamino)prop-2-en-1-one (56)



Molecular formula: C₂₃H₂₀ClN₃O

Molecular weight: 389.88 g/mol

Melting point: 125-130 °C

R_f-value: [EE] 0.29

Yield: 730 mg (1.87 mmol, 92 %) yellowish orange solid

Method of preparation:

7 ml (6.23 g, 52.28 mmol, 25.5 eq.) DMF-DMA was placed in a 25 ml round bottom flask. Under stirring, 683 mg (2.04 mmol, 1 eq.) of **55** was added. Then the mixture was heated under argon atmosphere to reflux for 3 h. After cooling, a yellowish orange solid began to fall. By the addition of 40 ml of diethyl ether the precipitation was completed, and after 30 minutes the desired product was collected by filtration through a Buchner funnel and dried in an open air.

¹H-NMR: [400 MHz, DMSO-d⁶] δ (ppm) = 3.03-3.25 (br 2 s, 6H, N-(CH₃)₂); 5.87 (s, 2H, N-CH₂-C₆H₅); 5.99 (d, *J* = 12.1 Hz, 1H, CO-CH=CH-N); 7.29-7.39 (m, 5H, N-CH₂-C₆H₅); 7.54 (d, *J* = 5.3 Hz, 1H, H-3); 7.81-7.86 (m, 2H, H-7, H-8); 8.24 (dd, *J* = 8.7 Hz, *J* = 1.1 Hz, 1H, H-2); 8.58 (d, *J* = 5.2 Hz, 1H, CO-CH=CH-N); 9.01 (s, 1H, H-5).

¹³C-NMR: [100 MHz, DMSO-d⁶] δ (ppm) = 31.1 (p, N-(CH₃)₂); 45.1 (s, CH₂-Bnz.); 91.3 (t, CO-CH=CH-N); 110.3 (t, C-8); 113.4 (q, C-4a); 117.2 (t, C-3); 118.8 (q, C-4b); 122.4 (t, C-5); 127.5-127.9 (t, 5x C-Bnz.); 129.1 (t, C-7); 133.8 (q, C-6); 137.5 (q, C-Bnz.); 141.2 (q, C-4); 147.4 (q, C-8a); 148.9 (t, C-2); 152.9 (t, CO-CH=CH-N); 154.4 (q, C-9a); 185.6 (q, C=O).

IR: (ATR) ν(cm⁻¹) = 3032 (w, Aryl-CH-stretch); 2923 (m, Alkyl-CH-stretch); 2854 (m, Alkyl-CH-stretch); 2805 (w, Alkyl-CH-stretch); 1633 (s, C=O-stretch); 1572 (s, C=C-stretch); 1293 (m, C=C-bending); 1218 (m, C=C-bending); 984 (m, CH-bending); 870 (m, CH-bending); 751 (m, CH-bending).

ESI-MS: m/z = 390.21 (M⁺).

9-benzyl-4-chloro-6-(1H-pyrazol-5-yl)-9H-pyrido[2,3-b]indole (57)

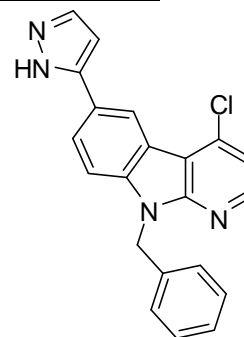
Molecular formula: C₂₁H₁₅ClN₄

Molecular weight: 358.82 g/mol

Melting point: 233-236 °C

R_f-value: [EE] 0.75

Yield: 86 mg (0.24 mmol, 92 %) yellow solid



Method of preparation:

In a 25 ml rounded flask, 100 mg (0.26 mmol, 1 eq.) of **56** was heated to reflux for 10 min. with 0.03 ml (0.31 mmol, 1.2 eq.) hydrazine hydrate in MeOH. Then, the reaction mixture was left stirring at RT overnight. The desired heterocyclic structure **57** precipitated and was collected by filtration and dried in an open air.

¹H-NMR: [400 MHz, DMSO-d₆] δ (ppm) = 5.75 (s, 2H, N-CH₂-C₆H₅); 6.75 (br, 1H, H-5"); 7.19-7.27 (m, 5H, N-CH₂-C₆H₅); 7.39 (d, *J* = 5.3 Hz, 1H, H-3); 7.70 (d, *J* = 8.6 Hz, 1H, H-7); 7.80 (s, 1H, H-5); 8.01 (d, *J* = 8.6 Hz, 1H, H-8); 8.45 (d, *J* = 5.2 Hz, 1H, H-2); 8.83 (br, 1H, H-4"); 12.83 (s, 1H, H-2").

¹³C-NMR: [100 MHz, DMSO-d₆] δ (ppm) = 44.5 (s, CH₂-Bnz.); 101.5 (t, C-5"); 110.5 (t, C-8); 112.6 (q, C-4a); 116.2 (t, C-3); 118.8 (q, C-4b); 125.4 (t, C-5); 127.0-128.6 (t, 5x C-Bnz.); 129.9 (t, C-7); 132.6 (q, C-6); 134.2 (q, C-Bnz.); 136.9 (q, C-4); 137.3 (t, C-4"); 139.9 (q, C-8a); 142.2 (q, C-1"); 146.7 (t, C-2); 152.1 (q, C-9a).

IR: (ATR) ν(cm⁻¹) = 3171 (m, Aryl-CH-stretch); 3105 (m, Aryl-CH-stretch); 3034 (m, Aryl-CH-stretch); 2945 (m, Alkyl-CH-stretch); 2880 (m, Alkyl-CH-stretch); 2753 (m, Alkyl-CH-stretch); 1631 (m, C=O-stretch); 1577 (m, C=C-stretch); 1296 (s, C=C-bending); 1209 (m, C=C-bending); 976 (m, CH-bending); 855 (m, CH-bending); 735 (m, CH-bending); 571 (m, CH-bending).

ESI-MS: *m/z* = 359.17 (M⁺).

4-chloro-6-(1H-pyrazol-5-yl)-9H-pyrido[2,3-b]indole (58)

Molecular formula: C₁₄H₉ClN₄

Molecular weight: 268.70 g/mol

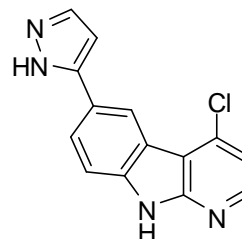
Melting point: 233-236 °C

R_f-value: [EE] 0.48

Yield: 45 mg (0.17 mmol, 60 %) white solid

Method of preparation:

To a 10 ml rounded flask contains 5 ml of 95% H₂SO₄, 100 mg (0.28 mmol) of compound **57** was added portion wise and very slowly. The mixture was left stirring overnight at RT. Then the reaction mixture was poured on 50 ml water and the precipitated solid collected by filtration and dried in air.



¹H-NMR: [400 MHz, DMSO-d₆] δ (ppm) = 6.72 (d, *J* = 2.1 Hz, 1H, H-5''); 7.31 (d, *J* = 5.3 Hz, 1H, H-7); 7.58 (d, *J* = 8.4 Hz, 1H, H-3); 7.72 (s, 1H, H-5); 7.96 (dd, *J* = 8.6 Hz, *J* = 1.7 Hz, 1H, H-8); 8.37 (d, *J* = 5.2 Hz, 1H, H-2); 8.75 (d, *J* = 1.2 Hz, 1H, H-4''); 12.44 (s, 1H, H-9); 12.99 (br, 1H, H-2'').

¹³C-NMR: [100 MHz, DMSO-d₆] δ (ppm) = 101.4 (t, C-5''); 111.7 (t, C-8); 112.7 (q, C-4a); 115.6 (t, C-3); 118.8 (q, C-4b); 119.3 (t, C-5); 125.2 (t, C-7); 136.6 (q, C-6); 138.4 (q, C-4); 139.3 (t, C-4''); 140.5 (q, C-8a); 143.1 (q, C-1''); 146.7 (t, C-2); 153.0 (q, C-9a).

IR: (ATR) ν(cm⁻¹) = 3389 (br, NH-stretch); 3207 (m, Aryl-CH-stretch); 3145 (m, Aryl-CH-stretch); 2924 (m, Alkyl-CH-stretch); 2849 (m, Alkyl-CH-stretch); 2733 (m, Alkyl-CH-stretch); 1651 (m, C=O-stretch); 1465 (m, C=C-stretch); 1312 (m, C=C-bending); 1259 (s, C=C-bending); 981 (m, CH-bending); 876 (w, CH-bending); 722 (m, CH-bending); 561 (m, CH-bending).

ESI-MS: *m/z* = 269.26 (M⁺+H⁺).

3-(6-(1H-pyrazol-5-yl)-9H-pyrido[2,3-b]indol-4-ylamino)phenol (59)

Molecular formula: C₂₀H₁₅N₅O

Molecular weight: 341.37 g/mol

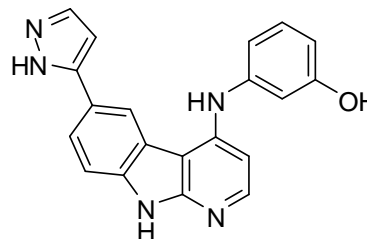
Melting point: > 300 °C

R_f-value: [EE] 0.38

Yield: 75 mg (0.22 mmol, 24 %) dark gray solid

Method of preparation:

250 mg (0.93 mmol, 1 eq.) of **58**, according to **GP-1**, is implemented with 1.015 g (9.3 mmol, 10 eq.) 3-Aminophenol.



¹H-NMR: [400 MHz, DMSO-d⁶] δ (ppm) = 6.68 (d, *J* = 1.4 Hz, 1H, H-3); 6.79 (s, 1H, H-2'); 6.80 (d, *J* = 10.7 Hz, 4H, H-4', H-6', H-5'' & H-4''); 7.22 (t, *J* = 7.9 Hz, 1H, H-5'); 7.49 (d, *J* = 8.4 Hz, 1H, H-7); 7.89 (d, *J* = 7.6 Hz, 1H, H-2); 8.13 (s, 1H, H-5); 8.47 (s, 1H, Aniline-NH); 9.46 (s, 1H, OH); 11.72 (s, 1H, H-9); 12.90 (br, 1H, H-2'').

¹³C-NMR: [100 MHz, DMSO-d⁶] δ (ppm) = 101.9 (t, C-3); 106.7 (t, C-2'); 110.5 (t, C-5''); 111.0 (t, C-6'); 111.7 (t, C-4'); 112.2 (q, C-4a); 118.9 (t, C-8); 120.0 (q, C-4b); 120.8 (t, C-5); 122.9 (q, C-6); 130.4 (t, C-7); 137.5 (t, C-5'); 139.3 (t, C-4''); 141.7 (q, C-8a); 142.9 (q, C-1''); 146.3 (q, C-1'); 148.5 (q, C-4); 149.2 (t, C-2); 154.3 (q, C-9a); 158.7 (q, C-3').

IR: (ATR) ν(cm⁻¹) = 3586 (br, NH-stretch); 3300 (m, Aryl-CH-stretch); 3145 (m, Aryl-CH-stretch); 2922 (s, Alkyl-CH-stretch); 2851 (m, Alkyl-CH-stretch); 2599 (w, Alkyl-CH-stretch); 1592 (s, C=O-stretch); 1452 (m, C=C-stretch); 1316 (m, C=C-bending); 1268 (m, C=C-bending); 969 (m, CH-bending); 888 (w, CH-bending); 734 (m, CH-bending); 547 (m, CH-bending).

ESI-MS: *m/z* = 342.29 (M⁺+H⁺).

N-(3-chlorophenyl)-6-(1H-pyrazol-5-yl)-9H-pyrido[2,3-b]indol-4-amine (60)

Molecular formula: C₂₀H₁₄ClN₅

Molecular weight: 359.81 g/mol

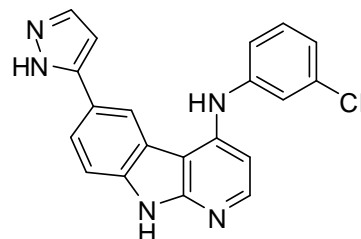
Melting point: 280-285 °C

R_f-value: [EE] 0.21

Yield: 70 mg (0.19 mmol, 21 %) gray solid

Method of preparation:

250 mg (0.93 mmol, 1 eq.) of **58**, according to **GP-1**, is implemented with 1.186 g (9.3 mmol, 10 eq.) 3-chloroaniline.



¹H-NMR: [400 MHz, Acetone-d₆] δ (ppm) = 6.62 (d, *J* = 1.6 Hz, 1H, H-2'); 6.96 (t, *J* = 5.6 Hz, 1H, H-5'); 7.10-7.12 (m, 1H, H-4'); 7.25-7.43 (m, 4H, H-6', H-5'', H-4'' & H-3); 7.57 (d, *J* = 8.4 Hz, 1H, H-8); 7.65 (d, *J* = 2.1 Hz, 1H, H-5); 7.97 (dd, *J* = 8.4 Hz, *J* = 1.5 Hz, 1H, H-7); 8.17 (d, *J* = 9.0 Hz, 1H, H-2); 8.49 (d, *J* = 1.9 Hz, 1H, Aniline-NH); 10.97 (br, 1H, H-9); H-2'' not detected.

¹³C-NMR: [100 MHz, Acetone-d₆] δ (ppm) = 102.3 (t, C-3); 111.6 (t, C-2'); 120.1 (t, C-5''); 120.2 (t, C-6'); 120.3 (t, C-4'); 121.5 (q, C-4a); 121.7 (t, C-8); 123.3 (q, C-4b); 123.4 (t, C-5); 124.1 (q, C-6); 131.5 (t, C-7); 135.3 (t, C-5'); 138.5 (t, C-4''); 140.1 (q, C-8a); 142.9 (q, C-1''); 146.7 (q, C-1'); 148.1 (q, C-4); 149.1 (t, C-2); 152.7 (q, C-9a); 155.9 (q, C-3').

IR: (ATR) ν(cm⁻¹) = 3581 (br, NH-stretch); 3205 (m, Aryl-CH-stretch); 3139 (m, Aryl-CH-stretch); 2917 (s, Alkyl-CH-stretch); 2849 (s, Alkyl-CH-stretch); 1577 (s, C=O-stretch); 1454 (m, C=C-stretch); 1319 (m, C=C-bending); 1272 (m, C=C-bending); 995 (m, CH-bending); 868 (m, CH-bending); 739 (m, CH-bending); 591 (m, CH-bending).

ESI-MS: *m/z* = 360.30 (M⁺+H⁺); 358.35 (M⁺-H⁺).

5-(9-benzyl-4-chloro-9H-pyrido[2,3-b]indol-6-yl)isoxazole (61)

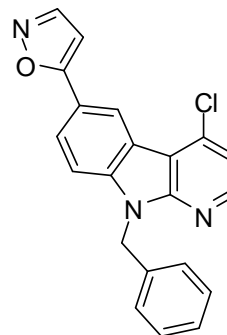
Molecular formula: C₂₁H₁₄ClN₃O

Molecular weight: 359.81 g/mol

Melting point: 165-172 °C

R_f-value: [EE] 0.95

Yield: 60 mg (0.17 mmol, 65 %) white solid



Method of preparation:

In a 25 ml rounded flask, 100 mg (0.26 mmol, 1 eq.) of **56** was heated to reflux for 1 h with 0.22 mg (0.31 mmol, 1.2 eq.) hydroxylamine HCl in absolute EtOH under argon atmosphere. Then, the reaction mixture was left stirring at RT overnight. The desired heterocyclic structure **61** precipitated and was collected by filtration and dried in an open air.

¹H-NMR: [400 MHz, DMSO-d⁶] δ (ppm) = 5.79 (s, 2H, N-CH₂-C₆H₅); 7.05 (d, *J* = 1.5 Hz, 1H, H-5"); 7.21-7.27 (m, 5H, N-CH₂-C₆H₅); 7.48 (d, *J* = 5.3 Hz, 1H, H-3); 7.87 (d, *J* = 8.6 Hz, 1H, H-7); 8.08 (d, *J* = 8.6 Hz, 1H, H-8); 8.52 (d, *J* = 5.3 Hz, 1H, H-2); 8.64 (d, *J* = 1.9 Hz, 1H, H-4"); 8.83 (s, 1H, H-5).

¹³C-NMR: [100 MHz, DMSO-d⁶] δ (ppm) = 45.1 (s, CH₂-Bnz.); 99.4 (t, C-5"); 111.9 (t, C-8); 112.9 (q, C-4a); 117.3 (t, C-3); 120.1 (q, C-4b); 125.9 (t, C-5); 127.0-128.6 (t, 5x C-Bnz.); 129.1 (t, C-7); 132.3 (q, C-6); 134.9 (q, C-Bnz.); 136.4 (q, C-4); 138.0 (t, C-4"); 140.7 (q, C-8a); 143.2 (q, C-1"); 147.9 (t, C-2); 152.3 (q, C-9a).

IR: (ATR) ν(cm⁻¹) = 3139 (m, Aryl-CH-stretch); 3108 (m, Aryl-CH-stretch); 3030 (w, Aryl-CH-stretch); 2973 (m, Alkyl-CH-stretch); 2926 (m, Alkyl-CH-stretch); 2676 (m, Alkyl-CH-stretch); 1596 (s, C=O-stretch); 1561 (m, C=C-stretch); 1291 (m, C=C-bending); 1210 (m, C=C-bending); 971 (m, CH-bending); 853 (m, CH-bending); 744 (m, CH-bending); 593 (m, CH-bending).

ESI-MS: m/z = 360.22 (M⁺).

5-(4-chloro-9H-pyrido[2,3-b]indol-6-yl)isoxazole (62)

Molecular formula: C₁₄H₈ClN₃O

Molecular weight: 269.69 g/mol

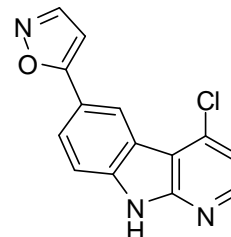
Melting point: 183-192 °C

R_f-value: [EE] 0.58

Yield: 55 mg (0.20 mmol, 73 %) white solid

Method of preparation:

To a 10 ml rounded flask contains 5 ml of 95% H₂SO₄, 100 mg (0.28 mmol) of compound **61** was added portion wise and very slowly. The mixture was left stirring overnight at RT. Then the reaction mixture was poured on 50 ml water and the precipitated solid collected by filtration and dried in air.



¹H-NMR: [400 MHz, DMSO-d₆] δ (ppm) = 7.11 (d, *J* = 1.9 Hz, 1H, H-5''); 7.47-7.57 (m, 1H, H-7); 7.76 (d, *J* = 8.6 Hz, 1H, H-3); 8.12 (dd, *J* = 8.5 Hz, *J* = 1.6 Hz, 1H, H-8); 8.51 (d, *J* = 5.3 Hz, 1H, H-5); 8.72 (d, *J* = 2.0 Hz, 1H, H-4''); 8.85 (d, *J* = 2.0 Hz, 1H, H-2); 12.60 (s, 1H, H-9).

¹³C-NMR: [100 MHz, DMSO-d₆] δ (ppm) = 99.1 (t, C-5''); 112.9 (t, C-8); 116.7 (q, C-4a); 117.2 (t, C-3); 119.6 (q, C-4b); 119.8 (t, C-5); 129.1 (t, C-7); 137.7 (q, C-6); 137.9 (q, C-4); 147.5 (t, C-4''); 147.9 (q, C-8a); 152.2 (q, C-1''); 153.3 (t, C-2); 169.3 (q, C-9a).

IR: (ATR) ν(cm⁻¹) = 3408 (br, NH-stretch); 3098 (m, Aryl-CH-stretch); 2923 (m, Alkyl-CH-stretch); 2852 (m, Alkyl-CH-stretch); 2750 (m, Alkyl-CH-stretch); 1650 (m, C=O-stretch); 1464 (s, C=C-stretch); 1342 (m, C=C-bending); 1170 (s, C=C-bending); 975 (m, CH-bending); 874 (m, CH-bending); 750 (m, CH-bending); 535 (m, CH-bending).

ESI-MS: *m/z* = 270.16 (M⁺+H⁺); 268.23 (M⁺-H⁺).

3-(6-(isoxazol-5-yl)-9H-pyrido[2,3-b]indol-4-ylamino)phenol (63)

Molecular formula: C₂₀H₁₄N₄O₂

Molecular weight: 342.35 g/mol

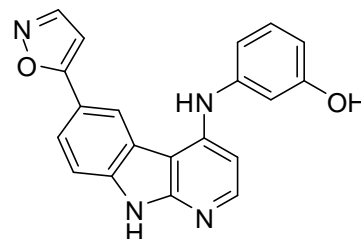
Melting point: 218-224 °C

R_f-value: [EE] 0.23

Yield: 80 mg (0.23 mmol, 25 %) brown solid

Method of preparation:

250 mg (0.93 mmol, 1 eq.) of **62**, according to **GP-1**, is implemented with 1.015 g (9.3 mmol, 10 eq.) 3-Aminophenol.



¹H-NMR: [400 MHz, Acetone-d₆] δ (ppm) = 6.65 (dd, *J* = 8.5 Hz, *J* = 2.8 Hz, 1H, H-5''); 6.72 (d, *J* = 1.8 Hz, 1H, H-2'); 6.88-6.94 (m, 4H, H-3, H-6', H-4' & H-8); 7.22-7.26 (m, 1H, H-5''); 7.67 (d, *J* = 8.1 Hz, 1H, H-7); 7.90 (dd, *J* = 8.5 Hz, *J* = 1.7 Hz, 1H, H-4''); 8.08 (s, 1H, H-5); 8.17 (d, *J* = 5.8 Hz, 1H, H-2); 8.41 (d, *J* = 1.9 Hz, 1H, H-Aniline-NH); 8.59 (d, *J* = 1.7 Hz, 1H, OH); 11.18 (br, 1H, H-9).

¹³C-NMR: [100 MHz, Acetone-d₆] δ (ppm) = 97.5 (t, C-5''); 102.2 (t, C-3); 109.3 (t, C-2'); 110.9 (t, C-6'); 111.1 (t, C-4'); 113.6 (q, C-4a); 119.9 (t, C-8); 122.7 (q, C-4b); 124.5 (t, C-5); 129.2 (q, C-6); 130.0 (t, C-7); 136.7 (t, C-5'); 139.5 (t, C-4''); 142.8 (q, C-8a); 144.3 (q, C-1''); 147.6 (q, C-1'); 147.9 (q, C-4); 149.8 (t, C-2); 150.9 (q, C-9a); 158.4 (q, C-3').

IR: (ATR) ν(cm⁻¹) = 3292 (br, NH-stretch); 2917 (s, Alkyl-CH-stretch); 2849 (m, Alkyl-CH-stretch); 1585 (s, C=O-stretch); 1448 (m, C=C-stretch); 1338 (m, C=C-bending); 1179 (m, C=C-bending); 952 (w, CH-bending); 881 (w, CH-bending); 760 (m, CH-bending); 544 (m, CH-bending).

ESI-MS: *m/z* = 343.26 (M⁺+H⁺); 341.32 (M⁺-H⁺).

N-(3-chlorophenyl)-6-(isoxazol-5-yl)-9H-pyrido[2,3-b]indol-4-amine (64)

Molecular formula: C₂₀H₁₃ClN₄O

Molecular weight: 360.80 g/mol

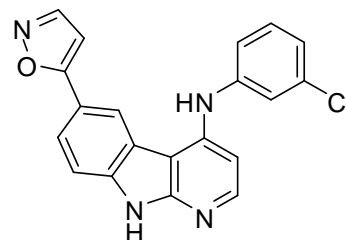
Melting point: 245-247 °C

R_f-value: [EE] 0.35

Yield: 85 mg (0.24 mmol, 25 %) dark brown solid

Method of preparation:

250 mg (0.93 mmol, 1 eq.) of **62**, according to **GP-1**, is implemented with 1.186 g (9.3 mmol, 10 eq.) 3-chloroaniline.



¹H-NMR: [400 MHz, Acetone-d₆] δ (ppm) = 6.72 (d, *J* = 1.9 Hz, 1H, H-5''); 6.97 (dd, *J* = 5.6 Hz, *J* = 2.9 Hz, 1H, H-2'); 7.15 (d, *J* = 7.7 Hz, 1H, H-4'); 7.38-7.45 (m, 4H, H-6', H-5', H-3 & H-7); 7.68 (d, *J* = 8.4 Hz, 1H, H-8); 7.92 (dd, *J* = 8.5 Hz, *J* = 1.5 Hz, 1H, H-5); 8.25-8.8.31 (m, 1H, H-4''); 8.42 (d, *J* = 1.9 Hz, 1H, H-2); 8.58 (d, *J* = 1.5 Hz, 1H, Aniline-NH); 11.19 (br, 1H, H-9).

¹³C-NMR: [100 MHz, Acetone-d₆] δ (ppm) = 97.5 (t, C-5''); 101.9 (t, C-3); 109.4 (t, C-2'); 110.5 (t, C-6'); 112.2 (t, C-4'); 113.4 (q, C-4a); 120.1 (t, C-8); 123.3 (q, C-4b); 125.1 (t, C-5); 129.3 (q, C-6); 130.6 (t, C-7); 135.7 (t, C-5'); 138.4 (t, C-4''); 142.4 (q, C-8a); 143.1 (q, C-1''); 146.0 (q, C-1'); 148.1 (q, C-4); 149.7 (t, C-2); 150.9 (q, C-9a); 159.5 (q, C-3').

IR: (ATR) ν(cm⁻¹) = 3293 (br, NH-stretch); 3069 (m, Aryl-CH-stretch); 2917 (s, Alkyl-CH-stretch); 2849 (s, Alkyl-CH-stretch); 1584 (s, C=O-stretch); 1479 (m, C=C-stretch); 1375 (m, C=C-bending); 1179 (m, C=C-bending); 952 (m, CH-bending); 834 (m, CH-bending); 761 (m, CH-bending); 542 (m, CH-bending).

ESI-MS: *m/z* = 361.18 (M⁺); 359.26 (M⁺-H⁺).

Bromination:

6-bromo-4-chloro-9H-pyrido[2,3-b]indole (67)

Molecular formula: C₁₁H₆BrClN₂

Molecular weight: 281.54 g/mol

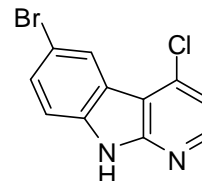
Melting point: 200-208 °C

R_f value: [Cyc : EE 75 : 25 v/v] 0.43

Yield: 952 mg (3.38 mmol, 69 %) beige solid

Method of preparation:

To a solution of 1 g (4.93 mmol, 1 eq.) **9** in 30 ml of glacial acetic acid, 300 μl (942 mg, 4.93 mmol, 1.2 eq.) elemental bromine were added dropwise under stirring. After the addition, the mixture was stirred for 24 h at RT. Then it was carefully added to 50 ml of 1 M sodium thiosulfate. The mixture was then cooled on an ice bath, by dropwise addition of conc. ammonia solution is alkalized, and is extracted three times with 50 ml of CHCl₃ and then three times with 50 ml ethyl acetate. The combined organic phases were dried over sodium sulfate, and the solvent was removed under reduced pressure. The product thus obtained was used without further purification in the next step.



¹H-NMR: [400 MHz, DMSO-d₆] δ (ppm) = 7.33 (d, *J* = 5.2 Hz, 1H, H-3); 8.60 (d, *J* = 7.5 Hz, 1H, H-8); 8.62 (d, *J* = 7.5 Hz, 1H, H-7); 8.39 (s, 1H, H-5); 8.40 (s, 1H, H-2).

¹³C-NMR: [100 MHz, DMSO-d₆] δ (ppm) = 111.6 (q, C-4a); 111.7 (q, C-6); 113.5 (t, C-8); 115.8 (t, C-3); 120.6 (q, C-4b); 124.2 (t, C-5); 129.6 (t, C-7); 136.8 (q, C-4); 137.4 (q, C-8a); 147.3 (t, C-2); 152.6 (q, C-9a).

IR: (KBr) ν(cm⁻¹) = 3436 (br, NH-stretch); 3224 (m, Aryl-CH-stretch); 3137 (m, Aryl-CH-stretch); 3074 (m, Aryl-CH-stretch); 1619 (m, NH-bending); 1585 (s, C=C-stretch); 1566 (s, C=C-stretch); 1456 (s, C=C-stretch); 750 (m, CH-bending); 643 (m, CH-bending).

EI-MS: *m/z* = 282 (100, M⁺); 245 (4, M⁺-Cl); 219 (8, C₉H₄BrN₂⁺); 202 (90, M⁺-Br); 174 (16, C₁₀H₅ClN⁺); 166 (41, C₁₁H₆N₂⁺); 113 (14, C₈H₃N⁺); 87 (11, C₃H₂ClN⁺).

6,8-dibromo-4-chloro-9H-pyrido[2,3-b]indole (68)

Molecular formula: C₁₁H₅Br₂ClN₂

Molecular weight: 360.43 g/mol

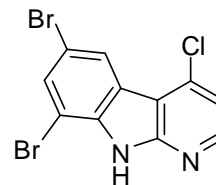
Melting point: 257-260 °C

R_f-value: [EE] 0.89

Yield: 890 mg (2.47 mmol, 50 %) light beige solid

Method of preparation:

To a solution of 1 g (4.93 mmol, 1 eq.) **9** in 30 ml of glacial acetic acid, excess (2.5 eq.) elemental bromine was added dropwise under stirring. Then the following procedure for preparing compound **67** was used.



¹H-NMR: [400 MHz, DMSO-d⁶] δ (ppm) = 7.51 (dd, *J* = 8.8 Hz, *J* = 3.5 Hz, 1H, H-3); 7.68 (dd, *J* = 8.7 Hz, *J* = 1.9 Hz, 1H, H-7); 8.39 (dd, *J* = 5.6 Hz, *J* = 2.5 Hz, 1H, H-2); 8.65 (s, 1H, H-5), 12.52 (s, 1H, H-9).

¹³C-NMR: [100 MHz, DMSO-d⁶] δ (ppm) = 111.1 (q, C-4a); 112.7 (q, C-6); 113.7 (q, C-8); 114.3 (t, C-3); 120.8 (q, C-4b); 125.0 (t, C-5); 130.9 (t, C-7); 136.4 (q, C-4); 138.5 (q, C-8a); 148.8 (t, C-2); 151.6 (q, C-9a).

IR: (ATR) ν(cm⁻¹) = 3442 (br, NH-stretch); 3195 (m, Aryl-CH-stretch); 3045 (m, Aryl-CH-stretch); 1621 (m, NH-bending); 1599 (m, C=C-stretch); 1561 (m, C=C-stretch); 1447 (s, C=C-stretch); 742 (m, CH-bending); 659 (m, CH-bending).

ESI-MS: *m/z* = 361.21 (M⁺+H⁺).

3-(6-bromo-9H-pyrido[2,3-b]indol-4-ylamino)phenol (69)

Molecular formula: C₁₇H₁₂BrN₃O

Molecular weight: 354.20 g/mol

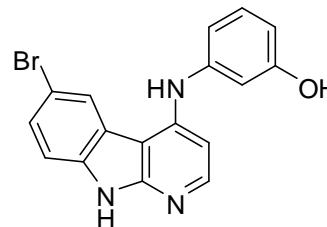
Melting point: 264-266 °C

R_f-value: [EE] 0.37

Yield: 60 mg (0.17 mmol, 19 %) dark beige solid

Method of preparation:

250 mg (0.89 mmol, 1 eq.) of **67**, according to **GP-1**, is implemented with 969 mg (8.9 mmol, 10 eq.) 3-Aminophenol.



¹H-NMR: [400 MHz, DMSO-d⁶] δ (ppm) = 6.45 (dd, *J* = 7.5 Hz, *J* = 1.8 Hz, 1H, H-2'); 6.69-6.79 (m, 3H, H-4', H-3 & H-6'); 7.09-7.17 (m, 1H, H-5'); 7.32-7.48 (m, 2H, H-7, H-8); 8.07-8.09 (m, 1H, H-5); 8.33 (d, *J* = 1.8 Hz, 1H, H-2); 8.49 (s, 1H, Aniline-NH); 9.41 (s, 1H, OH); 11.77 (s, 1H, H-9).

¹³C-NMR: [100 MHz, DMSO-d⁶] δ (ppm) = 102.4 (t, C-3); 103.9 (q, C-4a); 109.2 (t, C-2'); 110.3 (t, C-6'); 110.9 (t, C-8); 112.7 (t, C-4'); 119.2 (t, C-5); 120.5 (q, C-4b); 122.4 (q, C-6); 125.2 (t, C-7); 130.3 (t, C-5'); 138.0 (q, C-8a); 142.5 (q, C-1'); 147.1 (q, C-4); 147.9 (t, C-2); 154.4 (q, C-9a); 158.6 (q, C-3').

IR: (ATR) ν(cm⁻¹) = 3427 (br, NH-stretch); 3262 (m, Aryl-CH-stretch); 3055 (m, Aryl-CH-stretch); 2922 (m, Aryl-CH-stretch); 1875 (br, NH-bending); 1586 (s, C=C-stretch); 1520 (s, C=C-stretch); 1453 (m, C=C-stretch); 742 (m, CH-bending); 598 (m, CH-bending).

ESI-MS: *m/z* = 354.17 (M⁺).

6-bromo-N-(3-chlorophenyl)-9H-pyrido[2,3-b]indol-4-amine (70)

Molecular formula: C₁₇H₁₁BrClN₃

Molecular weight: 372.65 g/mol

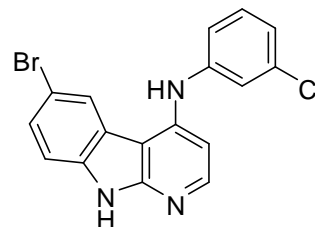
Melting point: 244-249 °C

R_f-value: [EE] 0.49

Yield: 63 mg (0.17 mmol, 19 %) dark gray solid

Method of preparation:

250 mg (0.89 mmol, 1 eq.) of **67**, according to **GP-1**, is implemented with 1.135 g (8.9 mmol, 10 eq.) 3-chloroaniline.



¹H-NMR: [400 MHz, DMSO-d₆] δ (ppm) = 6.83 (d, *J* = 5.5 Hz, 1H, H-3); 7.09 (d, *J* = 8.6 Hz, 1H, H-2'); 7.25 (d, *J* = 8.2 Hz, 1H, H-4'); 7.33-7.41 (m, 3H, H-6', H-7 & H-5'); 7.48 (dd, *J* = 8.6 Hz, *J* = 1.5 Hz, 1H, H-8); 8.15 (d, *J* = 5.7 Hz, 1H, H-5); 8.31 (d, *J* = 1.2 Hz, 1H, H-2); 8.75 (s, 1H, Aniline-NH); 11.87 (s, 1H, H-9).

¹³C-NMR: [100 MHz, DMSO-d₆] δ (ppm) = 102.8 (t, C-3); 103.5 (q, C-4a); 111.6 (t, C-2'); 112.9 (t, C-6'); 119.7 (t, C-8); 120.9 (t, C-4'); 122.1 (t, C-5); 122.8 (q, C-4b); 125.2 (q, C-6); 127.9 (t, C-7); 131.2 (t, C-5'); 134.0 (q, C-8a); 136.9 (q, C-1'); 143.4 (q, C-4); 146.2 (t, C-2); 148.2 (q, C-9a); 154.4 (q, C-3').

IR: (ATR) ν(cm⁻¹) = 3419 (br, NH-stretch); 3094 (m, Aryl-CH-stretch); 3034 (m, Aryl-CH-stretch); 2915 (m, Aryl-CH-stretch); 1883 (br, NH-bending); 1587 (s, C=C-stretch); 1507 (m, C=C-stretch); 1450 (s, C=C-stretch); 755 (m, CH-bending); 571 (m, CH-bending).

ESI-MS: *m/z* = 474.09 (M⁺+H⁺).

6-bromo-N-(3-nitrophenyl)-9H-pyrido[2,3-b]indol-4-amine (71)

Molecular formula: C₁₇H₁₁BrN₄O₂

Molecular weight: 383.20 g/mol

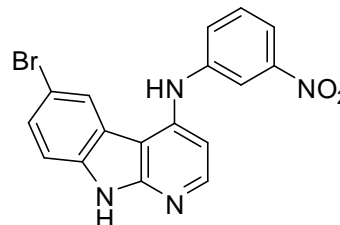
Melting point: 211-218 °C

R_f-value: [EE] 0.38

Yield: 58 mg (0.16 mmol, 17 %) yellow solid

Method of preparation:

250 mg (0.89 mmol, 1 eq.) of **67**, according to **GP-1**, is implemented with 1.229 g (8.9 mmol, 10 eq.) 3-nitroaniline.



¹H-NMR: [400 MHz, Acetone-d₆] δ (ppm) = 7.02 (s, 1H, H-2'); 7.04 (d, *J* = 5.6 Hz, 1H, H-3); 7.46-7.55 (m, 2H, H-7, H-6'); 7.66 (t, *J* = 8.2 Hz, 1H, H-5'); 7.81 (d, *J* = 1.4 Hz, 1H, H-8); 7.95 (d, *J* = 0.8 Hz, 1H, H-4'); 9.19 (d, *J* = 2.3 Hz, 1H, H-5); 8.27 (d, *J* = 1.1 Hz, 1H, H-2); 8.44 (s, 1H, Aniline-NH); 11.09 (br, 1H, H-9).

¹³C-NMR: [100 MHz, Acetone-d₆] δ (ppm) = 101.3 (t, C-3); 109.1 (q, C-4a); 111.9 (t, C-2'); 116.2 (t, C-6'); 118.4 (t, C-8); 120.6 (t, C-4'); 121.4 (t, C-5); 123.5 (q, C-4b); 125.1 (q, C-6); 128.6 (t, C-7); 130.4 (t, C-5'); 133.3 (q, C-8a); 138.6 (q, C-1'); 141.2 (q, C-4); 144.5 (t, C-2); 147.9 (q, C-9a); 156.1 (q, C-3').

IR: (ATR) ν(cm⁻¹) = 3420 (m, NH-stretch); 3093 (m, Aryl-CH-stretch); 3030 (m, Aryl-CH-stretch); 2921 (s, Aryl-CH-stretch); 1898 (br, NH-bending); 1594 (s, C=C-stretch); 1522 (s, C=C-stretch); 1451 (m, C=C-stretch); 767 (m, CH-bending); 541 (m, CH-bending).

ESI-MS: *m/z* = 383.33 (M⁺).

6-bromo-N-(3-methoxyphenyl)-9H-pyrido[2,3-b]indol-4-amine (72)

Molecular formula: C₁₈H₁₄BrN₃O

Molecular weight: 368.23 g/mol

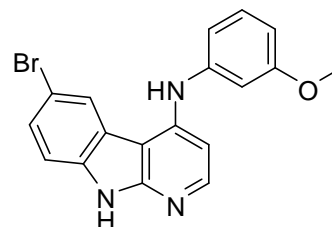
Melting point: 312-318 °C

R_f-value: [EE] 0.33

Yield: 59 mg (0.16 mmol, 18 %) white solid

Method of preparation:

250 mg (0.89 mmol, 1 eq.) of **67**, according to **GP-1**, is implemented with 1.096 g (8.9 mmol, 10 eq.) 3-anisidine.



¹H-NMR: [400 MHz, DMSO-d⁶] δ (ppm) = 3.75 (s, 3H, OCH₃); 6.67 (dd, *J* = 8.0 Hz, *J* = 1.9 Hz, 1H, H-2'); 6.79 (d, *J* = 5.7 Hz, 1H, H-4'); 6.88-6.91 (m, 2H, H-3, H-6'); 7.28 (t, *J* = 7.9 Hz, 1H, H-5'); 7.38 (d, *J* = 8.5 Hz, 1H, H-7); 7.47 (d, *J* = 1.9 Hz, 1H, H-8); 8.09 (d, *J* = 5.6 Hz, 1H, H-5); 8.35 (d, *J* = 1.9 Hz, 1H, H-2); 8.59 (s, 1H, Aniline-NH); 11.80 (s, 1H, H-9).

¹³C-NMR: [100 MHz, DMSO-d⁶] δ (ppm) = 23.6 (p, OCH₃); 101.9 (t, C-3); 102.4 (q, C-4a); 107.4 (t, C-2'); 108.7 (t, C-6'); 111.0 (t, C-8); 112.2 (t, C-4'); 113.9 (t, C-5); 121.8 (q, C-4b); 124.6 (q, C-6); 128.0 (t, C-7); 129.9 (t, C-5'); 136.3 (q, C-8a); 142.2 (q, C-1'); 146.6 (q, C-4); 147.6 (t, C-2); 153.9 (q, C-9a); 160.1 (q, C-3').

IR: (ATR) ν(cm⁻¹) = 3443 (m, NH-stretch); 3132 (m, Aryl-CH-stretch); 3029 (m, Aryl-CH-stretch); 2920 (m, Aryl-CH-stretch); 1892 (br, NH-bending); 1579 (s, C=C-stretch); 1510 (m, C=C-stretch); 1452 (m, C=C-stretch); 776 (m, CH-bending); 542 (m, CH-bending).

ESI-MS: m/z = 369.31 (M⁺+H⁺); 367.35 (M⁺-H⁺).

3-(6,8-dibromo-9H-pyrido[2,3-b]indol-4-ylamino)phenol (73)

Molecular formula: C₁₇H₁₁Br₂N₃O

Molecular weight: 433.10 g/mol

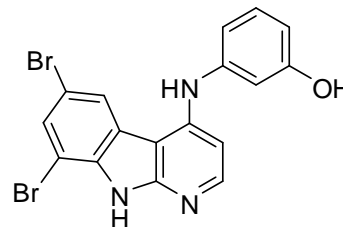
Melting point: 290-300 °C

R_f-value: [EE] 0.74

Yield: 27 mg (0.06 mmol, 9 %) pale green solid

Method of preparation:

250 mg (0.69 mmol, 1 eq.) of **68**, according to **GP-1**, is implemented with 753 mg (6.9 mmol, 10 eq.) 3-Aminophenol.



¹H-NMR: [400 MHz, DMSO-d⁶] δ (ppm) = 6.23-6.35 (m, 3H, H-2', H-4' & H-3); 6.98-7.02 (m, 2H, H-6', H-5'); 7.37 (d, *J* = 8.6 Hz, 1H, H-7); 7.44 (d, *J* = 7.2 Hz, 1H, H-5); 8.42 (d, *J* = 8.9 Hz, 2H, H-2, Aniline-NH); 9.17 (s, 1H, OH), 12.10 (s, 1H, H-9).

¹³C-NMR: [100 MHz, DMSO-d⁶] δ (ppm) = 104.9 (t, C-3); 106.2 (q, C-4a); 108.3 (t, C-2'); 109.0 (t, C-6'); 111.7 (q, C-8); 112.9 (t, C-4'); 121.3 (t, C-5); 126.9 (q, C-4b); 128.6 (q, C-6); 130.3 (t, C-7); 130.9 (t, C-5'); 137.6 (q, C-8a); 142.5 (q, C-1'); 143.9 (q, C-4); 149.2 (t, C-2); 153.2 (q, C-9a); 158.6 (q, C-3').

IR: (ATR) ν(cm⁻¹) = 3355 (s, NH-stretch); 3192 (m, Aryl-CH-stretch); 3039 (s, Aryl-CH-stretch); 2923 (s, Aryl-CH-stretch); 1859 (br, NH-bending); 1565 (s, C=C-stretch); 1509 (m, C=C-stretch); 1458 (s, C=C-stretch); 776 (m, CH-bending); 556 (m, CH-bending).

ESI-MS: *m/z* = 434.24 (M⁺+H⁺); 432.21 (M⁺-H⁺).

6,8-dibromo-N-(3-chlorophenyl)-9H-pyrido[2,3-b]indol-4-amine (74)

Molecular formula: C₁₇H₁₀Br₂ClN₃

Molecular weight: 451.54 g/mol

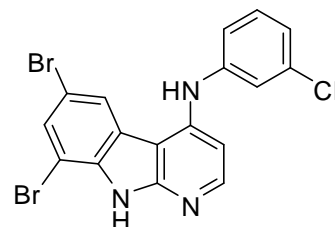
Melting point: 302-305 °C

R_f-value: [EE] 0.85

Yield: 27 mg (0.06 mmol, 9 %) beige solid

Method of preparation:

250 mg (0.69 mmol, 1 eq.) of **68**, according to **GP-1**, is implemented with 880 mg (6.9 mmol, 10 eq.) 3-chloroaniline.



¹H-NMR: [400 MHz, DMSO-d⁶] δ (ppm) = 6.69 (dd, *J* = 8.2 Hz, *J* = 1.5 Hz, 1H, H-2'); 6.87-6.93 (m, 2H, H-4', H-3); 7.16-7.21 (m, 2H, H-6', H-5'); 7.41 (d, *J* = 8.6 Hz, 1H, H-7); 7.48 (dd, *J* = 8.6 Hz, *J* = 1.9 Hz, 1H, H-2); 8.56 (s, 1H, H-5); 8.85 (s, 1H, Aniline-NH); 12.21 (br, 1H, H-9).

¹³C-NMR: [100 MHz, DMSO-d⁶] δ (ppm) = 107.0 (t, C-3); 109.2 (q, C-4a); 111.8 (t, C-2'); 113.4 (t, C-6'); 115.4 (q, C-8); 116.6 (t, C-4'); 120.6 (t, C-5); 120.9 (q, C-4b); 126.4 (q, C-6); 129.1 (t, C-7); 131.2 (t, C-5'); 134.1 (q, C-8a); 137.8 (q, C-1'); 141.5 (q, C-4); 144.6 (t, C-2); 149.5 (q, C-9a); 153.2 (q, C-3').

IR: (ATR) ν(cm⁻¹) = 3358 (s, NH-stretch); 3187 (m, Aryl-CH-stretch); 3040 (s, Aryl-CH-stretch); 2921 (s, Aryl-CH-stretch); 1860 (br, NH-bending); 1561 (m, C=C-stretch); 1503 (s, C=C-stretch); 1460 (m, C=C-stretch); 769 (m, CH-bending); 547 (m, CH-bending).

ESI-MS: *m/z* = 452.12 (M⁺+H⁺); 450.20 (M⁺-H⁺).

6,8-dibromo-N-(3-nitrophenyl)-9H-pyrido[2,3-b]indol-4-amine (75)

Molecular formula: C₁₇H₁₀Br₂N₄O₂

Molecular weight: 462.09 g/mol

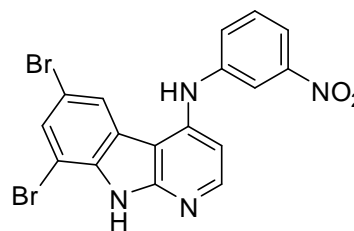
Melting point: > 300 °C

R_f-value: [EE] 0.62

Yield: 32 mg (0.07 mmol, 10 %) yellowish green solid

Method of preparation:

250 mg (0.69 mmol, 1 eq.) of **68**, according to **GP-1**, is implemented with 953 mg (6.9 mmol, 10 eq.) 3-nitroaniline.



¹H-NMR: [400 MHz, DMSO-d⁶] δ (ppm) = 6.84 (d, *J* = 5.6 Hz, 1H, H-2'); 7.48-7.67 (m, 3H, H-4', H-3 & H-6'); 7.75 (dd, *J* = 8.2 Hz, *J* = 1.5 Hz, 1H, H-7); 7.99 (t, *J* = 2.5 Hz, 1H, H-5'); 8.13 (d, *J* = 5.5 Hz, 1H, H-5); 8.25 (d, *J* = 1.6 Hz, 1H, H-2); 8.97 (s, 1H, Aniline-NH); 12.12 (s, 1H, H-9).

¹³C-NMR: [100 MHz, DMSO-d⁶] δ (ppm) = 103.4 (t, C-3); 104.2 (q, C-4a); 104.5 (t, C-2'); 111.6 (t, C-6'); 115.2 (q, C-8); 117.4 (t, C-4'); 123.1 (t, C-5); 124.5 (q, C-4b); 127.0 (q, C-6); 129.8 (t, C-7); 131.0 (t, C-5'); 136.1 (q, C-8a); 139.2 (q, C-1'); 143.1 (q, C-4); 146.2 (t, C-2); 149.1 (q, C-9a); 154.7 (q, C-3').

IR: (ATR) ν(cm⁻¹) = 3427 (s, NH-stretch); 3080 (m, Aryl-CH-stretch); 3040 (m, Aryl-CH-stretch); 2917 (m, Aryl-CH-stretch); 1881 (br, NH-bending); 1603 (s, C=C-stretch); 1520 (s, C=C-stretch); 1455 (m, C=C-stretch); 742 (w, CH-bending); 558 (m, CH-bending).

ESI-MS: *m/z* = 463.04 (M⁺+H⁺); 461.10 (M⁺-H⁺).

6,8-dibromo-N-(3-methoxyphenyl)-9H-pyrido[2,3-b]indol-4-amine (76)

Molecular formula: C₁₈H₁₃Br₂N₃O

Molecular weight: 447.12 g/mol

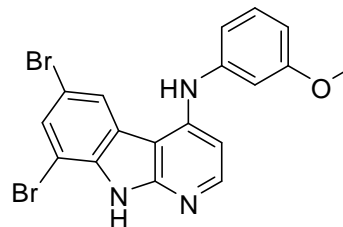
Melting point: 303-308 °C

R_f-value: [EE] 0.51

Yield: 27 mg (0.06 mmol, 9 %) white solid

Method of preparation:

250 mg (0.69 mmol, 1 eq.) of **68**, according to **GP-1**, is implemented with 850 mg (6.9 mmol, 10 eq.) 3-anisidine.



¹H-NMR: [400 MHz, DMSO-d⁶] δ (ppm) = 3.75 (s, 3H, OCH₃); 6.38 (dd, *J* = 7.7 Hz, *J* = 1.6 Hz, 1H, H-2'); 6.47 (t, *J* = 2.3 Hz, 1H, H-5'); 6.51 (dd, *J* = 8.2 Hz, *J* = 1.8 Hz, 1H, H-4'); 6.99-7.31 (m, 2H, H-3, H-6'); 7.47 (d, *J* = 1.9 Hz, 1H, H-7); 7.75 (d, *J* = 1.7 Hz, 1H, H-2); 8.52 (s, 1H, H-5); 8.57 (s, 1H, Aniline-NH); 12.13 (s, 1H, H-9).

¹³C-NMR: [100 MHz, DMSO-d⁶] δ (ppm) = 54.9 (p, OCH₃); 103.4 (t, C-3); 105.8 (q, C-4a); 106.7 (t, C-2'); 107.8 (t, C-6'); 109.8 (q, C-8); 111.1 (t, C-4'); 112.6 (t, C-5); 120.7 (q, C-4b); 122.9 (q, C-6); 126.3 (t, C-7); 130.4 (t, C-5'); 137.1 (q, C-8a); 141.8 (q, C-1'); 143.5 (q, C-4); 148.8 (t, C-2); 152.7 (q, C-9a); 160.2 (q, C-3').

IR: (ATR) ν(cm⁻¹) = 3399 (s, NH-stretch); 3189 (m, Aryl-CH-stretch); 3038 (m, Aryl-CH-stretch); 2940 (m, Aryl-CH-stretch); 1857 (br, NH-bending); 1599 (s, C=C-stretch); 1515 (s, C=C-stretch); 1457 (m, C=C-stretch); 780 (m, CH-bending); 546 (m, CH-bending).

ESI-MS: *m/z* = 448.19 (M⁺+H⁺); 446.19 (M⁺-H⁺).

Cyanation:

4-(3-hydroxyphenylamino)-9H-pyrido[2,3-b]indole-6-carbonitrile (78)

Molecular formula: C₁₈H₁₂N₄O

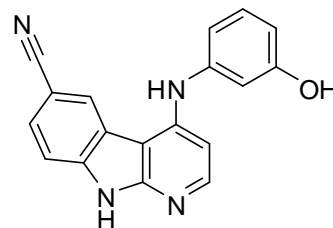
Molecular weight: 300.31 g/mol

Melting point: > 300 °C

Yield: 45 mg (0.15 mmol, 54 %) metallic-colored solid

Method of preparation:

A solution of 100 mg (0.28 mmol, 1 eq.) **69** and 68 mg (0.76 mmol, 2.7 eq.) copper (I) cyanide in 15 ml of NMP was heated for 7 hours under an argon atmosphere to reflux. After cooling, the solution was poured into 100 ml of ethyl acetate. This solution was washed with 50 ml of 20% ammonia solution and the washing solution was re-extracted four times with 50 ml ethyl acetate. The organic phases were combined and the solvent was removed under reduced pressure. The solid residue was washed with 50 ml of water and then filtered through a Buchner funnel and dried in an open air.



¹H-NMR: [400 MHz, DMSO-d⁶] δ (ppm) = 6.55 (dd, *J* = 7.8 Hz, *J* = 1.2 Hz, 1H, H-2'); 6.74-6.76 (m, 2H, H-4', H-6'); 6.80 (d, *J* = 5.9 Hz, 1H, H-3); 7.18 (t, *J* = 8.0 Hz, 1H, H-5'); 7.55 (d, *J* = 0.8 Hz, 1H, H-7); 7.71 (dd, *J* = 8.2 Hz, *J* = 1.6 Hz, 1H, H-8), 8.14 (br, 1H, OH); 8.54 (s, 1H, H-5); 8.67 (d, *J* = 1.2 Hz, 1H, H-2); 9.46 (s, 1H, Aniline-NH); 12.19 (br, 1H, H-9).

¹³C-NMR: [100 MHz, DMSO-d⁶] δ (ppm) = 101.3 (t, C-3); 104.5 (q, C-4a); 108.9 (t, C-2'); 110.6 (t, C-6'); 112.6 (t, C-8); 113.7 (t, C-4'); 118.6 (q, CN); 119.8 (t, C-5); 121.0 (q, C-4b); 124.8 (q, C-6); 127.4 (t, C-7); 130.5 (t, C-5'); 136.1 (q, C-8a); 140.9 (q, C-1'); 144.3 (q, C-4); 148.9 (t, C-2); 151.7 (q, C-9a); 155.5 (q, C-3').

ESI-MS: *m/z* = 301.27 (M⁺+H⁺); 299.39 (M⁺-H⁺).

Nitration:

4-chloro-6-nitro-9H-pyrido[2,3-b]indole (81)

Molecular formula: C₁₁H₆ClN₃O₂

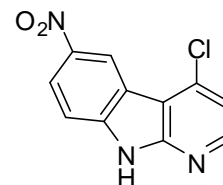
Molecular weight: 247.64 g/mol

Melting point: >320 °C

Yield: 1.47 g (5.93 mmol, 48 %) beige solid

Method of preparation:

15 ml of red fuming nitric acid were placed in a 50 ml round-bottomed flask and cooled on an ice bath. Then, at 0 ° C and under stirring, 2.5 g (12.33 mmol) of **9** were added portionwise. The ice bath was removed and the mixture stirred for 20 minutes at RT. Then the reaction mixture was poured onto crushed ice followed by the addition of 50 ml of water. A saturated sodium carbonate solution was added dropwise to alkalize the mixture. The reaction mixture was allowed to stand overnight, and then the precipitated solid was filtered through a Buchner funnel, washed with water and dried in an open air. The resulting crude product was recrystallized from DMF and then dried under vacuum over P₂O₅.



¹H-NMR: [400 MHz, DMSO-d₆] δ (ppm) = 7.41 (d, *J* = 5.3 Hz, 1H, H-3); 7.65 (d, *J* = 9.0 Hz, 1H, H-8); 8.35 (dd, *J* = 9.0 Hz, *J* = 2.3 Hz, 1H, H-7); 8.46 (d, *J* = 5.3 Hz, 1H, H-2); 9.00 (d, *J* = 2.3 Hz, 1H, H-5); 12.87 (s, 1H, H-9).

¹³C-NMR: [100 MHz, DMSO-d₆] δ (ppm) = 112.5 (t, C-8); 113.2 (t, C-5); 117.5 (t, C-7); 118.9 (t, C-3); 123.2 (q, C-4a); 131.0 (q, C-4b); 137.8 (q, C-4); 141.1 (q, C-8a); 143.0 (q, C-9a); 148.8 (t, C-2); 154.1 (q, C-6).

IR: (KBr) ν(cm⁻¹) = 3436 (br, NH-stretch); 1630 (m, NH-bending); 1604 (m, C=C-stretch); 1577 (m, C=C-stretch); 1527 (m, NO-stretch); 1490 (m, C=C-stretch); 1456 (m, C=C-stretch); 1341 (s, NO-stretch); 796 (m, CH-bending).

EI-MS: *m/z* = 247 (100, M⁺); 201 (39, M⁺-NO₂); 174 (20, C₉H₃ClN₂⁺); 166 (39, C₁₁H₆N₂⁺).

4-chloro-6,8-dinitro-9H-pyrido[2,3-b]indole (86)

Molecular formula: C₁₁H₅ClN₄O₄

Molecular weight: 292.63 g/mol

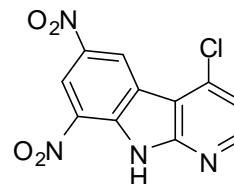
Melting point: > 300 °C

R_f-value: [EE] 0.65

Yield: 1.8 g (6.17 mmol, 50 %) yellowish solid

Method of preparation:

20 ml (excess) of red fuming nitric acid were placed in a 50 ml round-bottomed flask and cooled on an ice bath. Then, at 0 ° C and under stirring, 2.5 g (12.33 mmol) of **9** were added portionwise. The ice bath was removed and the mixture stirred for 45 minutes at RT. Then the reaction mixture was poured onto crushed ice followed by the addition of 50 ml of water. A saturated sodium carbonate solution was added dropwise to alkalize the mixture. The reaction mixture was allowed to stand overnight, and then the precipitated solid was filtered through a Buchner funnel, washed with water and dried in an open air. The resulting crude product was recrystallized from DMF and then dried under vacuum over P₂O₅.



¹H-NMR: [400 MHz, DMSO-d₆] δ (ppm) = 7.46 (d, *J* = 5.2 Hz, 1H, H-3); 8.15 (s, 1H, H-7); 8.49 (d, *J* = 5.3 Hz, 1H, H-2); 8.97 (d, *J* = 2.2 Hz, 1H, H-5); 13.49 (s, 1H, H-9).

¹³C-NMR: [100 MHz, DMSO-d₆] δ (ppm) = 109.8 (t, C-7); 116.3 (t, C-3); 118.1 (t, C-5); 119.7 (q, C-8); 122.4 (q, C-4a); 130.8 (q, C-4b); 139.0 (q, C-4); 142.3 (q, C-8a); 145.7 (q, C-6); 149.5 (t, C-2); 152.0 (q, C-9a).

IR: (ATR) ν(cm⁻¹) = 3183 (br, NH-stretch); 1635 (m, NH-bending); 15984 (m, C=C-stretch); 1581 (m, C=C-stretch); 1521 (m, NO-stretch); 1485 (m, C=C-stretch); 1465 (m, C=C-stretch); 1370 (s, NO-stretch); 783 (m, CH-bending).

ESI-MS: m/z = 291.33 (M⁺-H⁺).

3-(6-nitro-9H-pyrido[2,3-b]indol-4-ylamino)phenol (87)

Molecular formula: C₁₇H₁₂N₄O₃

Molecular weight: 320.30 g/mol

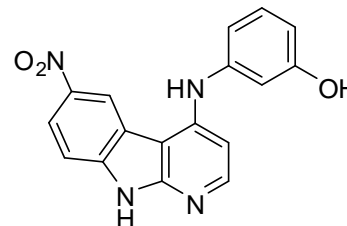
Melting point: 258-260 °C

R_f-value: [EE] 0.26

Yield: 80 mg (0.25 mmol, 25 %) yellow solid

Method of preparation:

250 mg (1.01 mmol, 1 eq.) of **81**, according to **GP-1**, is implemented with 1.102 g (10.1 mmol, 10 eq.) 3-Aminophenol.



¹H-NMR: [400 MHz, DMSO-d⁶] δ (ppm) = 6.62 (dd, *J* = 8.1 Hz, *J* = 1.5 Hz, 1H, H-2'); 6.76-6.82 (m, 3H, H-4', H-3 & H-6'); 7.23 (t, *J* = 7.9 Hz, 1H, H-5'); 7.64 (d, *J* = 9.0 Hz, 1H, H-8); 8.17 (d, *J* = 5.9 Hz, 1H, H-2); 8.31 (dd, *J* = 8.9 Hz, *J* = 2.3 Hz, 1H, H-7); 9.17 (d, *J* = 2.1 Hz, 1H, H-5); 9.28 (s, 1H, Aniline-NH); 9.57 (s, 1H, OH); H-9 not detected.

¹³C-NMR: [100 MHz, DMSO-d⁶] δ (ppm) = 102.7 (t, C-3); 105.2 (q, C-4a); 110.1 (t, C-2'); 111.1 (t, C-6'); 111.9 (t, C-8); 113.8 (t, C-4'); 118.9 (t, C-5); 119.6 (q, C-4b); 120.9 (q, C-6); 127.2 (t, C-7); 130.1 (t, C-5'); 137.4 (q, C-8a); 140.8 (q, C-1'); 141.3 (q, C-4); 148.7 (t, C-2); 155.6 (q, C-9a); 158.3 (q, C-3').

IR: (ATR) ν (cm⁻¹) = 3344 (br, NH-stretch); 1637 (m, NH-bending); 1595 (s, C=C-stretch); 1526 (m, NO-stretch); 1485 (m, C=C-stretch); 1406 (m, C=C-stretch); 1331 (s, NO-stretch); 785 (m, CH-bending).

ESI-MS: *m/z* = 319.43 (M⁺-H⁺).

N-(3-chlorophenyl)-6-nitro-9H-pyrido[2,3-b]indol-4-amine (88)

Molecular formula: C₁₇H₁₁ClN₄O₂

Molecular weight: 338.75 g/mol

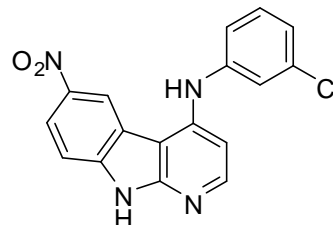
Melting point: > 300 °C

R_f-value: [EE] 0.39

Yield: 160 mg (0.47 mmol, 47 %) brown solid

Method of preparation:

250 mg (1.01 mmol, 1 eq.) of **81**, according to **GP-1**, is implemented with 1.288 g (10.1 mmol, 10 eq.) 3-chloroaniline.



¹H-NMR: [400 MHz, DMSO-d₆] δ (ppm) = 6.90 (d, *J* = 5.7 Hz, 1H, H-3); 7.16 (dd, *J* = 2.0 Hz, *J* = 0.9 Hz, 1H, H-2'); 7.29 (dd, *J* = 2.0 Hz, *J* = 0.9 Hz, 1H, H-4'); 7.35-7.42 (m, 2H, H-6', H-5'); 7.59 (d, *J* = 9.0 Hz, 1H, H-8); 8.23 (d, *J* = 5.6 Hz, 1H, H-2); 8.29 (dd, *J* = 9.0 Hz, *J* = 2.3 Hz, 1H, H-7); 9.03 (d, *J* = 2.5 Hz, 1H, H-5); 9.11 (s, 1H, Aniline-NH); 12.49 (s, 1H, H-9).

¹³C-NMR: [100 MHz, DMSO-d₆] δ (ppm) = 103.4 (t, C-3); 103.8 (q, C-4a); 110.7 (t, C-2'); 119.1 (t, C-6'); 119.5 (t, C-8); 119.7 (t, C-4'); 120.8 (t, C-5); 120.9 (q, C-4b); 122.7 (q, C-6); 128.7 (t, C-7); 130.8 (t, C-5'); 133.6 (q, C-8a); 140.1 (q, C-1'); 142.6 (q, C-4); 146.2 (t, C-2); 148.5 (q, C-9a); 154.9 (q, C-3').

IR: (ATR) ν (cm⁻¹) = 3396 (m, NH-stretch); 1608 (s, NH-bending); 1587 (m, C=C-stretch); 1570 (m, C=C-stretch); 1529 (m, NO-stretch); 1495 (m, C=C-stretch); 1450 (m, C=C-stretch); 1335 (s, NO-stretch); 798 (m, CH-bending).

ESI-MS: *m/z* = 339.32 (M⁺+H⁺); 337.40 (M⁺-H⁺).

N-(3-methoxyphenyl)-6-nitro-9H-pyrido[2,3-b]indol-4-amine (89)

Molecular formula: C₁₈H₁₄N₄O₃

Molecular weight: 334.33 g/mol

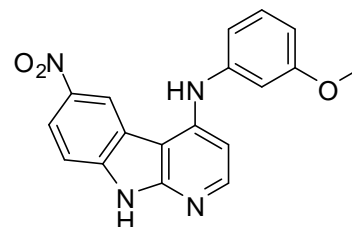
Melting point: 265-270 °C

R_f-value: [EE] 0.36

Yield: 61 mg (0.18 mmol, 18 %) yellow solid

Method of preparation:

250 mg (1.01 mmol, 1 eq.) of **81**, according to **GP-1**, is implemented with 1.244 g (10.1 mmol, 10 eq.) 3-anisidine.



¹H-NMR: [400 MHz, DMSO-d⁶] δ (ppm) = 3.81 (s, 3H, OCH₃); 6.77 (d, *J* = 2.5 Hz, 1H, H-2'); 6.96-6.99 (m, 3H, H-4', H-3 & H-6'); 7.35 (t, *J* = 8.1 Hz, 1H, H-5'); 7.69 (d, *J* = 9.0 Hz, 1H, H-8); 8.23 (d, *J* = 5.8 Hz, 1H, H-2); 8.32 (dd, *J* = 9.0 Hz, *J* = 2.3 Hz, 2H, H-7, H-5); 9.01 (d, *J* = 2.2 Hz, 1H, Aniline-NH); 11.43 (br, 1H, H-9).

¹³C-NMR: [100 MHz, DMSO-d⁶] δ (ppm) = 54.7 (p, OCH₃); 102.4 (t, C-3); 105.2 (q, C-4a); 110.4 (t, C-2'); 113.6 (t, C-6'); 118.4 (t, C-8); 119.9 (t, C-4'); 120.6 (t, C-5); 123.5 (q, C-4b); 126.1 (q, C-6); 129.3 (t, C-7); 130.1 (t, C-5'); 133.9 (q, C-8a); 141.7 (q, C-1'); 144.2 (q, C-4); 147.8 (t, C-2); 151.0 (q, C-9a); 157.8 (q, C-3').

IR: (ATR) ν (cm⁻¹) = 3390 (m, NH-stretch); 1696 (m, NH-bending); 1601 (m, C=C-stretch); 1583 (s, C=C-stretch); 1510 (m, NO-stretch); 1493 (m, C=C-stretch); 1459 (s, C=C-stretch); 1322 (s, NO-stretch); 779 (m, CH-bending).

ESI-MS: *m/z* = 335.18 (M⁺+H⁺); 333.29 (M⁺-H⁺).

N-(3-(benzyloxy)phenyl)-6-nitro-9H-pyrido[2,3-b]indol-4-amine (90)

Molecular formula: C₂₄H₁₈N₄O₃

Molecular weight: 410.42 g/mol

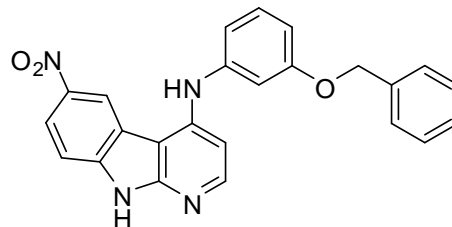
Melting point: 236-245 °C

R_f-value: [EE] 0.40

Yield: 290 mg (0.71 mmol, 70 %) yellow solid

Method of preparation:

250 mg (1.01 mmol, 1 eq.) of **81**, according to **GP-1**, is implemented with 2.011 g (10.1 mmol, 10 eq.) 3-benzyloxyaniline.



¹H-NMR: [400 MHz, DMSO-d₆] δ (ppm) = 5.11 (s, 2H, O-CH₂-C₆H₅); 6.78-6.80 (m, 2H, H-2', H-4'); 6.91-6.96 (m, 2H, H-3, H-6'); 7.28-7.43 (m, 6H, O-CH₂-C₆H₅; H-5'); 7.57 (d, *J* = 8.9 Hz, 1H, H-7); 8.14 (d, *J* = 5.6 Hz, 1H, H-8); 8.27 (dd, *J* = 9.0 Hz, *J* = 2.3 Hz, 1H, H-2); 8.96 (s, 1H, H-5); 9.07 (s, 1H, Aniline-NH); 12.42 (s, 1H, H-9).

¹³C-NMR: [100 MHz, DMSO-d₆] δ (ppm) = 69.7 (s, OCH₂); 103.5 (t, C-3); 103.8 (q, C-4a); 108.9 (t, C-2'); 110.6 (t, C-6'); 111.0 (t, C-8); 114.8 (t, C-4'); 119.5 (t, C-5); 120.2 (q, C-4b); 121.2 (q, C-6); 127.9-128.9 (t, 5x C-Bnz.); 130.6 (t, C-7); 131.9 (t, C-5'); 137.5 (q, C-1''); 140.6 (q, C-8a); 142.2 (q, C-1'); 142.5 (q, C-4); 148.8 (t, C-2); 155.4 (q, C-9a); 159.6 (q, C-3').

IR: (ATR) ν (cm⁻¹) = 3408 (m, NH-stretch); 1695 (m, NH-bending); 1607 (m, C=C-stretch); 1580 (s, C=C-stretch); 1496 (m, C=C-stretch); 1455 (m, C=C-stretch); 1319 (s, NO-stretch); 782 (m, CH-bending).

ESI-MS: m/z = 411.20 (M⁺+H⁺); 409.28 (M⁺-H⁺).

3-(6-amino-9H-pyrido[2,3-b]indol-4-ylamino)phenol (91)

Molecular formula: C₁₇H₁₄N₄O

Molecular weight: 290.32 g/mol

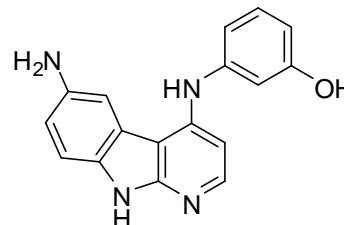
Melting point: 196-200 °C

R_f-value: [EE] 0.10

Yield: 190 mg (0.65 mmol, 93 %) black solid

Method of preparation:

224 mg (0.7 mmol) of compound **87** was suspended in 15 ml of 10% hydrochloric acid. Then, 800 mg (4.21 mmol) of tin-II-chloride was added and the reaction mixture was heated for 80 min under reflux. TLC was made to detect the reaction progression. After cooling, the mixture was poured into 25 ml water and the pH was adjusted to 12 using 10 M potassium hydroxide. The water phase was then extracted by ethyl acetate for 5 times (each with 25 ml) and the unified organic layers are dried over sodium sulfate. After filtration, the eluent is removed in vacuum and the amino derivative is obtained.



¹H-NMR: [400 MHz, DMSO-d⁶] δ (ppm) = 3.49 (s, 2H, -NH₂); 6.41 (d, *J* = 9.1 Hz, 1H, H-2'); 6.72-6.74 (m, 4H, H-4', H-3, H-6' & H-5'); 7.08-7.15 (m, 2H, H-8, H-7); 7.37 (d, *J* = 1.7 Hz, 1H, H-5); 7.97 (d, *J* = 5.6 Hz, 1H, H-2); 8.17 (s, 1H, Aniline-NH); 9.32 (s, 1H, OH); 11.06 (s, 1H, H-9).

¹³C-NMR: [100 MHz, DMSO-d⁶] δ (ppm) = 101.6 (t, C-3); 106.3 (q, C-4a); 109.6 (t, C-2'); 110.7 (t, C-6'); 112.3 (t, C-8); 115.1 (t, C-4'); 117.8 (t, C-5); 119.2 (q, C-4b); 120.5 (q, C-6); 123.8 (t, C-7); 130.9 (t, C-5'); 135.5 (q, C-8a); 141.7 (q, C-1'); 143.1 (q, C-4); 149.4 (t, C-2); 153.8 (q, C-9a); 155.1 (q, C-3').

IR: (ATR) ν (cm⁻¹) = 3287 (br, NH-stretch); 2923 (s, Aryl-CH-stretch); 1712 (m, NH-bending); 1586 (s, C=C-stretch); 1489 (m, C=C-stretch); 1470 (s, C=C-stretch); 781 (m, CH-bending).

ESI-MS: *m/z* = 291.31 (M⁺+H⁺).

N⁴-(3-chlorophenyl)-9H-pyrido[2,3-b]indole-4,6-diamine (92)

Molecular formula: C₁₇H₁₃ClN₄

Molecular weight: 308.76 g/mol

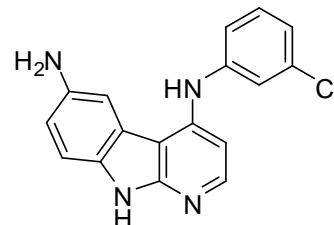
Melting point: 205-207 °C

R_f-value: [EE] 0.19

Yield: 120 mg (0.39 mmol, 56 %) dark brown solid

Method of preparation:

237 mg (0.7 mmol) of compound **88** was suspended in 15 ml of 10% hydrochloric acid. Then, 800 mg (4.21 mmol) of tin-II-chloride was added and the reaction mixture was heated for 80 min under reflux. TLC was made to detect the reaction progression. After cooling, the mixture was poured into 25 ml water and the pH was adjusted to 12 using 10 M potassium hydroxide. The water phase was then extracted by ethyl acetate for 5 times (each with 25 ml) and the unified organic layers are dried over sodium sulfate. After filtration, the eluent is removed in vacuum and the amino derivative is obtained.



¹H-NMR: [400 MHz, DMSO-d₆] δ (ppm) = 6.89 (dd, *J* = 5.7 Hz, *J* = 2.8 Hz, 1H, H-2'); 7.08-7.11 (m, 1H, H-3); 7.30-7.33 (m, 1H, H-4'); 7.35-7.39 (m, 4H, H-6', H-5', H-7 & H-5); 7.47 (d, *J* = 8.3 Hz, 1H, H-8); 8.16 (d, *J* = 5.6 Hz, 2H, H-2, Aniline-NH); 10.89 (s, 1H, H-9).

¹³C-NMR: [100 MHz, DMSO-d₆] δ (ppm) = 101.9 (t, C-3); 110.8 (q, C-4a); 112.5 (t, C-2'); 115.1 (t, C-6'); 117.5 (t, C-8); 118.8 (t, C-4'); 119.8 (t, C-5); 120.2 (q, C-4b); 120.8 (q, C-6); 123.3 (t, C-7); 129.9 (t, C-5'); 132.7 (q, C-8a); 138.4 (q, C-1'); 144.2 (q, C-4); 147.6 (t, C-2); 149.9 (q, C-9a); 152.0 (q, C-3').

IR: (ATR) ν(cm⁻¹) = 3062 (m, Aryl-CH-stretch); 2922 (s, Alkyl-CH-stretch); 2851 (s, Alkyl-CH-stretch); 1575 (s, C=O-stretch); 1471 (m, C=C-stretch); 1376 (m, C=C-bending); 1092 (m, C=C-bending); 995 (m, CH-bending); 856 (m, CH-bending); 754 (m, CH-bending); 512 (m, CH-bending).

ESI-MS: *m/z* = 309.55 (M⁺+H⁺).

3-(6,8-dinitro-9H-pyrido[2,3-b]indol-4-ylamino)phenol (93)

Molecular formula: C₁₇H₁₁N₅O₅

Molecular weight: 365.30 g/mol

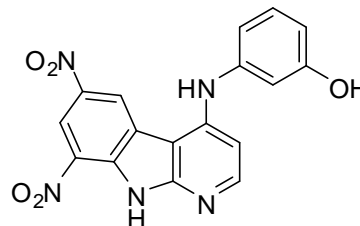
Melting point: > 300 °C

R_f-value: [EE] 0.58

Yield: 160 mg (0.44 mmol, 52 %) brown solid

Method of preparation:

250 mg (0.85 mmol, 1 eq.) of **86**, according to **GP-1**, is implemented with 928 mg (8.5 mmol, 10 eq.) 3-Aminophenol.



¹H-NMR: [400 MHz, DMSO-d⁶] δ (ppm) = 6.58 (dd, *J* = 8.1 Hz, *J* = 1.4 Hz, 1H, H-2'); 6.73-6.61 (m, 2H, H-4', H-6'); 6.89 (d, *J* = 5.8 Hz, 1H, H-3); 7.20 (t, *J* = 7.9 Hz, 1H, H-5'); 8.27 (d, *J* = 5.8 Hz, 1H, H-2); 8.97 (s, 1H, H-7); 9.11 (s, 1H, H-5); 9.33 (d, *J* = 1.7 Hz, 1H, Aniline-NH); 9.53 (s, 1H, OH); 13.07 (br, 1H, H-9).

¹³C-NMR: [100 MHz, DMSO-d⁶] δ (ppm) = 100.9 (t, C-3); 102.4 (q, C-4a); 103.2 (t, C-2'); 104.0 (t, C-6'); 105.3 (q, C-8); 109.7 (t, C-4'); 111.5 (t, C-5); 113.4 (q, C-4b); 116.3 (q, C-6); 123.2 (t, C-7); 124.8 (t, C-5'); 129.3 (q, C-8a); 130.1 (q, C-1'); 138.8 (q, C-4); 141.1 (t, C-2); 158.0 (q, C-9a); 158.3 (q, C-3').

IR: (ATR) ν(cm⁻¹) = 3428 (br, NH-stretch); 1654 (m, NH-bending); 1630 (m, C=C-stretch); 1582 (s, C=C-stretch); 1526 (s, NO-stretch); 1508 (m, C=C-stretch); 1462 (m, C=C-stretch); 1380 (s, NO-stretch); 776 (m, CH-bending).

ESI-MS: *m/z* = 366.30 (M⁺+H⁺); 364.39 (M⁺-H⁺).

N-(3-chlorophenyl)-6,8-dinitro-9H-pyrido[2,3-b]indol-4-amine (94)

Molecular formula: C₁₇H₁₀ClN₅O₄

Molecular weight: 383.75 g/mol

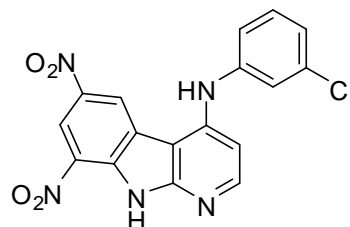
Melting point: > 300 °C

R_f-value: [EE] 0.91

Yield: 221 mg (0.58 mmol, 68 %) yellow solid

Method of preparation:

250 mg (0.85 mmol, 1 eq.) of **86**, according to **GP-1**, is implemented with 1.084 g (8.5 mmol, 10 eq.) 3-chloroaniline.



¹H-NMR: [400 MHz, DMSO-d₆] δ (ppm) = 6.97 (d, *J* = 5.7 Hz, 1H, H-6'); 7.20 (dd, *J* = 7.9 Hz, *J* = 1.1 Hz, 1H, H-2'); 7.30 (dd, *J* = 8.1 Hz, *J* = 1.1 Hz, 1H, H-4'); 7.39-7.46 (m, 2H, H-3, H-5'); 8.33 (d, *J* = 5.7 Hz, 1H, H-2); 8.99 (d, *J* = 2.0 Hz, 1H, H-5); 9.34 (d, *J* = 2.0 Hz, 2H, H-7, Aniline-NH); 13.09 (br, 1H, H-9).

¹³C-NMR: [100 MHz, DMSO-d₆] δ (ppm) = 100.9 (t, C-3); 102.9 (q, C-4a); 104.3 (t, C-2'); 105.0 (t, C-6'); 108.3 (q, C-8); 110.7 (t, C-4'); 112.1 (t, C-5); 115.7 (q, C-4b); 120.6 (q, C-6); 127.1 (t, C-7); 130.6 (t, C-5'); 133.4 (q, C-8a); 137.8 (q, C-1'); 140.1 (q, C-4); 144.2 (t, C-2); 151.4 (q, C-9a); 155.8 (q, C-3').

IR: (ATR) ν (cm⁻¹) = 3416 (br, NH-stretch); 1737 (m, NH-bending); 1585 (s, C=C-stretch); 1535 (s, NO-stretch); 1509 (s, C=C-stretch); 1469 (m, C=C-stretch); 1378 (m, NO-stretch); 782 (m, CH-bending).

ESI-MS: *m/z* = 384.26 (M⁺+H⁺); 382.33 (M⁺-H⁺).

N-(4-bromo-3-methoxyphenyl)-6,8-dinitro-9H-pyrido[2,3-b]indol-4-amine (95)

Molecular formula: C₁₈H₁₂BrN₅O₅

Molecular weight: 458.22 g/mol

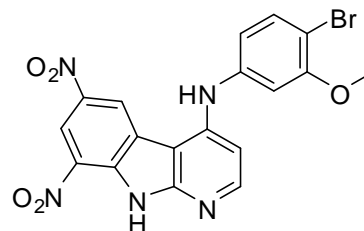
Melting point: 282-287 °C

R_f-value: [EE] 0.82

Yield: 245 mg (0.54 mmol, 63 %) yellow solid

Method of preparation:

250 mg (0.85 mmol, 1 eq.) of **86**, according to **GP-1**, is implemented with 1.717 g (8.5 mmol, 10 eq.) 3-methoxy-4-bromoaniline.



¹H-NMR: [400 MHz, DMSO-d₆] δ (ppm) = 3.63 (s, 3H, OCH₃); 6.77-6.96 (m, 3H, H-2', H-6' & H-3); 7.18 (d, *J* = 8.1 Hz, 1H, H-5'); 8.14 (dd, *J* = 12.3 Hz, *J* = 5.7 Hz, 1H, H-2); 8.84 (d, *J* = 2.2 Hz, 1H, H-5); 9.05 (s, 1H, H-7); 9.22 (d, *J* = 2.2 Hz, 1H, Aniline-NH); 12.95 (s, 1H, H-9).

¹³C-NMR: [400 MHz, DMSO-d₆] δ (ppm) = 55.2 (p, OCH₃); 102.4 (t, C-3); 104.0 (q, C-4a); 107.1 (t, C-2'); 108.4 (t, C-6'); 109.8 (q, C-8); 114.9 (q, C-4'); 115.6 (t, C-5); 116.4 (q, C-4b); 122.1 (q, C-6); 124.6 (t, C-7); 130.5 (t, C-5'); 133.2 (q, C-8a); 138.9 (q, C-1'); 141.3 (q, C-4); 147.7 (t, C-2); 156.1 (q, C-9a); 160.2 (q, C-3').

IR: (ATR) ν (cm⁻¹) = 3413 (br, NH-stretch); 1707 (w, NH-bending); 1580 (s, C=C-stretch); 1527 (s, NO-stretch); 1504 (m, C=C-stretch); 1465 (m, C=C-stretch); 1379 (m, NO-stretch); 779 (m, CH-bending).

ESI-MS: *m/z* = 458.21 (M⁺); 456.24 (M⁺-H⁺).

N-(3-(benzyloxy)phenyl)-6,8-dinitro-9H-pyrido[2,3-b]indol-4-amine (96)

Molecular formula: C₂₄H₁₇N₅O₅

Molecular weight: 455.42 g/mol

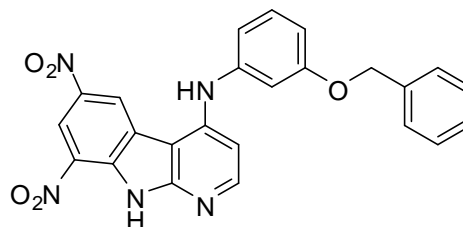
Melting point: 254-259 °C

R_f-value: [EE] 0.88

Yield: 310 mg (0.68 mmol, 80 %) yellow solid

Method of preparation:

250 mg (0.85 mmol, 1 eq.) of **86**, according to **GP-1**, is implemented with 1.694 g (8.5 mmol, 10 eq.) 3-benzyloxyaniline.



¹H-NMR: [400 MHz, DMSO-d₆] δ (ppm) = 5.12 (s, 2H, O-CH₂-C₆H₅); 6.84 (dd, *J* = 8.5 Hz, *J* = 3.6 Hz, 2H, H-2', H-4'); 6.94-6.97 (m, 2H, H-3, H-6'); 7.31-7.42 (m, 6H, O-CH₂-C₆H₅, H-5'); 8.25 (d, *J* = 5.8 Hz, 1H, H-2); 8.97 (d, *J* = 2.0 Hz, 1H, H-5); 9.19 (s, 1H, H-7); 9.32 (s, 1H, Aniline-NH); 13.08 (s, 1H, H-9).

¹³C-NMR: [100 MHz, DMSO-d₆] δ (ppm) = 69.2 (s, OCH₂); 102.5 (t, C-3); 104.1 (q, C-4a); 109.1 (t, C-2'); 109.5 (t, C-6'); 110.9 (q, C-8); 115.0 (t, C-4'); 116.4 (t, C-5); 123.1 (q, C-4b); 124.6 (q, C-6); 127.5-128.4 (t, 5x C-Bnz.); 130.2 (t, C-7); 131.4 (t, C-5'); 136.9 (q, C-1''); 138.8 (q, C-8a); 141.4 (q, C-1'); 147.6 (q, C-4); 149.3 (t, C-2); 155.9 (q, C-9a); 159.2 (q, C-3').

IR: (ATR) ν (cm⁻¹) = 3419 (br, NH-stretch); 1584 (s, C=C-stretch); 1521 (m, NO-stretch); 1506 (m, C=C-stretch); 1468 (m, C=C-stretch); 1381 (s, NO-stretch); 784 (m, CH-bending).

ESI-MS: *m/z* = 456.19 (M⁺+H⁺); 454.35 (M⁺-H⁺).

Biological Part

Kinase Assay:

These compounds were studied in collaboration with the *ProQinase GmbH* Company (Freiburg, www.proqinase.com). A radiometric protein kinase assay (³³PanQinase[®] Activity Assay) was used for measuring the kinase activity of the two protein kinases (Brk and HER2). All kinase assays were performed in 96-well FlashPlates[™] from PerkinElmer (Boston, AM, USA) in a 50 µl reaction volume. The reaction cocktail was pipetted in four steps in the following order:

- 20 µl of assay buffer (standard buffer)
- 5 µl of ATP solution (in H₂O)
- 5 µl of test compound (in 10% DMSO)
- 10 µl of substrate/ 10 µl of enzyme solution (premixed)

The assay for all protein kinases contained 70 mM HEPES-NaOH pH 7.5, 3 mM MgCl₂, 3 mM MnCl₂, 3 µM Na-orthovanadate, 1.2 mM DTT, 50 µg/ml PEG₂₀₀₀₀, 1 µM ATP, [γ -³³P]-ATP (approx. 5 x 10⁵ cpm per well), protein kinase (variable amounts), and substrate (variable amounts).

The following amounts of enzyme and substrate were used per well:

#	Kinase	Kinase	Kinase	Kinase Conc.	Kinase Conc.	ATP Conc.	Substrate	Substrate	Substrate
	Name	ProQinase Lot	External/Vendor Lot	ng/50µl	nM*	µM	Name	Lot	µg/50µl
1	Brk	003		25	6.1	1.0	Poly(Glu, Tyr) 4:1	SIG_20K5903	0.125
2	HER2	012		25	5.3	1.0	Poly(Glu, Tyr) 4:1	SIG_20K5903	0.125

* Maximal molar enzyme assay concentrations, implying enzyme preparations exclusively containing 100% active enzyme

Table 3. Assay parameters for the tested protein kinases.

The reaction cocktails were incubated at 30 °C for 60 minutes. The reaction was stopped with 50 µl of 2 % (v/v) H₃PO₄, plates were aspirated and washed two times with 200 µl 0.9 % (w/v) NaCl. Incorporation of ³³P_i was determined with a microplate scintillation counter (Microbeta, Wallac). All assays were performed with a BeckmanCoulter/SAGIAN[™] Core System.

For determining the inhibitory activity of the protein kinases to tested compounds, the assay was performed in the presence of each test compound, in ten different concentrations range of 3 nM to 100 μ M, and the control, in the absence of tested compound which was taken as the “high control” whereas in absence of the kinase as “low control”. The difference between high and low control was taken as 100 % residual activity and was calculated according to equation 1.

$$\text{Res. Activity (\%)} = 100 \times \frac{\text{cpm of compound} - \text{low control}}{\text{high control} - \text{low control}}$$

Equation 1. Calculation of the percentage residual activity

The residual activities for each concentration and the compound IC₅₀ values (50 % inhibition concentration) were calculated using *Quattro Workflow V3.1.0* (Quattro Research GmbH, Munich, Germany; www.quattro-research.com). The fitting model for the IC₅₀ determinations was “Sigmoidal response (variable slope)” with parameters “top” fixed at 100 % and “bottom” at 0 %. The fitting method used was least-squares fit.

The IC₅₀ value is the concentration of the tested substance that inhibits half-maximal activity of the particular kinase, and is a measure of the strength of the inhibitory effect of the tested substance.

As a parameter for assay quality, the Z'-factor (Zhang et al., *J. Biomol. Screen.* 2:67-73, 1999) for the low and high controls of each assay plate was used. The Z'-factors for this project did not drop below 0.44 and were above 0.6 in most cases, indicating a good to an excellent assay quality.

The substances in this work were tested against the Brk and HER2 kinases. The determination of IC₅₀ values were performed *via* double measurements. IC₅₀ values represent the arithmetic mean of the two measurements values obtained for a single substance measurement in each case.

60-Cell-Line-Screenings:

The screening is a two-stage process, beginning with the evaluation of all compounds against the 60 cell lines at a single dose of 10^{-5} M. The output from the single dose screen is reported as a mean graph and is available for analysis by the COMPARE program. Compounds which exhibit significant growth inhibition are evaluated against the 60 cell panel at five concentration levels. The human tumor cell lines of the cancer screening panel are grown in RPMI 1640 medium containing 5 % fetal bovine serum and 2 mM L-glutamine. For a typical screening experiment, cells are inoculated into 96 well microtiter plates in 100 μ l at plating densities ranging from 5000 to 40,000 cells/well depending on the doubling time of individual cell lines. After cell inoculation, the microtiter plates are incubated at 37°C, 5% CO₂, 95% air and 100% relative humidity for 24 h prior to addition of experimental drugs. After 24 h, two plates of each cell line are fixed in situ with TCA, to represent a measurement of the cell population for each cell line at the time of drug addition (Tz). Experimental drugs are solubilized in dimethylsulfoxide at 400-fold the desired final maximum test concentration and stored frozen prior to use. At the time of drug addition, an aliquot of frozen concentrate is dissolved and diluted to twice the desired final maximum test concentration with complete medium containing 50 mg/ml gentamicin. Additional four, 10-fold or ½ log serial dilutions are made to provide a total of five drug concentrations plus control. Aliquots of 100 μ l of these different drug dilutions are added to the appropriate microtiter wells already containing 100 μ l of medium, resulting in the required final drug concentrations. Following drug addition, the plates are incubated for an additional 48 h at 37 °C, 5% CO₂, 95% air, and 100% relative humidity. For adherent cells, the assay is terminated by the addition of cold TCA. Cells are fixed in situ by the gentle addition of 50 μ l of cold 50 % (w/v) TCA (final concentration, 10% TCA) and incubated for 60 min at 4 °C. The supernatant is discarded, and the plates are washed five times with tap water and air dried. Sulforhodamine B (SRB) solution (100 μ l) at 0.4% (w/v) in 1% acetic acid is added to each well, and plates are incubated for 10 min at room temperature. After staining, unbound dye is removed by washing five times with 1% acetic acid and the plates are air dried. Bound stain is subsequently solubilized in 10 μ M trizma base, and the absorbance is read on an automated plate reader at a wavelength of 515 nm. For suspension cells, the methodology is the same except that the assay is terminated by fixing settled cells at the bottom of the wells by gently adding 50 μ l of 80% TCA (final concentration, 16% TCA). Using the seven absorbance measurements [time zero, (Tz), control growth, (C), and test growth in the presence of drug at the five concentration levels (Ti)], the percentage growth is

calculated at each of the drug concentrations levels. Percentage growth inhibition is calculated as:

$$\begin{array}{ll} [(Ti-Tz)/(C-Tz)] \times 100 & \text{for concentrations for which } Ti \geq Tz \\ [(Ti-Tz)/Tz] \times 100 & \text{for concentrations for which } Ti < Tz \end{array}$$

Three dose response parameters are calculated for each experimental agent. Growth inhibition of 50% (GI_{50}) is calculated from $[(Ti-Tz)/(C-Tz)] \times 100 = 50$, which is the drug concentration resulting in a 50% reduction in the net protein increase (as measured by SRB staining) in control cells during the drug incubation. The drug concentration resulting in total growth inhibition (TGI) is calculated from ($Ti = Tz$). The LC_{50} (concentration of drug resulting in a 50% reduction in the measured protein at the end of the drug treatment as compared to that at the beginning) indicating a net loss of cells following treatment is calculated from $[(Ti-Tz)/Tz] \times 100 = -50$. Values are calculated for each of these three parameters if the level of activity is reached; however, if the effect is not reached or is exceeded, the value for that parameter is expressed as greater or less than the maximum or minimum concentration tested.¹⁶⁹

Appendix

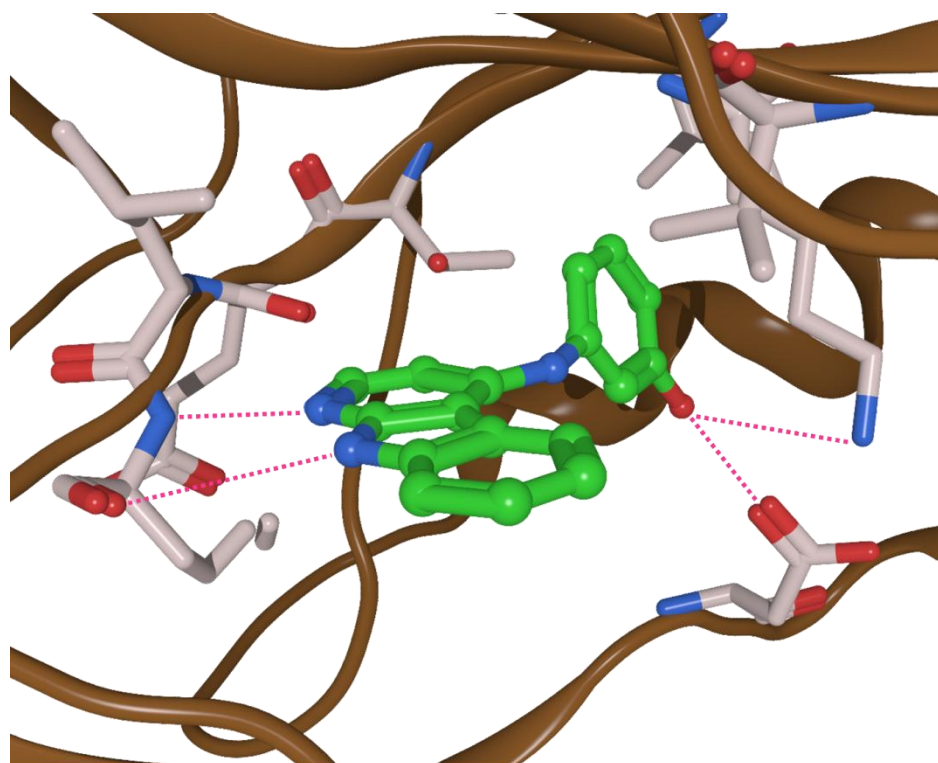


Fig. 79. Docking of the active *meta*-hydroxyaniline derivative (12) to Brk (active form). Hydrogen bonds are shown in magenta.

Results of the NCI 60-Cell-Line Screenings:

A) One-dose Screening data:

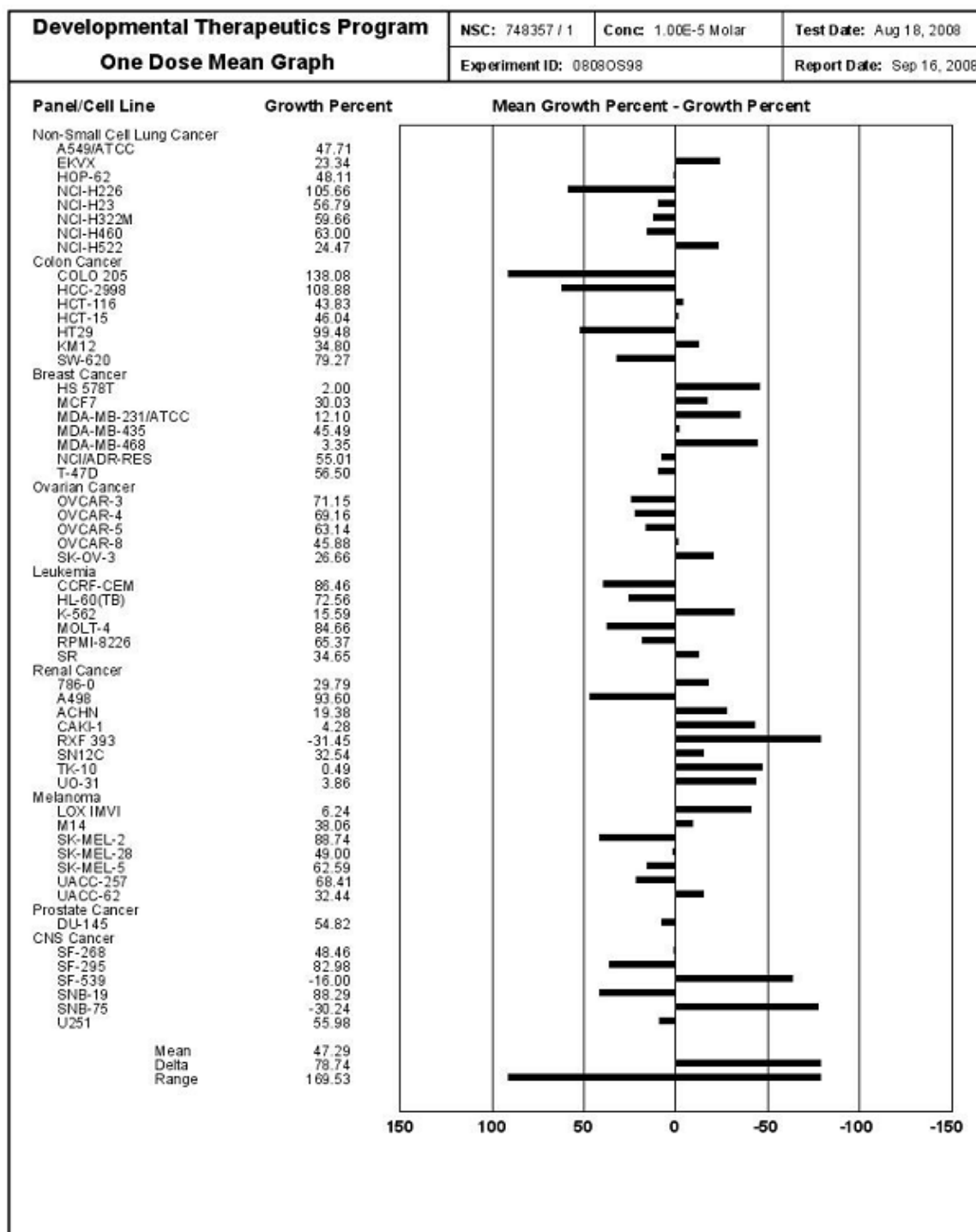


Fig. 80. Results of One-dose screenings of compound 12.

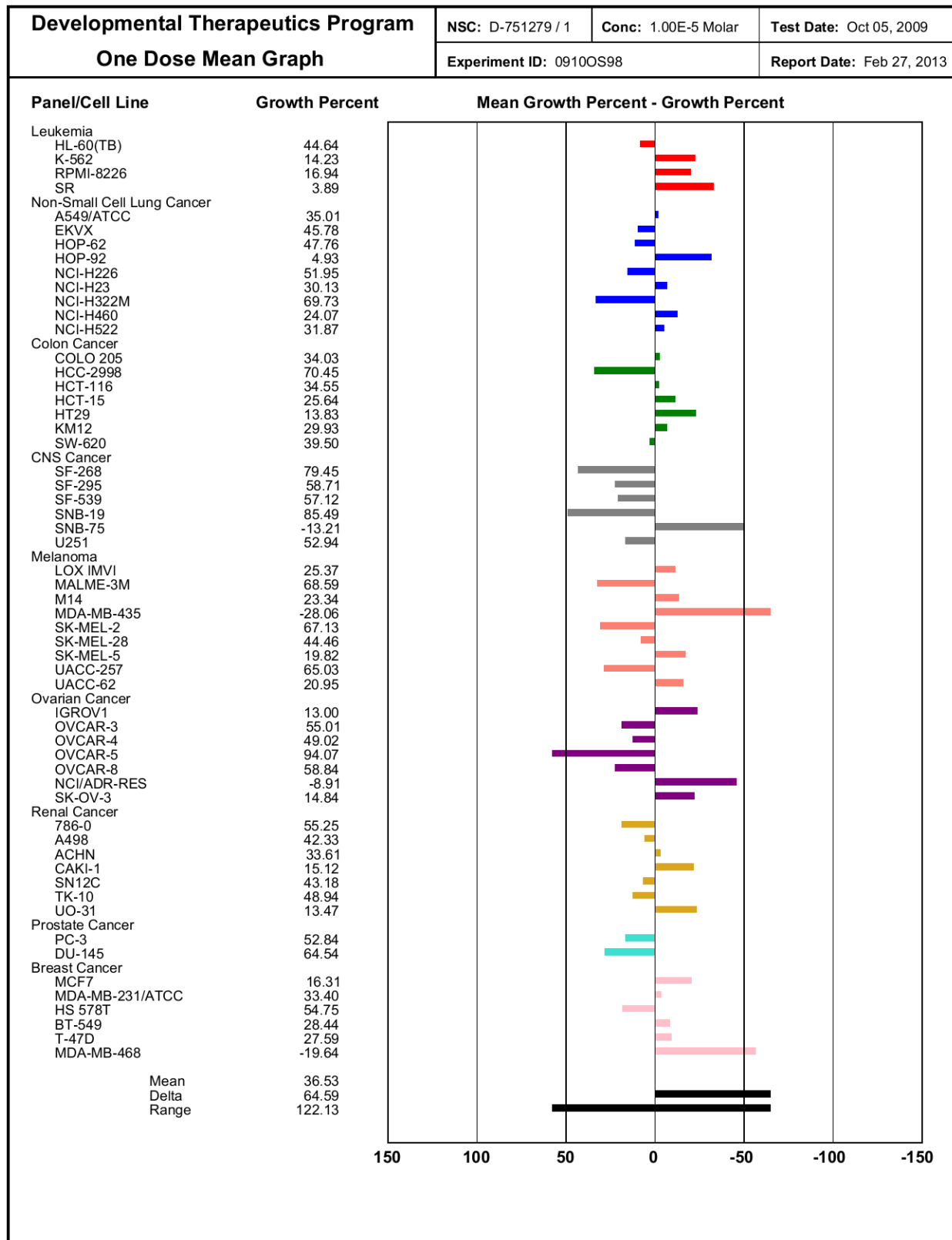


Fig. 81. Results of One-dose screenings of compound 13.

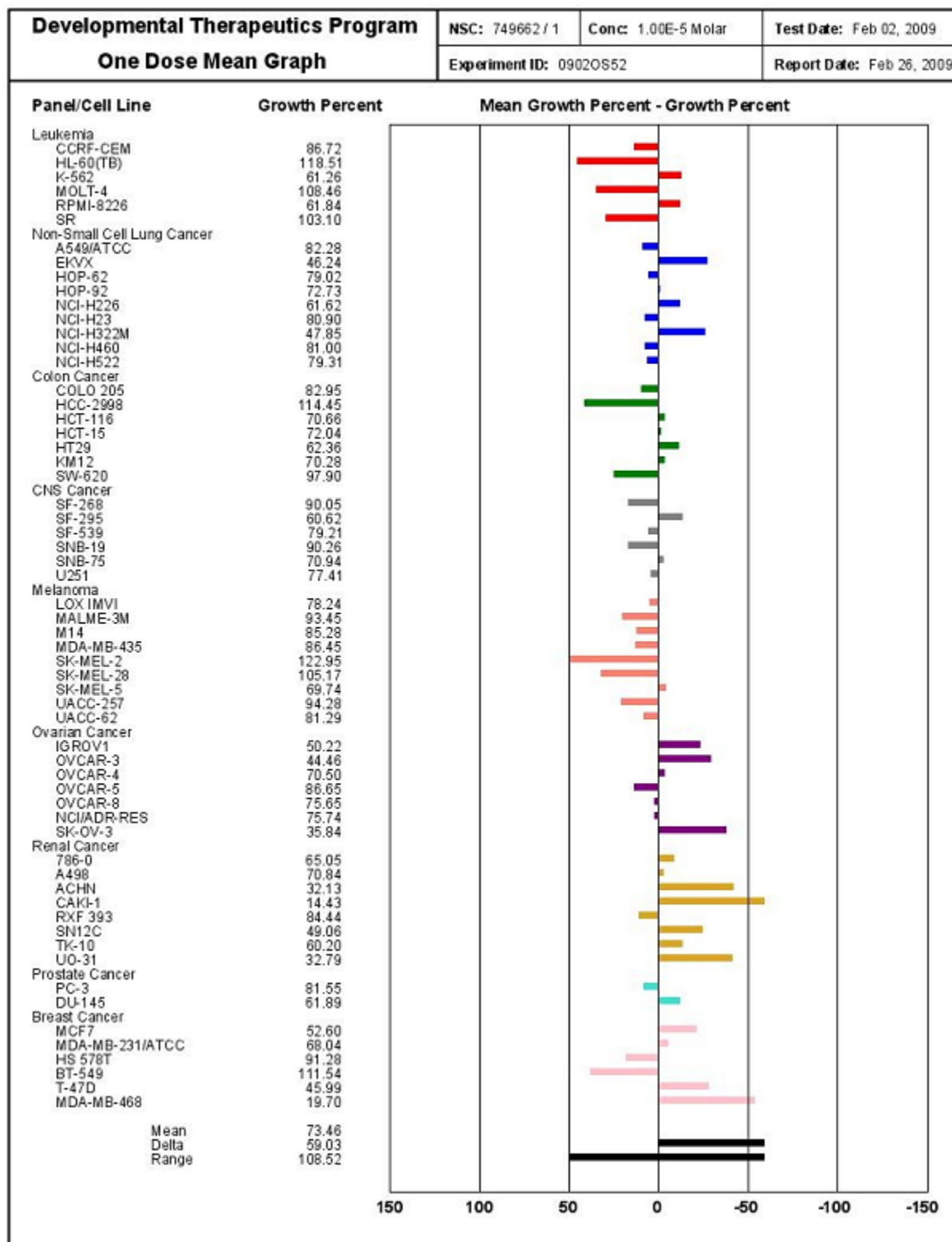


Fig. 82. Results of One-dose screenings of compound 15.

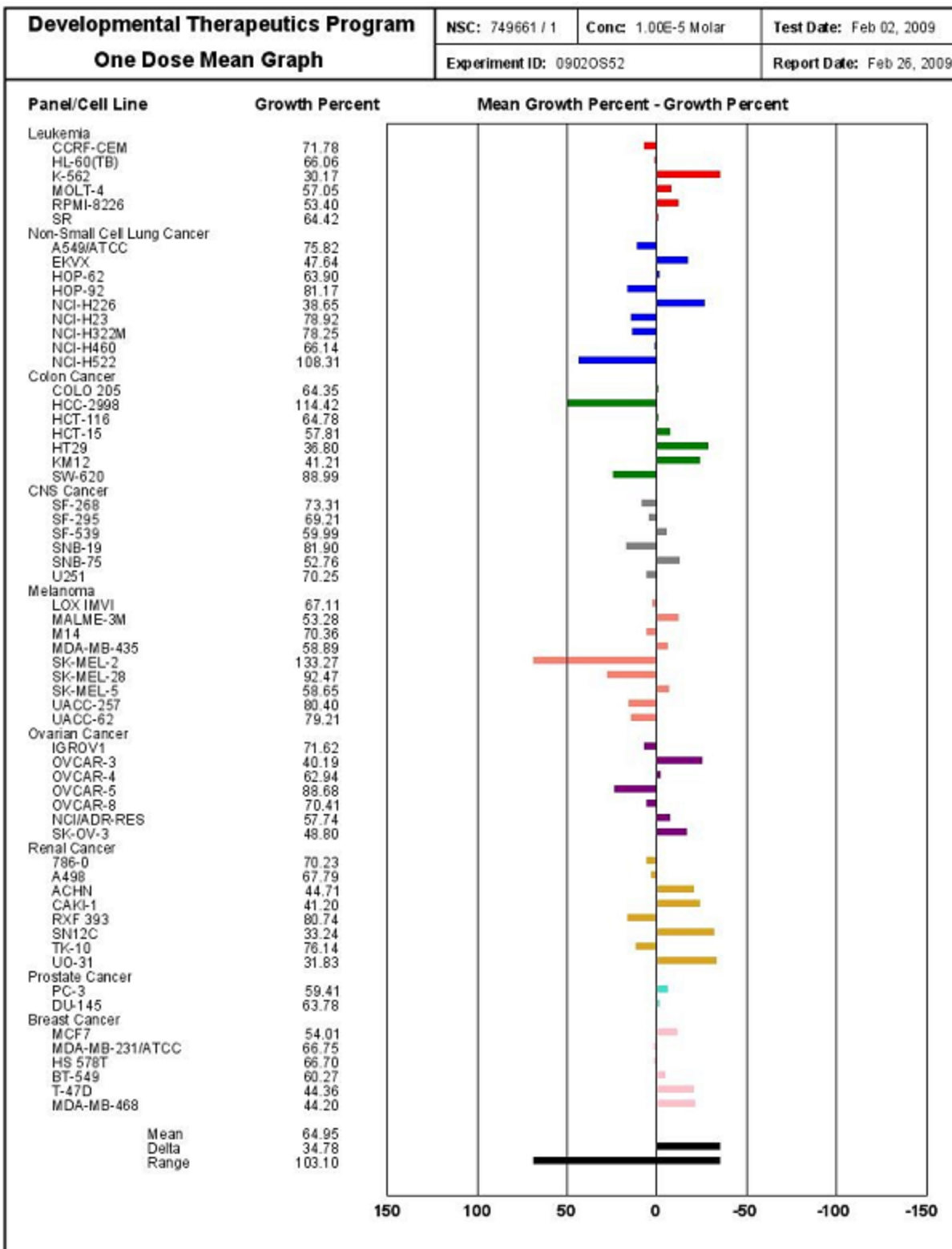


Fig. 83. Results of One-dose screenings of compound 20.

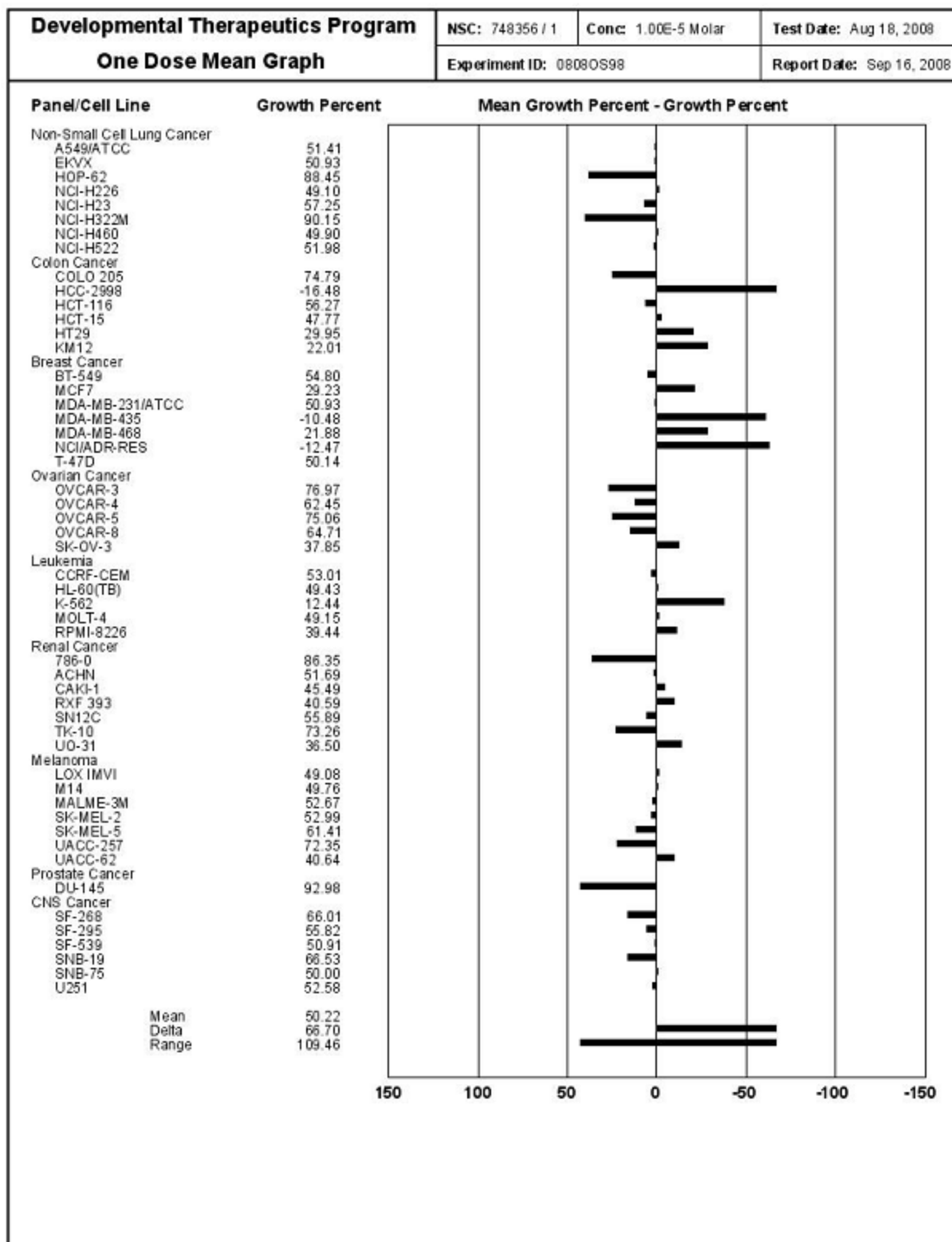


Fig. 84. Results of One-dose screenings of compound 21.

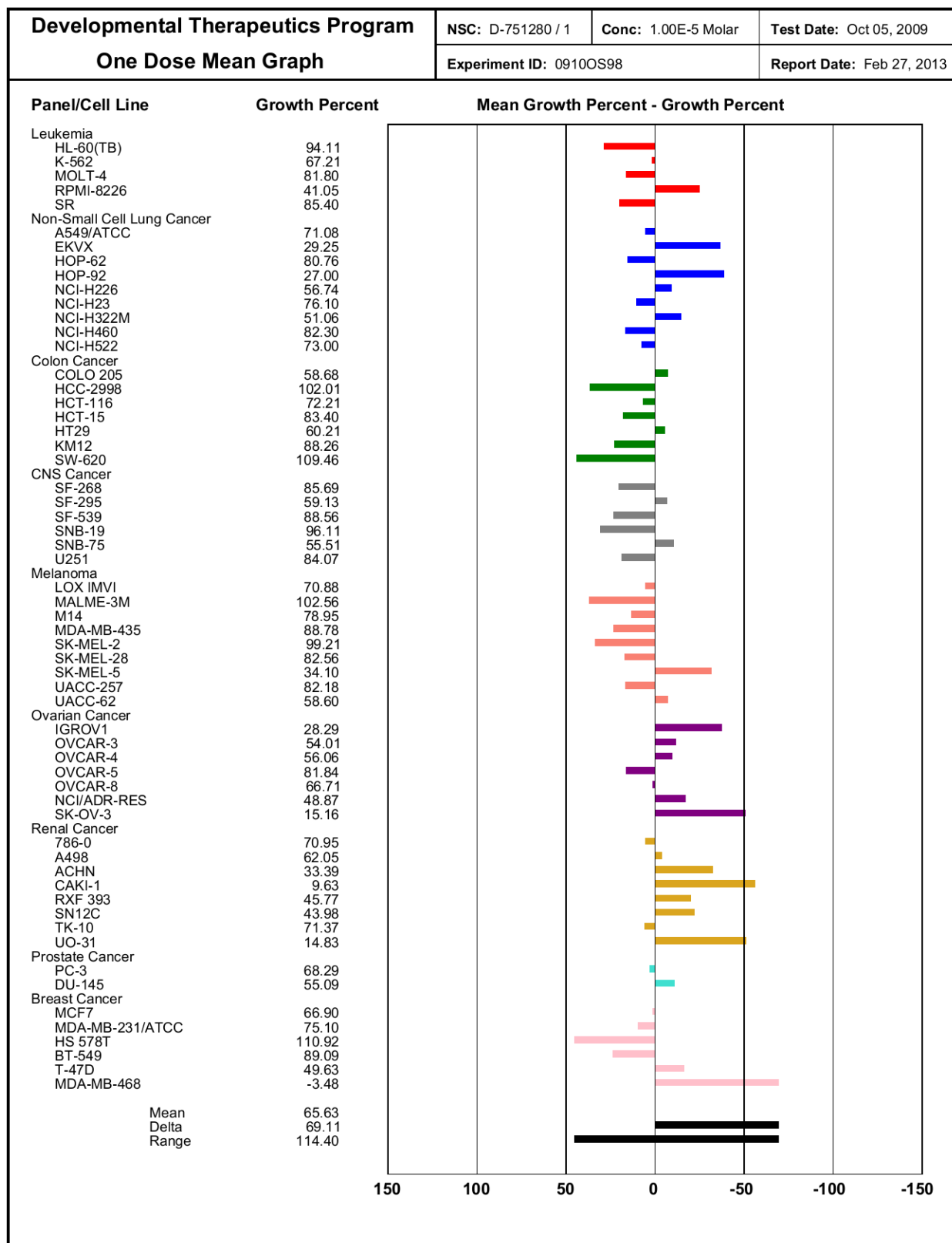


Fig. 85. Results of One-dose screenings of compound 24.

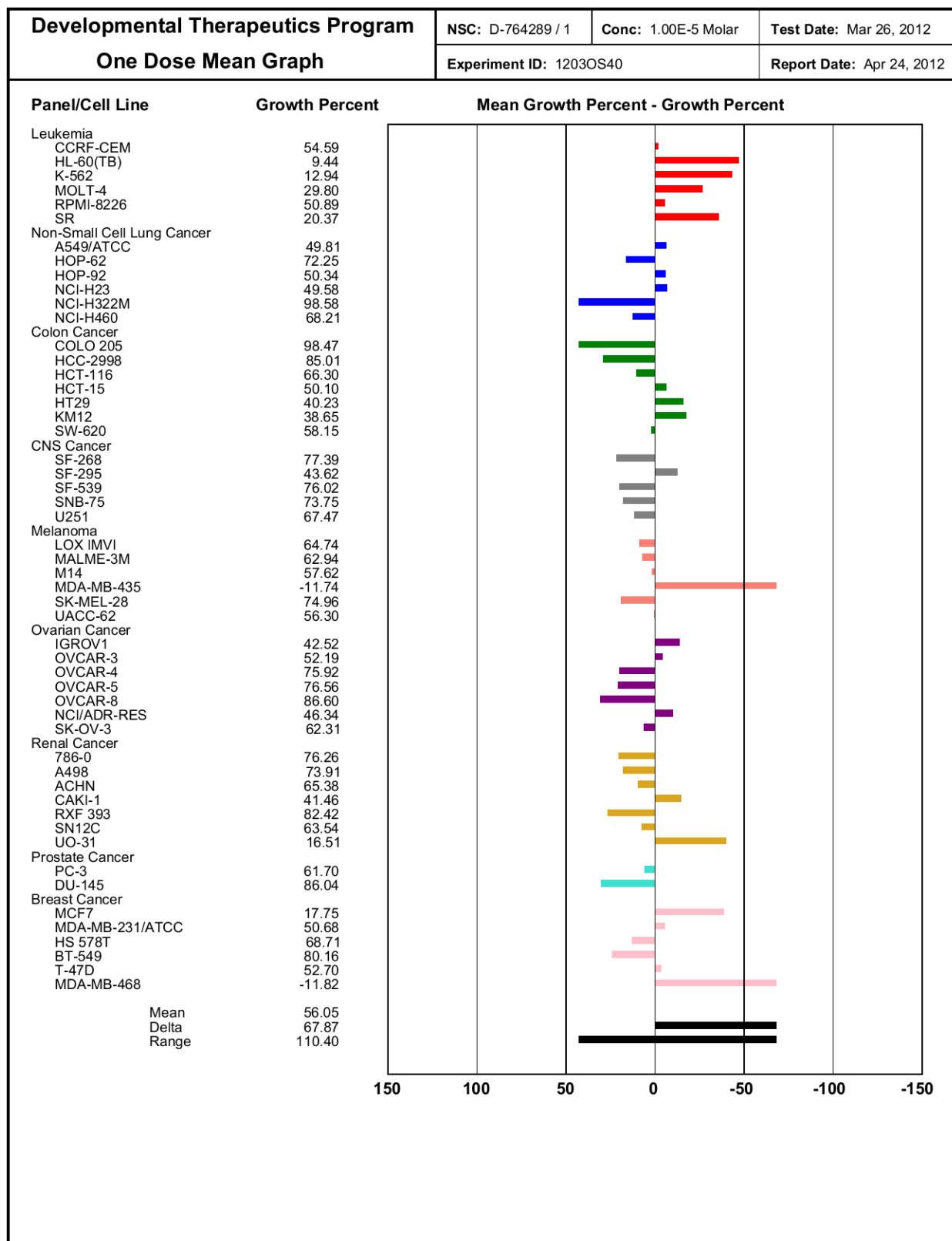


Fig. 86. Results of One-dose screenings of compound 27.

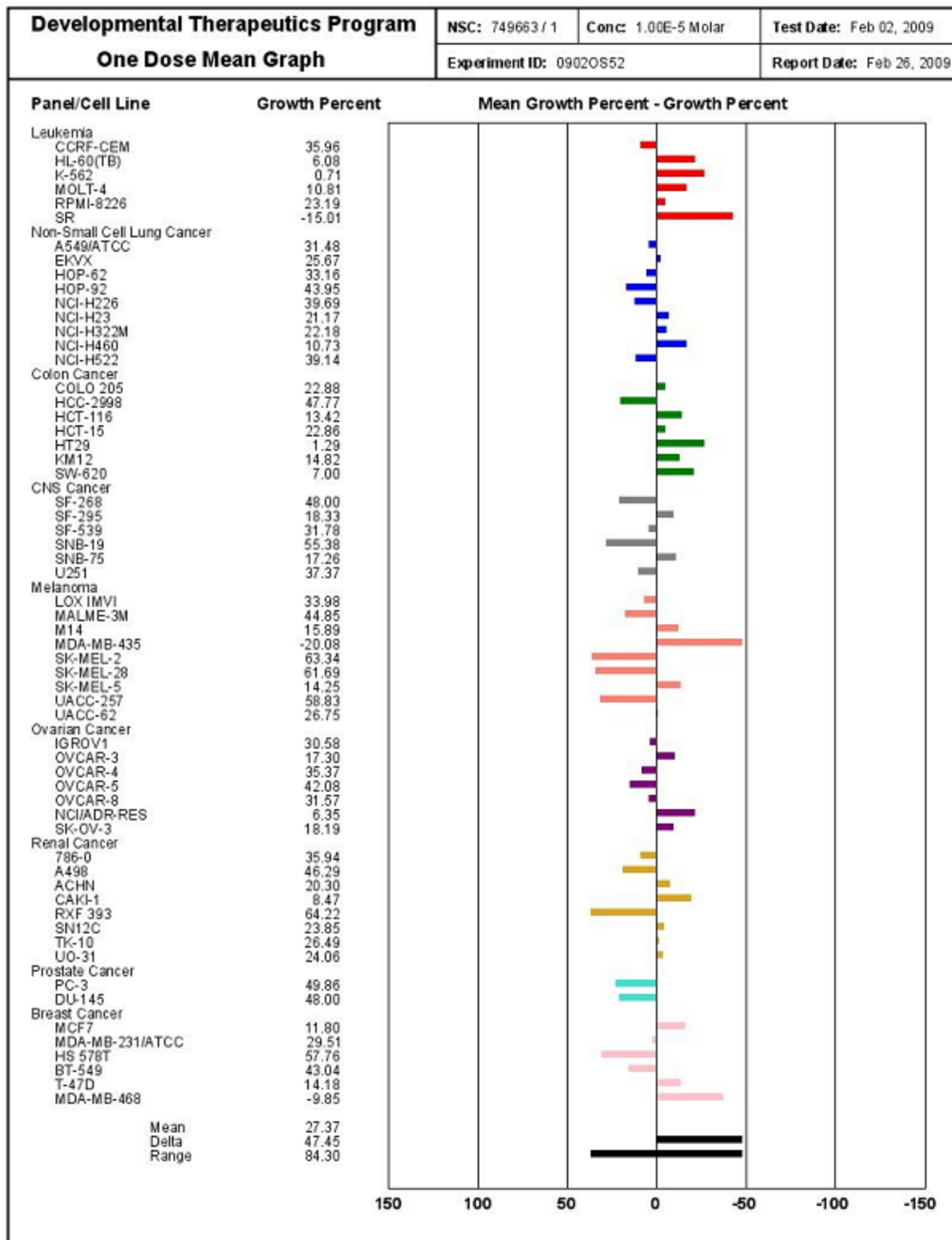


Fig. 87. Results of One-dose screenings of compound 28.

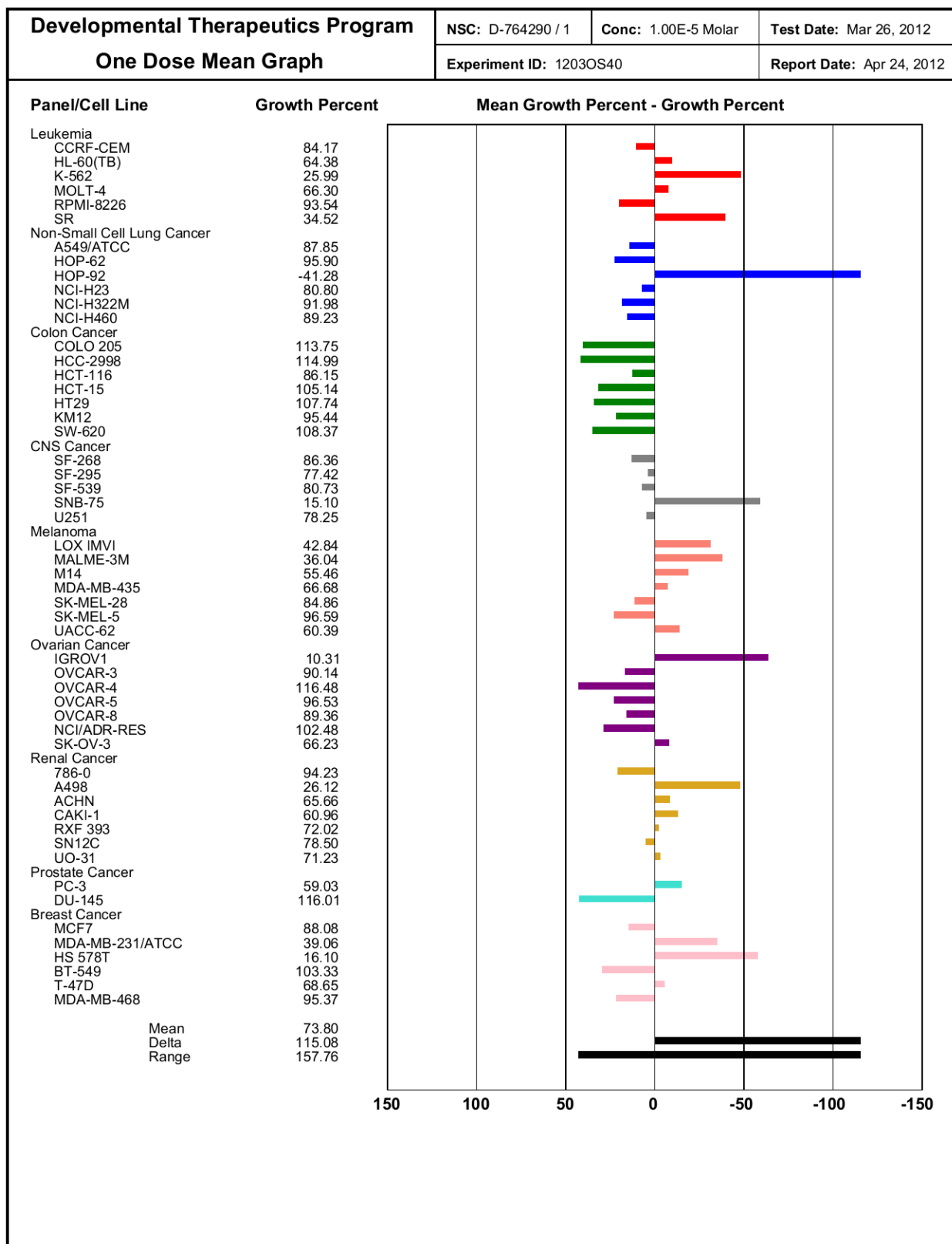


Fig. 88. Results of One-dose screenings of compound 37.

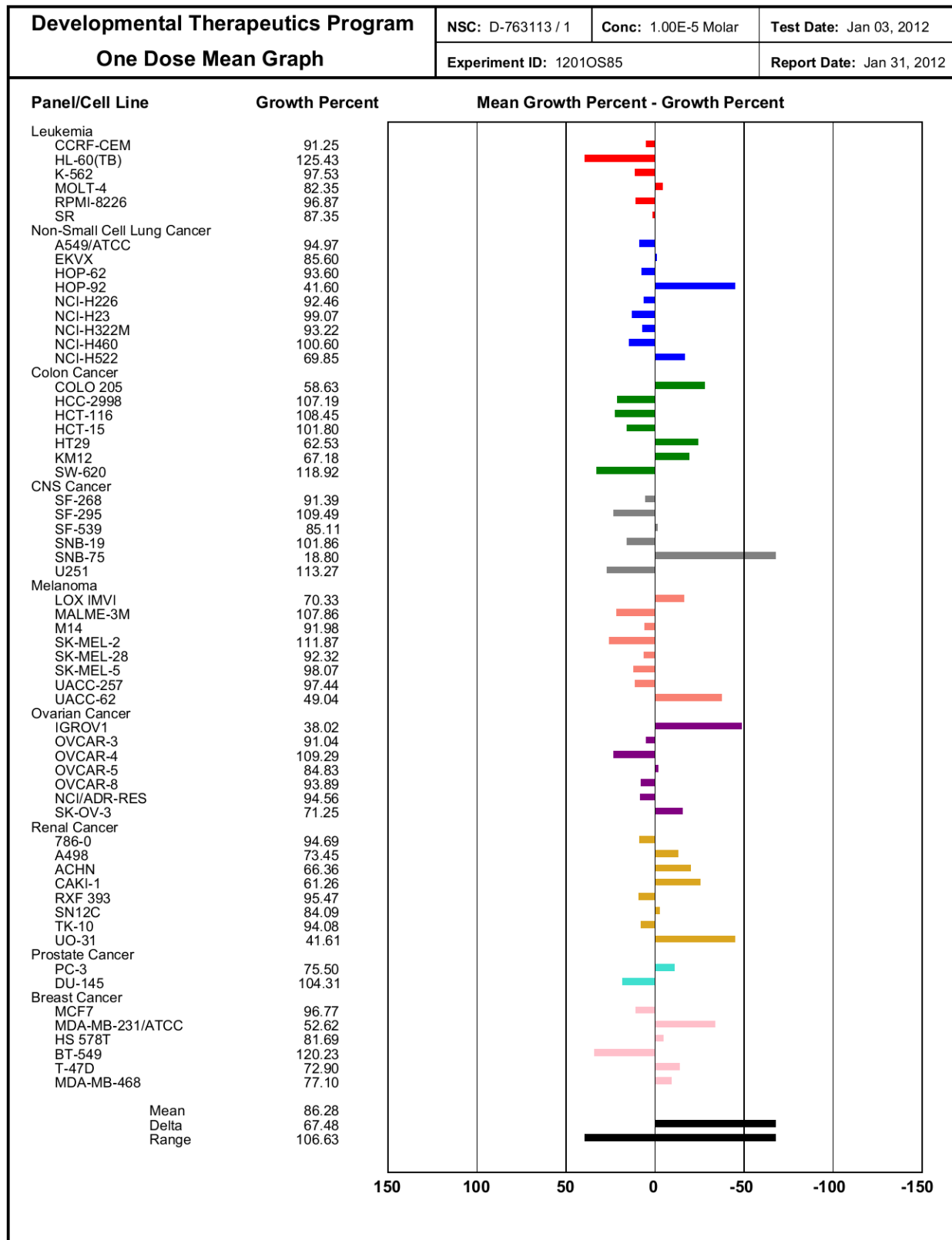


Fig. 89. Results of One-dose screenings of compound 38.

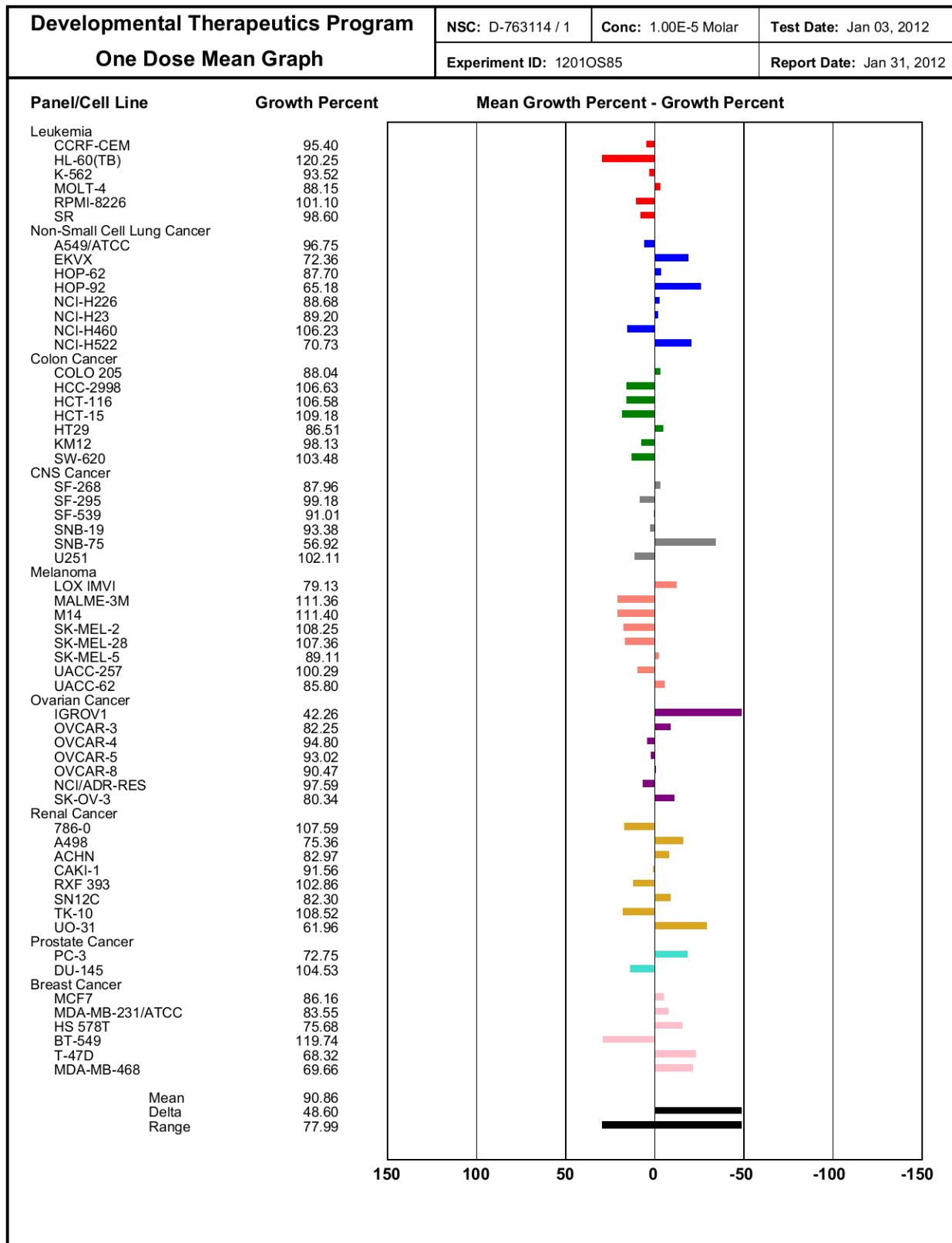


Fig. 90. Results of One-dose screenings of compound 42.

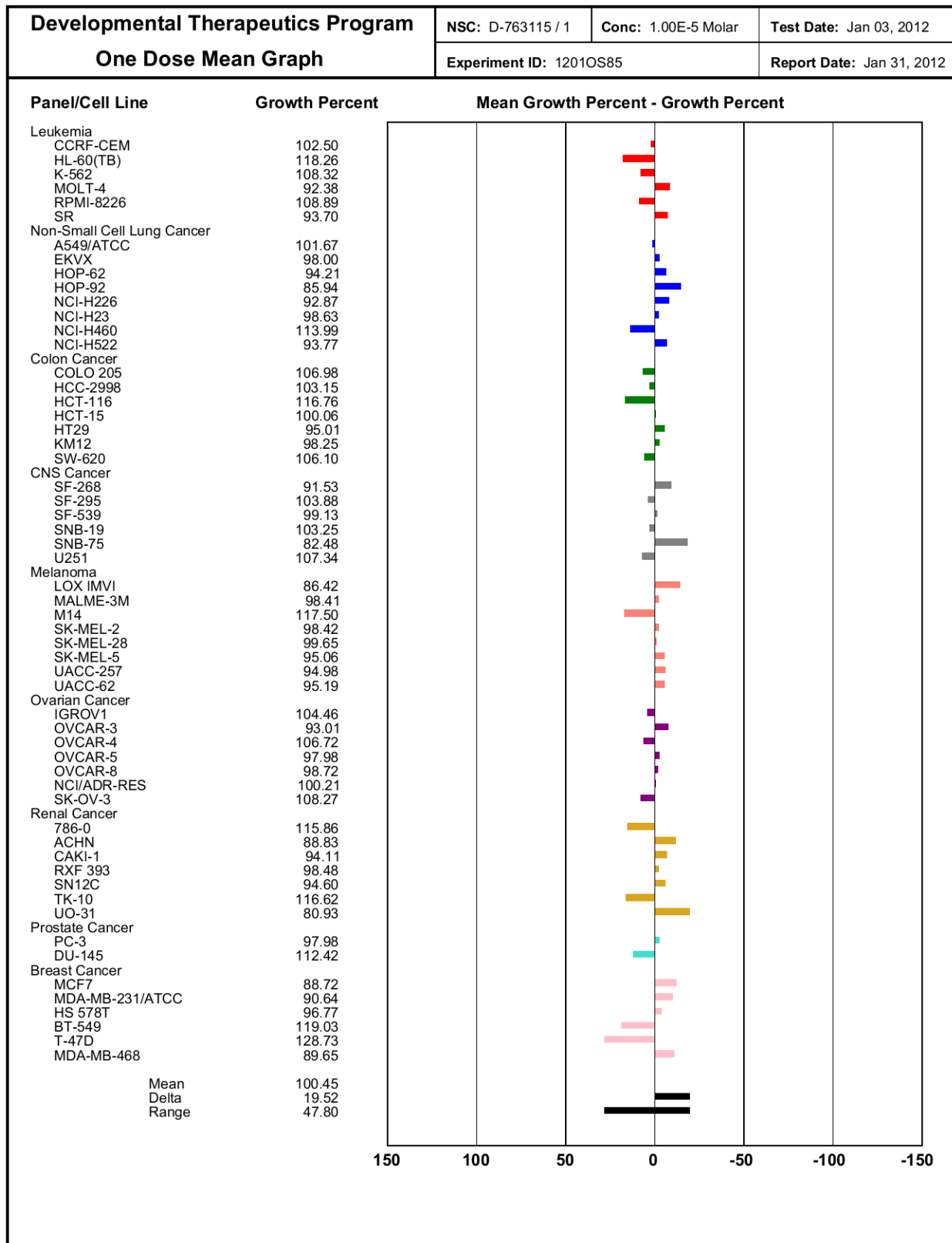


Fig. 91. Results of One-dose screenings of compound 43.

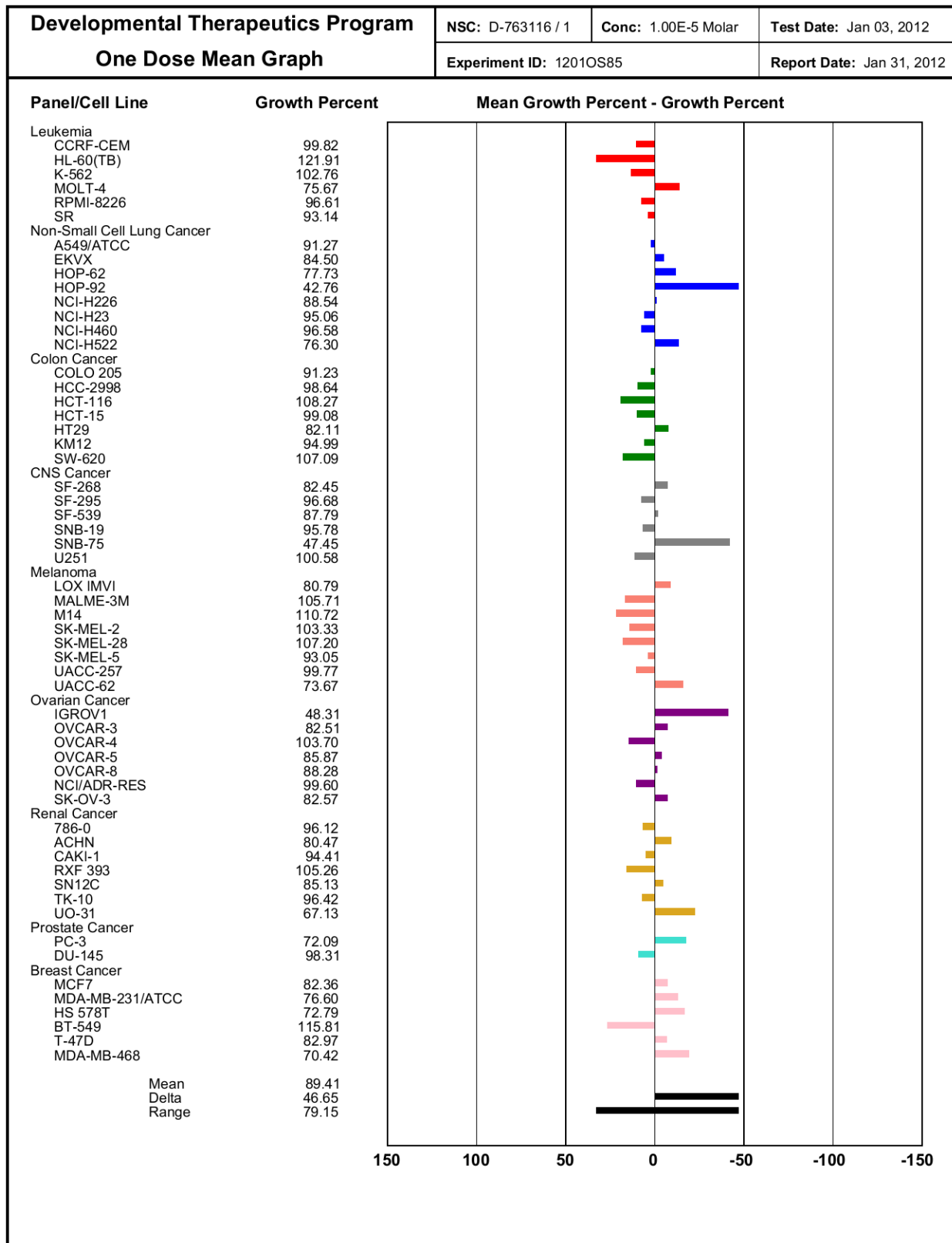


Fig. 92. Results of One-dose screenings of compound 44.

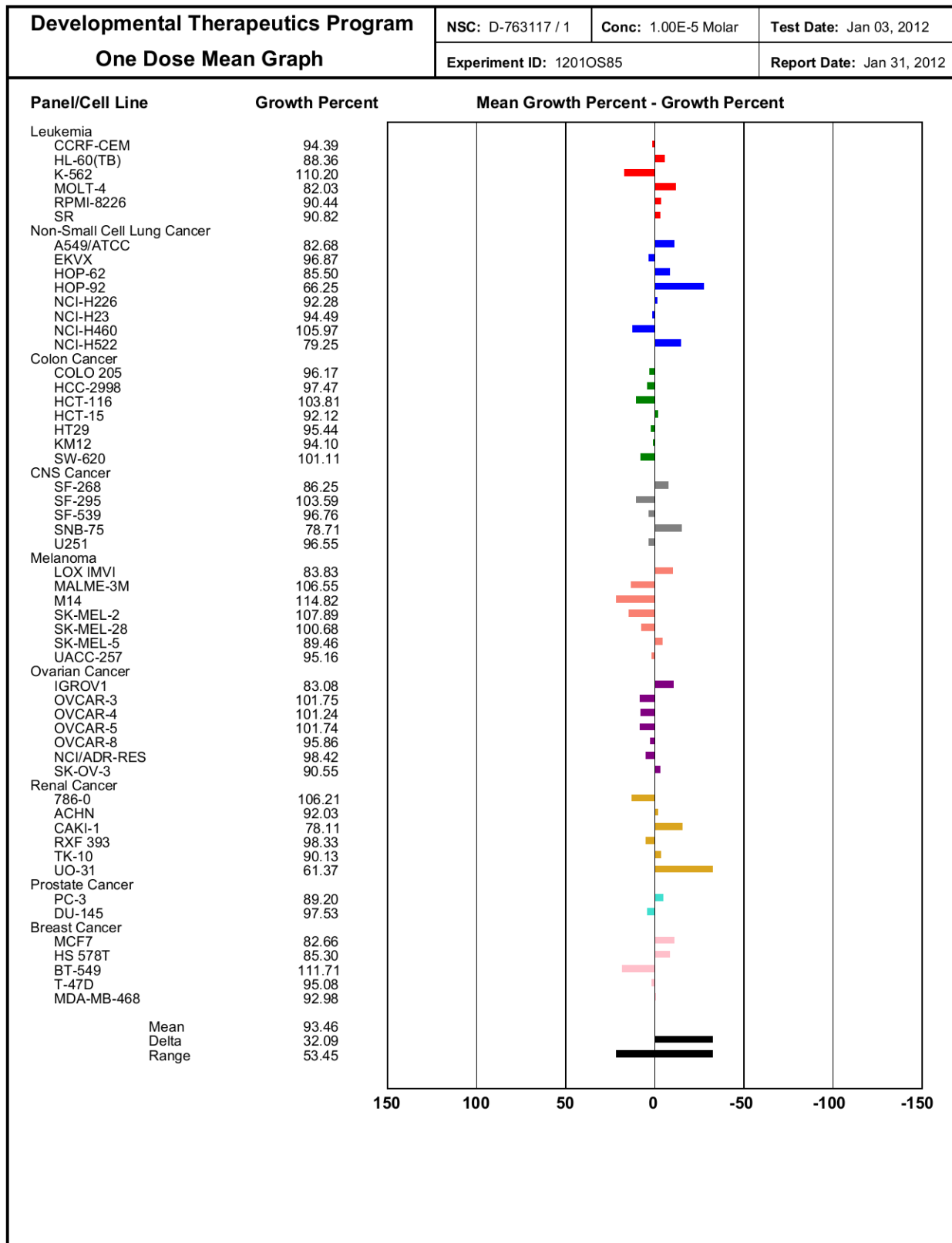


Fig. 93. Results of One-dose screenings of compound 45.

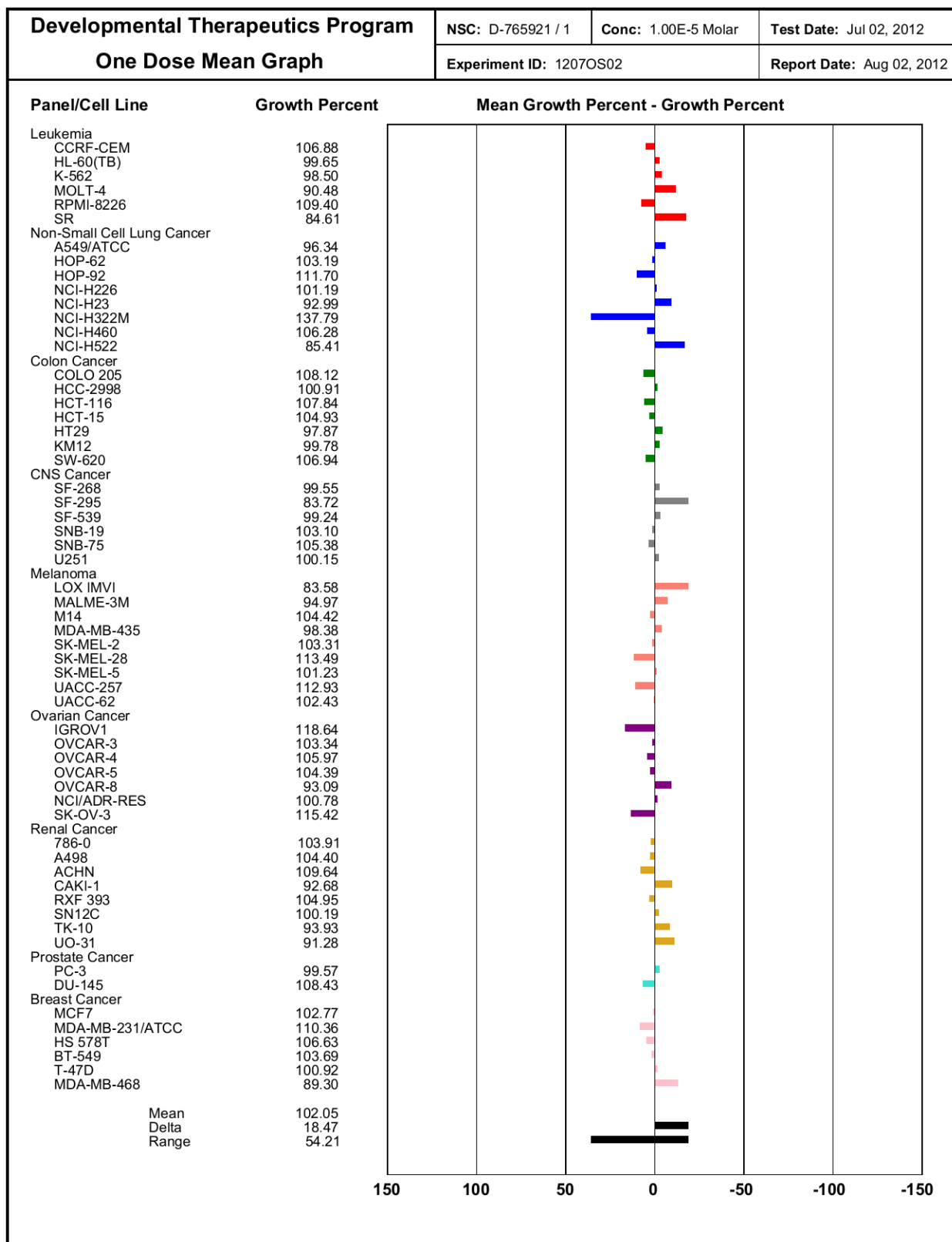


Fig. 94. Results of One-dose screenings of compound 59.

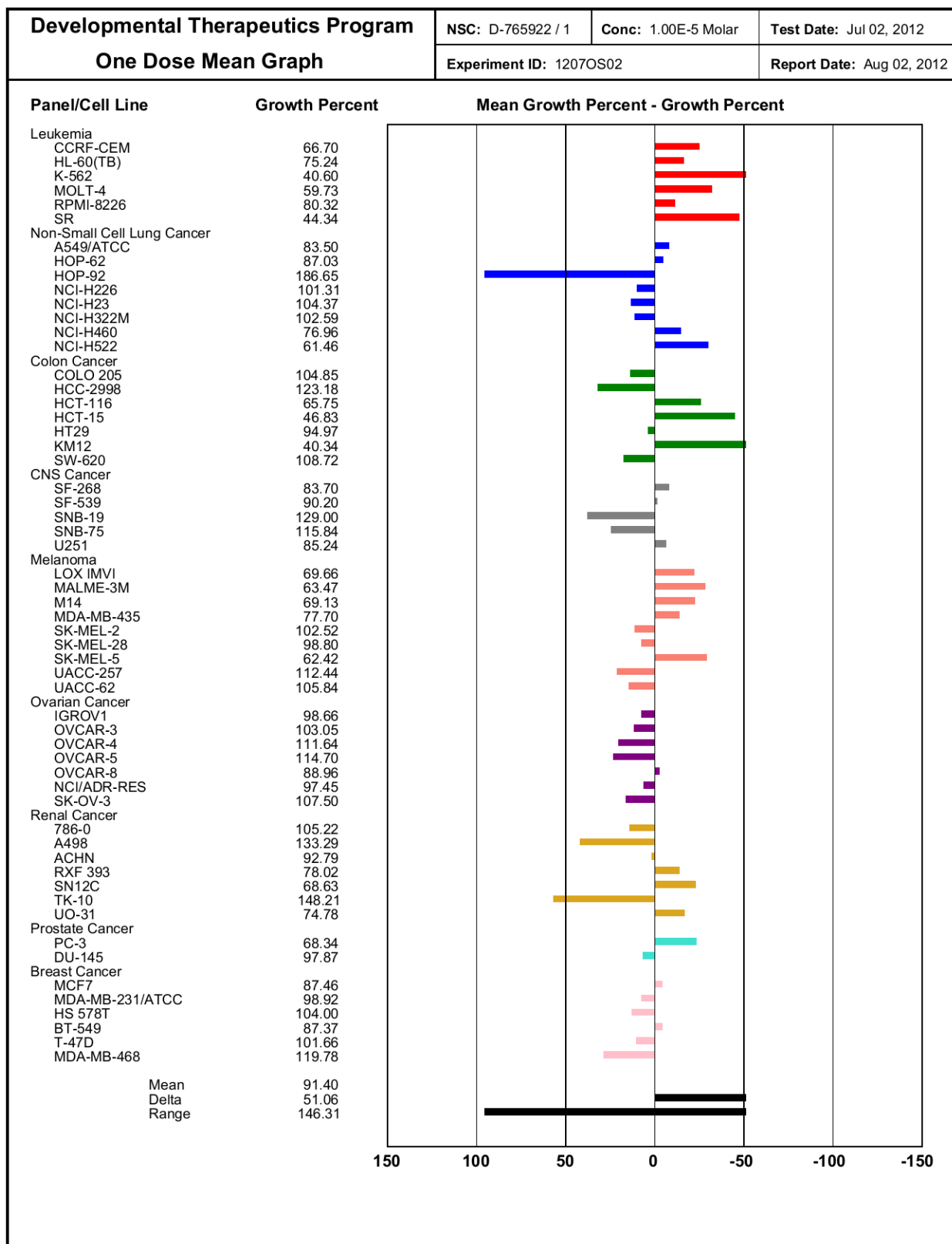


Fig. 95. Results of One-dose screenings of compound 60.

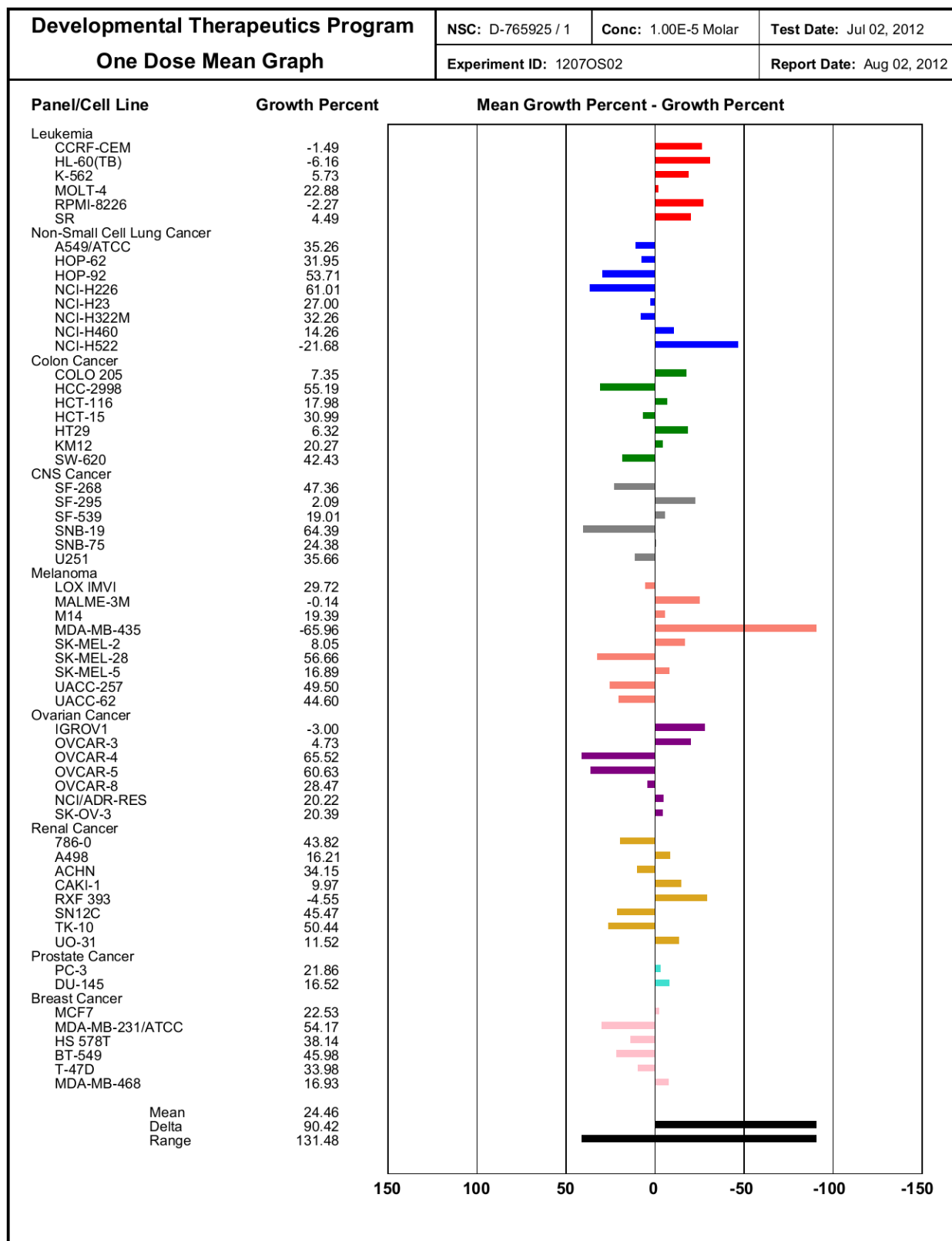


Fig. 96. Results of One-dose screenings of compound 70.

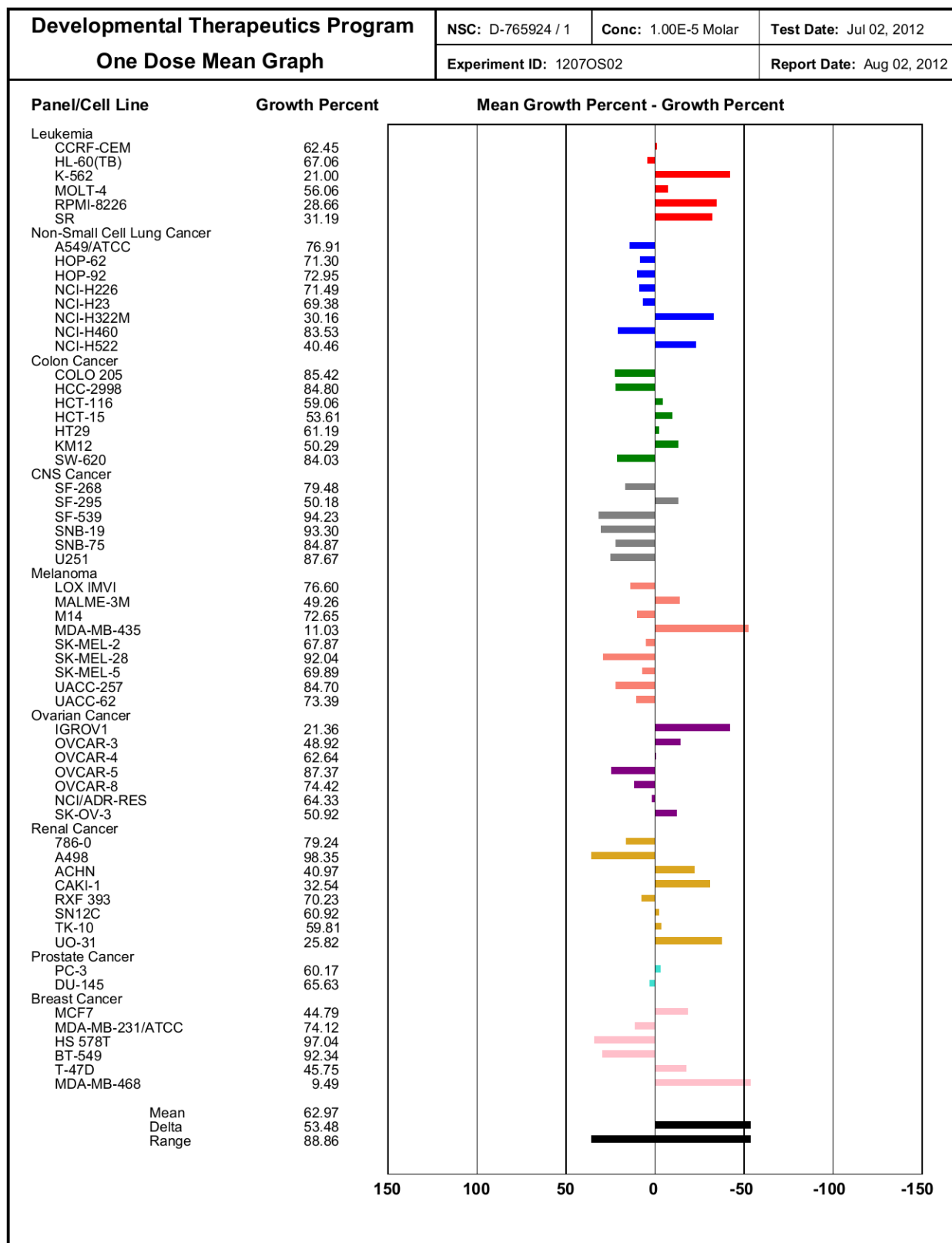


Fig. 97. Results of One-dose screenings of compound 71.

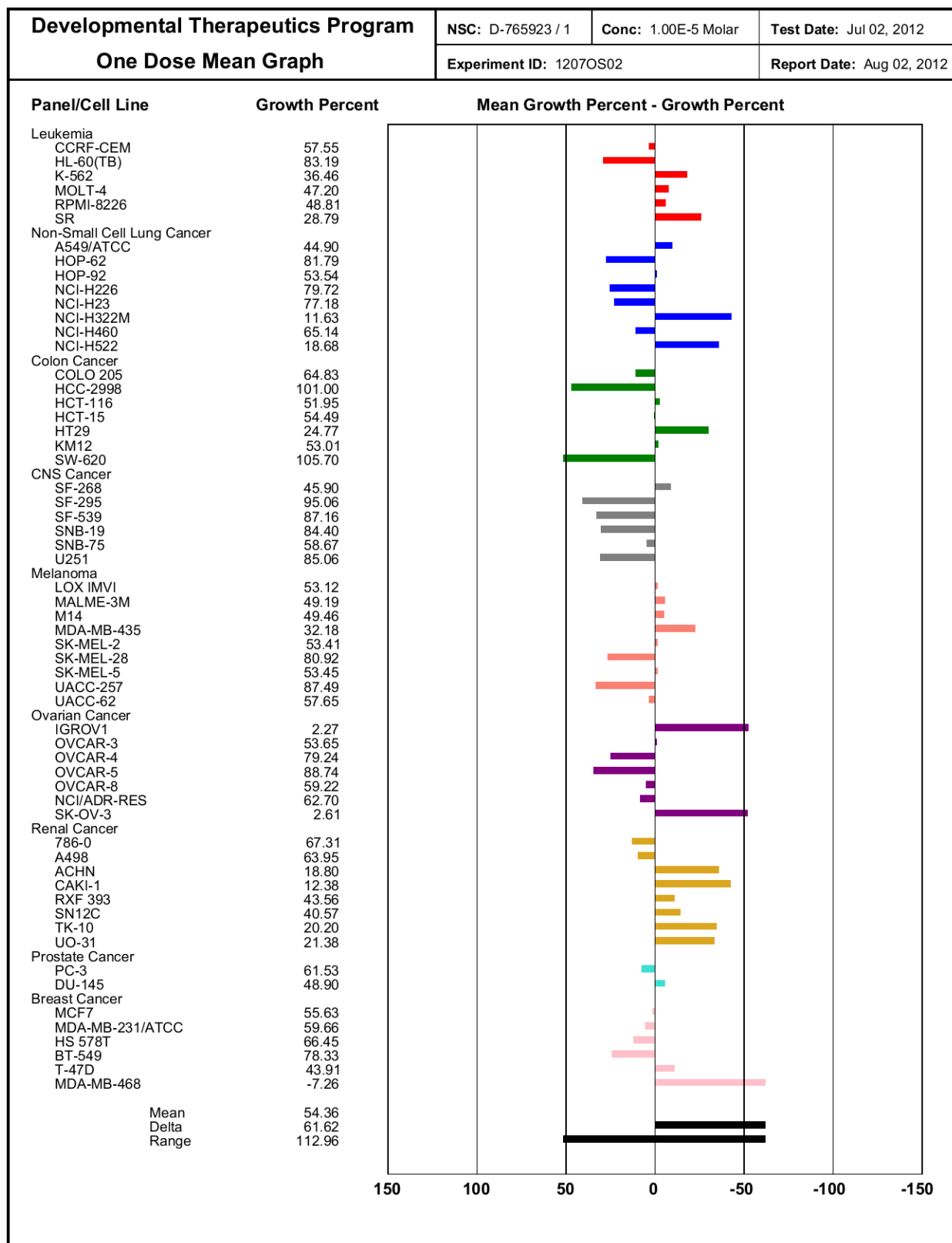


Fig. 98. Results of One-dose screenings of compound 73.

B) Five-dose Screenings data:

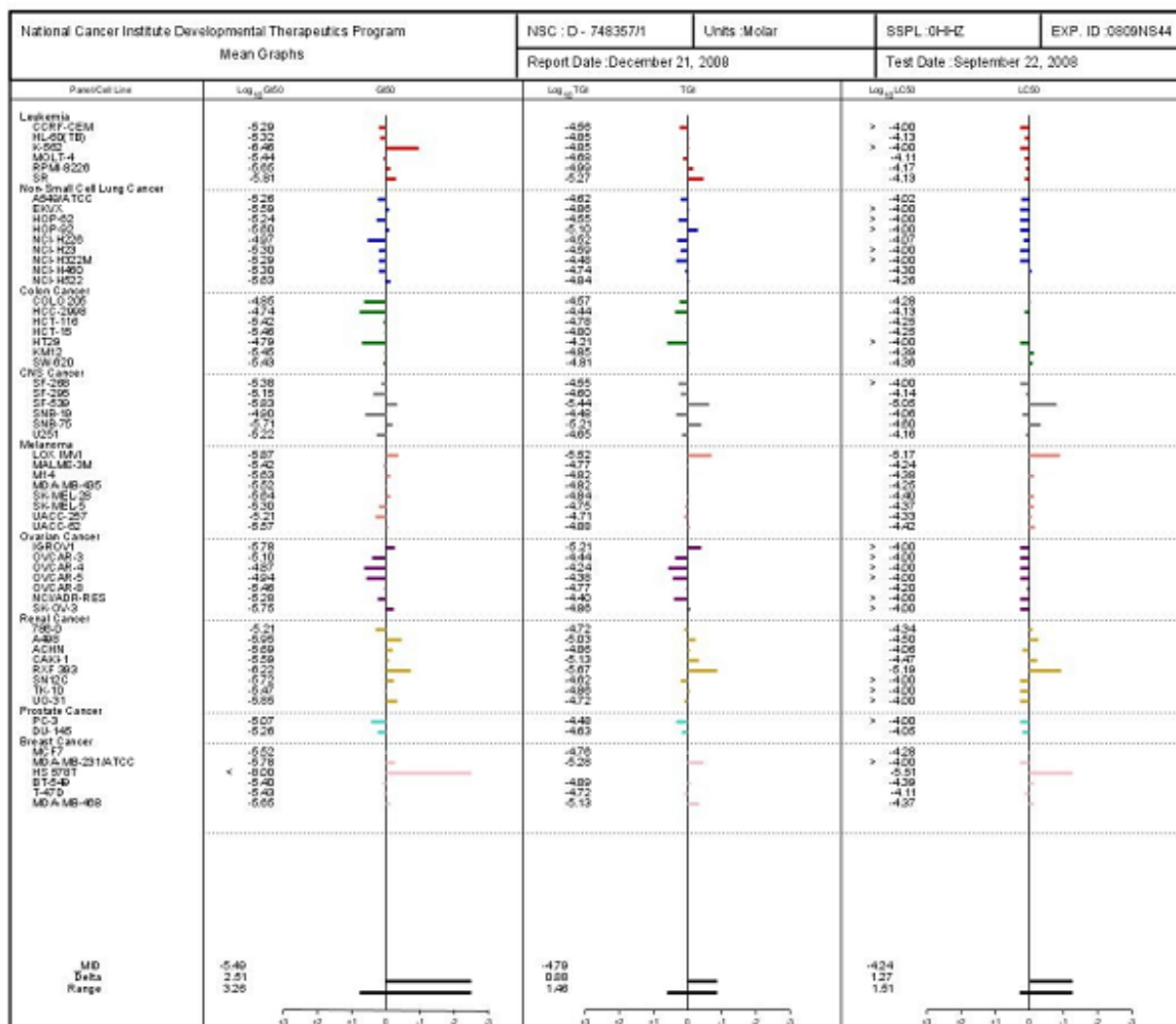


Fig. 99. Results of Five-dose screenings of compound 12 (first).

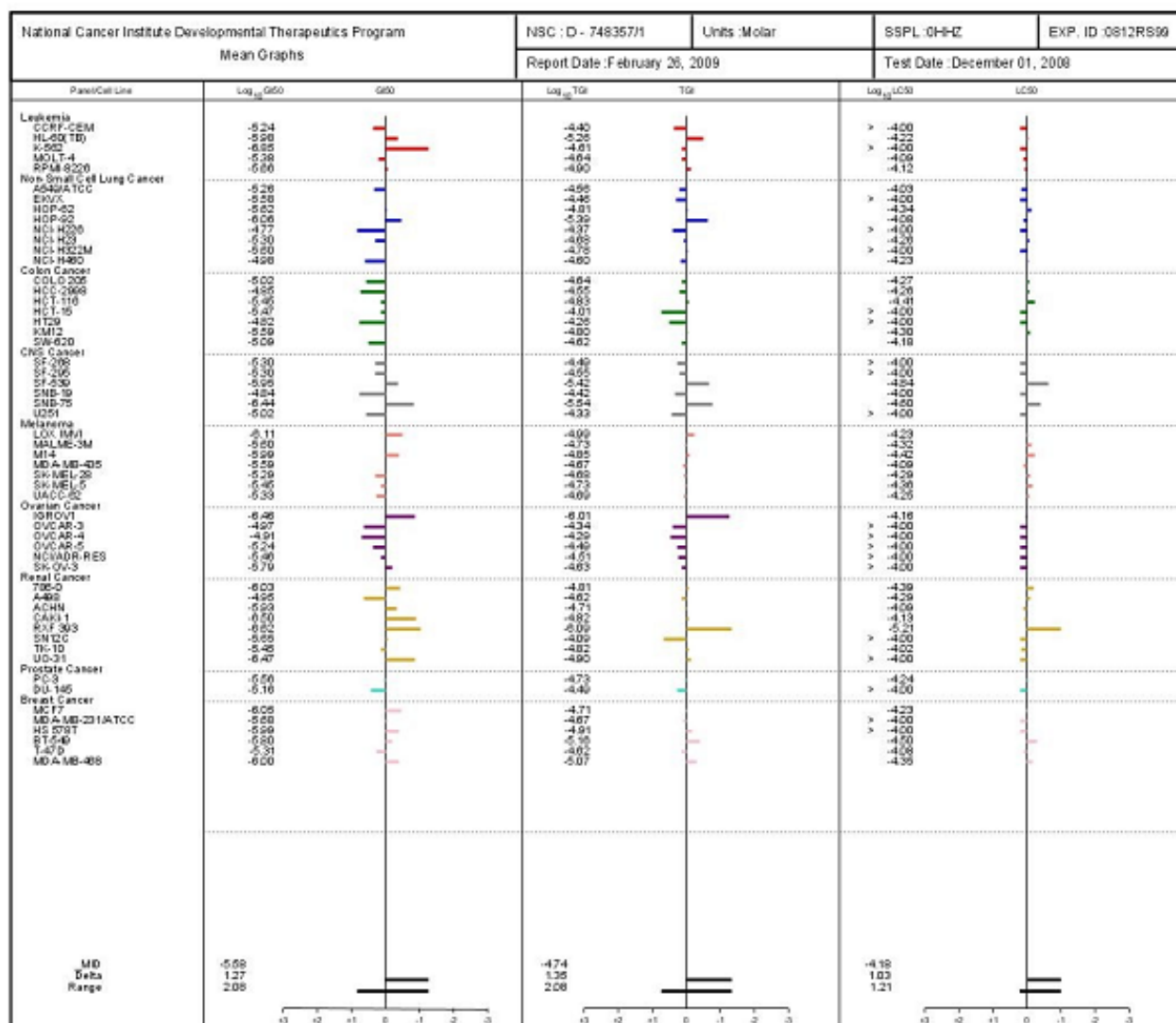


Fig. 100. Results of Five-dose screenings of compound 12 (second).

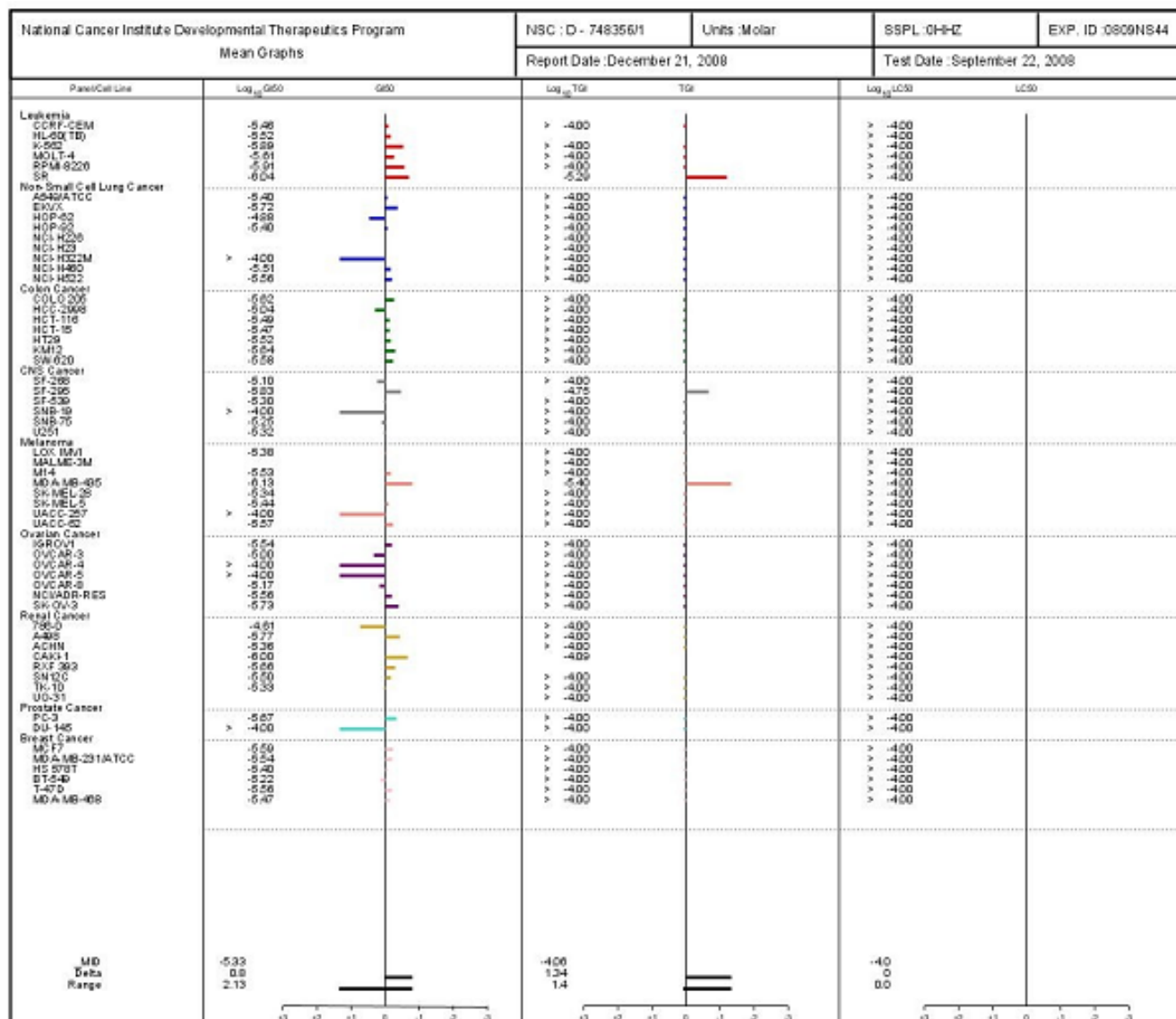


Fig. 101. Results of Five-dose screenings of compound 21.

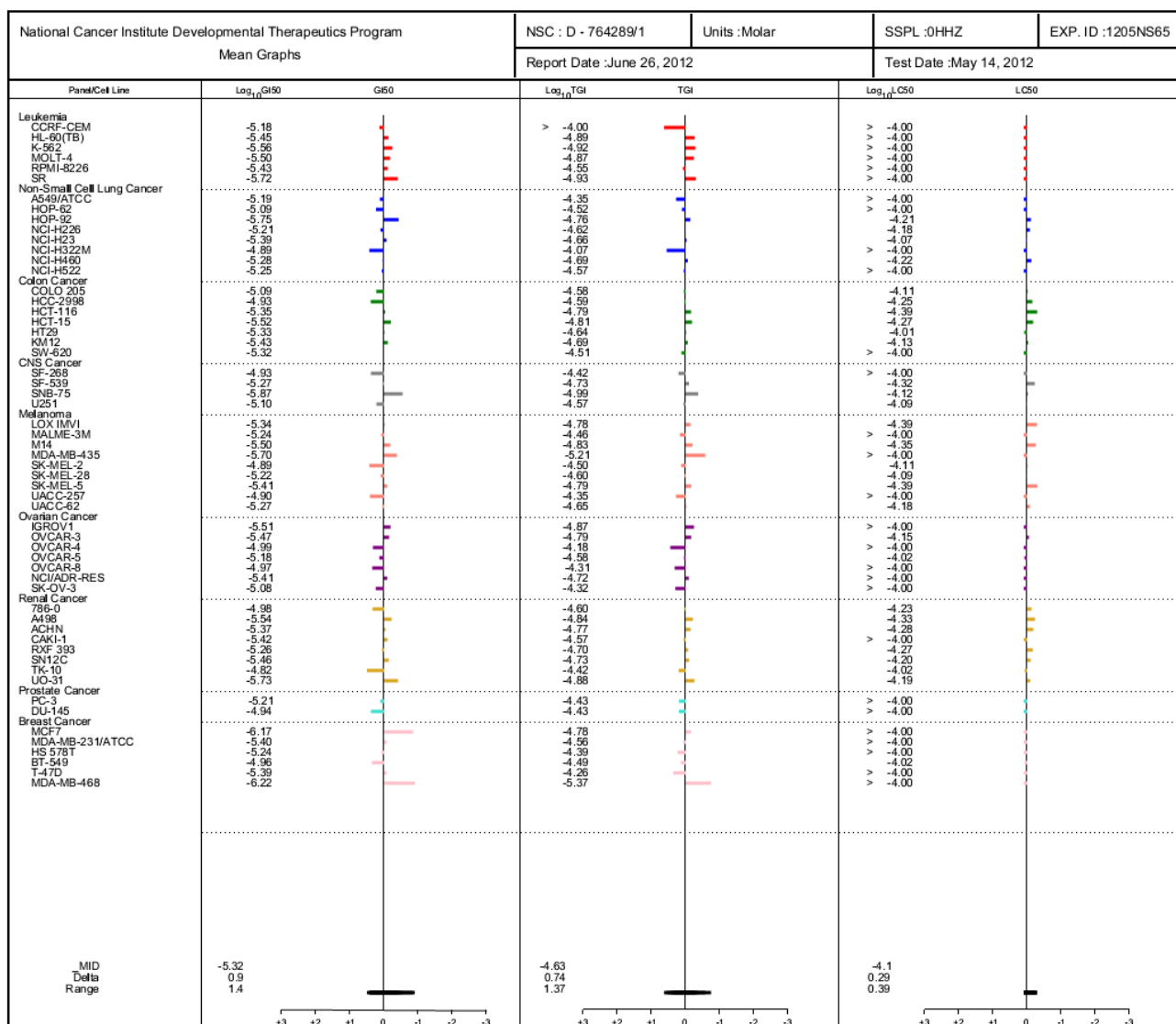


Fig. 102. Results of Five-dose screenings of compound 27.

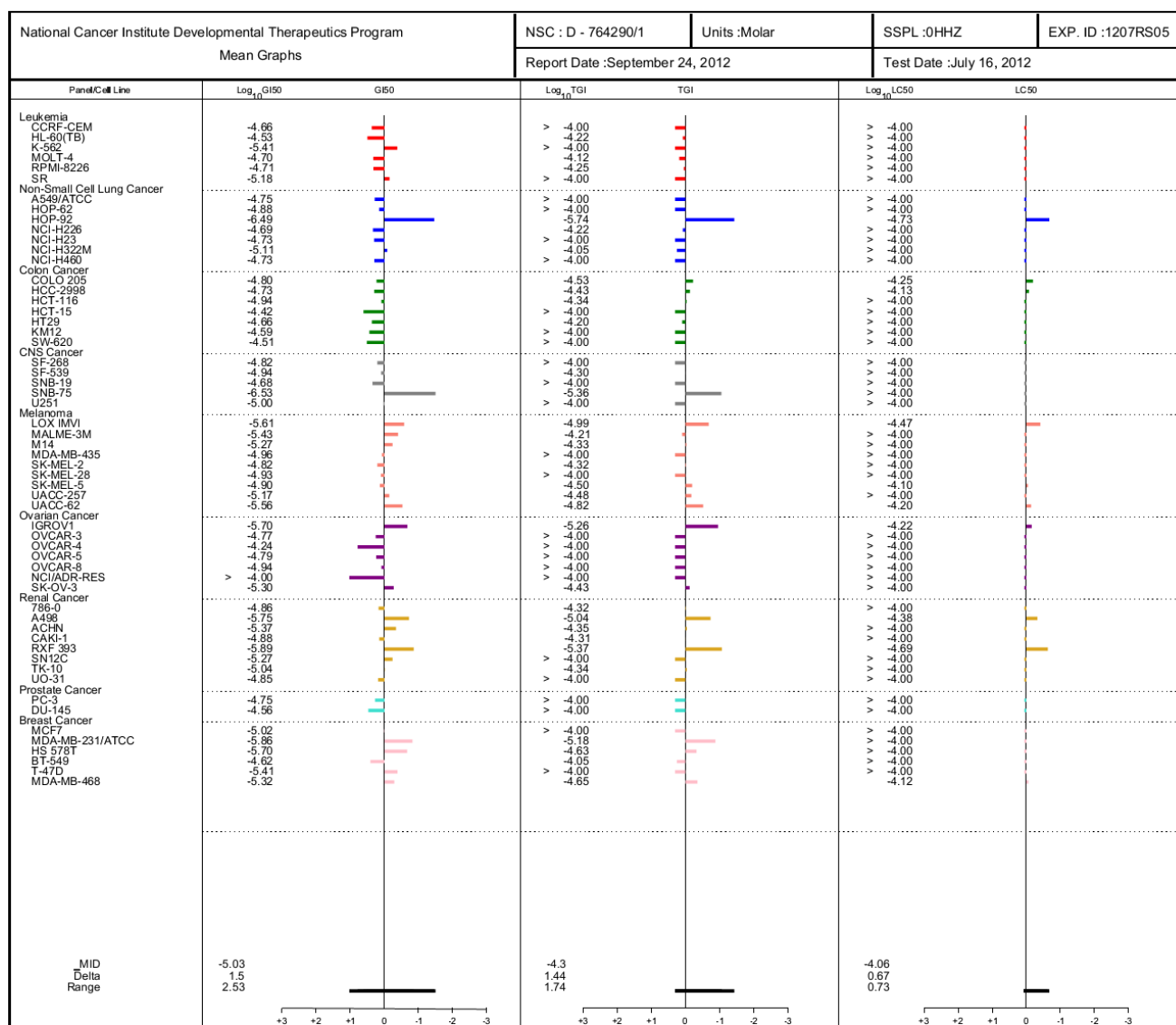


Fig. 103. Results of Five-dose screenings of compound 37 (second).

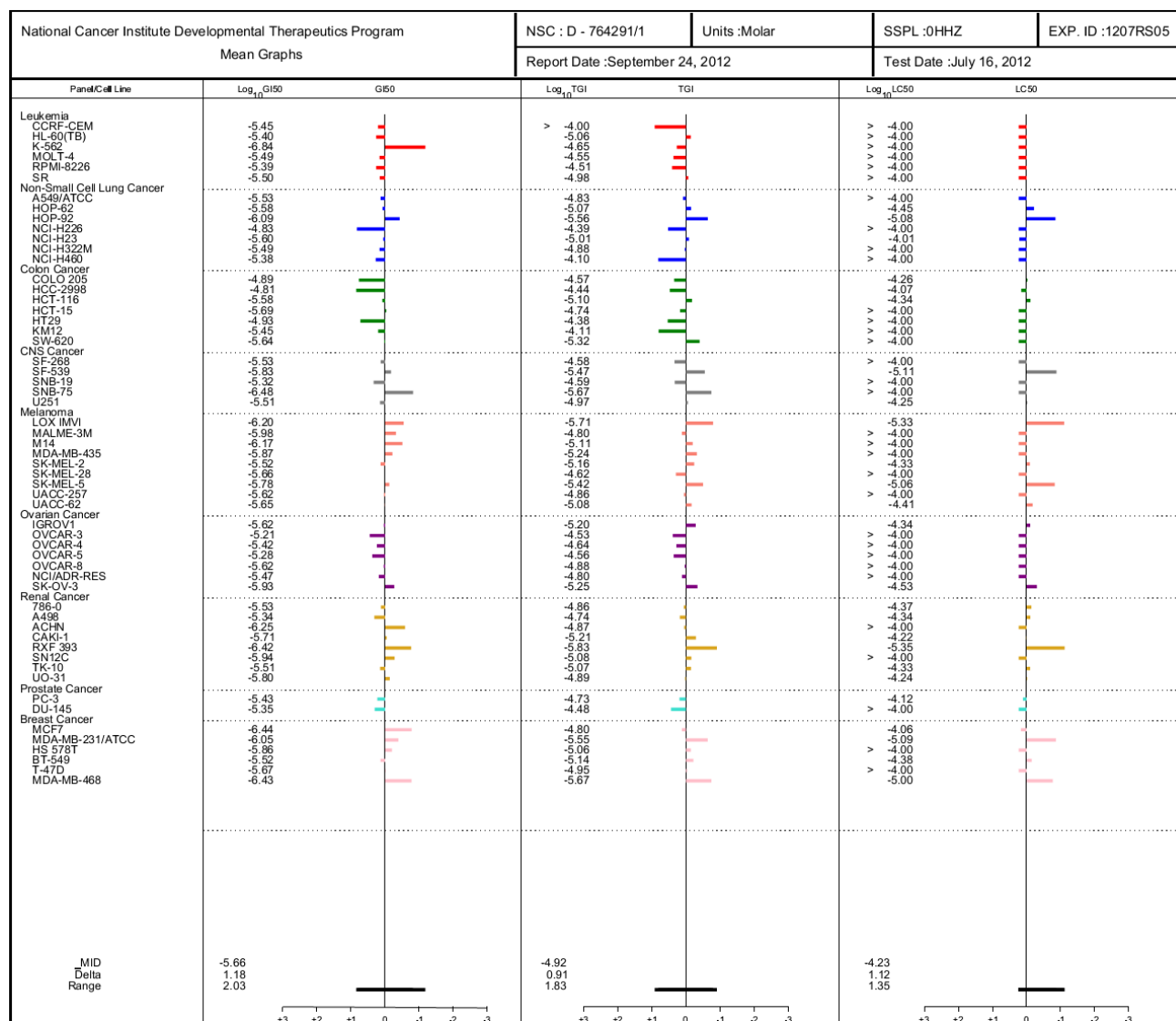


Fig. 104. Results of Five-dose screenings of compound 69 (second).

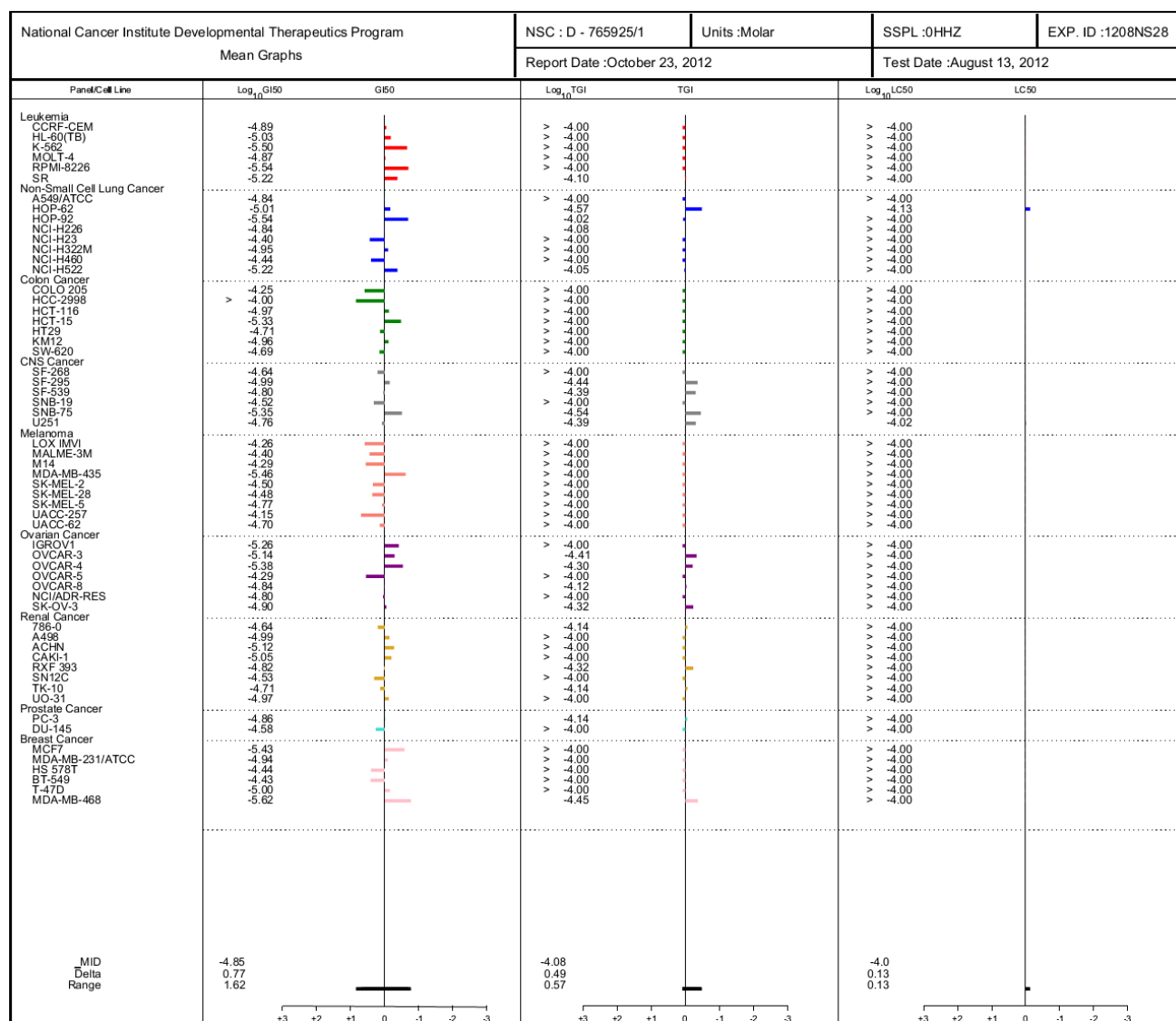


Fig. 105. Results of Five-dose screenings of compound 70.

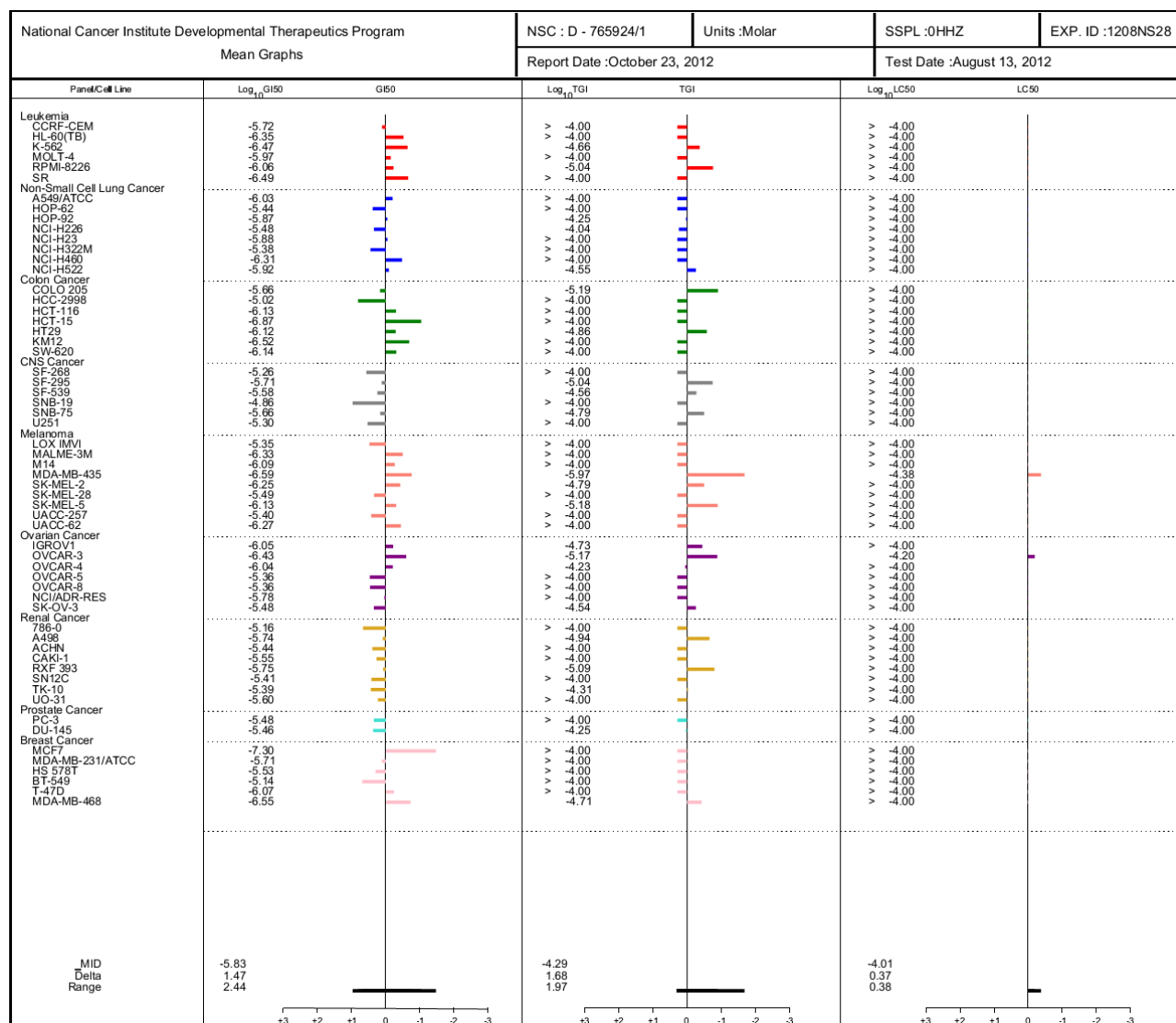


Fig. 106. Results of Five-dose screenings of compound 71.

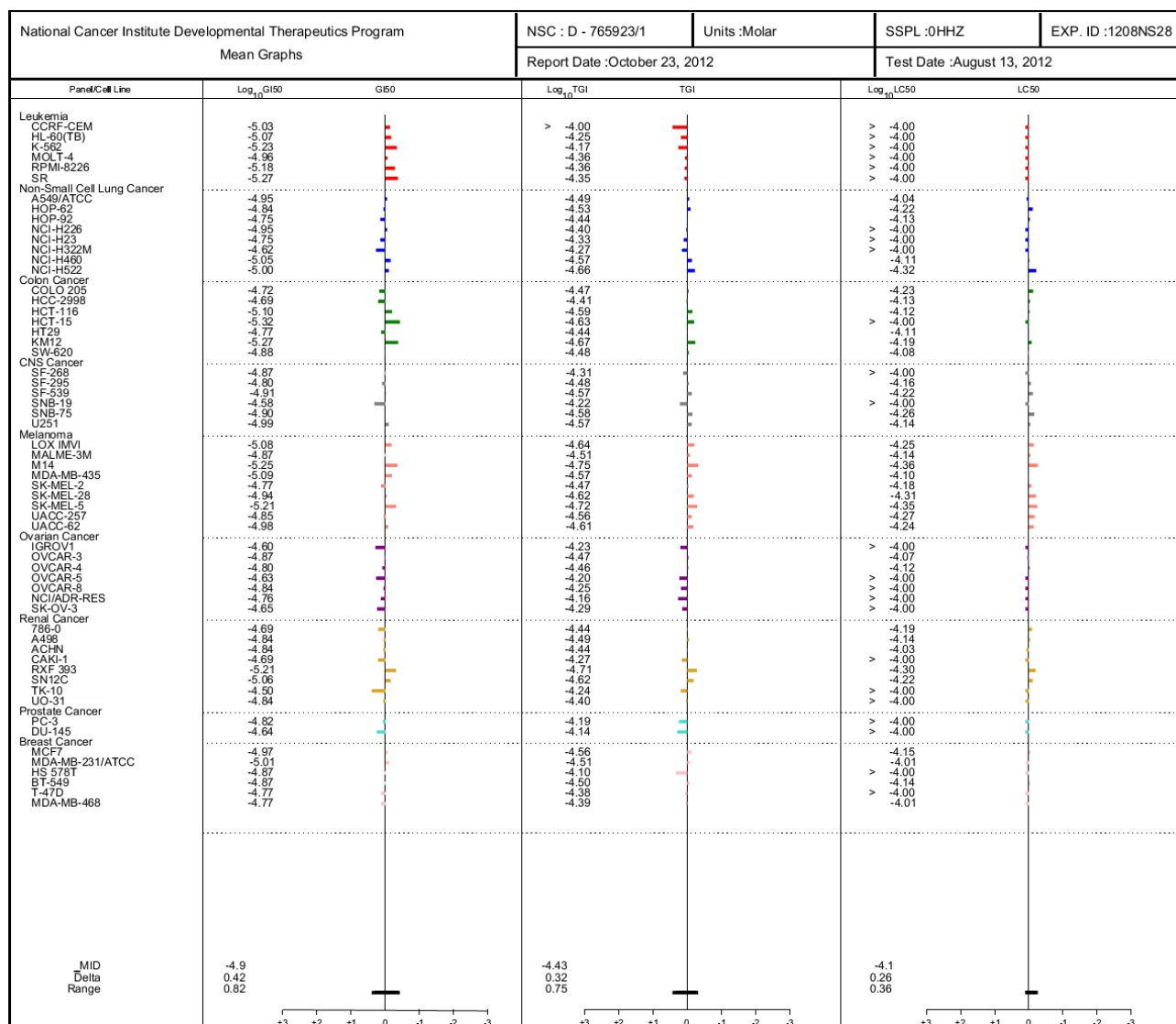


Fig. 107. Results of Five-dose screenings of compound 73.

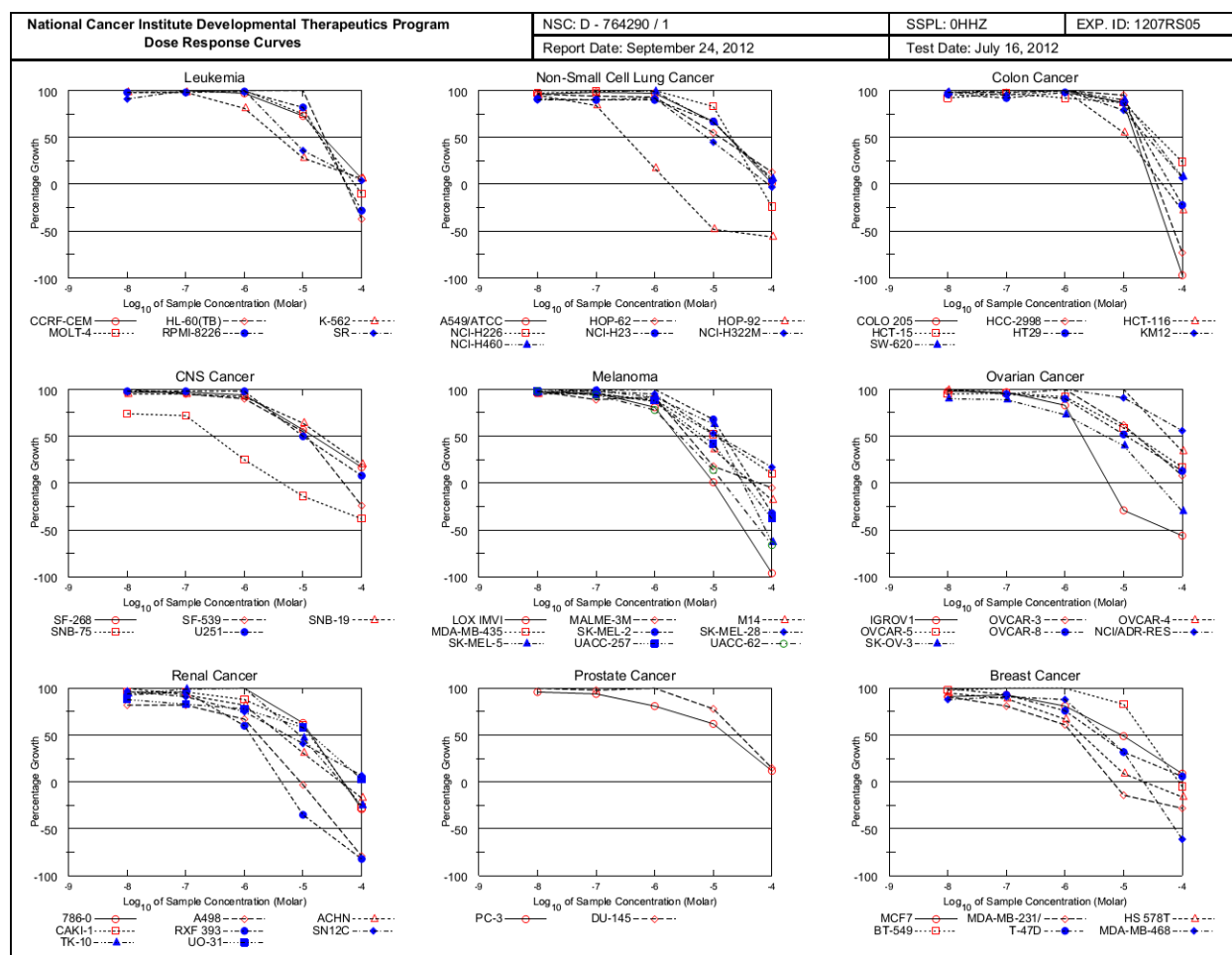


Fig. 108. Dose-response curves for the second Five-dose screenings of compound 37.

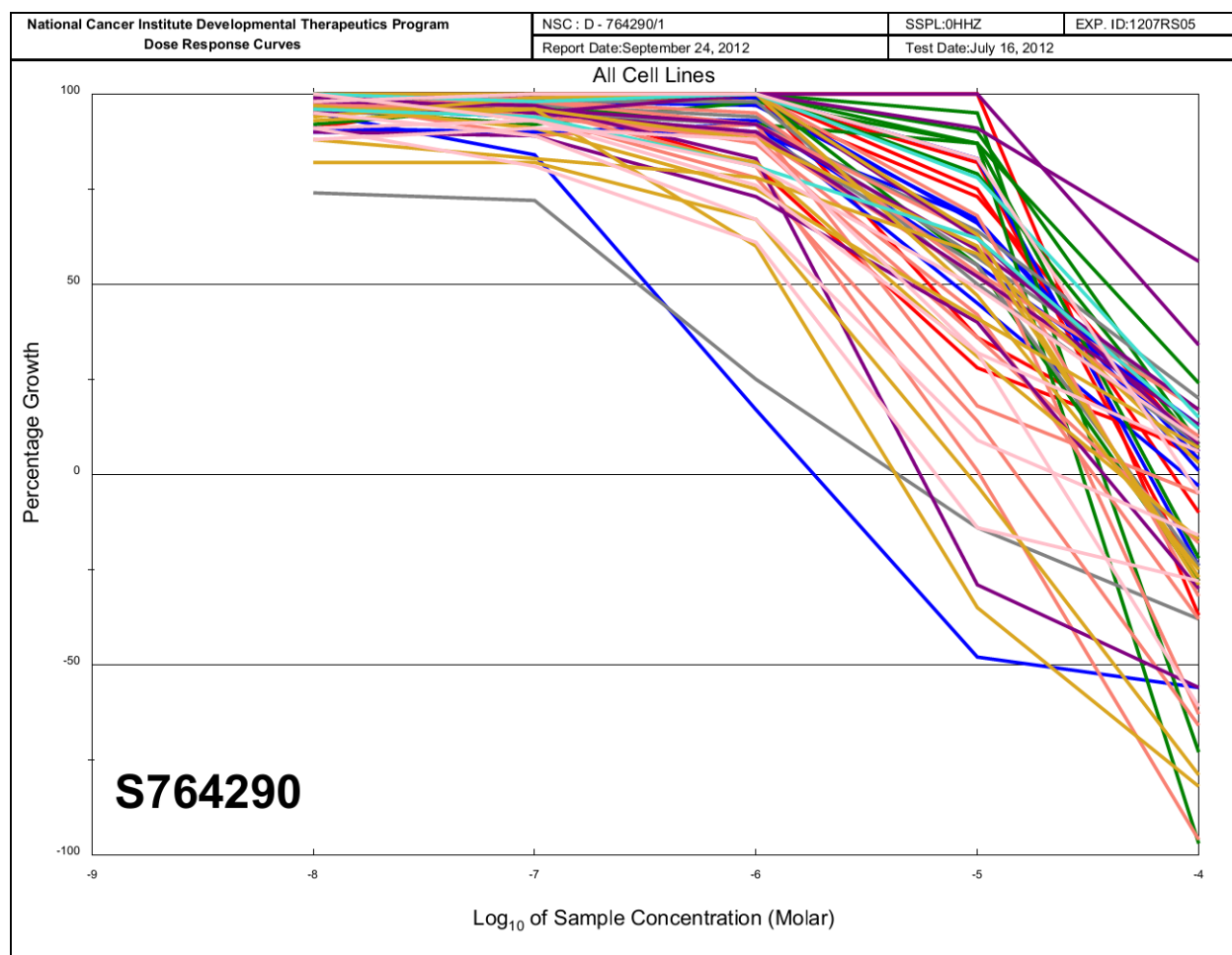


Fig. 109. Superposition of all the growth curves for compound 37 (second screenings).

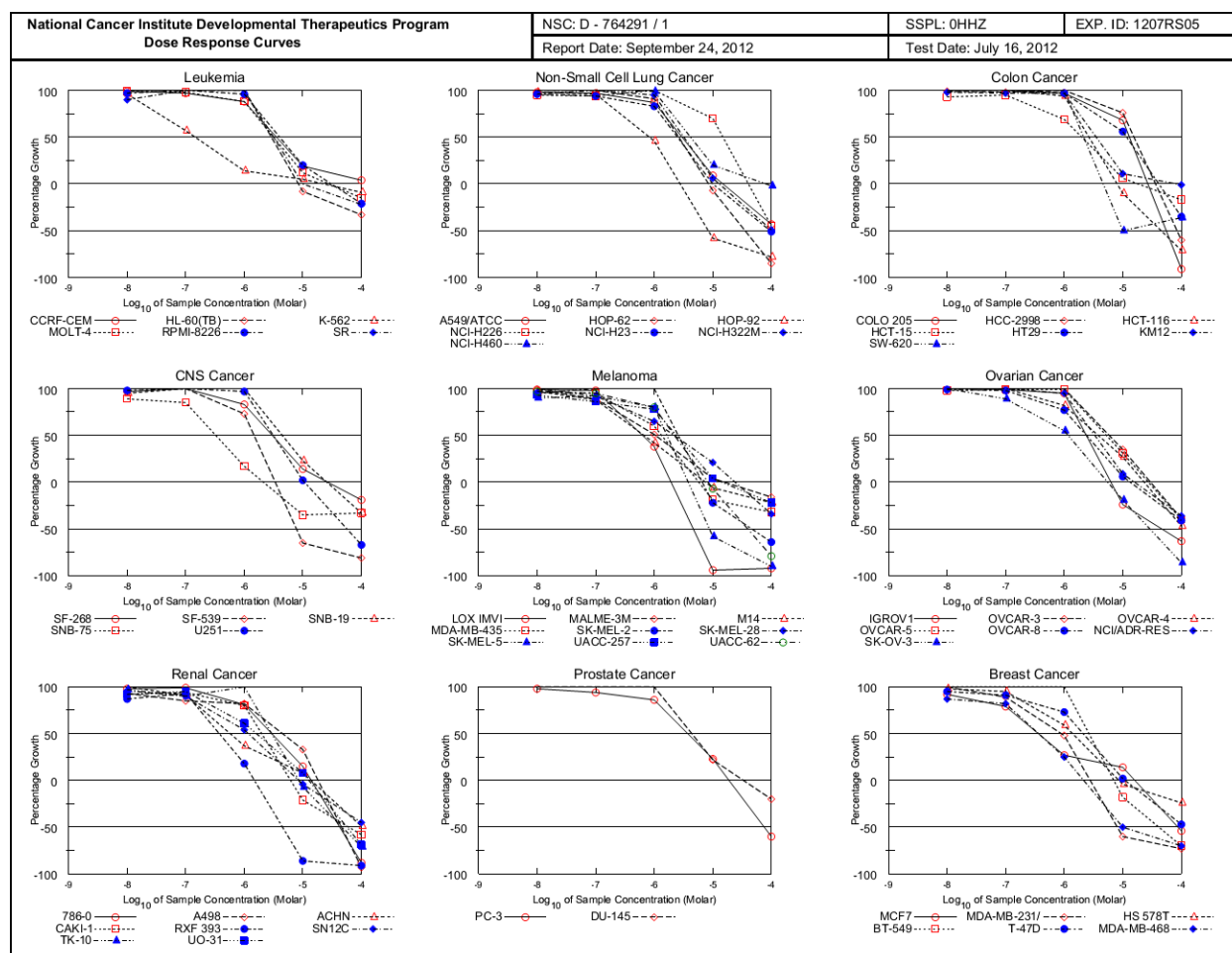


Fig. 110. Dose-response curves for the second Five-dose screenings of compound 69.

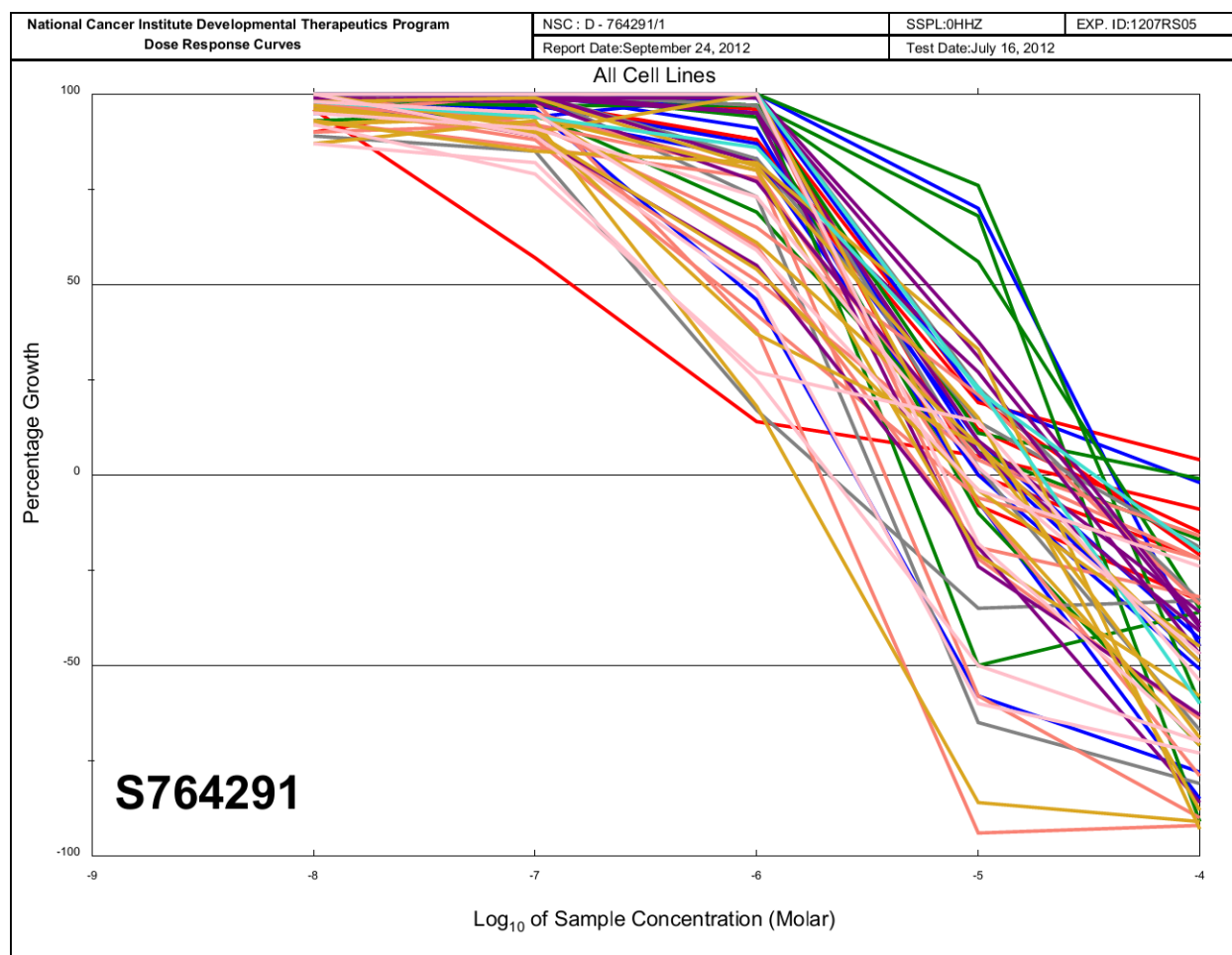


Fig. 111. Superposition of all the growth curves for compound 69 (second screenings).

Curriculum Vitae

Name: Kazem Ahmed Mahmoud
Date of birth: 06.01.1981
Place of birth: Sohag, Egypt
Marital status: Married, 2 children
E-mail: kazem.mahmoud@pharmazie.uni-halle.de
kazem.ahmed81@yahoo.com

Education:

1987-1992 Primary School
1992-1995 Secondary School
1995-1998 High School (Science Session)
1998-2003 Bachelor of Pharmacy & Pharmaceutical Sciences
Faculty of Pharmacy, Assiut University, Egypt
6/2009-3/2010 Diplomarbeit, Institute for Pharmacy, Martin
Luther University Halle-Wittenberg, Germany,
with PD Dr. A. Hilgeroth, grade "Sehr gut"
4/2010 to present PhD student, Institute for Pharmacy, Martin Luther
University Halle-Wittenberg, Germany,
with PD Dr. A. Hilgeroth

Work Experience:

7/2003-6/2005 Pharmacist at a Community Pharmacy, Cairo,
Egypt
6/2005-12/2005 Medical Representative at *Sanofi-Aventis*, Cairo,
Egypt
2/2006-10/2008 Pharmacist at a Community Pharmacy, Riyadh,
Saudi Arabia

Publications & Activities

Reviews:

- ✓ Mardia Telep El-Sayed, **Kazem Mahmoud**, Andreas Hilgeroth; *Synthesis of β -Nitroamines via Classical Mannich and Aza-Henry Reactions*; Curr. Org. Chem. (E-Pub Ahead-of-Schedule, Volume 17, 24 Issues, **2013**).

Papers:

- ✓ Volkmar Tell, **Kazem Ahamed Mahmoud**, Kanin Wichapong, Christoph Schächtele, Frank Totzke, Wolfgang Sippl and Andreas Hilgeroth. *Novel aspects in structure-activity relationships of profiled 1-aza-9-oxafluorenes as inhibitors of alzheimer disease-relevant kinases cdk1, cdk5 and gsk3 β* . Med. Chem. Comm. **2012**, **3**, 1413-1418.
- ✓ Volkmar Tell, Max Holzer, Lydia Herrmann, **Kazem Ahmed Mahmoud**, Christoph Schächtele, Frank Totzke, Andreas Hilgeroth. *Multitargeted drug development: Discovery and profiling of dihydroxy substituted 1-aza-9-oxafluorenes as lead compounds targeting Alzheimer disease relevant kinases*. Bioorg. Med. Chem. Lett. **2012**, **22**, 6914-6918.

Posters:

- ✓ Mardia Teleb, E., **Kazem, A. M.**, Hilgeroth, A. *Novel Bis-Indolyl Cytostatics*. 6th Summer School in Medicinal Chemistry, Regensburg, Germany, 26-28 September **2012**.

Oral Presentations:

- ✓ Mardia Teleb, E., **Kazem, A. M.**, Hilgeroth, A. *Synthesis of Novel Indolo-Spirocyclic Compounds*. International Congress of Young Chemists "YoungChem2012", Gdańsk, Poland, 10-14 October **2012**.

Thesis:

- ✓ Diplomarbeit thesis, *New 1-Aza-9-oxafluorenes as inhibitors of Alzheimer disease-relevant kinases*, Institute of Pharmacy, Martin-Luther-University Halle-Wittenberg under supervision of **PD Dr. A. Hilgeroth**, **2010**.

Bibliography

1. a) Paik, S. A multigene assay to predict recurrence of tamoxifen-treated, node-negative breast cancer. *N. Engl. J. Med.* **2004**, 351, 2817–2826. b) Ferlay J, Shin HR, Bray F, Forman D, Mathers C, Parkin DM. GLOBOCAN **2008** v1.2, Cancer Incidence and Mortality Worldwide: IARC CancerBase No. 10 [Internet]. Lyon, France: International Agency for Research on Cancer, 2010. Available from: <http://globocan.iarc.fr>. Accessed May **2011**. c) The global burden of disease: 2004 update; 2008. Accessed May **2011**.
2. van't Veer, L. J. Gene expression profiling predicts clinical outcome of breast cancer. *Nature* **2002**, 415, 530–536.
3. Chin, K. et al. Genomic and transcriptional aberrations linked to breast cancer pathophysiologies. *Cancer Cell* **2006**, 10, 529–541.
4. Bergamaschi, A. Distinct patterns of DNA copy number alteration are associated with different clinicopathological features and gene-expression subtypes of breast cancer. *Genes Chromosom. Cancer* **2006**, 45, 1033–1040.
5. Perou, C. M. Molecular stratification of triple-negative breast cancers. *Oncologist* **2011**, 16, 61–70.
6. Sorlie, T. Repeated observation of breast tumor subtypes in independent gene expression data sets. *Proc. Natl Acad. Sci. USA* **2003**, 100, 8418–8423.
7. Foulkes, W. D. Germline BRCA1 mutations and a basal epithelial phenotype in breast cancer. *J. Natl Cancer Inst.* **2003**, 95, 1482–1485.
8. Carey, L. A. et al. Race, breast cancer subtypes, and survival in the Carolina Breast Cancer Study. *J. Am. Med. Assoc.* **2006**, 295, 2492–2502.
9. <http://emedicine.medscape.com/article/1947145-overview>
10. Koboldt DC, Fulton RS, McLellan MD, Schmidt H, Kalicki-Veizer J, McMichael JF. Comprehensive molecular portraits of human breast tumours. *Nature* **2012**, 490, 61–70.
11. National Comprehensive Cancer Network. NCCN Clinical Practice Guidelines in Oncology. Breast Cancer, v.2.2011. Available at http://www.nccn.org/professionals/physician_gls/pdf/breast.pdf. Accessed June 3 2011.
12. Hennipman A, van Oirschot BA, Smits J, Rijksen G, Staal GE. Tyrosine kinase activity in breast cancer, benign breast disease, and normal breast tissue. *Cancer Res* **1989**, 49: 516–521.
13. Bolla M, Rostaing-Puissant BR, Chedin M. Protein tyrosine kinase activity as a prognostic parameter in breast cancer, a pilot study. *Breast Cancer Res Treat* **1993**, 26: 283–307.

References

- 14.Liu X, Pawson T. Biochemistry of the Src protein-tyrosine kinase: regulation by SH2 and SH3 domains. *Recent Prog Horm Res* **1994**, 49: 149-160.
- 15.Marshall CJ. Specificity of receptor tyrosine kinase signaling: transient versus sustained extracellular signal-regulated kinase activation. *Cell* **1995**, 80: 179-185.
- 16.Schlessinger J. Cell signaling by receptor tyrosine kinases. *Cell* **2000**, 103: 211-125.
- 17.Schlessinger J. New roles for Src kinases in control of cell survival and angiogenesis. *Cell* **2000**, 100: 293-306.
- 18.a) Mitchell PJ, Barker KT, Martindale JE. Cloning and characterisation of cDNAs encoding a novel non-receptor tyrosine kinase, brk, expressed in human breast tumours. *Oncogene* **1994**, 9: 2383-2390. b) Xue-Kui L., Xin-Rui Z., Qian Z., Man-Zhi L., Zhi-Min L., Zhi-Rui L., Di W. and Mu-Sheng Z. Low expression of PTK6/Brk predicts poor prognosis in patients with laryngeal squamous cell carcinoma. *Journal of Translational Medicine* **2013**, 11:59-68.
- 19.Easty, D. J., P. J. Mitchell, K. Patel, V. A. Florenes, R. A. Spritz, and D. C. Bennett.. Loss of expression of receptor tyrosine kinase family genes PTK7 and SEK in metastatic melanoma. *Int J Cancer* **1997**, 71:1061-1065.
- 20.Derry, J. J., G. S. Prins, V. Ray, and A. L. Tyner. Altered localization and activity of the intracellular tyrosine kinase BRK/Sik in prostrate tumor cells. *Oncogene* **2003**, 22:4212-4220.
- 21.Kasprzycka, M., M. Majewski, Z. J. Wang, A. Ptasznik, M. Wysocka, Q. Zhang, M. Marzec, P. Gimotty, M. R. Crompton, and M. A. Wasik. Expression and oncogenic role of Brk (PTK6/Sik) protein tyrosine kinase in lymphocytes. *Am J Pathol* **2006**, 168:1631-1641.
- 22.Llor, X., M. S. Serfas, W. Bie, V. Vasioukhin, M. Polonskaia, J. Derry, C. M. Abbott, and A. L. Tyner. BRK/Sik expression in the gastrointestinal tract and in colon tumors. *Clin Cancer Res* **1999**, 5:1767-1777.
- 23.Schmandt, R. E., M. Bennett, S. Clifford, A. Thornton, F. Jiang, R. Broaddus, C. Sun, K. Lu, A. Sood, and D. Gershenson. The BRK tyrosine kinase is expressed in high-grade serous carcinoma of the ovary. *Cancer Biol Ther.* **2006**, 5:1136-1141.
- 24.Serfas, M. S., and A. L. Tyner. Brk, Srm, Frk, and Src42A form a distinct family of intracellular Src-like tyrosine kinases. *Oncol Res* **2003**, 13:409-419.
- 25.Mitchell, P. J., K. T. Barker, J. E. Martindale, T. Kamalati, P. N. Lowe, M. J. Page, B. A. Gusterson, and M. R. Crompton. Cloning and characterisation

- of cDNAs encoding a novel non-receptor tyrosine kinase, brk, expressed in human breast tumours. *Oncogene* **1994**, 9:2383-2390.
26. Qiu H, Miller WT. Regulation of the nonreceptor tyrosine kinase Brk by autophosphorylation and by autoinhibition. *J Biol Chem* **2002**, 277, 34634-34641.
27. Qiu H, Miller WT. Role of the Brk SH3 domain in substrate recognition. *Oncogene* **2004**, 23, 2216-2223.
28. Hong, E., J. Shin, H. I. Kim, S. T. Lee, and W. Lee. Solution structure and backbone dynamics of the nonreceptor tyrosine kinase PTK6 SH2 domain. *J Biol Chem.* **2004**, 279 (28): 29700-29708.
29. Xiang B, Chatti K, Qiu H, Lakshmi B, Krasnitz A, Hicks J, Yu M, Miller WT, Muthuswamy SK: Brk is coamplified with ErbB2 to promote proliferation in breast cancer. *Proc Natl Acad Sci USA* **2008**, 105:12463-12468.
30. Ostrander J, Daniel A, Lange C. Brk/PTK6 signaling in normal and cancer cell models. *Current Opinion in Pharmacology* **2010**, 10: 662-669.
31. Derry, J. J., S. Richard, C. H. Valderrama, X. Ye, V. Vasioukhin, A. W. Cochrane, T. Chen, and A. L. Tyner. Sik (BRK) phosphorylates Sam68 in the nucleus and negatively regulates its RNA binding ability. *Mol Cell Biol* **2000**, 20:6114-6126.
32. Haegebarth, A., D. Heap, W. Bie, J. J. Derry, S. Richard, and A. L. Tyner. The nuclear tyrosine kinase BRK/Sik phosphorylates and inhibits the RNA-binding activities of the Sam68-like mammalian proteins SLM-1 and SLM-2. *J Biol Chem* **2004**, 279:54398-54404.
33. Lukong, KE, Hout ME, Richard S. BRK phosphorylates PSF promoting its cytoplasmic localization and cell cycle arrest. *Cell Signal* **2009**, 21:1415-1422.
34. Liu L, Gao Y, Qiu H, Miller WT, Poli V, Reich NC. Identification of STAT3 as a specific substrate of breast tumor kinase. *Oncogene* **2006**, 25: 4904-4912.
35. Weaver AM, Silva CM. Signal transducer and activator of transcription 5b: a new target of breast tumor kinase/protein tyrosine kinase 6. *Breast Cancer Res* **2007**, 9: R79.
36. Liu X, Robinson GW, Hennighausen L. Activation of Stat5a and Stat5b by tyrosine phosphorylation is tightly linked to mammary gland differentiation. *Mol Endocrinol* **1996**, 10: 1496-1506.
37. Philp JA, Burdon TG, Watson CJ. Differential activation of STATs 3 and 5 during mammary gland development. *FEBS Lett* **1996**, 396: 77-80.
38. Petit V, Boyer B, Lentz D, Turner CE, Thiery JP, Valles AM: Phosphorylation of tyrosine residues 31 and 118 on paxillin regulates cell

References

- migration through an association with CRK in NBT-II cells. *J Cell Biol* **2000**, 148:957-970.
39. Bradley WD, Hernandez SE, Settleman J, Koleske AJ: Integrin signaling through Arg activates p190RhoGAP by promoting its binding to p120RasGAP and recruitment to the membrane. *Mol Biol Cell* **2006**, 17:4827-4836.
40. Moran MF, Polakis P, McCormick F, Pawson T, Ellis C: Protein-tyrosine kinases regulate the phosphorylation, protein interactions, subcellular distribution, and activity of p21rasGTPase-activating protein. *Mol Cell Biol* **1991**, 11:1804-1812.
41. Mitchell PJ, Sara EA, Crompton MR. A novel adaptor-like protein which is a substrate for the non-receptor tyrosine kinase, BRK. *Oncogene* **2000**, 19: 4273-4282.
42. Ikeda O, Miyasaka Y, Sekine Y, et al. STAP-2 is phosphorylated at tyrosine-250 by Brk and modulates Brk-mediated STAT3 activation. *Biochem Biophys Res Commun* **2009**, 384: 71-75.
43. Lukong KE, Richard S. Breast tumor kinase BRK requires kinesin-2 subunit KAP3A in modulation of cell migration. *Cell Signal* **2008**, 20: 432-442.
44. Zheng Y, Peng M, Wang Z, Asara JM, Tyner AL. Protein tyrosine kinase 6 directly phosphorylates AKT and promotes AKT activation in response to epidermal growth factor. *Mol Cell Biol* **2010**, 30: 4280-4292.
45. Palka-Hamblin HL, Gierut JJ, Bie W, et al. Identification of beta-catenin as a target of the intracellular tyrosine kinase PTK6. *J Cell Sci* **2010**, 123: 236-245.
46. Kamalati T, Jolin HE, Mitchell PJ, et al. Brk, a breast tumor-derived non-receptor protein-tyrosine kinase, sensitizes mammary epithelial cells to epidermal growth factor. *J Biol Chem* **1996**, 271: 30956-63.
47. Kamalati T, Jolin HE, Fry MJ, Crompton MR. Expression of the BRK tyrosine kinase in mammary epithelial cells enhances the coupling of EGF signalling to PI3-kinase and Akt, via erbB3 phosphorylation. *Oncogene* **2000**, 19: 5471-6.
48. Xiang B, Chatti K, Qiu H. Brk is coamplified with ErbB2 to promote proliferation in breast cancer. *Proc Natl Acad Sci USA* **2008**, 105: 12463-12468.
49. Qiu H, Zappacosta F, Su W, Annan RS, Miller WT: Interaction between Brk kinase and insulin receptor substrate-4. *Oncogene* **2005**, 24:5656-5664.
50. Castro NE, Lange CA. Breast tumor kinase and extracellular signal-regulated kinase 5 mediate Met receptor signaling to cell migration in breast cancer cells. *Breast Cancer Res* **2010**, 12: R60.

51. Chen HY, Shen CH, Tsai YT, Lin FC, Huang YP, Chen RH. Brk activates rac1 and promotes cell migration and invasion by phosphorylating paxillin. *Mol Cell Biol* **2004**, 24: 10558-10572.
52. Ostrander JH, Daniel AR, Lofgren K, Kleer CG, Lange CA. Breast tumor kinase (protein tyrosine kinase 6) regulates heregulin-induced activation of ERK5 and p38 MAP kinases in breast cancer cells. *Cancer Res* **2007**, 67: 4199-4209.
53. Harvey AJ, Pennington CJ, Porter S. Brk protects breast cancer cells from autophagic cell death induced by loss of anchorage. *Am J Pathol* **2009**, 175:1226-1234.
54. Haegebarth A, Bie W, Yang R. Protein tyrosine kinase 6 negatively regulates growth and promotes enterocyte differentiation in the small intestine. *Mol Cell Biol* **2006**, 26: 4949-57.
55. Aroian, R.V., Koga, M., Mendel, J.E., Ohshima, Y., Sternberg, P.W. The let-23 gene necessary for *Caenorhabditis elegans* vulval induction encodes a tyrosine kinase of the EGF receptor subfamily. *Nature* **1990**, 348, 693–699.
56. Livneh, E., Glazer, L., Segal, D., Schlessinger, J., Shilo, B.Z. The *Drosophila* EGF receptor gene homolog: conservation of both hormone binding and kinase domains. *Cell* **1985**, 40, 599–607.
57. a) Burgess, A.W., Cho, H.S., Eigenbrot, C., Ferguson, K.M., Garrett, T.P., Leahy, D.J., Lemmon, M.A., Sliwkowski, M.X., Ward, C.W., Yokoyama, S. An open-and-shut case? Recent insights into the activation of EGF/ErbB receptors. *Mol. Cell* **2003**, 12, 541–552. b) Holbro, T., Civenni, G., and Hynes, N.E. The ErbB receptors and their role in cancer progression. *Exp. Cell Res.* **2003**, 284, 99–110. c) Yarden, Y., and Sliwkowski, M.X. Untangling the ErbB signaling network. *Nat. Rev. Mol. Cell Biol.* **2001**, 2, 127-137.
58. Stein, R.A., and Staros, J.V. Evolutionary analysis of the ErbB receptor and ligand families. *J. Mol. Evol.* **2000**, 50, 397–412.
59. a) Jorissen, R.N., Walker, F., Pouliot, N., Garrett, T.P., Ward, C.W., and Burgess, A.W. Epidermal growth factor receptor: mechanisms of activation and signalling. *Exp. Cell Res.* **2003**, 284, 31–53. b) Schlessinger, J. Cell signaling by receptor tyrosine kinases. *Cell* **2000**, 103, 211–225. c) Falls, D.L. Neuregulins: functions, forms, and signaling strategies. *Exp. Cell Res.* **2003**, 284, 14–30.
60. Nahta R, Esteva FJ. Herceptin: mechanisms of action and resistance. *Cancer let* **2006**, 232(5), 123-138.
61. Yeon CH, Pegram MD. Anti-erbB2 antibody trastuzumab in the treatment of HER2-amplified breast cancer. *Invest New Drugs* **2005**, 23(5), 391-409.

References

- 62.Ménard S, Tagliabue E, Campiglio M, Pupa SM. Role of HER2 gene overexpression in breast carcinoma. *J Cell Physiol.* **2000**,182:150-162.
- 63.Jones KL, Buzdar AU. Evolving novel anti-HER2 strategies. *Lancet Oncol.* **2009**,10:1179-1187.
- 64.Conleth GM, Patrick GM. Recent advances in novel targeted therapies for HER2-positive breast cancer. *Anti-Cancer Drugs* **2012**, 23, 765-776.
- 65.Landgraf R. HER2 (ERBB2): functional diversity from structurally conserved building blocks. *Breast Can Res.* **2007**, 9:202-211.
- 66.Sliwkowski MX. Ready to partner. *Nat Struct Biol.* 2003; 10:158-159.
- 67.Tymoczko, J. L. J. M. B. L. S. *Biochemistry: a short course*; W.H. Freeman and Co.: New York, NY, **2010**.
- 68.Li E, H. K. Role of receptor tyrosine kinase transmembrane domains in cell signaling and human pathologies. *Biochemistry* **2006**, 45 (20), 6241-6251.
- 69.Arpino G, Gutierrez C, Weiss H. Treatment of human epidermal growth factor receptor 2-overexpressing breast cancer xenografts with multiagent HER-targeted therapy. *J Natl Cancer Inst.* **2007**, 99:694-705.
- 70.Hsieh AC, Moasser MM. Targeting HER proteins in cancer therapy and the role of the non-target HER3. *Br J Cancer.* **2007**, 97:453-457.
- 71.Jones KL, Buzdar AU. Evolving novel anti-HER2 strategies. *Lancet Oncol.* **2009**, 10:1179-1187.
- 72.Gutierrez C, Schiff R. HER2: biology, detection, and clinical implications. *Arch Pathol Lab Med.* **2011**, 135:55-62.
- 73.Rosen LS, Ashurst HL, Chap L. Targeting signal transduction pathways in metastatic breast cancer: a comprehensive review. *Oncologist.* **2010**, 15:216-235.
- 74.Amin DN, Sergina N, Ahuja D. Resiliency and vulnerability in the HER2-HER3 tumorigenic driver. *Sci Transl Med.* **2010**, 2:16ra7.
- 75.Ménard S, Tagliabue E, Campiglio M, Pupa SM. Role of HER2 gene overexpression in breast carcinoma. *J Cell Physiol.* **2000**,182:150-162.
- 76.Holbro T, Civenni G, Hynes NE. The ErbB receptors and their role in cancer progression. *Exp Cell Res.* **2003**, 284:99-110.
- 77.McCubrey JA, Steelman LS, Franklin RA. Targeting the RAF/MEK/ERK, PI3K/AKT and p53 pathways in hematopoietic drug resistance. *Adv Enzyme Regul.* **2007**, 47:64-103.
- 78.Brown MD, Sacks DB. Protein scaffolds in MAP kinase signalling. *Cell Signal.* **2009**, 21:462-469.
- 79.Liu P, Cheng H, Roberts TM, Zhao JJ. Targeting the phosphoinositide 3-kinase pathway in cancer. *Nat Rev Drug Discov.* **2009**, 8:627-644.

80. Nahta R, Yu D, Hung MC. Mechanisms of disease: understanding resistance to HER2-targeted therapy in human breast cancer. *Nat Clin Pract Oncol*. **2006**, 3:269-280.
81. Koutras AK, Fountzilas G, Kalogeras KT. The upgraded role of HER3 and HER4 receptors in breast cancer. *Crit Rev Oncol Hematol*. **2010**, 74:73-78.
82. Hurvitz SA. Current approaches and future directions in the treatment of HER2-positive breast cancer. *Cancer Treat Rev* **2012**, <http://dx.doi.org/10.1016/j.ctrv.2012.04.008>
83. Hongbo Z., Belanger D., Curran P., Shipps G., Malkowski M., Wang Y. Discovery of novel imidazo[1,2- α]pyrazin-8-amines as Brk/PTK6 inhibitors. *Bioorg. Med. Chem. Lett*. **2011**, 21, 5870-5875.
84. Hochhaus, A. Management of Bcr-Abl-positive leukemias with dasatinib. *Exp. Rev. Anticancer Ther*. **2007**, 7, 1529-1536.
85. Fab Hyun-Soo Cho, Karen Mason, Kasra X. Ramyar, Ann Marie Stanley, Sandra B. Gabelli, Dan W. Denney Jr & Daniel J. Leahy. Structure of the extracellular region of HER2 alone and in complex with the Herceptin. *Nature* **2003**, 421, 756-760.
86. Kute, T; Lack CM, Willingham M, Bishwokama B, Williams H, Barrett K, Mitchell T, Vaughn JP. "Development of Herceptin resistance in breast cancer cells". *Cytometry* **2004**, 57A (2): 86–93.
87. Albanell, J; Codony J, Rovira A, Mellado B, Gascon P. "Mechanism of action of anti-HER2 monoclonal antibodies: scientific update on trastuzumab and 2C4". *Advances in Experimental Medicine and Biology* **2003**, 532: 253–268.
88. Izumi Y, Xu L, di Tomaso E, Fukumura D, Jain RK. Tumour biology: herceptin acts as an anti-angiogenic cocktail. *Nature* **2002**; 416:279–280.
89. Clynes, RA; Towers, TL; Presta, LG; Ravetch, JV. "Inhibitory Fc receptors modulate in vivo cytotoxicity against tumor targets". *Nat Med* **2000**, 6 (4): 443-446.
90. Perez EA, Romond EH, Suman VJ, Jeong JH, Davidson NE, Geyer CE Jr. Four-year follow-up of trastuzumab plus adjuvant chemotherapy for operable human epidermal growth factor receptor 2-positive breast cancer: joint analysis of data from NCCTG N9831 and NSABP B-31. *J Clin Oncol* **2011**, 29:3366–3373.
91. Burris HA. "Dual kinase inhibition in the treatment of breast cancer: initial experience with the EGFR/ErbB-2 inhibitor lapatinib". *Oncologist* **2004**, 9 Suppl 3: 10–5.
92. Higa GM & Abraham J. Lapatinib in the treatment of breast cancer. *Expert Review of Anticancer Therapy* **2007**, 7 (9): 1183–1192.

References

93. Denny WA, Rewcastle GW, Bridges AJ, Fry DW, Kraker AJ. Structure activity relationships for 4- anilinoquinazolines as potent inhibitors at the ATP binding site of the epidermal growth factor receptor *in vitro*. *Clin Exp Pharmacol Physiol*. **1996**, 23: 424-427.
94. Rusnak DW, Lackey K, Affleck K, et al. The effects of the novel reversible epidermal growth factor/ErbB-2 tyrosine kinase inhibitor GW2016 on the growth of human normal and tumor derived cell lines in vitro and in vivo. *Mol Cancer Ther* **2001**, 1:85-94.
95. Konecny GE, Pegram MD, Venkatesan N, Finn R, Yang G, Rahmeh M. Activity of the dual kinase inhibitor lapatinib (GW572016) against HER-2-overexpressing and trastuzumab-treated breast cancer cells. *Cancer Res* **2006**, 66:1630–1639.
96. de Bono, Johann S.; Bellmunt, J; Attard, G; Droz, JP; Miller, K; Flechon, A; Sternberg, C; Parker, C. Open-Label Phase II Study Evaluating the Efficacy and Safety of Two Doses of Pertuzumab in Castrate Chemotherapy-Naive Patients With Hormone-Refractory Prostate Cancer. *Journal of Clinical Oncology* **2007**, 25 (3): 257–262.
97. Keating GM. Pertuzumab: in the first-line treatment of HER2-positive metastatic breast cancer. *Drugs* **2012**, 12; 72 (3): 353-60.
98. Baselga J, Cortés J, Kim SB, and the CLEOPATRA Study Group. Pertuzumab plus trastuzumab plus docetaxel for metastatic breast cancer. *N Engl J Med* **2012**, 12; 366 (2): 109-19.
99. http://www.ema.europa.eu/ema/index.jsp?curl=pages/medicines/human/medicines/002547/smops/Positive/human_smop_000457.jsp&mid=WC0b01ac058001d127
100. Rabindran SK, Discafani CM, Rosfjord EC, Baxter M, Floyd MB, Golas J, Hallett WA, Johnson BD, Nilakantan R, Overbeek E, Reich MF, Shen R, Shi X, Tsou HR, Wang YF, Wissner A. Antitumor activity of HKI-272, an orally active, irreversible inhibitor of the HER-2 tyrosine kinase. *Cancer Res*. **2004**, 1;64(11):3958-65.
101. Awada A, Dirix L, Manso Sanchez L, Xu B, Luu T, Diéras V, Hershman DL, Agrapart V, Ananthakrishnan R, Staroslawska E. Safety and efficacy of neratinib (HKI-272) plus vinorelbine in the treatment of patients with ErbB2-positive metastatic breast cancer pretreated with anti-HER2 therapy. *Ann Oncol*. **2013**, 24(1):109-116.
102. Yoshinori Ito, Mitsukuni Suenaga, Kiyohiko Hatake, Shunji Takahashi, Masahiro Yokoyama, Yusuke Onozawa, Kentaro Yamazaki, Shuichi Hironaka, Kiyoshi Hashigami, Hirotaka Hasegawa, Nobuko Takenaka and Narikazu Boku. Safety, Efficacy and Pharmacokinetics of

- Neratinib (HKI-272) in Japanese Patients with Advanced Solid Tumors: A Phase 1 Dose-escalation Study. *Jpn J Clin Oncol* **2012**, 42(4)278–286.
103. Krug M, Wichapong K, Erlenkamp G, Sippl W, Schächtele C, Totzke F, Hilgeroth A. Discovery of 4-benzylamino-substituted α -carboline as a novel class of receptor tyrosine kinase inhibitors. *Chem Med Chem.* **2011**, 6(1):63-72.
104. Martin Krug, Entwicklung, Synthese und biologische Evaluation neuartiger selektiver Proteinkinaseinhibitoren. *Dissertation*, MLU Halle-Wittenberg, **2009**.
105. Harvey, A.J., Pennington, C.J., Porter, S., Burmi, R.S., Edwards, D.R., Cout, W., Eccles, S.A., Crompton, M.R. Brk Protects Breast Cancer Cells from Autophagic Cell Death Induced by Loss of Anchorage. *Am J. Pathol.* **2009**, 175:1226-1234.
106. Cold Spring Harbor Laboratory (2008, August 26). Scientists Identify New Drug Target Against Virulent Type Of Breast Cancer. *ScienceDaily*. Retrieved December 6, **2010**, from <http://www.sciencedaily.com/releases/2008/08/080825103533.htm>.
107. Born, M., Quintanilla-Fend, L., Braselmann, H., Reich, U., Richter, M., Hutzler, P., Aubele, M. Simultaneous over-expression of Her2/neu and PTK6 tyrosine kinase in archival invasive ductal breast carcinomas. *J. Pathol.* **2005**, 205:592-596.
108. Irie, H.Y., Shestra, Y., Selfors, L.M., Frye, F., Iida, N., Wang, Z., Zou, L., Yao, J., Lu, Y., Epstein, C.B., Natesan, S., Richardson, A.L., Polyak, K., Mills, G.B., Hahn, W.C., Brugge, J.S. PTK6 regulates IGF-1-induced anchorage-independent survival. *PLoS One* **2010**, 5:e11729.
109. Brauer, P.M., Tyner, A.L. Building a better understanding of the intracellular tyrosine kinase PTK6-Brk by Brk. *Biochim. Biophys. Acta* **2010**, 1806:66-73.
110. Frisch, S.M., Francis, H. Disruption of epithelial cell-matrix interactions induces apoptosis. *J. Cell. Biol.* **1994**, 124:619-626.
111. Barker, K.T., Jackson, L.E., Crompton, M.R. Brk tyrosine kinase expression in a high proportion of human breast carcinoma. *Oncogene* **1997**, 15:799-805.
112. Bianco, R., Shin, I., Ritter, C.A., Yakes, F.M., Basso, A., Rosen, N., Tsurutani, J., Dennis, P.A., Mills, G.B., Arteaga, C.L. Loss of PTEN/MMAC1/TEP in EGF receptor-expressing tumor cells counteracts the anti-tumor action of EGFR tyrosine kinase inhibitors. *Oncogene* **2003**, 22: 2812-2822.
113. a) Graebe, C.; Ullmann, F. Ueber eine neue Carbazolsynthese. *Justus Liebigs Ann. Chem.* **1896**, 291, 16-17. b) Nantka-Namirski, P. Graebe-

References

- Ullmann method in the synthesis of carbolines. II. Synthesis of 2,4-dimethyl- α -carboline derivatives. *Acta. Pol. Pharm.* **1961**, 18, 449-460.
- c) Vera-Luque, P.; Alajarin, R.; Alvarez-Builla, J.; Vaquero, J. An improved synthesis of α -carbolines under microwave irradiation. *Org. Lett.* **2006**, 8, 415-418.
114. A. R. Katritzky, J. Wu, W. Kuzmierkiewicz, S. Rachwal, M. Balasubramanian, P. J. Steel. Unusual reactivity of lithiated 2-alkylbenzotriazoles. *Liebigs Ann. Chem.*, **1994**, 7-12.
115. Witkop, B. Studies on Carboline Anhydronium Bases. *J. Am. Chem. Soc.* **1953**, 75, 3361-3370.
116. Marky, M.; Schmid, H.; Hansen, H. Photoreactions of 1-Alkyl benzotriazoles. *Helv. Chim. Acta.* **1979**, 62, 2129-2153.
117. Mathias, I.; Burkett, D. N-Alkylations of Benzimidazoles and Benzotriazole via Phase Transfer Catalysis. *Tetrahedron Lett.* **1979**, 20, 4709-4712.
118. Bergman, J., Sand, P. A new simple procedure for alkylation of nitrogen heterocycles using dialkyl oxalates and alkoxides. *Tetrahedron Lett.* **1984**, 25, 1957-1960.
119. Claramunt, R.; Elguero, J.; Garceran, R. Synthesis by Phase Transfer Catalysis of *N*-Benzyl, *N*-Diphenylmethyl and *N*-Triphenylmethyl Azoles and Benzazoles: Proton NMR and Chromatographic Data as a Tool for Identification. *Heterocycles*, **1985**, 23, 2895-2906.
120. Semenov, A.; Tolstikhina, V. Pyrido[2,3-*b*]indoles (α -carbolines). *Chem. Heterocycl. Compd.* **1984**, 20, 345-356.
121. Elks, J.; Webb, J. B.; Gregory, G. J.; Cocker, J. D. *deutsches Patent Nr. 1913124*, **1970**, Chem. Abstr. 72, 43636.
122. Stephenson, L.; Warburton, W. K.; Gregory, G. J.; Cocker, J. D.; Clark, M. V. *britisches Patent Nr. 1268771*; **1972**, Chem. Abstr. 77, 48432.
123. Stephenson, L.; Warburton, W. K.; Gregory, G. J.; Cocker, J. D.; Clark, M. V. *deutsches Patent Nr. 1913120*; **1971**, Chem. Abstr. 74, 13126.
124. Bellamy, F.D.; Ou, K. Selective reduction of aromatic nitro compounds with stannous chloride in non acidic and non aqueous medium. *Tetrahedron Lett.* **1985**, 26, 11, 1362.
125. Xing, W.-K., Ogata, Y. Steric acceleration by ortho substituents of the stannous chloride reduction of nitrobenzenes in aqueous ethanol. *Journal of Organic Chemistry* **1982**, 47, 18, 3577-3581.
126. Emmanuil I. Troyansky "Phenyl Isocyanate" in Encyclopedia of Reagents for Organic Synthesis, **2001** John Wiley & Sons doi:10.1002/047084289X.rp073

127. Muñoz, M. A.; Balon, M.; Carmona, C.; Hidalgo, J.; Lopez Poveda, M. Sulphonation of β -Carbolines in Concentrated Sulphuric Acid Solutions *Heterocycles* **1988**, 27, 2067-2070.
128. Carmona Guzman, M.C.; Balon Almeida, M.; Hidalgo Toledo, J.; Munoz Perez, M. A.; Lopez Poveda, M. Sulfonation reactions of b-carbolines. *Can. J. Chem.* **1989**, 67, 720-726.
129. Neef, G.; Eder, U.; Huth, A.; Rahtz, D.; Schmiechen, R.; Seidelmann, D. Synthesis of 4-substituted b-carbolines. *Heterocycles* **1983**, 20, 1295-313.
130. Neef, G.; Eder, U.; Schmiechen, R.; Huth, A.; Rathz, D.; Seidelmann, D.; Kehr, W.; Palenschat, D.; Braestrup, C. T.; Christensen, J. A.; Engelstraf, M. *Eur. Pat. Appl. 54.507* **1982**, Chem. Abstr. 98,16663.
131. Wang S, Wan NC, Harrison J, Miller W, Chuckowree I, Sohal S, Hancox TC, Baker S, Folkes A, Wilson F, Thompson D, Cocks S, Farmer H, Boyce A, Freathy C, Broadbridge J, Scott J, Depledge P, Faint R, Mistry P, Charlton P. Design and synthesis of new templates derived from pyrrolopyrimidine as selective multidrug-resistance-associated protein inhibitors in multidrug resistance. *J. Med. Chem.* **2004**, 47, 1339-1350.
132. S. S. Kiselev, M. K. Polievktov, V. G. Granik. Enamines. 8. Polarographic study of the reactions of a number of enamino ketones with nucleophilic reagents. *Chemistry of Heterocyclic Compounds* **1981**, 17(3), 256-260.
133. Kealey, S.; Long, N. J.; Miller, P. W.; White, A. J. P.; Hitchcock, P. B.; Gee, A. Variable coordination behaviour of pyrazole-containing N,P and N,P(O) ligands towards palladium(II). *Dalton Trans.* **2007**, 26, 2823-2832.
134. Marson, C. M.; Hobson, A. D. *ComprehensiVe Organic Functional Group Transformations*; Katritzky, A. R., Meth-Cohn, O., Rees, C. W., Eds.; Pergamon Press: New York, **1995**; Vol. 5, p 302.
135. Thomas Rosenau, Andreas Hofinger, Antje Potthast, and Paul Kosma A General, Selective, High-Yield N-Demethylation Procedure for Tertiary Amines by Solid Reagents in a Convenient Column Chromatography-like Setup. *Org. Lett.*, **2004**, 6(4), 541-544.
136. Ottoni O.; Cruz R.; Alves R. Efficient and Simple Methods for the Introduction of the Sulfonyl, Acyl and Alkyl Protecting Groups on the Nitrogen of Indole and its Derivatives. *Tetrahedron* **1998**, 54, 13915-13928.
137. Kowalski, P.; Majka, Z.; Kowalska, T. Acid-catalyzed N-debenzylation of (benzylamino) pyridines. *Chemistry of Heterocyclic Compounds* **1998**, 34(6), 740-741.
138. Powell, Dennis; Gopalsamy, Ariamala; Wang, Yanong D.; Zhang, Nan; Miranda, Miriam; McGinnis, John P.; Rabindran, Sridhar K. Pyrazolo[1,5-a]pyrimidin-7-yl phenyl amides as novel antiproliferative

References

- agents: Exploration of core and headpiece structure–activity relationships. *Bioorg. Med Chem Lett* **2007**, 17, 1641 – 1645.
139. Fernanda A. Rosa, Pablo Machado, Helio G. Bonacorso, Nilo Zanatta and Marcos A. P. Martins Reaction of β -Dimethylaminovinyl Ketones with Hydroxylamine: a Simple and Useful Method for Synthesis of 3- and 5-Substituted Isoxazoles. *Journal of Heterocyclic Chemistry*, **2008**, 45, 879-885.
140. Al-Shiekh, M.; El-Din, A.; Hafez, E.; Elnagdi, M. α -Enones in heterocyclic synthesis, part I. Classical synthetic and environmentally friendly synthetic approaches to alkyl and acyl azoles and azines. *J. Chem. Res* **2004**, 3, 174-179.
141. Carlo Mustazza, Maria Rosaria Del Giudice, Anna Borioni, Franco Gatta. Synthesis of pyrazolo[1,5-*a*]-, 1,2,4-triazolo[1,5-*a*]- and imidazo[1,2-*a*]pyrimidines related to zaleplon, a new drug for the treatment of insomnia. *Heterocycl. Chem.* **2001**, 38, 1119-1129.
142. Dormagala, J. M.; Peterson, P. J. New 7-substituted quinolone antibacterial agents. II. The synthesis of 1-ethyl-1,4-dihydro-4-oxo-7-(pyrazoyl, isoxazoyl, and pyrimidinyl)-1,8-naphthyridine and quinolone-3-carboxylic acids Domagala, J.M.; Peterson, P.; *J. Heterocyclic Chem.* **1989**, 26 1147-1158.
143. Al-Omran, N.; Al-Awadi, A.; El-Khair, A.; Elnagdi, M. Synthesis of new aryl and heteroaromatic substituted pyridines, pyrazoles, pyrimidines and pyrazolo[3,4-*d*]pyridazines. *Org. Prep. Proced. Int.* **1997**, 29, 285-292.
144. Miyaura, N.; Yamada, K.; Suzuki, A. A new stereospecific cross-coupling by the palladium-catalyzed reaction of 1-alkenylboranes with 1-alkenyl or 1-alkynyl halides. *Tetrahedron Letters* **1979**, 20 (36): 3437–3440.
145. Miyaura, N.; Suzuki, A. Stereoselective synthesis of arylated (E) alkenes by the reaction of alk-1-enylboranes with aryl halides in the presence of palladium catalyst. *Chem. Comm.* **1979**, 19: 866–867.
146. Schultz, C.; Link, A.; Leost, M.; Zaharevitz, D. W.; Gussio, R.; Sausville, E. A.; Meijer, L.; Kunick, C. The paullones, a series of cyclin-dependent kinase inhibitors: synthesis, evaluation of CDK1/cyclin B inhibition, and in vitro antitumor activity. *J. Med. Chem.* **1999**, 42, 2909-2919.
147. Rosenmund, K. W.; Struck, E. Das am Ringkohlenstoff gebundene Halogen und sein Ersatz durch andere Substituenten. I. Mitteilung: Ersatz des Halogens durch die Carboxylgruppe. *Chem. Ber.* **1916**, 52, 1749-1756.
148. von Braun, J.; Manz, G. Fluoranthen und seine Derivate. III. Mitteilung. *Justus Liebigs Ann. Chem.* **1931**, 488, 111-126.

149. SMITHKLINE BEECHAM CORPORATION, Indole derivatives and use thereof as kinase inhibitors in particular IKK2 inhibitors. Patent: WO2005/67923 A1, **2005**.
150. Bernhard G., Dominique R., Oliver K. Synthesis of 5-Substituted 1H-Tetrazoles from Nitriles and Hydrazoic Acid by Using a Safe and Scalable High-Temperature Microreactor Approach. *Angew. Chem. Int. Ed.* **2010**, 49, 7101-7105.
151. Mologni L., Rostagno R., Brussolo S., Knowles P.P., Kjaer S., Murray-Rust J., Rosso E., Zambon A., Scapozza L., McDonald N.Q., Lucchini V., Gambacorti-Passerini C. Synthesis, structure-activity relationship and crystallographic studies of 3-substituted indolin-2-one RET inhibitors. *Bioorg. Med. Chem.* **2010**, 18, 1482-1496.
152. Shoemaker, R.H. The NCI60 human tumour cell line anticancer drug screen. *Nat. Rev. Cancer* **2006**, 6, 813-823.
153. Boyd MR, Paull KD. Some practical considerations and applications of the National Cancer Institute in vitro anticancer drug discovery screen. *Drug Dev Res* **1995**, 34:91-109.
154. NCI, <http://dtp.nci.nih.gov/branches/btb/ivclsp.html>
155. NCI, http://dtp.nci.nih.gov/docs/dtp_search.html
156. Marc Lacroix and Guy Leclercq. Relevance of breast cancer cell lines as models for breast tumours: an update. *Breast Cancer Research and Treatment* **2004**, 83: 249–289.
157. Merlin J.-L., Barberi-Heyob M. & Bachmann N. In vitro comparative evaluation of trastuzumab (Herceptin®) combined with paclitaxel (Taxol®) or docetaxel (Taxotere®) in HER2-expressing human breast cancer cell lines. *Annals of Oncology* **2002**, 13: 1743–1748.
158. Filmus, J.; Pollack, M. N.; Cailleau, R.; Buick, R. N. MDA-468, a human breast cancer cell line with a high number of epidermal growth factor (EGF) receptors, has an amplified EGF receptor gene and is growth inhibited by EGF. *Biochem. Biophys. Res. Commun.* **1985**, 128, 898-905.
159. Vickie S. W., Kathy B. and L. Earl G. Jr. Development and Characterization of a Cell Line That Stably Expresses an Estrogen-Responsive Luciferase Reporter for the Detection of Estrogen Receptor Agonist and Antagonists. *Toxicological Sciences* **2004**, 81, 69–77.
160. Nicholson, K. M., Streuli, C. H., and Anderson, N. G. Autocrine signalling through erbB receptors promotes constitutive activation of protein kinase B/Akt in breast cancer cell lines. *Breast Cancer Res Treat*, **2003**, 81: 117-128.

References

161. The UniProt Consortium. Reorganizing the protein space at the Universal Protein Resource (UniProt). *Nucleic Acids Res.* 40: D71-D75 (2012).
162. Laskowski, R.A., MacArthur, M.W., Moss, D.S., Thornton, J.M.: PROCHECK: a program to check the stereochemical quality of protein structures (International Union of Crystallography), *Journal of applied crystallography* **1993**, 26(2), 283–291.
163. LigPrep, version 2.5. Schrödinger, LLC, New York, NY, **2012**.
164. Jones, G, Willett, P, Glen, R C: Molecular recognition of receptor sites using a genetic algorithm with a description of desolvation., *J. Mol. Biol.* **1995**, 245(1), 43–53.
165. Jones, G, Willett, P, Glen, R C, Leach, A R, Taylor, R: Development and validation of a genetic algorithm for flexible docking., *J. Mol. Biol.* **1997**, 267(3), 727–748.
166. Molecular Operating Environment (MOE), 2012.10; Chemical Computing Group Inc., 1010 Sherbooke St. West, Suite #910, Montreal, QC, Canada, H3A 2R7, **2012**.
167. Guimarães, Cristiano R W, Rai, Brajesh K, Munchhof, Michael J, Liu, Shenping, Wang, Jian, Bhattacharya, Samit K, Buckbinder, Leonard: Understanding the impact of the P-loop conformation on kinase selectivity., *J Chem Inf Model* **2011**, 51(6), 1199–1204.
168. Becker, H. G. O., Beckert, R.; Domschke, G.; Fanghanel, E.; Habicher, W. D.; Metz, P.; Pavel, D.; Schwetlick, K. *Organikum*, **2000**, 21. Auflage, 741.
169. a) Grever, M. R.; Schepartz, S. A.; Chabner, B. A. The National Cancer Institute: cancer drug discovery and development program. *Semin. Oncol.* **1992**, 19, 622-638. b) Monks, A.; Scudiero, D.; Skehan, P.; Shoemaker, R.; Paull, K.; Vistica, D.; Hose, C.; Langley, J.; Cronise, P.; Vaigro-Wolff, A.; Gray-Goodrich, M.; Campbell, H.; Mayo, J.; Boyd, M. Feasibility of a high-flux anticancer drug screen using a diverse panel of cultured human tumor cell lines. *J. Natl. Cancer Inst.* **1991**, 83, 757-766. c) Monks, A.; Scudiero, D. A.; Johnson, G. S.; Paull, K. D.; Sausville, E. A. The NCI anti-cancer drug screen: a smart screen to identify effectors of novel targets. *Anti-Cancer Drug Des.* **1997**, 12, 533-541. d) Weinstein, J. N.; Myers, T. G.; O'Connor, P. M.; Friend, S. H.; Fornace Jr., A. J.; Kohn, K. W.; Fojo, T.; Bates, S. E.; Rubinstein, L. V.; Anderson, N. L.; Buolamwini, J. K.; van Osdol, W. W.; Monks, A. P.; Scudiero, D. A.; Sausville, E. A.; Zaharevitz, D. W.; Bunow, B.; Viswanadhan, V. N.; Johnson, G. S.; Wittes, R. E.; Paull, K. D. An information-intensive approach to the molecular pharmacology of cancer.

Science **1997**, 275, 343-349. **e)** Paull, K. D.; Shoemaker, R. H.; Hodes, L.; Monks, A.; Scudiero, D. A.; Rubinstein, L.; Plowman, J.; Boyd, M. R. Display and analysis of patterns of differential activity of drugs against human tumor cell lines: development of mean graph and COMPARE algorithm. *J. Natl. Cancer Inst.* **1989**, 81, 1088 - 1092. **f)** <http://www.ncbi.nlm.nih.gov/pmc/articles/PMC2868078/> **g)** S.A.F. Rostom, Synthesis and in vitro antitumor evaluation of some indeno[1,2-c]pyrazol(in)es substituted with sulfonamide, sulfonylurea(-thiourea) pharmacophores, and some derived thiazole ring systems. *Bioorg. Med. Chem.* **2006**, 14, 6475e-6485. **h)** Malleshappa N. Synthesis and anticancer evaluation of novel 2-cyclopropylimidazo[2,1-*b*][1,3,4]-thiadiazole derivatives. *European Journal of Medicinal Chemistry* **2011**, 46, 4411-4418.